ADVANCES IN PHYSIOLOGICAL SCIENCES

Proceedings of the 28th International Congress of Physiological Sciences Budapest 1980

Volumes

1 — Regulatory Functions of the CNS. Principles of Motion and Organization
2 — Regulatory Functions of the CNS. Subsystems
3 — Physiology of Non-excitable Cells
4 — Physiology of Excitable Membranes
5 — Molecular and Cellular Aspects of Muscle Function
6 — Genetics, Structure and Function of Blood Cells
7 — Cardiovascular Physiology. Microcirculation and Capillary Exchange
8 — Cardiovascular Physiology. Heart, Peripheral Circulation and Methodology
9 — Cardiovascular Physiology. Neural Control Mechanisms
10 — Respiration
11 — Kidney and Body Fluids
12 — Nutrition, Digestion, Metabolism
13 — Endocrinology, Neuroendocrinology, Neuropeptides — I
14 — Endocrinology, Neuroendocrinology, Neuropeptides — II
15 — Reproduction and Development
16 — Sensory Functions
17 — Brain and Behaviour
18 — Environmental Physiology
19 — Gravitational Physiology
20 — Advances in Animal and Comparative Physiology
21 — History of Physiology

Satellite symposia of the 28th International Congress of Physiological Sciences

22 — Neurotransmitters in Invertebrates
23 — Neurobiology of Invertebrates
24 — Mechanism of Muscle Adaptation to Functional Requirements
25 — Oxygen Transport to Tissue
26 — Homeostasis in Injury and Shock
27 — Factors Influencing Adrenergic Mechanisms in the Heart
28 — Saliva and Salivation
29 — Gastrointestinal Defence Mechanisms
30 — Neural Communications and Control
31 — Sensory Physiology of Aquatic Lower Vertebrates
32 — Contributions to Thermal Physiology
33 — Recent Advances of Avian Endocrinology
34 — Mathematical and Computational Methods in Physiology
35 — Hormones, Lipoproteins and Atherosclerosis
36 — Cellular Analogues of Conditioning and Neural Plasticity

(Each volume is available separately.)

ADVANCES IN
PHYSIOLOGICAL SCIENCES

Proceedings of the 28th International Congress of Physiological Sciences
Budapest 1980

Volume 3

Physiology of Non-excitable Cells

Editor

J. Salánki
Tihany, Hungary

Co-editors

E. L. Boulpaep, *USA*
P. Fasella, *Italy*
A. Kleinzeller, *USA*
W. R. Loewenstein, *USA*
H. H. Ussing, *Denmark*

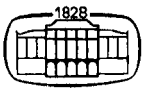

PERGAMON PRESS

AKADÉMIAI KIADÓ

Pergamon Press is the sole distributor for all countries, with the exception of the socialist countries.

HUNGARY	Akadémiai Kiadó, Budapest, Alkotmány u. 21. 1054 Hungary
U.K.	Pergamon Press Ltd., Headington Hill Hall, Oxford OX3 0BW, England
U.S.A.	Pergamon Press Inc., Maxwell House, Fairview Park, Elmsford, New York 10523, U.S.A.
CANADA	Pergamon of Canada, Suite 104, 150 Consumers Road, Willowdale, Ontario M2J 1P9, Canada
AUSTRALIA	Pergamon Press (Aust.) Pty. Ltd., P.O. Box 544, Potts Point, N.S.W. 2011, Australia
FRANCE	Pergamon Press SARL, 24 rue des Ecoles, 75240 Paris, Cedex 05, France
FEDERAL REPUBLIC OF GERMANY	Pergamon Press GmbH, 6242 Kronberg-Taunus, Hammerweg 6, Federal Republic of Germany

British Library Cataloguing in Publication Data

International Congress of Physiological Sciences
(28th : 1980 : Budapest)
Advances in physiological sciences
Vol. 3: Physiology of non-excitable cells
1. Physiology - Congresses
I. Title II. Salánki, J
591.1 QP1 80-41874

Pergamon Press	ISBN 0 08 026407 7 (Series) ISBN 0 08 026815 3 (Volume)
Akadémiai Kiadó	ISBN 963 05 2691 3 (Series) ISBN 963 05 2729 4 (Volume 3)

In order to make this volume available as economically and as rapidly as possible the authors' typescripts have been reproduced in their original forms. This method unfortunately has its typographical limitations but it is hoped that they in no way distract the reader.

Printed in Hungary

FOREWORD

This volume is one of the series published by Akadémiai Kiadó, the Publishing House of the Hungarian Academy of Sciences in coedition with Pergamon Press, containing the proceedings of the symposia of the 28th International Congress of Physiology held in Budapest between 13 and 19 July, 1980. In view of the diversity of the material and the "taxonomic" difficulties encountered whenever an attempt is made to put the various subdisciplines and major themes of modern physiology into the semblance of some systematic order, the organizers of the Congress had to settle for 14 sections and for 127 symposia, with a considerable number of free communications presented either orally or as posters.

The Congress could boast of an unusually bright galaxy of top names among the invited lecturers and participants and, naturally, the ideal would have been to include all the invited lectures and symposia papers into the volumes. We are most grateful for all the material received and truly regret that a fraction of the manuscripts were not submitted in time. We were forced to set rigid deadlines, and top priority was given to speedy publication even at the price of sacrifices and compromises. It will be for the readers to judge whether or not such an editorial policy is justifiable, for we strongly believe that the value of congress proceedings declines proportionally with the gap between the time of the meeting and the date of publication. For the same reason, instead of giving exact transcriptions of the discussions, we had to rely on the introductions of the Symposia Chairmen who knew the material beforehand and on their concluding remarks summing up the highlights of the discussions.

Evidently, such publications cannot and should not be compared with papers that have gone through the ordinary scrupulous editorial process of the international periodicals with their strict reviewing policy and high rejection rates or suggestions for major changes. However, it may be refreshing to read these more spontaneous presentations written without having to watch the "shibboleths" of the scientific establishment.

September 1, 1980

J. Szentágothai

President of the
Hungarian Academy of Sciences

PREFACE

This Volume contains two plenary lectures and most of the papers of five symposia of the Section "General Cell Physiology" at the 28th International Congress of Physiological Sciences. Cell physiology has become an extremely wide field of biological sciences, and it was impossible to cover its entire spectrum in the program. A number of important, fast developing subjects were, therefore, selected for discussion concerning the general aspects of both non-excitable cells and neuronal membranes. Papers of this Volume deal with recent results on metabolism and transport, cell-to-cell communication, and time dimensions of intracellular processes in non-excitable cells.

The chairmen of the symposia acted not only as organizers of their topics by selecting the invited speakers, but most of them have also made a contribution to the proceedings by compiling an introduction and concluding remarks to the respective symposia. Furthermore, they were also active as co-editors of the Volume for which I wish to express my sincere gratitude.

I wish to thank Dr. T. Kiss, Secretary of the Section, and Mrs. Maria Kiss for their careful and enthusiastic work during the Congress and for their help in compiling this Volume.

J. Salánki

Adv. Physiol. Sci. Vol. 3. Physiology of Non-excitable Cells
J. Salánki (ed.)

OXIDATIVE METABOLISM OF PHAGOCYTOSING LEUKOCYTES*

Shigeki Minakami and Koichiro Takeshige
Department of Biochemistry, Kyushu University School of Medicine, Fukuoka 812, Japan

The phagocytotic oxidative metabolism of polymorphonuclear leukocytes and macrophages have been studied by many investigators during this decade. The cells form a large amount of reactive oxygen species such as superoxide anions and hydrogen peroxide, and the metabolism is closely related to the bactericidal action of the phagocytes which was proposed by Metchnikoff in 1883, about a century ago.

Historical Development

Before presenting our own study, we would like to give brief historical review on the study of this problem.

Respiratory burst

Just a half century after Metchnikoff proposed the phagocyte theory, a short but very important paper with a title of "The Extra Respiration of phagocytosis" was published by physiologists, Baldridge and Gerard(1933).They observed a "burst of extra respiration" which lasted for 10 to 15 min on the addition of bacteria to dog leukocytes. They did the experiment with the anticipation that "the respiration of leukocytes would increase during active phagocytic ingestion" to supply energy, so that it is natural for them to conclude that the burst respiration represents "the excess energy liberation of engulfment". Their important observation and the concept, however, did not seem to draw much attention at that time, because it was generally believed by the influences of eminent physiologists, Fenn and Ponder, that phagocytosis is a passive process and no energy is necessary for the engulfment of particles (see Mudd et al.,1934). A quarter century had elapsed before their observation was confirmed and the nature of the extra respiration was studied.

Cyanide-insensitive respiration

In 1958, Becker et al.(1958) published a paper on the metabolism of leukocytes during phagocytosis. They showed that the respiratory burst

* The study presented here was done in collaboration with our former colleagues, Drs. Kakinuma, Matsumoto, Nabi, Nakagawara, Nakamura and Tatscheck. The work was supported in part by grants from Yamanouchi Foundation of Metabolism and Disease, the Ministry of Education,Science and Culture, and the Ministry of Health and Welfare,Japan.

of the cells is not inhibited by cyanide, which clearly indicates that the extra respiration is not the energy-yielding process as concluded by Baldridge and Gerard(1933). Their another finding is that the lactate production as well as the catabolism of glycogen is accelerated by phagocytosis, the finding which is in accord with many previous reports (for example, Fleischmann, 1927) that phagocytosis depends on glycolysis and not on respiration. Sbarra and Karnovsky(1959) reported more intensive investigation on the problem.

The respiratory burst is also characterized by a concomitant acceleration of hexose monophosphate oxidative pathway. It was found by Stähelin et al. (1957) and more intensively studied by Sbarra and Karnovsky(1959). They observed the increased appearance of C-1 of glucose as carbon dioxide relative to C-6 of glucose when guinea pig leukocytes were incubated with bacteria or inert particles. Because hexose monophosphate oxidative pathway is coupled to reoxidation of NADPH and the oxidation is usually accompanied by little or no oxidative phosphorylation, the oxidation of NADPH can be related to the respiratory burst.

Formation of hydrogen peroxide

In 1961, Quastel's group presented an important proposal (Iyer et al. 1961). They suggested that guinea pig polymorphonuclear leukocytes produce hydrogen peroxide during phagocytosis. Their conclusion was based on the observation that the cells oxidize radioactive formate to carbon dioxide in the presence of catalase. Later, the extracellular appearance of hydrogen peroxide was actually shown by several investigators(Paul and Sbarra, 1968; Zatti et al.,1968). The formation of hydrogen peroxide has important meaning in view of the intracellular killing of bacteria: the presence of peroxidase(myeloperoxidase) in granulocytes and the bactericidal action of hydrogen peroxide have been known for long time.

One of the earliest experiments on the bactericidal effect of peroxidase-hydrogen peroxide system was carried out by Kojima(1931) a half century ago at our university, though he used horseradish peroxidase. He suggested that phenols he added in the test systems are oxidized to quinones which exert bactericidal action. More recently, a study was done by Agner(1950) who had purified myeloperoxidase(Agner, 1941). He showed that certain donor substances are oxidized by the enzyme in the presence of hydrogen peroxide to products which destroy the toxic properties of diphtheria toxin. Halide ions such as chloride, iodide and bromide, were shown by Klebanoff(1967) to be the donor substances and the myeloperoxidase-hydrogen peroxide-halide system has become an important bactericidal system of leukocytes.

Formation of superoxide radicals

At the close of 1960s, superoxide anions became an actual compound for biochemists. The existence of the radicals, the product of univalent reduction of oxygen molecules, had been proposed based on the reaction mechanisms of peroxidase and xanthine oxidase, but because of their lability in aqueous media, they could not be detected. In 1969, McCord and Fridovich(1961) showed that hemocuprein, a cupper protein which had been known for long time, catalyses dismutation of superoxide radicals to hydrogen peroxide and oxygen molecules. The enzyme, superoxide dismutase, becomes an important reagent to detect the formation of superoxide radicals in biological systems.

The formation and extracellular release of superoxide anions by

phagocytosing leukocytes was first reported by Babior et al.(1973). It was based on the observation that the cells reduce exogenously added cytochrome c and the reduction is inhibited by the addition of superoxide dismutase.

Mechanism of NADPH oxidation

From the foregoing discussions, it may become clear that the oxidation of NADPH is a crucial step in the respiratory burst. The oxidation should be accelerated by phagocytosis, reduce oxygen molecules to superoxide radicals and hydrogen peroxide and be able to release them to the extracellular medium or into the vacuoles in which bacteria are trapped. Several enzyme or enzyme systems have been assigned to the reaction: for example, myeloperoxidase(Roberts and Quastel,1964), a soluble NADH oxidase coupled with a transhydrogenase(Cagan and Karnovsky,1964) and a particulate NADPH oxidase (Iyer and Quastel,1963). At present, most investigators seem to agree that a particulate-bound NADPH oxidase is catalyzing the oxidation of NADPH during phagocytosis. Rossi and Zatti(1964) found that the granule fraction obtained from phagocytosing cells exhibited an increase of both NADH and NADPH oxidase activities, the latter being stimulated several-fold with respect to the activity found in the granules of resting cells. The activation has been ascribed to the decrease of Km for NADPH(Patriarca et al., 1971). The enzyme produces superoxide anions(Curnutte et al.,1975) and seems to be localized on the plasma membrane. These properties of the particulate NADPH oxidase make the enzyme as the best candidate responsible for the respiratory burst.

General Process of Phagocytosis

Because we have reviewed only a rather special facet of phagocytosis, it may be necessary to relate them with more general complex process of phagocytosis and bactericidal actions.

Phagocytosis (Table I)

First, leukocytes move to the direction of bacteria in response to a concentration gradient of a chemotactic factor (Chemotaxis). When bacteria are in contact with the cells, metabolic changes take place. Both oxygen-uptake and hexose monophosphate oxidative pathway are stimulated, which can be explained by the activation of the NADPH oxidase. Glycolysis is

Table I.Phagocytotic process

Chemotaxis
Metabolic changes
Respiratory burst
Stimulation of HMP-shunt
Stimulation of glycolysis
Adhesion and Engulfment
Phagosome formation
Degranulation
Phagolysosome formation
Bactericidal action
Digestion

Table II. Bactericidal mechanism

Oxidative killing
Superoxide anions (O_2^-)
Hydrogen peroxide
Myeloperoxidase-H_2O_2-halide
Hydroxy radicals ($HO\cdot$)
Singlet oxygen ($^1O_2$)
Non-Oxidative killing
Hydrolytic enzymes
Bactericidal proteins
Cationic proteins
Lactoferrin
Acid

also stimulated to prepare energy for the activation of the NADPH oxidase and for the ingestion process. By adhesion of bacteria to the plasma membrane, vacuoles (phagosomes) are formed by the invagination of the membrane, the activated NADPH oxidase facing the interior of the phagosomes. Then, lysosomes (granules) are fused with phagosomes and thus the contents of the granules, hydrolytic enzymes and bactericidal proteins, are released into phagolysosomes formed by the fusion. Killing and digestion of bacteria take place in the phagolysosomes.

Bactericidal actions (Table II)

Two groups of intracellular killings exist: one group is related to the respiratory burst and the other group needs no oxygen. The former is the killing by reactive oxygen species, i.e. superoxide anions, hydrogen peroxide, hydroxy radicals and singlet oxygen, of which the killing by myeloperoxidase system is most intensively studied. Related to the oxidative killing, a hereditary disease with recurrent infection, chronic granulomatous disease, has been known (Berendes et al.,1957). Polymorphonuclear leukocytes of the patients can ingest bacteria but can not kill them because the cells do not form superoxide anions. Patients with leukocytes deficient in myeloperoxidase are also known. The bactericidal capacity of the cells are somewhat impaired but the patients are usually healthy without recurrent infections. Related to the non-oxidative killing, no clear demonstration of clinical cases is made. Thus, the non-oxidative killings seem to be auxillary to the oxidative killing or of only bacteriostatic nature.

Non-particulate Substances which Induce Metabolic Changes

Difficulty in the study of phagocytotic metabolism is that the changes induced by particles are complicated by the endocytotic process, including the internalization of the plasma membrane. This can be avoided by using non-particulate reagents which trigger metabolic changes characteristic to phagocytosis (Table III). They are sometimes called as "mimickers" because they mimic phagocytosis. Many of them are surfactants (Graham et al.,1967; Zatti and Rossi,1967) and most of them are the reagents which interact with plasma membrane, for example lectins (Romeo et al.,1974), antibodies (Rossi et al.,1970) and phospholipase C (Patriarca et al.,1970). The triggering of the metabolic changes by the stimulation of the plasma membrane is in accord with the concept that the activation of the NADPH oxidase happens by the contact of particles with the plasma membrane and is not related to the ingestion process. We will discuss two kinds of the mimickers, surfactants and cytochalasins, as examples.

Table III. Agents which trigger phagocytotic metabolism

Surfactants
Digitonin
Fatty acids
Phorbol myristate acetate
Lectins
Antibodies and Complements
Cytochalasin D (E)
Calcium ionophore

Surfactants

Detergents are a group of well-defined chemical substances among the mimickers. Steroid surfactants, such as deoxycholate (Graham et al.,1967) and saponin (Zatti and Rossi,1967), have been shown to induce phagocytotic metabolic changes. A systematic examination of surfactants showed that fatty acids and some of their derivatives also trigger the respiratory burst without showing any appreciable pinocytotic process by electron microscopic observations (Kakinuma,1974; Kakinuma et al.,1976). It was shown that among saturated fatty acids of different alkyl chain lengths, myristate (C = 14) have the strongest activating effect. A comparison of the respiration stimulated by various surfactants which have an alkyl chain corresponding to that of laurate (C = 12) showed that only anionic surfactants

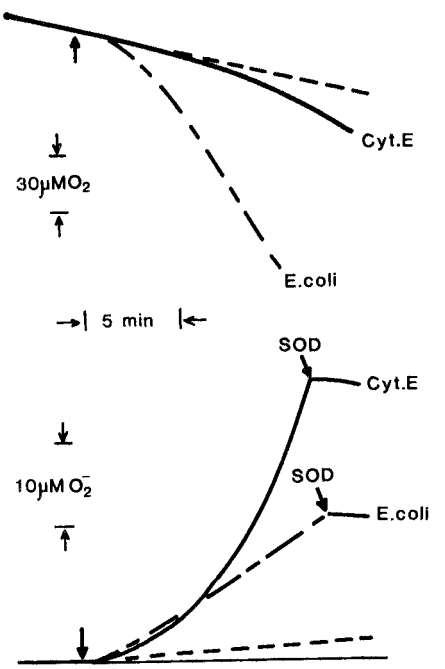

Fig. 1. Oxygen uptake and superoxide release by leukocytes

Polymorphonuclear leukocytes(1.4×10^7) of guinea pig peritoneal exudates were suspended in 2.0 ml Krebs Ringer phosphate solution(Ca:0.6 mM) containing 5 mM glucose at 37°C. The reaction was started either with cytochalasin E(Cyt.E) or heat-killed E. coli(0.85 mg dry weight). The dotted lines indicated the control experiments without stimulation. Upper figure: traces with oxygen electrode. Lower figure: absorbancy changes at 550-540 nm in the presence of 75 μM ferricytochrome c. Superoxide dismutase(SOD) was added at the points indicated. (Nakagawara et al.,1976)

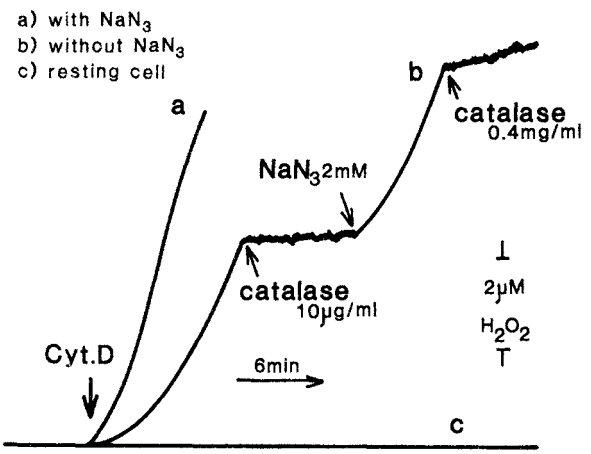

Fig. 2. Hydrogen peroxide formation by leukocytes.

Guinea pig leukocytes(10^6) were added to 1.0 ml Krebs Ringer phosphate solution(Ca:0.6 mM) containing 2 mM glucose, 2 mM azide, 0.4 nM horseradish peroxidase and 0.5 mM homovanillic acid. The fluorescence change on the surface of the cuvette was measured at 37°C with a excitation filter (313-366 nm) and a emission filter(400-3000 nm). The reaction was started by 5 μg cytochalasin D. (Nabi et al.,1979)

such as lauryl sulfate and laurate trigger the burst, whereas cationic surfactants such as laurylbetaine and non-ionic surfactants such as lauryldimethylamine do not stimulate the respiration. The effects of anionic surfactants are apparently related to the electrostatic strengths of the ionic sites, suggesting the interaction of the anions with cationic groups of the membrane on the one hand, and the interaction of the alkyl chain with the non-polar groups of the membrane on the other hand.

Cytochalasins

Cytochalasins are a family of antibiotics from molds which exert an inhibitory effect on various cellular motile functions including membrane movement. One of the members, cytochalasin B, is known to inhibit the transport of monosaccharides(Zigmond and Hirsch, 1972) and the particle ingestion (Malawista et al., 1971) by leukocytes. Stimulation of the cytochalasin B-treated leukocytes with particles have been used for the study of phagocytotic metabolism (Root and Metcalf, 1977).

We have found that two members of the six congeners, cytochalasins D and E, stimulate the cyanide-insensitive respiration, hexose monophosphate oxidative pathway and the release of superoxide anions (Nakagawara et al., 1974; Nakagawara and Minakami,1975; Nakagawara et al.,1976) at low concentrations of less than 10 μM. The cytochalasins are ideal tools for the study of the metabolic changes in a simplified system, because they completely inhibit endocytotic process at the same time. We are going to show experimental results obtained by using cytochalasins D or E.

Oxidative Metabolism Induced by the Cytochalasins

The uptake of oxygen and the release of superoxide anions by guinea pig polymorphonuclear leukocytes stimulated either by cytochalasin E or bacteria are shown in Fig. 1. The oxygen-uptake trace was obtained by using a Clark-type oxygen electrode and the trace of superoxide release is the reduction of exogenously added cytochrome c as measured at 550 nm relative to 540 nm by a dual-wavelength spectrophotometer with an end-on photomultiplier tube. Superoxide dismutase (SOD) completely inhibits the reduction. The cytochalasin is a relatively weak stimulant of the oxygen uptake compared with bacteria, but the former caused the release of a large amount of superoxide anions than the latter. Quantitative comparison will be made later.

The cytochalasins (D and E) also stimulate the formation of hydrogen peroxide which can be measured continuously by the fluorescence increase due to the formation of a fluorescent product from homovanillic acid in the presence of horseradish peroxidase. The traces are shown in Fig. 2. Curve a gives the standard condition with azide which inhibits contaminated catalase. Curve b shows the effect of catalase and azide, and the curve c the trace with non-stimulated cells.

Quantitative comparison of the oxygen metabolism

The oxygen uptake and the formations of superoxide and hydrogen peroxide of guinea pig polymorphonuclear leukocytes induced by cytochalasin D and bacteria are shown in Table IV. The rates at steady-state in the presence of azide are shown except that of the superoxide release by the phagocytosing cells given in parenthesis which is the initial rate. If we compare the rates of the superoxide and hydrogen peroxide formation which are measured separately, the ratio is 2 : 1 for the cytochalasin-treated cells in agreement with the stoichiometry of the dismutation in the medium,

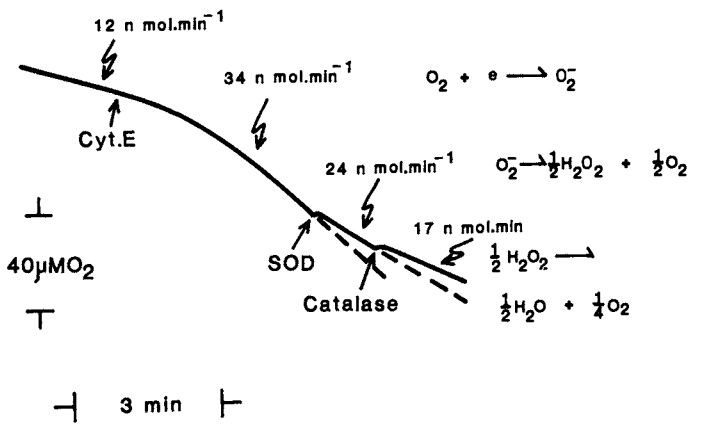

Fig. 3. Decrease of oxygen uptake on addition of superoxide dismutase

Guinea pig leukocytes(2.4×10^7) were suspended in 2.0 ml of an isotonic surcose solution buffered with 15 mM Tris-HCl,pH7.4, and containing 5 mM glucose. The concentrations of cytochalasin E(Cyt.E), superoxide dismutase (SOD) and catalase were 10 μM, 10 μg/ml and 0.35 μg/ml, respectively. (Minakami et al.,1977)

whereas the ratio is 1 : 10 for the cells ingesting bacteria indicating that hydrogen peroxide is not the one formed in the medium from superoxide anions but is the one directly released from the cells.

The ratio of the oxygen uptake and the hydrogen peroxide formation is 2 : 1 for the cytochalasin-treated cells, whereas it is 4 : 1 for the phagocytosing cells. We propose for the cytochalasin-treated cells that all of the oxygen consumed is converted to superoxide which is released to the medium and converted to hydrogen peroxide. The theoretical ratio of the oxygen uptake and the hydrogen peroxide formation in this case should be 1 : 1, but a part of the superoxide are utilized on the cell membrane before it is scavenged by ferricytochrome c or dismutated spontaneously in the medium As shown below, the oxygen uptake is decreased and the hydrogen peroxide formation is increased if they are measured in the presence of superoxide dismutase.

Effect of superoxide dismutase on the respiration

Fig. 3 shows the decrease of the oxygen uptake on addition of superoxide dismutase. The addition of catalase further decreases the rate. These changes can be explained by the equations given at the right side of the trace. If we measure the respiration in the presence of ferricytochrome c , the respiration is activated by superoxide dismutase as expected(not shown).

Effect of superoxide dismutase on the hydrogen peroxide formation

The effect of superoxide dismutase on the hydrogen peroxide formation is different whether the cells are triggered with the cytochalasin or with bacteria (Fig. 4). When the cells are triggered with the cytochalasin, the steady-state rate of the hydrogen peroxide formation is stimulated, whereas when the cells are stimulated with bacteria, the steady-state rate is not affected but an initial slow formation of hydrogen peroxide is replaced by a fast one. The latter phenomenon can be explained by the trace of superoxide release given in Fig. 5 (and also in Table IV). The superoxide release from the cytochalasin-treated cells is linear with some lag time, whereas the release from the cells ingesting bacteria is initially fast but it soon subsides. The addition of superoxide dismutase may affect only at the initial stage when the cells are ingesting bacteria, whereas it may affect the steady-state when the cells are stimulated with the cytochalasin. The phagocytosing cells release superoxide while the phagosomes have openings but they release only hydrogen peroxide when the phagosomes are completely sealed.

Table IV. Quantitative comparison of the oxidative metabolism
(Nabi et al.,1979)

	oxygen uptake	superoxide release	H_2O_2 release
cytochalasin D	4.5 ± 0.3	4.0 ± 0.3	1.9 ± 0.1
E. coli	8.0 ± 1.0	0.2 ± 0.04 [2.1 ± 0.3]	2.1 ± 0.1

The activities were measured in the presence of 2 mM NaN_3 and linear portion of the curves were taken, except that in parenthesis which is the initial rate. The values are mean ± SEM of 10 independent experiments and expressed as nmol/min per 10^6 cells.

Hydrogen peroxide formation in the presence of ferricytochrome c (Fig. 6)

The situation can be more clearly shown when the hydrogen peroxide formation is measured in a medium containing ferricytochrome c. The hydrogen peroxide formation by the cells stimulated with the cytochalasin is negligibly slow in the presence of the scavenger but it is strongly activated by superoxide dismutase. In contrast, the steady-state rate of hydrogen peroxide formation by the cells ingesting bacteria is not affected by the enzyme and only the initial lag disappears.

Effects of permeant and non-permeant SH-inhibitors

The possibility that the superoxide forming NADPH oxidase faces the extracellular medium when the cells are triggered with the cytochalasin and it moves to the phagosome membrane when the cells are actively ingesting particles , can be supported by experiments comparing the effects of

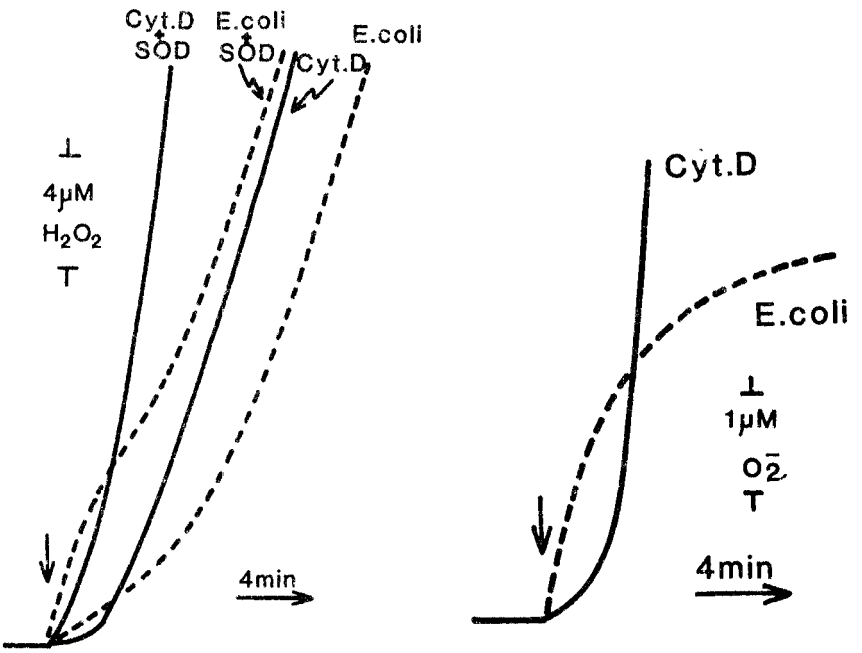

Fig.4(left). Effect of superoxide dismutase on hydrogen peroxide formation
The experimental conditions were essentially the same as in Fig. 2. The cytochalasin D(5 μg) or E.coli(0.9 mg dry wt) was added at the point indicated by an arrow. The concentration of superoxide dismutase was 10 μg/ml. (Nabi et al.,1979)

Fig.5(right). The time-course of the superoxide release
The experiment was carried out with the same batch of the cells as in Fig. 4. The experimental conditions were essentially the same as above, except that horseradish peroxidase and homovanillic acid were omitted and 80 μM cytochrome c was added. The reduction of the pigment was measured as in Fig. 2. (Nabi et al.,1979)

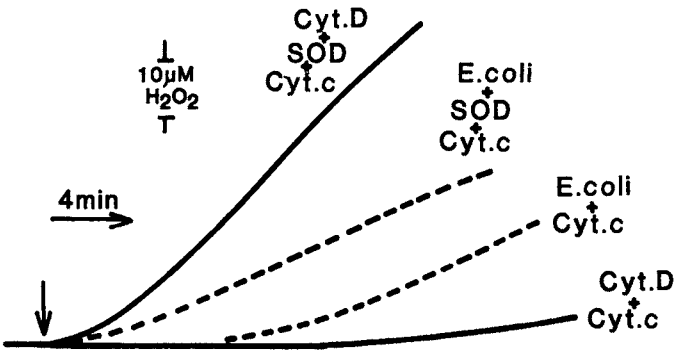

Fig. 6. Hydrogen peroxide fomration in the presence of cytochrome c.
The experimental conditions were essentially the same as in Fig. 4 and with the same batch of the cells, except that 100 μM cytochrome c was added in the reaction mixture. (Nabi et al.,1979)

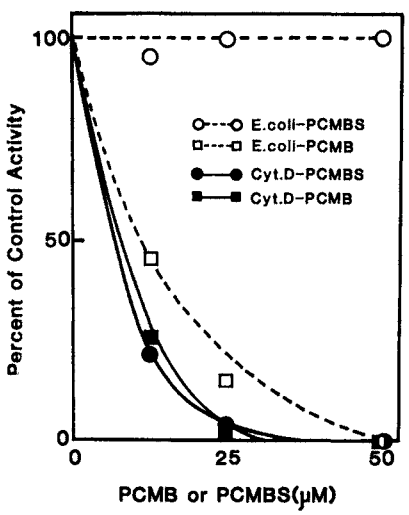

Fig. 7. Effect of SH-inhibitors on the hydrogen peroxide formation
Guinea pig leukocytes were stimulated with cytochalasin D or E. coli and after 4 min, p-chloromercuribenzoate(PCMB) or p-chloromercuribenzene sulfonate(PCMBS), the concentrations of which are on the abscissa, were added. (Nabi et al.,1979)

permeant and non-permeant SH-inhibitors on the hydrogen formation by the cytochalasin-treated cells and the phagocytosing cells. Mercurials have been known to inhibit the particulate NADPH oxidase. As shown in Fig. 7, a permeant inhibitor, p-chloromercuribenzoate(PCMB) , inhibits the hydrogen peroxide formation induced by both bacteria and the cytochalasin, whereas a non-permeant SH-inhibitor, p-chloromercuribenzenesulfonate (PCMBS), inhibits only the hydrogen peroxide formation by the cytochalasin-treated cells, without inhibiting the formation of the cells ingesting bacteria.

Electron microscopic observations

Electron microscopic observations of the cytochalasin treated cells done by Drs. Hatae and Shibata of the Anatomy Department are also in accord with the above discussed concept. The cells treated with cytochalasin D or cytochalasin E are characterized by the disappearance of pseudopods and the subsequent appearance of vacuole-like structures which resemble phagosomes at first sight (Fig. 8). Some of the vacuole-like structures, however, have openings to the extracellular medium, suggesting that they are a part of the plasma membrane linked to the cell surface. This can be ascertained by fixing the cells in a fixative containing tannic acid which is impermeant of plasma membrane. Tannic acid is found lining the inner-surface of the vacuole-like structure as well as the cell surface (Nabi et al.,1979).

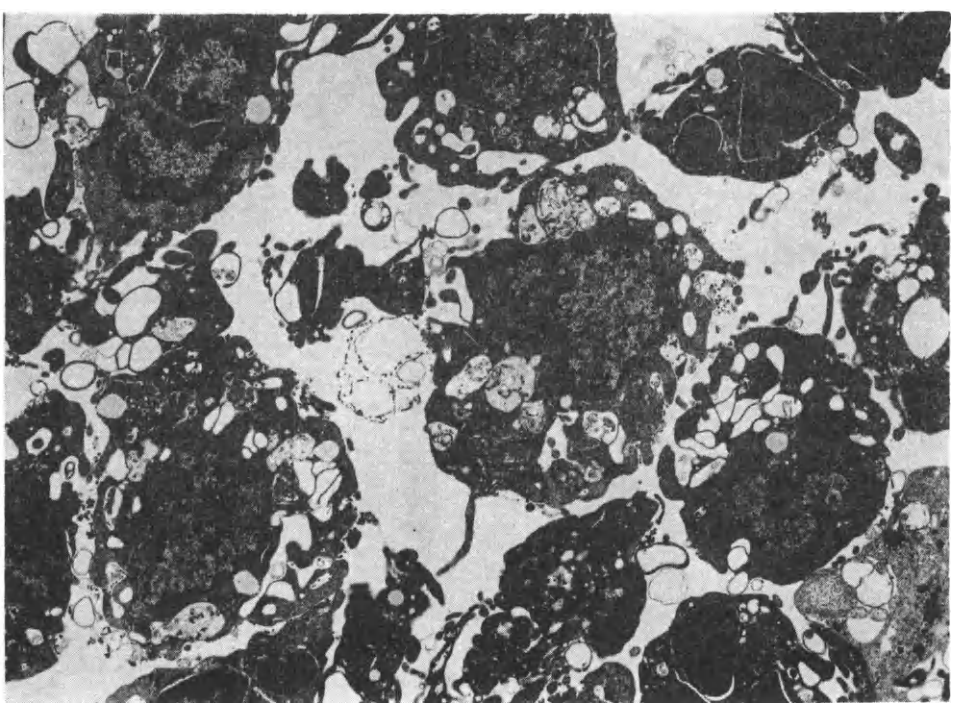

Fig. 8. Electron-micrograph of leukocytes treated with cytochalasin D.
Guinea pig polymorphonuclear leukocytes were incubated with the cytochalasin(5 μg/ml) for 10 min at 37°C, fixed with 2.5 % glutaraldehyde-0.1M cacodylate solution,pH 7.4 and postfixed with 1 % osmium tetraoxide. (courtesy of Dr. Hatae)

Table V. Effects of cytochalasins and inhibitors (Nabi et al.,1979)

	Superoxide release (nmol/min per 10^6 cell)	NADPH oxidase (nmol/min per mg prot.)
Control	0	2.0
Cytochalasin B	0	2.5
Cytochalasin C	0.5	2.9
Cytochalasin E	3.8	13.0
Cytochalasin D	4.0	16.5
+ 3mM dibutyryl cAMP	0.08	2.6
+ 1mM theophylline	1.4	3.8
+ 1mM N-ethylmaleimide	0	1.4
+10mM 2-deoxyglucose	0	1.0

The cells were incubated with cytochalasins(10 μg/ml) at 37°C for 10 and 30 min, for the superoxide release and NADPH oxidase activation,respectively.

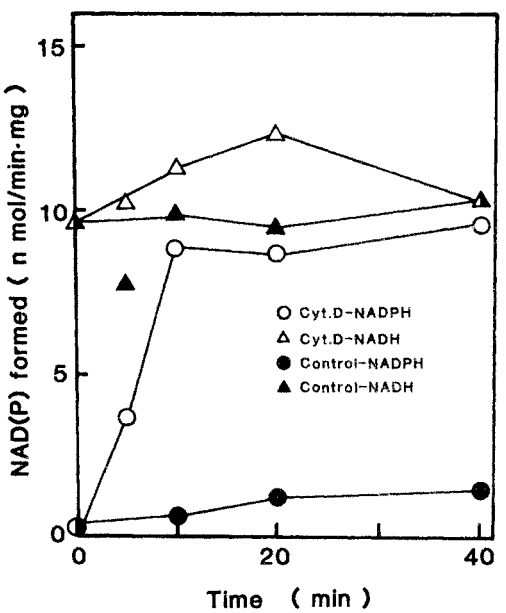

Fig. 9 Activation of NADPH oxidase by cytochalasin treatment
Guinea pig leukocytes in the Ringer solution were incubated with cytochalasin D(10 μg/ml) at 37°C for time intervals given on the abscissa. The cells were homogenized with a Polytron homogenizer for 2 min in a buffered 0.34 M sucrose solution. The particulate fraction (between 150 g x 10 min and 100 000 g x 30 min) was used for the assays. The NADH- and NADPH oxidase activities were measured at pH 5.5 in the presence of 1 mM of NADH or NADPH and 2 mM KCN. The oxidized coenzymes were measured fluorometrically after alkaline treatment. The open symbols are the control experiments incubated without cytochalasin D. (Nabi et al.,1979)

Activation of the NADPH Oxidase

Cytochalasin D(or E) activates the particulate NADPH oxidase as expected from the stimulation of the cellular metabolism. A particulate fraction (between 250 g for 10 min and 100 000 g for 30 min in 0.34 M sucrose solution) oxidizes both NADH and NADPH. The NADPH oxidase activity is low in the resting cells but it increases several-fold during incubation of the cells with cytochalasin D , while the NADH oxidase activity is only slightly activated during the incubation (Fig. 9). The lineweaver-Burk plot of the NADPH oxidase becomes biphasic with two Km values. The larger one corresponds to the NADPH oxidase of the resting cells and the smaller Km value seems to be responsible for the respiratory burst.

Cellular response and the activation of the enzyme

Conditions for the activation of the NADPH oxidase are essentially similar to those for the cellular release of superoxide anions. As shown in Table V, cytochalasins B and C do not activate the enzyme, and cytochalasins D and E activate it; the activation of the enzyme is parallel with the stimulation of the cellular response. Dibutyrl cyclic AMP, theophylline, N-ethylmaleimide and 2-deoxyglucose which inhibit the superoxide release triggered with cytochalasin D also suppress the activation of the enzyme. The cytochalasins as well as other known mimicers do not activate the enzyme when they are added to the homogenate.

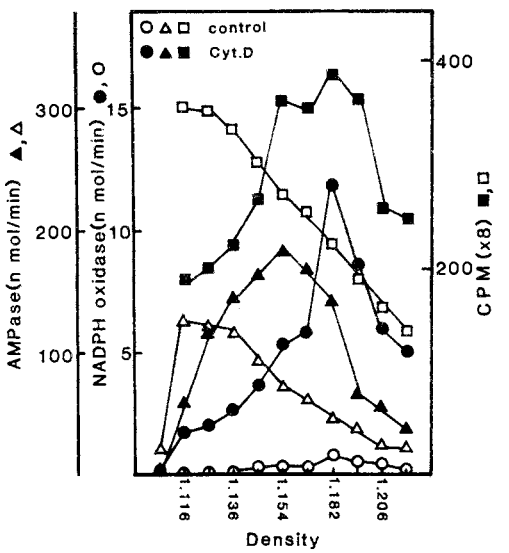

Fig. 10 Subcellular localization of the activated NADPH oxidase
Guinea pig leukocytes were iodinated with radioactive iodide and lactoperoxidase, and washed. The cells were activated with cytochalasin D and the particulate fraction was prepared as in Fig. 9. It was centrifuged on a linear sucrose density gradient from 30-60 % at 77 000 g for 60 min. The open symbols are for the control cells incubated without cytochalsin D.

Localization of the NADPH oxidase

Subcellular localization of the activated NADPH oxidase is studied by an isopycnic centrifugation of the homogenate (Fig. 10). In order to label the plasma membrane, we pretreated the cells first with radioactive iodide and lactoperoxidase, and washed the cells with saline. Then the cells were incubated with or without cytochalasin D. The radioactivity of the control cells is located in the fractions of low density, corresponding to the location of 5'-AMPase, a marker enzyme of plasma membrane. When the cells are stimulated with the cytochalasin, the radioactivity is found in heavier fractions forming 2 peaks, a lighter peak corresponding to 5'-AMPase and a heavier one corresponding to the activated NADPH oxidase.

A scheme on the activation of the NADPH oxidase

Foregoing discussions may be summarized in a scheme presented in Fig. 11. A stimulant interacts with a receptor on the plasma membrane and the NADPH oxidase located on the membrane is activated by some mechanism. The activated NADPH oxidase reduces oxygen molecules to superoxide anions on the outer surface of the membrane and oxidizes NADPH at the cytosol-side of the membrane. At present, we are ignorant of the activation mechanism. We only know that several conditions influence the activation, for example calcium ions, lectins and deuterium oxide, can potentiate the induction and cyclic AMP is antagonistic. Involvement of microtubule system may be considered (Nakagawara and Minakami, 1979), but it can not be said with certainty.

Before discussing the possible involvement of calcium ions in the activation process, we will show the effect of concanavalin A because strong synergistic action of concanavalin A and cytochalasin E (D) can be used in a clinical laboratory test.

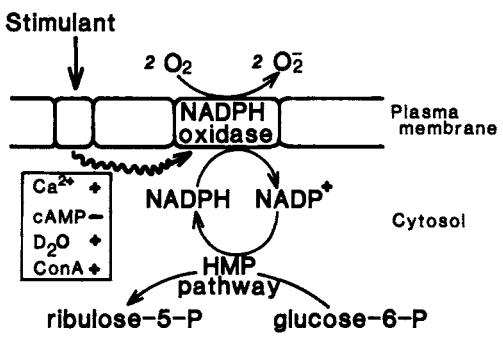

Fig. 11 A scheme of phagocytotic metabolic stimulation

Synergism of concanavalin A and the cytochalasin

Concanavalin A has been known to trigger the metabolic changes (Romeo et al., 1974) but it triggers the superoxide release of human blood leukocytes only weakly. It, however, stimulates the superoxide release of human

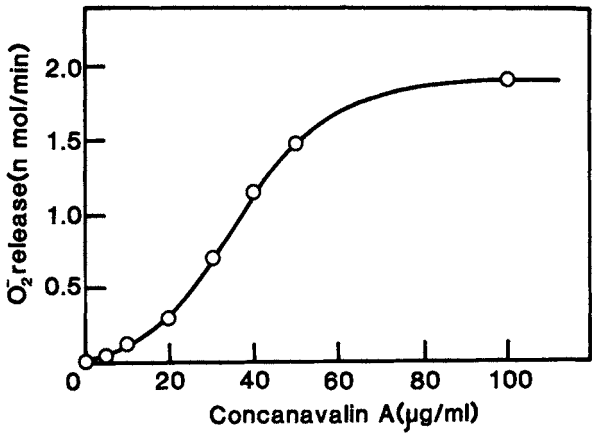

Fig. 12 Stimulation of the superoxide release by concanavalin A
Human polymorphonuclear leukocytes(2×10^5) were treated with concanavalin A(concentration given on the abscissa) and after 1 min cytochalasin E(5 μg/ml) was added. (Nakagawara and Minakami,1979)

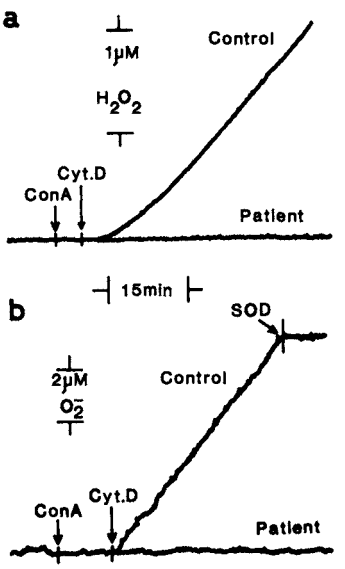

Fig. 13. Hydrogen peroxide and superoxide formation by human leukocytes
The assays were carried out essentially by similar methods as given in Fig. 1 and Fig. 2, but with 10 μl of human whole blood. The cells were treated with 100 μg concanavalin A(Con A) and 20 μg of cytochalasin D(Cyt D) after 5 min. (Takeshige et al.,1979)

cells if both concanavalin A and cytochalasin E are combined. Almot fifty-time acivation is obtained when the cells are treated with both, compared with either one (Fig. 12). This strong activating effect together with the methods of superoxide and hydrogen peroxide assays, can be used as clinical tests for the diagnosis of chronic granulomatous disease. As shown in Fig. 13, the formations of superoxide and hydrogen peroxide in control normal leukocytes can be measured with only 10 μl of whole blood without separating red cells, whereas the formations are negligible in patients.

Possible Role of Cytosol Calcium

Role of calcium in the activation of the oxygen metabolism has been discussed based on the observations that the enhancement of the oxygen uptake is induced by a calcium ionophore A23187 in the presence of calcium (Romeo et al.,1975) and the superoxide release induced by digitonin is inhibited by a calcium chelator EGTA(Cohen and Chovaniec,1978). These observations are mainly related to the influx of calcium through plasma membrane, but if we think of the role of calcium in analogy with other stimulus-secretion or stimulus-contraction coupling processes, we need to consider a possibility of an intracellular translocation of the ions between an intracellular pool and cytosol.

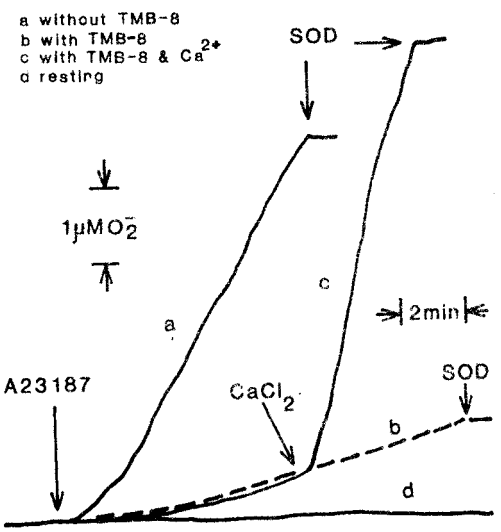

Fig. 14 Superoxide release induced with ionophore A23187
Guinea pig leukocytes(2 x 10^6) in calcium-free Tris-Ringer solution containing 2 mM glucose and 50 μM cytochrome c were incubated at 37°C with or without 100 μM 8-(N,N-diethylamino)-octyl-3,4,5-trimethoxybenzoate (TMB-8). The cells were stimulated with 5 μM A23187. The inhibition by TMB-8 was reversed by the addition of 1 mM $CaCl_2$ (Matsumoto et al.,1979)

Effect of TMB-8

A new intracellular calcium antagonist, 8-(N,N-diethylamino)-octyl-3,4,5-trimethoxybenzoate (TMB-8) has been used in the studies on muscles (Malagodi and Chiou,1974) and platelets (Charo et al.,1976). We used this reagent in our study on leukocytes.

The addition of a calcium ionophore A23187 to polymorphonuclear leukocytes induces the superoxide release even without calcium as shown in Fig. 14(curve a). The release is inhibited by TMB-8 as shown by curve b and is restored by the subsequent addition of calcium ions as shown by curve c. The effect of extracellular calcium concentration on the superoxide release induced by the calcium ionophore is different whether TMB-8 is present or absent. The superoxide release is essentially proportional to the calcium concentrations when the cells have been treated with TMB-8, whereas in the absence of TMB-8 the release is independent of calcium at low concentrations but it increased linearly at higher concentrations(Fig. 15).

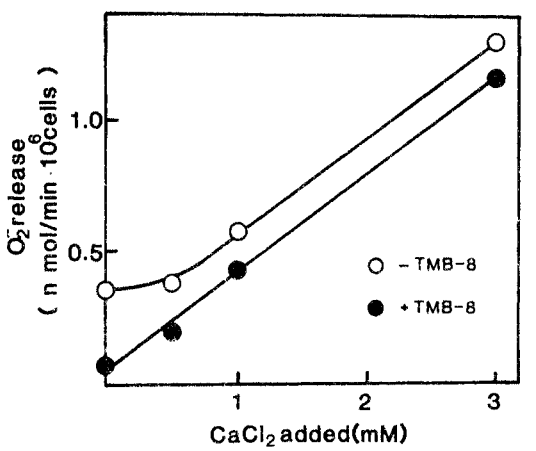

Fig. 15. The effect of calcium ions on the superoxide release
The conditions were the same as in Fig. 14. (Matsumoto et al.,1979)

Table VI Effect of TMB-8 on the superoxide release (Matsumoto et al.,1979)

		Activated with		
		E. coli (0.9 mg)	Cytochalasin D (10 μg)	A23187 (5 nmol)
Control		0.84	1.20	2.49
TMB-8	50 μM	0.49	0.40	2.49
	100 μM	0.42	0.13	1.06
	200 μM	0.14	0	0.51
	300 μM	0.04	0	0.07

The conditions were as in Fig. 14. The cells were stimulated at 5 min after preincubation with or without TMB-8.

This observation supports a proposal that TMB-8 inhibits the superoxide release by inhibiting the release of calcium from a storage pool.

The inhibition of superoxide release by TMB-8 is not limited to the release induced by the ionophore. As shown in Table VI, the release induced by the ingestion of bacteria or by cytochalasin D is similarly inhibited by TMB-8. This suggests the general role of intracellular calcium ions in the regulation of the oxidative metabolism. Inhibitors such as verapamil which has been used to inhibit the influx of extracellular calcium showed only weak inhibition of the superoxide release induced by cytochalasin D.

Fluorescence change of leukocytes loaded with chlortetracycline

If calcium ions are stored in a membrane compartment and released by the stimulation, we may be able to detect the change by using chlortetracycline. It is a very sensitive fluorescent probe which can monitor the mobilization of intracellular calcium from cellular hydrophobic environment. It is preferentially partitioned in membranes, gives stronger fluorescence with calcium than with magnesium, and the spectra of the both chelates are different. Chlortetracycline has been used as a probe to investigate intracellular events associated with the divalent cations and their interaction with membranes such as mitochondria and sarcoplasmic reticulum (Caswell and Hutchinson,1971).

As shown in Fig. 16, when polymorphonuclear leukocytes are loaded with chlortetracycline and stimulated with bacteria or with cytochalasin D, a rapid decrease of the fluorescence is observed. The excitation and emission spectra change, suggesting that the calcium ions in hydrophobic environment is displaced by magnesium ions. Dose-responses of the fluorescence change and the superoxide-release of the cells loaded with chlortetracycline are essentially parallel as shown in Fig. 17 which indicates that bothe reactions are closely related.

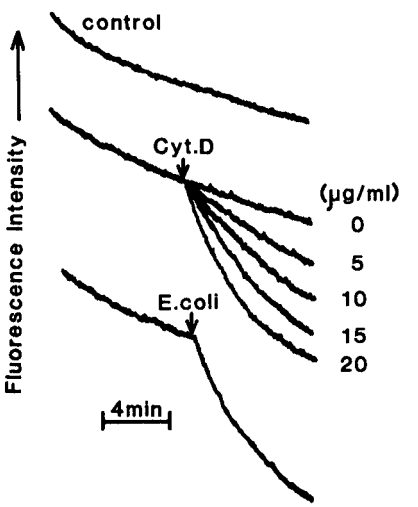

Fig. 16 Fluorescence change of CTC-loaded leukocytes
Guinea pig leukocytes(1×10^7) were incubated with chlortetracycline (CTC) for 30 min at 30°C and washed. The fluorescence change was monitored at 514 nm with the excitation wavelength of 401 nm. Cytochalasin D or E.coli were added at the points indicated by arrows. (Takeshige et al.1980)

Effect of TMB-8 on the fluorescence change

The relation can also be shown by the titration of the cells with TMB-8. As shown in Fig. 18, the intracellular calcium antagonist affects both fluorescence change and the superoxide release in parallel. This again suggests that the release of calcium ions from an intracellular hydrophobic pool to cytosol is an essential process in the oxidative metabolism of the stimulated cells. A concept that calcium functions as a link between stimuli and secretion in various cells has generally been accepted. The present observation may provide another evidence for the translocation of membrane calcium ions and its close association with the functions of the cells.

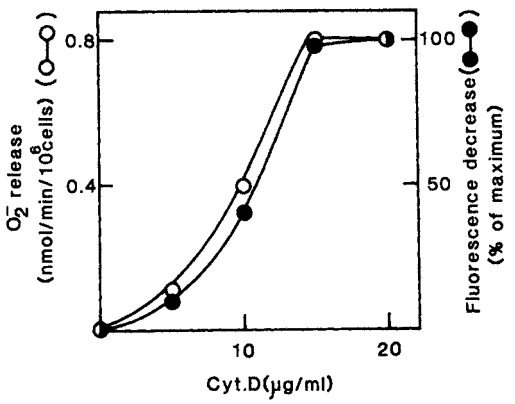

Fig. 17. Fluorescence change and superoxid release by cytochalasin D
The conditions were the same as in Fig. 16. The fluorescence change and the superoxide release(0.8 nmol/min per 10^6 cells) at 20 μg/ml cytochalasin D are set as 100 %. (Takeshige et al.,1980)

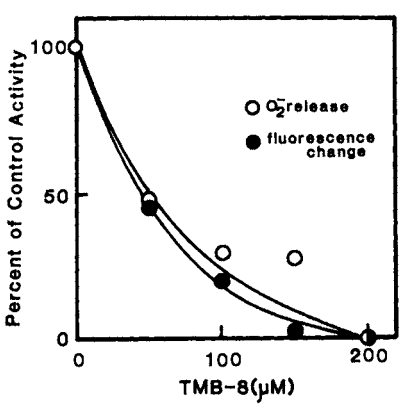

Fig. 18. Inhibition of the fluorescence change by TMB-8
The conditions were as in Fig. 17, except that the cells were stimulated with cytochalasin D at 5 min after treatment with various concentrations of TMB-8(given on the abscissa). (Takeshige et al.,1980)

Before finising, we would like to stress that many problems on phagocytosis are remaining unsolved. Two of them are of special importance. One is on the nature of the activation process, both at cellular and at enzyme level. The second is on the mechanism of killing, not only the killing of bacteria, but also the killing of tumor cells by macrophages. We expect that the coming decade is fruitful in solving these important problems.

REFERENCES

Agner,K.(1941): Verdoperoxidase. A ferment isolated from leukocytes. Acta Physiol.Scand. (Suppl.8), 2,1-62.

Agner,K.(1950):Studies on peroxidative detoxification of purified diphtheria toxin. J.Exp.Med. 92,337-347

Babior,B.M.,Kipnes,R.S. and Curnutte,J.T.(1973): Biological defense mechanism. The production by leukocytes of superoxide, a potential bactericidal agent. J.Clin;Invst.,52,741-744.

Baldridge,C.W. and Gerard,R.W.(1933): The extra respiration of phagocytosis. Amer.J.Physiol.,103,235-236.

Becker,H.,Munder,G. and Fischer,H.(1958): Ueber den Leukocytenstoffwechsel bei der Phagocytose. Hoppe-Seylers Z.physiol.Chem. 313,266-275

Berendes,H.,Bridges,R.A. and Good,R.A.(1957): A fatal granulomatosis of childhood. The clinical study of a new syndrome. Minn.Med. 40,309-312.

Cagan,R.H. and Karnovsky,M.L.(1964): Enzymic basis of the respiratory stimulation during phagocytosis. Nature(Lond.),204, 255-257.

Caswell,A.H. and Hutchinson,J.D.(1971): Visualization of membrane bound cations by a fluorescent technique. Biochem.Biophys.Res.Commun.42,43-49.

Charo,I.F.,Feinman,R.D. and Detwiler,T.C.(1976): Inhibition of platelet secretion by an antagonist of intracellular calcium. Biochem.Biophys.Res.Commun. 72,1462-1467.

Cohen,H.J. and Chovaniec,M.E.(1978): Superoxide production by digitonin-stimulated guinea pig granulocytes. The effects of N-ethylmaleimide, divalent cations, and glycolytic and mitochondrial inhibitors on the activation of the superoxide generating system. J.Clin.Invest. 61, 1088-1096.

Curnutte,J.T.,Kipnes,R.S. and Babior,B.M.(1975): Defect in pyridine nucleotide dependent superoxide production by a particulate fraction from the granulocytes of patients with chronic granulomatous disease. New Engl.J.Med.,293,628-632.

Fleischmann,W.(1927): Ueber Anoxybiose von Leucocyten. Biochem.Z.,184,385-389.

Graham,R.C.,Jr.,Karnovsky,M.J.,Shafer,A.W.,Glass,E.A. and Karnovsky,M.L. (1967): Metabolic and morphological observations on the effect of surface-active agents on leukocytes. J.Cell Biol.,32,629-647.

Iyer,G.Y.N.,Islam,D.M.F. and Quastel,J.H.(1961): Biochemical aspects of phagocytosis. Nature(Lond.) 192,535-541.

Iyer,G.Y.N. and Quastel,J.H.(1963): NADPH and NADH oxidation by guinea pig polymorphonuclear leukocytes. Canad.J.Biochem.,41,427-434.

Kakinuma,K.(1974): Effects of fatty acids on the oxidative metabolism of leukocytes. Biochim.Biophys.Acta, 348,76-85.

Kakinuma,K.,Hatae,T. and Minakami,S.(1976): Effect of ionic sites of surfactants on leukocyte metabolism. J.Biochem.(Tokyo) 79,795-802.

Klebanoff,S.J.(1967): A peroxidase-mediated anti-microbial system in leukocytes. J.Clin.Invest.46,1078.

Kojima,S.(1931): Studies on peroxidase. II. The effect of peroxidase on the bactericidal action of phenols. J.Biochem.(Tokyo) 14,95-109.

Malagodi,M.H. and Chiou,C.Y.(1974): Pharmacological evaluation of a new Ca^{2+} antagonist,8-(N,N-diethylamino)-octyl-3,4,5-trimethoxybenzoate hydrochloride(TMB-8):Studies in smooth muscles. Eur.J.Pharmacol.27,25-33.

Malawista,S.E.,Gee,J.B.L. and Bensch,K.G.(1971): Cytochalasin B reversibly inhibits phagocytosis: Functional,metabolic, and ultrastructual effects in human blood leukocytes and rabbit alveolar macrophages. Yale J.Biol.Med.,44,286-300.

Matsumoto,T.,Takeshige,K. and Minakami,S.(1979): Inhibition of phagocytotic metabolic changes of leukocytes by an intracellular calcium-antagonist 8-(N,N-diethylamino)-octyl-3,4,5-trimethoxybenzoate. Biochem.Biophys.Res. Commun.88,974-979.

McCord,J.M. and Fridovich,I.(1969): Superoxide dismutase. An enzyme function for erythrocuprein(hemocuprein). J.Biol.Chem. 244,6049-6055.

Minakami,S.,Nakagawara,A. and Nakamura,M.(1977):Generation and release of superoxide anions by leucocytes. In "Biochemical and Medical Aspects of Active Oxygen"(Hayaishi,O. and Asada,K.Eds.),pp.229-246, University of Tokyo Press.

Mudd,S.,McCutcheon,M. and Lucke,B.(1934): Phagocytosis. Physiol.Rev. 14,210-275.

Nabi,F.Z.,Takeshige,K.,Hatae,T. and Minakami,S.(1979): Hydrogen peroxide formation of polymorphonuclear leukocytes stimulated with cytochalasin D. Exp.Cell Res.,124,293-300.

Nakagawara,A.,Takeshige,K. and Minakami,S.(1974):Induction of phagocytosis-like metabolic pattern in polymorphonuclear leukocytes by cytochalasin E. Exp.Cell Res. 87,392-394.

Nakagawara,A. and Minakami,S.(1975): Generation of superoxide anions by leukocytes treated with cytochalasin E. Biochem.Biophys.Res.Commun.64, 760-767.

Nakagawara,A.,Shibata,R.,Takeshige,K. and Minakami,S.(1976): Action of cytochalasin E on polymorphonuclear leukocytes of guinea pig peritoneal exudates. Exp.Cell Res.,101,225-234.

Nakagawara,A. and Minakami,S.(1979): Role of cytoskeletal elements in cytochalasin E-induced superoxide production by human polymorphonuclear leukocytes. Biochim.Biophys.Acta,584,143-148.

Patriarca,P.,Zatti,M.,Cramer,R. and Rossi,F.(1970): Stimulation of the respiration of polymorphonuclear leukocytes by phospholipase C. Lefe Sci.,9, 841-849.

Patriarca,P.,Cramer,R.,Moncalvo,S.,Rossi,F. and Romeo,D.(1971): Enzymatic basis of metabolic stimulation in leukocytes during phagocytosis: The role of activated NADPH oxidase. Arch.Biochem.Biophys. 145,255-262.

Paul,B. and Sbarra,A.J.(1968): The role of the phagocyte in host-parasite interactions. XIII. The direct quantitative estimation of H_2O_2 in phagocytizing cells. Biochim.Biophys.Acta,156,168-178.

Roberts,M.M. and Quastel,J.H.(1964): Oxidation of reduced triphosphopyridine nucleotide by guinea pig polymorphonuclear leukocytes. Nature(Lond.) 202,85-86.

Romeo,D.,Jug,M.Zabucchi,G. and Rossi,F.(1974): Perturbation of leukocyte metabolism by nonphagocytosable concanavalin A-coated beads. FEBS Lett.,42,90-93.

Romeo,D.,Zabucchi,G.,Niani,N. and Rossi,F.(1975): Ion movement across leukocytes plasma membrane and excitation of their metabolism. Nature(Lond.) 253,542-544.

Root,R.K. and Metcalf,J.(1977):H_2O_2 release from human granulocytes during phagocytosis. Relationship to superoxide anion formation and cellular catabolism of H_2O_2: Studies with normal and cytochalasin B-treated cells. J.Clin.Invest.,60,1266-1279.

Rossi,F. and Zatti,M.(1964): Biochemical aspects of phagocytosis in polymorphonuclear leukocytes. NADH and NADPH oxidation by the granules of resting and phagocytizing cells. Experientia,20,21-23.

Rossi,F.,Zatti,M.,Patriarca,P. and Cramer,R.(1970): Stimulation of the respiration of polymorphonuclear leukocytes by anti-leukocytes antibodies. Experientia, 26, 491-492.
Sbarra,AJ. and Karnovsky,M.L.(1959): The biochemical basis of phagocytosis. I.Metabolic changes during the ingestion of particles by polymorphonuclear leukocytes. J.Biol.Chem. 234, 1355-1362.
Stähelin,H.,Suter,E. and Karnovsky,M.L.(1956): Studies on the interaction between phagocytes and tubercle bacilli. I. Observations on the metabolism of guinea pig l. Observations on the metabolism of guinea pig leukocytes and the influence of phagocytosis. J.Exp.Med.,104,121-136.
Takeshige,K.,Matsumoto,T.,Shibata,R. and Minakami,S.:Simple and rapid method for the diagnosis of chronic granulomatous disease, measuring hydrogen peroxide and superoxide anions released from leukocytes in whole blood. Clin.Chim.Acta,92,329-335.
Takeshige,K.,Nabi,Z.F.,Tatscheck,B. and Minakami,S.(1980): Release of calcium from membranes and its relation to phagocytotic metabolic changes: A fluorescence study on leukocytes loaded with chlortetracycline. Biochem.Biophys.Res.Commun. in press.
Zatti,M. and Rossi,F.(1967): Relationship between glycolysis and respiration in surfactant-treated leukocytes. Biochim.Biophys.Acta,148,553-555.
Zatti,M.,Rossi,F. and Patriarca,P.(1968): The H_2O_2-production by polymorphonuclear leukocytes during phagocytosis. Experientia, 24,669-670.
Zigmond,S.H. and Hirsch,J.G.(1972): Cytochalasin B: Inhibition of D-2-deoxyglucose transport into leukocytes and fibroblast. Science,176,1432-1434.

Adv. Physiol. Sci. Vol. 3. Physiology of Non-excitable Cells
J. Salánki (ed.)

PHYSIOLOGY OF GLIAL CELLS

George G. Somjen
Department of Physiology, Duke University, Durham, North Carolina 27710, USA

Ideas concerning the possible functions of glial cells used to be as numerous as the investigators working with this, the "other" tissue of the central nervous system (CNS). The main morphological types of glia are credited with different functions, but the correlation of form with function may not always be absolute. Thus microglia are thought to be the principal phagocytes of the CNS, but astrocytes are also believed to be capable of phagocytosis, if appropriately provoked. Scaffolding formed by radial glia is said to guide the growth of neural processes during embryonal development of the CNS; Schwann cells fulfill a similar role in the regeneration of injured peripheral axons. Myelination is the exclusive task of oligocytes in the CNS, and of Schwann cells in the periphery. Schwann cells embrace C-fibers in a single unit-layer of sheathing, and tether them by a mesaxon. This wrapping may provide electrical insulation, and prevent cross-talk between fibers. Many think that satellite cells in ganglia, and glia in contact with neural elements in gray matter, may render metabolic service to their associated neurons, but for this suggestion, as for many others, a solid experimental foundation is as yet lacking.

Astrocytes are the least well understood of the main classes of glial cells and, perhaps for this reason, they have been the subject of the most speculation. A long list could be compiled of the functions of which they have been suspected. The most important of these have been discussed in some detail in a recent report (Varon & Somjen, 1979). I will repeat here only the highlights, with emphasis on more recent additions to our understanding of astrocytic function. The final part of this short review will concern the evidence linking astrocytes to the regulation of the composition of interstitial fluid of the central nervous system, especially of the level of inorganic ions.

Suspected functions of astrocytes.

(1) The idea that glia is the connective tissue of the central nervous system originated with Virchow (1858), who gave glia its name. He began his investigation out of the conviction that all organs need mesenchyma as well as parenchyma, and that brain could be no exception. That astrocytes (and also oligocytes) originate from ectoderm, not from mesoderm, has, of course, been established already in the latter part of the nineteenth century. More recently Wolff (1965) expressed doubt that glia would possess the resilience or the rigidity required to give

shape to the brain. Grossman remarked, however, (page 15 in Varon & Somjen, 1979) on the resistance to penetration with glass microelectrodes offered by glial scar tissue, which attests of a mechanical strength superior to that of un-scarred cortex of which glia forms a smaller component. Palay raised the further point (page 15 in Varon & Somjen, 1979) that live brain is soft, though coherent, and glia needs to provide only adhesion and not a skeletal frame in order to deserve credit as the Nervenkitt (nerve-cement) of Virchow (1858).

(2) Ramón y Cajal appears to have been the first to suggest that astrocytes fill the spaces vacated by dying neurons. That this is so, has since been accepted as a basic fact of neuropathology.

(3) Like roots of a tree, so Golgi (1903) thought, dendrites nourish neurons. Since astrocytes appeared to him as consisting of nothing but dendrite-like processes, he naturally attributed to them the supply of nutrients to neurons. Biochemical symbiosis of neurons and glial cells, if not the supply of metabolic substrates to the former by the latter, remains a concept attractive to many. Thus, for example, Hydén and collaborators (Hydén & Egyházi, 1963; Lange, 1973; also Pevzner, 1978) found indications of a reciprocal interaction between neuronal and glial cells in nucleic acid metabolism. Chan-Palay and Palay (1979) demonstrated the predominant presence of cyclic GMP in glial cells, and point to the potential significance of its modulation with neuronal activity. A growing body of data suggests that glutamine, generated in glia, is being supplied to presynaptic terminals, which then convert it to glutamate which, in turn, after having been released in the course of synaptic transmission, is taken up again by glia, for reconversion to glutamine (Martinez-Hernandez, 1977; Quastel, 1978; Hamberger et al., 1978; 1979 a and b).

(4) Glial endfeet surrounding capillary walls suggested the formation of a physical barrier at the interface between blood and brain. These glial envelopes have, however, been shown to be too leaky to be an effective hindrance to diffusion. Seams of tight junctions between endothelial cells of the capillary wall are now believed to form the barrier (e.g. Maynard et al., 1957; Lasansky, 1971). That nothing stands between cerebral interstitium and blood plasma but a layer of endothelium, was at first difficult to reconcile with the results of balance studies and clearance rates which seemed to indicate that ions are actively transported between brain and blood. Exchange by way of cerebrospinal fluid could not account for this transport (Cserr, 1965; Bito, 1969; Bradbury et al., 1972). Cerebral capillary endothelium became a more plausible site of such transport since the abundant presence of mitochondria (Oldendorf et al., 1977) and of Na^+,K^+ activated ATPase (Eisenberg & Sudith, 1979) in these cells has come to light. Additional new light on capillary function was shed by the demonstration of the variable permeability to water of brain capillaries (Raichle et al., 1975), its regulation by catecholamines and peptides, and the newly discovered nerve supply of cerebral capillaries (for review and references see: Raichle, in press).

(5) Granted that glial endfeet ensheath capillaries in part only, the fact remains that glial processes are usually interposed between neurons and blood vessels. That glia rather than neurons have first chance

at sampling what has come from the blood plasma into the interstitium of the central nervous system, strongly suggests that glia has some role in the regulation or in the processing of the transported material. The incorporation into carbonic acid of the CO_2 which has traversed the capillary wall, as well as that produced locally by cellular respiration, may be a case in point, for carbonic anhydrase has been reported to be the sole property of glial cells in the CNS (Giacobini, 1962). It may or may not be significant in this context that carbonic anhydrase activity is apparently influenced by catecholamines (Church et al., 1980). A complex role has also been suggested for the hydration of CO_2, and perhaps to an associated "chloride shift" across the cell membrane, in pathologic movements of water and cell swelling and in cerebral oedema (Kimelberg, 1979). Carbonic anhydrase has also an evident key role in the regulation of tissue pH. Beyond that, insofar as the interstitial pH of the brain stem governs the rate of alveolar ventilation (Pappenheimer, 1967), and tissue pH in its turn is determined by the rate of entry of CO_2 and of its conversion into carbonic acid, glial carbonic anhydrase may be important in the regulation of respiration as well.

(6) Lugaro (1907) was probably the first to suggest that neuroglia may remove and detoxify the end products of neuronal metabolism. The predominant presence of glutamine synthetase in glial cells has recently been demonstrated by immunohistochemical methods by Martinez-Hernandez et al., (1977), who point to its importance in rendering harmless the ammonia produced by protein catabolism.

(7) DeRobertis (1965) and Peters and Palay (1965) have called attention to the perisynaptic dams made of glia which separate presynaptic terminals spaced closely on the surface of neurons. Glia also forms the capsules around synaptic glomeruli, wherever they occur. These wrappings may prevent the spread of synaptic transmitters outside their target area.

(8) Closely related to the idea of a physical barrier to the diffusion of transmitter substances is the suggestion that glial cells accumulate, and dispose of, the endproducts of synaptic action. At a time when chemical transmission was only a vaguely perceived possibility, Lugaro's (1907) attention was caught by the ubiquitous presence of glial processes near "neuronal articulations", and he inferred that these may serve the breakdown of chemical substances by means of which one neuron may excite another. This idea was revived after the demonstration that satellite cells in insect nervous systems take up glutamate with greater avidity than the neurons which are believed to utilize it as a transmitter (Faeder & Salpeter, 1970); and that glial cells of vertebrates as well as invertebrates possess a high-affinity uptake system for gamma-amino butyric acid (GABA) (Orkand & Kravitz, 1971; Iversen and Kelly, 1975).

(9) Glial cells are equipped to accumulate, and in fact have been observed to contain GABA even in parts of the nervous system where GABA-ergic synapses are not found (Kelly & Dick, 1978). Mammalian neurons generally are sensitive to GABA, which has been shown to increase the permeability to chloride of the neuronal membrane, regardless whether the cell is the target of GABA-ergic innervation or not (Krnjevic, 1976; Curtis, 1978). When depolarized by an excess of external potassium, or subjected to pulsed electric current, glial cells can be made to give up their content of GABA (Minchin and Nordmann, 1975; Bowery et al., 1979).

Similarly the Schwann cells which displace degenerating nerve ending at denervated nerve-muscle junctions can be made to release acetylcholine by like means (Dennis and Miledi, 1974). From these observations it would be tempting to conclude that glial cells could regulate the excitability of neurons by releasing GABA and other neuro-active substances at a rate dictated by the glial membrane potential, were it not that in order to achieve such release the concentration of K^+ in interstitial fluid must be raised to levels presumably never occurring in healthy tissue. Furthermore, the currents required to induce Schwann or glial cells to give up their content, are of a magnitude likely to cause injury to cell membranes (Dennis & Miledi, 1974; Bowery et al., 1979). Still, glia could yet turn out to influence neuronal function, if but a physiological stimulus other than external potassium would be discovered for its release. Besides GABA, glial cells and other satellite cells have been shown to accumulate or synthesize a number of other neuro-active substances, such as acetylcholine, 5-hydroxytryptamine, catecholamines, and certain other amino acids (e.g. Haber et al., 1978; Villegas, 1978; Hösli & Hösli, 1980). If any or several of these could be shown to be released in a controlled manner and influence the neurons in the vicinity of the glial cell, this would justify Nageotte (1910) who had called glia an organ of internal secretion. Hints at the possibility of such a regulatory mechanism are contained in an experiment by Schrier & Thompson (1974). Interpretation of all available data remains uncertain, however, because many of the substances discussed, such as glutamate and GABA, are also involved in biochemical reactions not related to membrane function.

But even if the neuro-active substances stored in glial cells would have no part in the normal functioning of nervous tissue, the discovery that they are released when external potassium activity ($[K^+]_o$) rises above 15 or 20mM is important. In the state known as spreading cortical depression, which by no means is limited to neocortical tissue (Bureš et al., 1974), $[K^+]_o$ does rise to the high levels (Vyskočil et al., 1972) at which glial cells appear to spill their content of amino acids and biogenic amines. Thus, in this case, they inevitably do affect neuronal membranes.

(10) From time to time the thought was expressed that glial tissue may have functions more important than the support and protection of neurons; that perhaps glial cells may be key elements in the processing and storage of information. Observations and reasoning which led to this conclusion have been multiform. For the time being, they remain controversial. In this space they cannot be outlined, not even in summary form (but see: Galambos, 1961; Hydén & Egyházy, 1963; Hertz, 1965; Schrier on page 144-145 of Varon & Somjen, 1979).

In summary the most influential of the various suggestions concerning the possible role of astrocytic tissue in the CNS have revolved around two groups of topics: neurochemical interaction with neurons, and the regulation of the composition of the interstitial fluid of the CNS. The latter topic, especially the regulation of the activity of potassium ions, will occupy the second half of this review.

Neuroglia and sustained potential (SP) shifts.

In the 1960's Kuffler and his collaborators (Kuffler et al., 1966; Orkand et al., 1966; Kuffler & Nicholls, 1966; Kuffler, 1967) reported

four important observations. First, that glial cells sustain a resting membrane potential, usually of higher voltage than the neurons in the same tissue. Second, that concommittant to the activation of neurons, glial cells can undergo slow depolarization of a very characteristic timecourse. Third, that their membrane potential is a logarithmic function of the ratio of internal and external potassium activities, the slope of which is accurately predicted by the Nernst equation. Fourth, that glial cells are coupled one to another by electrically patent junctions.

About the same time as these studies were published, Goldring and collaborators (Sugaya et al., 1964; Karahashi & Goldring, 1966) found that cells in the mammalian central nervous system presumed to be glia were depolarized when neurons in their vicinity were activated. That the cells showing such behavior were indeed glia, was subsequently demonstrated by the intracellular deposition of marker dies (Kelly et al., 1967; Grossman & Hampton, 1968; Sugaya et al., 1971), and in the most recent and technically best of such studies it was shown that they are astrocytes (Takato & Goldring, 1979). This does not necessarily mean that oligocytes and ependymal cells have different membrane properties, only that the exploring microelectrode is more likely to penetrate astrocytes than the other types of glia.

When two microelectrodes are used, one in an intracellular position the other in the immediate vicinity of the cell, it becomes clear that depolarization of glial cells is mirrored by a sustained negative shift of extracellular potential, which is as it were its inverted and slightly distorted replica (Fig. 1). By waveform and duration sustained potential (SP) shifts are readily distinguished from other extracellular potential variations, such as nerve impulses and focal synaptic potentials. Detailed investigations in the cerebral cortex (Karahashi & Goldring, 1966; Castellucci & Goldring, 1970; Sugaya et al., 1971) and spinal cord (Somjen, 1969; 1970) have led to the conclusion that SP shifts are generated in large part by the depolarization of glial cells (reviewed by Somjen, 1973; 1975). The argument rests on the precise correlation of the amplitude of glial depolarization and extracellular SP shifts (Fig.2); while neither the magnitude nor the waveform of neuronal membrane responses shows such correlation. Nor is there a consistent relationship between neuronal firing rates and SP shifts; or between the profiles of the distribution within the tissue of bona fide neuronally generated extracellular potentials (such as focally recorded EPSPs) and SP shifts. If one samples the responses of many glial cells to repeated standardized stimulus trains, by recording the potential of each and every one encountered during exploratory penetration by a microelectrode, and also the extracellular SP shift concurrently recorded in their immediate vicinity, mapping these two sets of measurements yields profiles which are, roughly, mirror images of one another (Fig. 3). Finally, when neuronal activity is depressed by a drug, the depolarizations of glial cells and the associated SP shifts are depressed also, but the ratio between the two is essentially unaltered (Fig. 4).

While these data seem to show convincingly that under the conditions specified in these experiments glial cells make the major contribution to extracellular SP shifts, the electrical activity of neurons must presumably also influence any recording of extracellular potential in the CNS. This may explain why SP shifts are not exact mirror images of glial depolarization (see e.g. Fig. 14 in Somjen 1970; also: Speckmann et al., 1972; Heinemann et al.,1979). The relative magnitudes of neuronal and glial contributions to SP shifts may vary widely with the conditions

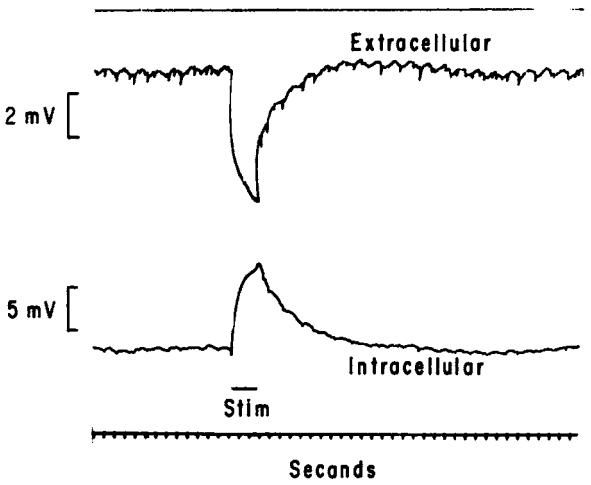

Fig. 1. Potentials in the spinal cord of a cat, simultaneously recorded from within a glial cell and from its vicinity with two micropipette electrodes the tips of which were separated by 40 μm. At the mark a large mixed function peripheral afferent nerve was stimulated repeatedly at a frequency of 300 pulses per sec. Upward excursion of the pens signals positive shift of potential. (From: Somjen, 1973, by permission of the Publisher).

under which they are generated, and must be determined separately for each newly encountered experimental situation.

From the comparable behavior of the glial cells of mammals and of poikilotherms during neuronal activation, and the demonstrated sensitivity of the latter to changing levels of $[K^+]_o$, it seemed probable that the depolarizing shifts of glial cells in mammalian nervous systems also are brought about by rising $[K^+]_o$. The influence of $[K^+]_o$ on the membrane potential of mammalian glial cells was soon also demonstrated experimentally, but the responses of membrane potential to changing $[K^+]_o$ seemed less than expected from the Nernst equation (Dennis & Gerschenfeld, 1965; Pape and Katzman, 1972; Ransom and Goldring, 1973; Adams and Brown, 1979). Such a deviation from the predicted value could have two reasons: (1) the membrane may be significantly permeable to ions other than potassium (as is indeed the case for nerve and muscle membranes); or (2) the distribution of potassium over the glial surface could be uneven, and the intracellular electrode could record an average of more and of less depolarized regions. Glial cells are supposed to be joined by electrically patent junctions, (see earlier in this text) and, therefore, neighboring cells might influence each other's membrane potential if, and only if, the electrotonic "space constant" of the network is longer than the variations

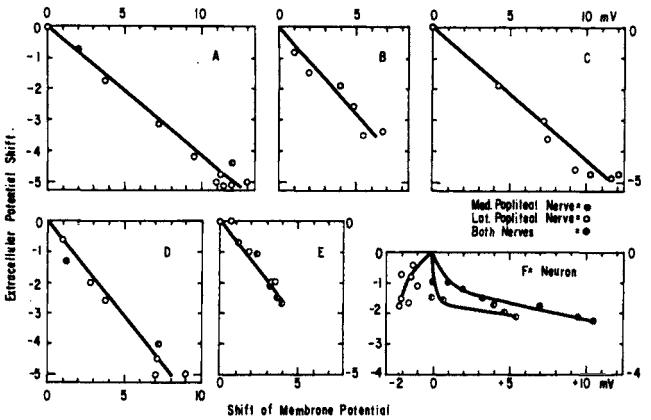

Fig. 2. Correlation between the amplitude of the responses of the membrane potential of five glial cells (A-E) and the extracellular SP shift recorded simultaneously, as in Fig. 1; and the lack of similar correlation in the case of one neuron (F). Symbols defined in inset indicate the identity of the peripheral nerve, which was stimulated by trains of electric pulses of varying intensity and frequency to evoke responses of varying magnitude. (From: Somjen, 1970, by permission).

in the distribution of $[K^+]_o$.

In other investigations where $[K^+]_o$, extracellular SP shifts, and glial membrane potential were concurrently observed, (Fig. 5), mammalian glial cells appeared, however, to obey Nernst's law quite faithfully (Fig. 6; also Lothman & Somjen, 1975; Futamachi & Pedley, 1976). Deviations were found only during very brief but intense bursts of neuronal activity such as occur during interictal epileptiform discharges (Futamachi & Pedley, 1976); in these cases the distribution of $[K^+]_o$ over the glial surface may indeed have been so unequal that condition (2), explained in the preceding paragraph, may have been applicable. During sustained neuronal activity, when $[K^+]_o$ could distribute itself more evenly, the glial membrane potential seemed to be entirely governed by the transmembrane distribution of $[K^+]_i$ / $[K^+]_o$, and thus the contribution of other ions appears negligible. Sugaya et al.,(1979) confirmed this in measurements on glial cells cultured in vitro.

We thus have two divergent opinions concerning the dependence of glial membrane potential on $[K^+]_o$, and should attempt to reconcile them. One possible source of error is introduced when $[K^+]_o$ is not measured, but is estimated from the composition of a solution to which the surface of

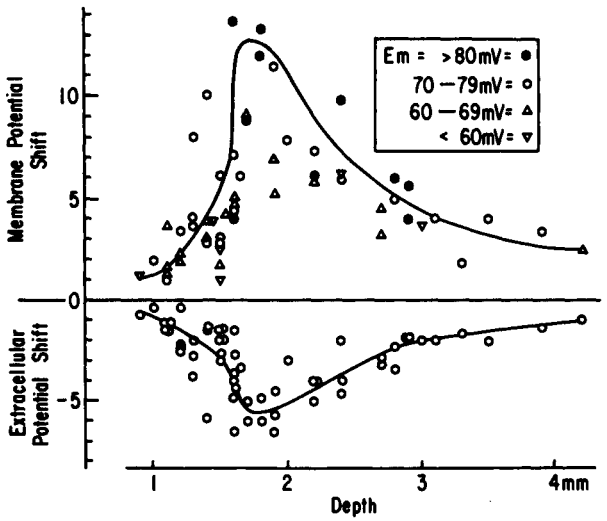

Fig. 3. Amplitude of glial responses (upper graph) and of SP shifts (lower graph) recorded, as in Fig. 1, from many locations in several spinal cords, by essentially identical standardized pulse trains. Abscissa indicates distance from the dorsal surface of the spinal cord; the electrode trajectory was similar in all experiments. Symbols defined in inset indicate "resting" membrane potential of glial cells; note that cells with low membrane potentials generate smaller responses. Note, also, that line of upper graph has been drawn with bias favoring high resting membrane potential cells, but that the responses of the others follow the same trend. (From: Somjen, 1970, by permission).

the preparation is exposed. Fisher et al., (1976) reported that $[K^+]_o$ declined along a steep gradient during prolonged superfusion of the cortical surface with a solution containing high $[K^+]$. Therefore, in the experiments of Pape & Katzman (1972) and of Ransom & Goldring (1973) the level of $[K^+]_o$ may have been overestimated. In slices of hippocampal tissue, about 200 μm from the washed surface, we (Dingledine & Somjen, unpublished) have found that, after a sudden change of either $[K^+]$ or of $[Ca^{2+}]$ in the continuously flowing bathing solution, it takes an average of 9 minutes to reach half the intended change in the tissue, and 20 to 40 minutes until there is no detectable difference between the readings of two ion-selective electrodes, one in the slice, the other in the bath. Recordings published by Adams and Brown (1979) suggest that the membrane potential of their glial cells had not reached a steady state at the time it was measured; thus presumably $[K^+]_o$ had not reached its final value,

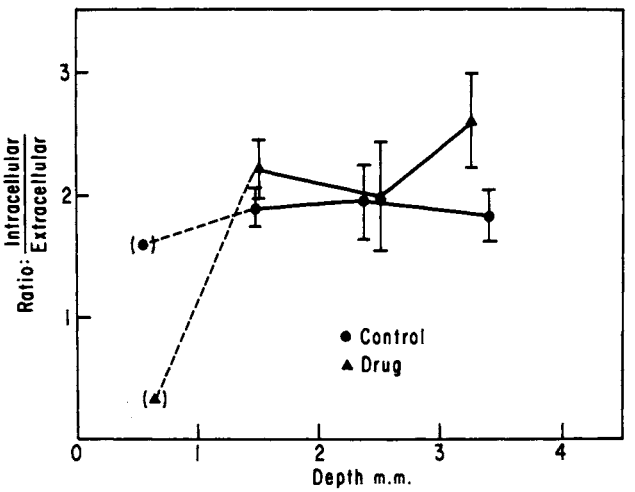

Fig. 4. Ratio of the amplitudes of the membrane voltage responses of glial cells and of the extracellular SP shifts. Data collected as in Fig. 3, but from a different group of cats, before and after the i.v. injection of either pentobarbital (30 to 60 mg/kg body wt), or thiopental (25 to 50 mg/kg) or diphenylhydantoin (20 to 40 mg/kg). Abscissal position of points indicates mean depth in tissue. Vertical bars show standard error. Number of observations, n:6, 36,36 and 16 for the four groups of control observations (points on graph from left to right), and 2, 36, 40, 14, for drug-treated group. The two sets of measurements are statistically not different. (From: Strittmatter and Somjen, 1973, by permission).

and it had been overestimated for the purpose of their calculations. Besides the possibility of exaggerating changes of $[K^+]_o$, the glial membrane potential response may be underestimated if only the intracellular potential is recorded relative to a distant "indifferent" potential, and possible shifts of extracellular potential are ignored. Extracellular SP shifts do occur during deposition of K^+ from an extraneous source in cortex (Heinemann et al., 1978; Gardner-Medwin et al., 1979) and presumably under all experimental conditions in which a gradient of $[K^+]_o$ is established in the tissue. Finally, it is also possible that under relatively hypoxic conditions of tissue kept in vitro, glial cells become more than usually leaky to ions other than K^+.

Discussion of the glial membrane potential would also require knowledge of the intracellular activity of K (K^+_i). This has not yet been

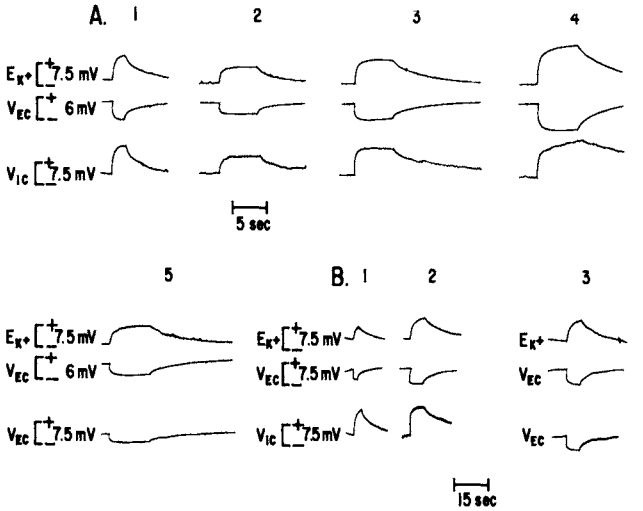

Fig. 5. Simultaneous recordings of extracellular potassium potential (E_K; recorded with ion-selective microelectrode), extracellular electric potential (V_{EC}), and intracellular potential of a glial cell (V_{IC}) in the spinal cord of a cat. E_K and V_{EC} recorded from the two channels of a double-barreled micropipette; V_{IC} from a separate electrode about 50 µm distant. Note that A, 5, and B , 3, are control recordings for which the previously intracellular electrode was withdrawn into an extracellular position, so that the two voltage channels (middle and lower tracings) recorded essentially identical responses. A and B are from two different glial cells. All recordings are referred to "ground" potential.

directly measured, except in the retina of insects (Coles and Tsacopoulos, 1979). The average $[K^+]_i$ estimated by Brown & Scholfield (1974) for the rat's superior cervical ganglion for all tissue elements, including glia and neurons, exceeded 200 mM. Adams & Brown (1979) consider this estimate to be confirmed for glial cells in their measurements of membrane potential as a function of $[K^+]_o$, which when extrapolated toward zero yields an abscissal intercept over 200 mM. These data would indicate hypertonicity of the intracellular fluid. Even the lower estimate of $[K^+]_i$ of Woodward et al., (1969) and those compiled in table 6.2 of Katzman & Pappius(1973), if added to $[Na^+]_i$, yield a hypertonic total. If true, this would force a revival of the notion of an active membrane transport of water, abandoned since the appearance of the well-known review by Robinson in 1960. Extrapolating the membrane potential measurements of Sugaya et al., (1979) to zero leads however to an estimate

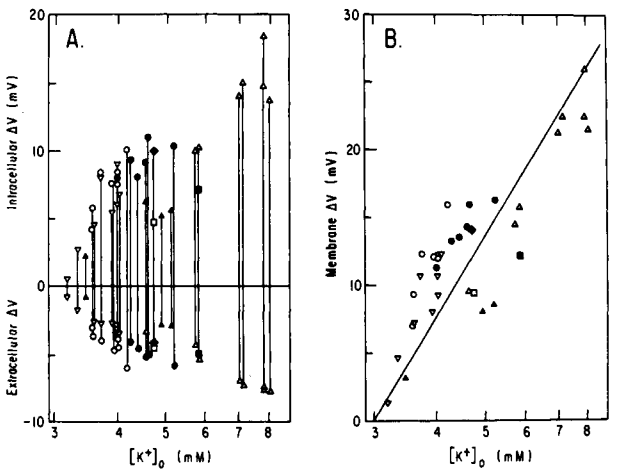

Fig. 6. A: Amplitude of responses such as those illustrated in Fig. 5, plotted to show the dependence of both intra- and extracellular potential shifts on the logarithm of the extracellular potassium activity ($[K^+]_o$). To calculate the change of membrane potential, extracellular and intracellular voltage responses must be summed; the graph of part (B) shows the result. The straight line drawn in B shows the Nernst function (at 37.5°C).

of $[K^+]_i$ of between only 90 and 110mM; and considerations of the previous paragraph make this the more plausible value. If the chemically and the electrically derived estimates of intracellular cation concentration disagree, then part of the intracellular potassium must either be bound or sequestered, and is neither ionically nor osmotically active.

Neuroglia and the passive movements of potassium ions in tissue.

In his review of 1967, Kuffler had suggested that a network of glial cells could function as a conveyor of K^+ ions through CNS tissue. This theory later became consolidated under the phrase "spatial buffering of potassium" (Trachtenberg & Pollen, 1970). It is based on the twin notions, that the membrane of glial cells is selectively permeable to K^+ ions, and that glial cells are joined so that ions can freely pass from one to another. Fig. 7 illustrates the way in which it is supposed to work. Neurons discharge K^+ ions into interstitial fluid in the course of generating impulses and synaptic potentials. The excess K^+ causes depolarization of glial cells lying amongst the active group of neurons, thus creating a gradient of potential. The potential gradient drives a current of ions, the current is carried by K^+ inward at the active focus and outward

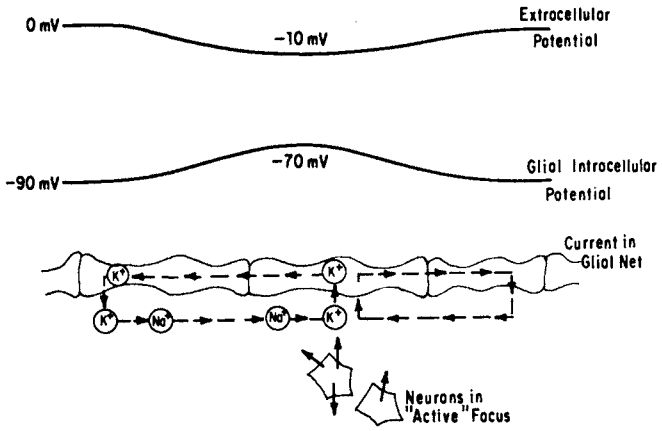

Fig. 7. Schematic representation of the transport of K^+ by electric current through a hypothetical network of glial cells. The numerical values of the voltages assigned to the potential profiles were arbitrarily chosen.

into the inactive surround, through the glial membrane, and K^+ is also the charge carrier within the glial net. The return current is, however, carried mainly by Na^+ in the interstitial fluid. The net effect is a redistribution of K^+ from regions of high toward regions of low activity.

Numerous observations agree well with this theory. Voltage profiles mapped in spinal tissue are not unlike the potential gradients expected on theoretical grounds (compare Fig. 3 and Fig. 7). Voltage gradients occur whether K^+ was released from neurons, or $[K^+]_o$ was raised by the experimenter (Heinemann et al,1978; Gardner-Medwin et al., 1979). Potassium activity does indeed rise during neuronal activation (Vyklicky et al. 1972; Krnjević & Morris, 1972; Prince et al., 1973). There is a consistent three-way correspondence between the magnitudes and the spatial profiles of the responses of $[K^+]_o$, glial depolarization, and extracellular SP shift (Somjen, 1970; Lothman & Somjen, 1975; Cordingley & Somjen, 1978). The plasma membrane of glial cells is highly selective for K^+ ions in the mammalian CNS (see earlier & Fig. 6) as also in cold-blooded animals. And finally, in a recent series of experiments by Gardner-Medwin (1977; in press) it was shown that when current is driven by an artificially imposed voltage gradient through cortical tissue, the share of the charge carried by potassium ions is greater than could be expected if all the current flowed through the interstitial spaces. Such a disproportionate displacement of K^+ is however expected, if much of the current has passed

through those cell membranes which selectively allow the passage of K^+ ions.

The one point of uncertainty in the theory of glial transport of K^+ concerns the occurrence of electrotonic junctions between the glial cells of the mammalian CNS. Their existence has been shown in some invertebrate and amphibian nervous tissues (Kuffler & Nicholls, 1966),and also in mammalian glial cells grown in culture(Moonen & Nelson, 1978). Gap junctions between glial processes have been noted in electron micrographs from intact mammalian CNS (Brightman et al., 1978) but the frequency with which they occur has not been established, nor their patency explored by electrophysiological means. The matter is further complicated by the consideration that, in lieu of electrotonic coupling between glial cells, transport of K^+ could also be achieved by individual cellular elements, provided that their processes spanned long enough distances. This condition is clearly met by the Müller cells of the retina (cf. Karwoski & Proenza, 1977; 1980; Newman, 1980) and by the Bergman fibers of the cerebellar cortex. The architecture of the astrocytic processes in the gray matter of other parts of the CNS has however not been worked out yet in sufficient detail.

Granted that glial transport of K^+ can and does occur, the next question concerns its magnitude compared to all the other modes of dissipating an excess of $[K^+]_o$. When neurons lose K^+, they usually exchange it for an equivalent amount of Na^+. This certainly is so when the K^+ exited with impulse discharge and probably also with synaptic current. The rise of $[Na^+]_i$ will stimulate Na^+, K^+-ATPase of the neuronal cell membrane (Skou, 1975). Consequently, neurons will tend to rapidly recapture most of the K^+ they had lost. Since however a gradient of K^+ demonstrably can exist, some will inevitably be dispersed. Loss to the blood stream may be minimal, if the capillary endothelium is as impermeable to the passage of ions from brain to blood, as from blood to brain (References in Somjen, 1979). Active transport of K^+ from cerebral interstitium into the circulation has, however, been inferred (Cserr, 1965; Bito, 1969; Bradbury et al., 1972; Betz et al., 1980).

Diffusion through the interstitial spaces is too slow a process to account for the dislocation of substantial amounts of K^+, at least when many neurons simultaneously release K^+ throughout a sizeable volume of gray matter. (For calculations and reasoning see Vern et al., 1977; Cordingley & Somjen, 1978). Dispersion by diffusion may account for a larger fraction of the released K^+ when only scattered neurons are sporadically active, so that they can be considered to be point-sources rather than volume-sources of excess ion (Krnjević & Morris, 1975; Lux & Neher, 1973). In this case however the quantity of K^+ spilled into the interstitial fluid would be small, and the recovery process would present no stress on the system.

While diffusion over appreciable distances takes time, transport by electric current is practically instantaneous. As indicated by the scheme of Fig. 7, as soon as K^+ enters through the membrane of the glial net at one point, an equivalent amount exits where the current leaves the net. In this case the limit is set by the electric resistance. The maximum quantity of ion conceivably carried by this mechanism can be calculated from the voltage gradient, and the tissue resistance. Such a calculation indicates that under intense afferent stimulation in the spinal cord, but less so in cortex, the current flowing through cellular processes may carry a significant minority of the K^+ ions spilled into the extracellular space (Somjen, in press; Gardner-Medwin, in press).

Whenever K^+ has been dispersed throughout the tissue, no matter by which mechanism, a deficit of $[K^+]_o$ must occur, once neurons have recovered their intracellular content of ${}^oK^+$. The deficit manifests itself as an

"undershooting" of $[K^+]_o$ below its "resting" baseline level (Heinemann & Lux, 1975; Krnjević & Morris, 1975; Lothman & Somjen, 1975). The magnitude of post-activation undershooting of $[K^+]_o$ is variable and unpredictable, thus dispersal of K^+ in tissue presumably is also variable. The drop of $[K^+]_o$ below the baseline level provides a reversed gradient of activity which drives wayward K^+ ions home when neuronal excitation has ceased.

Besides providing a path for ion current, glial cells could, in principle, allow for the dissipation of an excess of $[K^+]_o$ also by simple diffusion. Insofar as the glial membrane admits K^+ ions freely, it would be "transparent" not only for K^+ ions driven by electric current, but also those propelled by a gradient of concentration. Calculations show however that even if diffusion was entirely unhindered by cell membranes, it would be too slow to account for the measured rate of disappearance of an excess $[K^+]_o$ (Cordingley & Somjen, 1978). Glial cells may also admit K^+ together with Cl^- and water under the influence of Donnan forces (cf. e.g. Bourke et al., 1978). A simple calculation (see p. 165 of Varon & Somjen, 1979) can show that glial cells could, in principle, accommodate the entire load of excess K^+ spilled by neurons in the course of an epileptiform seizure by increasing their K^+ content by about 2%, and a concommittant shrinkage of the interstitial space by not more than 7%. Such a shift of water would not be detected as "swelling" of tissue, and would presumably not disturb the functioning of the nervous system. Whether in fact such uptake does occur under normal conditions depends on the permeability to Cl^- ions of the membrane of glial cells in undisturbed, normally circulated central nervous tissue. This datum is not known today.

Are glial cells actively clearing K^+ from interstitial fluid?

The thought that glial cells may regulate $[K^+]_o$ by active transport is in fact older than that they may do so by the passive, dissipative processes discussed in the preceding section (e.g. Cummins & Hydén, 1962; Hertz, 1965; Henn et al., 1972; Hertz & Schousboe, 1975). There are three ways in which glial cells could clear K^+ from the interstitium: (1) by exchanging intracellular Na^+ for extracellular K^+; (2) by admitting K^+ coupled with an equivalent amount of anion, and equiosmolar volume of water, (this would be an "active" counterpart to the "passive" uptake mechanism by Donnan forces discussed earlier); and (3) by actively pumping K^+ inward at regions of high $[K^+]_o$ and simultaneously pumping an equivalent amount outward in regions of low $[K^+]_o$, (i.e.by ion current, the generator of which would, however, be active ion transport, unlike the mechanism sketched in Fig. 7, for which the driving force was the "passive" depolarization of the glial membrane) (Orkand, 1977).

Without a doubt, glial cells are capable of accumulating K^+ and extruding Na^+, or else they could not maintain the composition of intracellular fluid. Na^+, K^+-ATPase has indeed been demonstrated in glial material, separated from neurons in one manner or other (e.g. Cummins & Hydén, 1962; Henn et al., 1972; Hertz, 1977), although its identification in glia by histochemical methods is apparently difficult (Stahl & Broderson, 1976). Undisturbed glial cells probably can maintain their intracellular ion balance with minimal expenditure of energy and minimal activation of ATPase, because of the low permeability of their membrane to cations other than K^+. The question is, how does the glial Na^+, K^+-ATPase react to elevations of $[K^+]_o$ above the normal level? If glial ATPase reacted like the similar enzyme of other cells, then during excitation of neurons it probably would be stimulated less than neuronal ATPase, for although both glial cells and neurons are exposed to the same high $[K^+]_o$, only neurons

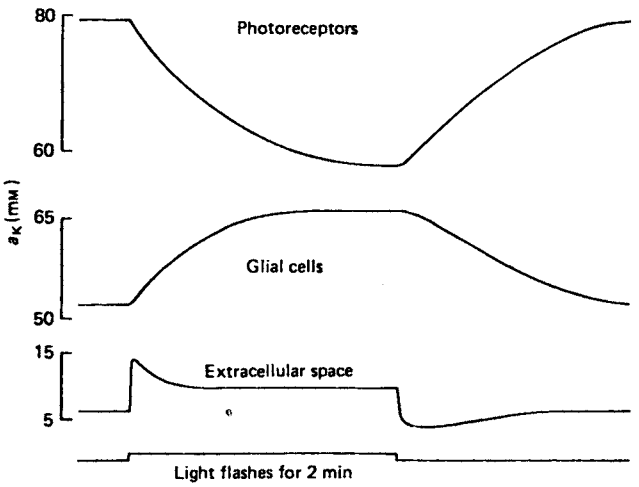

Fig. 8. Schematic summary of changes observed in potassium activity (a_K) in the eye of the honeybee drone, during stimulation by a series of light flashes. Resting and peak levels and timecourse are the means observed in a series of experiments. (From: Coles & Tsacopoulos, 1979, by permission of Authors and Publisher).

gain in $[Na^+]_i$ (cf. Skou, 1975). Potassium dependent activation of glial ATPase has, however, been demonstrated by a number of investigators (e.g. Franck et al., 1978).

In drawing conclusions from observations made on glial cell material in vitro it must be kept in mind that in healthy central nervous tissue $[K^+]_o$ probably rarely rises above 4mM and almost certainly never above 5 mM (Somjen, 1979; Varon & Somjen, 1979). Many of the early experiments have been conducted with "control" solutions containing 5 or 6 mM $[K^+]$, and a "stimulated condition" being represented by $[K^+]$ levels of 10, 20mM or even higher. In intact brain K^+ rises to about 10 or maximally 12mM during seizures, and above that level only during spreading depression. Changes occurring in glia at these high levels of $[K^+]_o$ are thus relevant only for the pathophysiology of the brain. Thus, for example, Kimelberg (1979)and Bourke et al., (1978) consider that the HCO_3^- dependent swelling of glial cells which occurs in brain slices exposed to high $[K^+]_o$ may be a model of cerebral oedema. In considering the mechanism by which brain tissue can become water-logged in situ, the transfer of water from blood into brain, and hence the behavior of the newly discovered blood-brain barrier for water (cf. Raichle, in press), must, however, also be considered.

Recently Hertz (1978) and Hertz & Franck (1978) have shown, however, that the uptake of radio-labelled K^+ into glial cells is stimulated by

relatively small increments of $[K^+]_o$, close to the normal level of 3mM. It remains to be determined how much of this uptake is in fact K^+-K^+ exchange, and therefore of no use in clearing $[K^+]_o$; and whether glia in intact tissue is stimulated in a like manner.

While the role of glial cells in regulating $[K^+]_o$ in the mammalian CNS is still the subject of much theoretical argumentation, it has been demonstrated beyond reasonable doubt by the elegant intracellular measurements of $[K^+]_i$ in cells of the insect eye by Coles and Tsacopoulos(1979). In this organ pigment cells are the analogues of glia. They apparently are the temporary receptacles of the K^+ ions discharged from stimulated photoreceptors, for which the interstitial fluid is the vehicle (Fig. 8). Coles and Tsacopoulos concluded, that K^+ is taken up by the glial cells in exchange for Na^+. The exact mechanism of the exchange has not yet been determined. Gardner-Medwin and Coles (in press) have however found evidence of current flow in the sense of a "spatial buffering" system through and around these glial cells.

Conclusions.

From the data available today, the role of glial cells in regulating the extracellular potassium activity in the mammalian central nervous system cannot be determined with certainty as yet. The following propositions are however at the least not contradicted by any of the known facts.

(1) Neurons which have discharged K^+ ions into interstitial space probably regain much or most by stimulated membrane transport, before it could be dispersed into the surrounding tissue. (2) The variable that is regulated by neuronal membrane transport is probably the intracellular ion content of the neuron. (3) Since single neurons and their environment do not form a closed two-compartment system, neurons cannot simultaneously regulate (be attuned to) both their intracellular ion content, and extracellular ion activities. There must be another agency taking care of the latter (cf. Varon & Somjen, 1979, p. 168). (4) Passive dissipation of spatial gradients of $[K^+]_o$ by diffusion and by electric current flowing through the "glial buffer network" may be an adjuvant in regulating $[K^+]_o$, but: (5) accurate homeostasis presupposes both, a sensing mechanism, and an active process governed by the sensor. Glial and/or endothelial cells are the candidates for "fine tuning" $[K^+]_o$ in the interstitial space of the CNS.

REFERENCES

Adams, P. R. and Brown, D.A. , 1979, Electrical responses of presumed sympathetic neuroglial cells to K^+ ions and to preganglionic nerve stimulation., J. Physiol. 293: 95-98.

Betz, A.L, Firth, J.A.,Goldstein, G.W.1980,Polarity of the blood-brain barrier: Distribution of enzymes between the luminal and antiluminal membranes of capillary endothelial cells., Brain Res. 192:17-28.

Bito, L.Z., 1969, Blood-brain barrier. Evidence for active cation transport between blood and the extracellular fluid of brain., Science, 165: 81-83.

Bourke, R.S., Daze, M.A., Kimelberg, H.K., 1978, Chloride transport in mammalian astroglia, Dynamic Properties of Glia Cells, Schoffeniels, E., Franck, G., Hertz, L., Tower, D.B. (eds), Pergamon Press, Oxford, pp. 337-346.

Bowery, N.G., Brown, D.A, and Marsh, S., 1979, Gamma-aminobutyric acid efflux from sympathetic glial cells: effect of "depolarizing" agents. J. Physiol. 293: 75-101.
Bradbury, M.W.B., Segal, M.B. and Wilson, J., 1972, Transport of potassium at the blood-brain barrier. J. Physiol. 221: 617-632.
Brightman, M.W., Anders, J.J., Schmechel, D., and Rosenstein, J.M., 1978, The lability of the shape and content of glial cells. In: Schoffeniels et al. (eds), pp. 21-44.
Brown, D.A., Scholfield,C.N.1974, Changes of intracellular sodium and potassium ion concentration in isolated rat superior cervical ganglia induced by depolarizing agents. J. Physiol. 242: 307-319.
Bureš, J. Burešová, O., Křivánek,J. 1974, The Mechanism and Applications of Leao's Apreading Depression of Electroencephalographic Activity. Academia, Prague.
Castellucci, V.F., and Goldring, S., 1970, Contribution to steady potential shifts of slow depolarization in cells presumed to be glia. Electroencephalogr. Clin. Neurophysiol. 28: 109-118.
Chan-Palay, V., Palay, S.L., 1979, Immunocytochemical localization of cyclic GMP: light and electromicroscope evidence for involvement of neuroglia. Proc. Natl. Acad. Sci. USA 76: 1485-1488.
Church, G.A., Kimelberg, H.K., Sapirstein, V.S., 1980, Stimulation of carbonic anhydrase activity and phosphorylation in primary astroglial cultures by norepinephrine. J. Neurochem. 34: 873-879.
Coles, J.A., and Tsacopoulos, M., 1979, Potassium activity in photoreceptors, glial cells and extracellular space in the drone retina: changes during photostimulation. J. Physiol. 290: 525-549.
Cordingley, G. E. and Somjen, G.G., 1978, The clearing of excess potassium from extracellular space in spinal cord and cerebral cortex. Brain Res. 151: 291-306.
Cserr, H., 1965, Potassium exchange between cerebrospinal fluid, plasma and brain. Am. J. Physiol. 209: 1219-1226.
Cummins, J. and Hydén, H., 1962, Adenosine triphosphate levels and adenosine triphosphatases in neurone, glia, and neuronal membranes of the vestibular nucleus. Biochim. Biophys. Acta 60: 271-283.
Curtis, D.R., 1978, Pre-and nonsynaptic activities of GABA and related amino acids in the mammalian nervous system. in: Amino Acids As Chemical Transmitters, Fonnum, F., (ed), Plenum Press, New York, pp. 55-86.
Dennis, M. and Gerschenfeld, H.M., 1965, Some physiological properties of identified mammalian glial cells. J. Physiol. 203: 211-222.
Dennis, M. J. and Miledi, R., 1974, Electrically induced release of acetylcholine from denervated Schwann cells. J. Physiol. 237: 431-452.
DeRobertis, E.D., 1965, Some new electron microscopical contributions to the biology of neuroglia. in: Biology of Neuroglia; Progress in Brain Research, Vol.15, DeRobertis, E., Carrea, R. , pp. 1-11.
Eisenberg, H.M. and Sudith, R.L. 1979, Cerebral vessels have the capacity to transport sodium and potassium., Science 206: 1083-1085.
Faeder, Isabelle R., and Salpeter, Miriam M., 1970, Glutamate uptake by a stimulated insect nerve muscle preparation., J.Cell Biol. 46: 300-307.
Fisher, R.S., Pedley, T.A. and Prince, D.A., 1976, Kinetics of potassium movement in normal cortex., Brain Res. 101: 223-237.
Futamachi, K., and Pedley, T.A., 1976, Glial cells and potassium: their relationship in mammalian cortex. , Brain Res. 109: 311-322.
Galambos, R., 1961, A glia-neural theory of brain function. Proc. Natl. Acad. Sci. USA 47: 129-136.
Gardner-Medwin, A.R., 1977, The migration of potassium produced by electric current through brain tissue., J. Physiol. 269: 32P.33P.

Gardner-Medwin, A. R., in press, The role of cells in the dispersal of brain extracellular K^+. in: Ion-selective Microelectrodes and Their Use in Excitable Tissues. Sykova, E. and Vyklicky, L. (eds), Plenum, New York.
Gardner-Medwin, A.R. and Coles, J.A., in press, Dispersal of potassium through glia. Proc. 28th Internat'l. Cong. Physiol. Abstr., Budapest.
Gardner-Medwin, A.R., Gibson, Josephine L., and Willshaw, D.J., 1979, The mechanism of potassium dispersal in brain tissue., J. Physiol. 293: 37P.
Giacobini, E., 1962, A cytochemical study of the localization of carbonic anhydrase in the nervous system., J. Neurochem. 9:169-177.
Golgi, C., 1903, Opera Omnia, Milano, U. Hoepli.
Grossman, R.G. and Hampton, T., 1968, Depolarization of cortical glial cells during electrocortical activity. Brain Res. 11: 316-324.
Haber, Bernard, Suddith, Robert L., Pacheco, Mauro, Gonzalez, Arturo, Ritchie, Terry L., and Glusman, Sylvio, 1978, Model systems for the glial transport of biogenic amines and GABA: clonal cell lines and the filum terminale of the frog spinal cord. in: Schoffeniels et al., (eds).
Hamberger, Anders, Chiang, Grace, Nylen, Eric S., Scheff, Stephen W. and Cotman, Carl W., 1978, Stimulus evoked increase in the biosynthesis of the putative neuro-transmitter glutamate in the hooopcampus. Brain Res. 143: 549-555.
Hamberger, A., Chiang, G., Sandoval, E. and Cotman, C. 1979, Glutamate as CNS transmitter. II.Regulation of synthesis in the releasable pool. Brain Res. 168: 531-541.
Hamberger, A. C., Chiang, G H., Nylen, E.S., Scheff, S.W., and Cotman, C.W. 1979, Glutamate as a CNS transmitter. 1. evaluation of glucose and glutamine as presursors for the synthesis of preferentially released glutamate., Brain Res. 168: 513-530.
Hamberger, A., Cotman, C.W., Sellstrom, A., and Weiler, C.T., 1978, Glutamine, glial cells and their relationship to transmitter glutamate. in: Schoffeniels et al., (eds), pp. 163-172.
Heinemann, U., and Lux, H.D. 1975, Undershoots following stimulus-induced rises of extracellular potassium concentration in cerebral cortex of cat. Brain Res. 93: 63-76.
Heinemann, U., Lux, H.D. and Gutnick, M.J., 1978, Changes in extracellular free calcium and potassium activity in the somatosensory cortex of cats. Abnormal Neuronal Discharges, Chalazonitis, N., and Boisson, M. (eds), Raven Press, New York.
Heinemann, U., Lux, H.D., Marciani, M.G., and Hofmeier, G., 1979, Slow potentials in relation to changes in extracellular potassium activity in the cortex of cats. in: Origin of Cerebral Field Potentials, Speckmann, E.J., Caspers, H. (eds), G. Thieme, Stuttgart., pp. 33-48.
Henn, F.A., Haljamae, H., and Hamberger, A., 1972, Glial cell function: active control of extracellular K^+ concentration., Brain Res. 43:437-443.
Hertz, L., 1965, Possible role of neuroglia: a potassium-mediated neuronal-neuroglial-neuronal impulse transmission system., Nature 206: 1091-1094.
Hertz, L., 1977, Drug-induced alterations of ion distribution at the cellular level of the central nervous system., Pharmac. Rev. 29: 35-65.
Hertz, L., 1978, An intense potassium uptake into astrocytes, its further enhancement by high potassium, and its possible involvement in potassium homeostasis at the cellular level.,. Brain Res. 145: 202-208.
Hertz, L, and Franck, G., 1978, Effect of increased potassium concentrations on potassium fluxes in brain slices and in glial cells., in: Schoffeniels et al., (eds), pp 383-388.
Hösli, E. and Hösli, L, 1980, Cellular localization of the uptake of [^{3}H] taurine and [^{3}H] alanine in cultures of the rat central nervous system. , Neuroscience 5: 145-152.

Hydén, H. and Egyházi, E., 1963, Glial RNA changes during learning experiment in rats.,Proc. Natl. Acad. Sci. USA 49: 618-624.
Iversen, L.L. and Kelly, J.S., 1975, Uptake and metabolism of γ-aminobutyric acid by neurones and glial cells. , Biochem. Pharmac. 24: 933-938.
Karahashi, Y. and Goldring, S., 1966, Intracellular potentials from "idle" cells in cerebral cortex of cat. Electroencephalogr. Clin. Neurophysiol. 20: 600-607.
Karwoski, C. J. and Proenza, L.M., 1977, Relationship between Müller cell responses, a local transretinal potential, and potassium flux., J. Physiol.40: 244-259.
Karwoski, C.J., and Proenza, L.M., 1980, Neurons, potassium, and glia in proximal retina of necturus., J. gen. Physiol. 75: 141-162.
Katzman, R. and Pappius, H.M., 1973, Brain Electrolytes and Fluid Metabolism, Williams and Wilkins, Baltimore.
Kelly, J.S. and Dick, F., 1978, GABA in glial cells of the peripheral and central nervous system. in: Schoffeniels et al. (eds), pp. 183-192.
Kimelberg, H.K., 1979, Glial enzymes and ion transport in brain swelling. Neural Trauma, Popp, A.J. et al. (ed), Raven Press, New York.
Krnjević, K., 1976, Inhibitory action of GABA and GABA-mimetics on vertebrate neurons. in:GABA In Nervous System Function, Roberts, E., Chase, T. N., Tower, D.B. (eds), Raven Press, New York,pp. 269-281.
Krnjević, K., and Morris, M.E., 1972, Extracellular K^+ activity and slow potential changes in spinal cord and medulla. Canadian J. Physiol. and Pharmac. 50: 1214-1217.
Krnjević, K., and Morris, M.E., 1975, Factors determining the decay of K^+ potentials and focal potentials in the central nervous system. Can. J. Physiol. Pharmac. 53: 923-934.
Kuffler, S.W., 1967, Neuroglial cells: physiological properties and a potassium mediated effect of neuronal activity on the glial membrane potential., Proc. R. Soc.B. 168: 1-21.
Kuffler, S.W. and Nicholls, J.G., 1966, The physiology of neuroglial cells., Ergebn. Physiol. 57: 1-90.
Kuffler, S.W., Nicholls, J.G., and Orkand, R.K., 1966, Physiological properties of glial cells in the central nervous system of amphibia., J. Physiol. 29: 768-787.
Lange, P.W., 1978, Nucleic acids and proteins. In: Schoffeniels et al., (eds).pp. 231-245.
Lasansky, A., 1971, Nervous function at the cellular level., Glia.Ann. Rev. Physiol. 33: 241-256.
Lothman, E.W. and Somjen, G.G., 1975, Extracellular potassium activity, intracellular and extracellular potential responses in the spinal cord., J. Physiol. 252: 115-136.
Lugaro, E., 1907, Sulle funzioni della nevroglia., Riv. Pat. Nerv. Ment.12: 225-233.
Lux, H.D. and Neher, E. , 1973, The equilibration time course of $[K+]_o$ in cat cortex., Exp. Brain Res. 17: 190-205.
Martinez-Hernandez, A., Bell, K.P., and Norenberg, M.D., 1977, Glutamine synthetase: glial localization in brain., Science 195: 1356-1358.
Maynard, E.A., Schultz, R.Y., Pease, D.C., 1957, Electromicroscopy of the vascular bed of rat cerebral cortex., Am. J. Anat.100: 409-434.
Minchin, M.C.W., and Nordmann, J.J., 1975, The release of [^{3}H] gamma - aminobutyric acid and neurophysin from the isolated rat posterior pituitary., Brain Res. 90: 75-84.
Moonen, G. and Nelson, P.G., 1978, Some physiological properties of astrocytes in primary cultures. In: Schoffeniels et al., (eds)pp. 389-393.

Nageotte, J., 1910, Phenomènes de secrétion dans le protoplasma des cellules nevrogliques de la substance grise.,C.r.Soc. Biol.68: 1068-1069.
Newman, Eric A., 1980, Current source-density analysis of the b-wave of frog retina., J. Neurophysiol. 43: 1355-1366.
Oldendorf, W.H., Cornford, M.E. and Brown, W.J., 1977, The large apparent work capability of the blood-brain barrier: A study of the mitochondrial content of capillary endothelial cells in brain and other tissues of the rat., Ann. Neurol. 1: 409-417.
Orkand, R.K., 1977, Glial cells. In: Handbook of Physiology, Sec.1,Vol.I, Part 2, Amer. Physiol.Soc., Bethesda, MD, pp. 855-875.
Orkand, P.M. and Kravitz, E.A., 1971, Localization of the sites of gamma-amino butyric acid uptake in lobster nerve-muscle preparation., J. Cell. Biol. 49: 75-89.
Orkand, R.K., Nicholls, J.G. and Kuffler, S.W., 1966, Effect of nerve impulses on the membrane potential of glial cells in the central nervous system of amphibia., J. Neurophysiol. 29: 788-806.
Pape, L.G. and Katzman, R., 1972, Response of glia in cat sensorymotor cortex to increased extracellular potassium., Brain Res. 38: 71-92.
Pappenheimer, John R., 1967, The ionic composition of cerebral extracellular fluid and its relation to the control of breathing., Harvey Lecture Series 61: Academic Press, New York, pp. 71-94.
Peters, A., and Palay, S.L., 1965, An electron microscope study of the distribution and patterns of astroglial processes in the central nervous system., J. Anat. 99: 419.
Pevzner, L.Z., 1978, Phasic interrelations between neuronal and neuroglial macromolecular metabolism. In: Schoffeniels et al., (eds).pp. 223-229.
Prince, D.A,, Lux, H.D. and Neher, E., 1973, Measurement of extracellular potassium activity in cat cortex., Brain Res. 50: 489-495.
Quastel, J.H., 1978, Cerebral glutamate-glutamine interrelations in vivo and in vitro., In: Schoffeniels et al., (eds).pp. 153-162.
Raichle, M.E., in press, Hypotheses: a central neuroendocrine system regulates brain ion homeostasis and volume.In:Neurosecretion and Brain Peptides: Implications for Brain Function and Neurological Disease, Martin, J.B (ed), Raven Press.
Raichle, Marcus E., Hartman, Boyd K., Eichling, John O., and Sharpe, L.G, 1975, Central noradrenergic regulation of cerebral blood flow and vascular permeability., Proc. Natl. Acad. Sci. USA 72: 3726-3730.
Ransom, B.R., Goldring, S., 1973, Ionic determinants of membrane potential of cells presumed to be glia in cerebral cortex of cat., J. Neurophysiol. 36:855-868.
Robinson, J.R., 1960, Metabolism of intracellular water., Physiol. Rev.40: 112-149.
Schoffeniels, E., Franck, G., Hertz, L., and Tower, D.B., 1978, Dynamic Properties of Glia Cells, Pergamon Press, Oxford.
Skou, J.C., 1975, The (Na^+, K^+) activated enzyme system and its relationship to transport of sodium and potassium., Q. Rev. Biophys. 7:401-434.
Somjen, G.G., 1969, Sustained evoked potential changes of the spinal cord. Brain Res. 12:268-272.
Somjen, G.G., 1970, Evoked sustained focal potentials and membrane potential of neurons and of unresponsive cells of the spinal cord., J. Neurophysiol. 33:562-582.
Somjen, G.G., 1973, Electrogenesis of sustained potentials., Progr. Neurobiol. 1: 199-237.
Somjen, G.G., 1975, Electrophysiology of neuroglia., Ann. Rev. Physiol. 37: 163-190.

Somjen, G.G., 1979, Extracellular potassium in the mammalian central nervous system., Ann. Rev. Physiol. 41:159-177.
Somjen, G.G., in press, The why and the how of measuring the activity of ions in extracellular fluid of the spinal cord and cerebral cortex. In: The Application of Ion-Selective Electrodes.Zeuthen, T. (ed). Amsterdam, Elsevier.
Speckmann, E.J., Caspers, H., and Janzen, R.W., 1972, Relations between cortical DC shifts and membrane potential changes of cortical neurons associated with seizure activity. In: Synchronization of EEG Activity in Epilepsies. Petsche, H. and Brazier, M.A.B.(eds).Springer-Verlag/ Wien, New York. pp. 93-111.
Stahl, L.W. and Broderson, S.H., 1976, Localization of Na^+, K^+-Adenosinetriphosphatase in brain., Fed. Proc. 35: 1260-1265.
Strittmatter, W.J. and Somjen, G.G., 1973,Depression of sustained evoked potentials and of glial depolarization in the spinal cord by barbiturates and by diphenylhydantoin., Brain Res. 55: 333-342.
Sugaya, E., Goldring, S., and O'Leary, J.L., 1964, Intracellular potentials associated with direct cortical response and seizure discharge in the cat. Electroencephalogr. Clin. Neurophysiol.17: 661-669.
Sugaya, E., Karahashi, Y., Sugaya, A., and Haruki, F., 1971, Intra- and extracellular potentials from "idle" cells in cerebral cortex of cats., Japan. J. Physiol. 21: 149-157.
Sugaya, E., Sekiya, Y., Kobori, T., and Noda, Y., 1979, Glial membrane potential and extracellular potassium concentration in cultured glial cells., Expl. Neurol. 66: 403-408.
Takato, M., and Goldring, S., 1979, Intracellular marking with lucifer yellow and horseradish peroxidase of cells electrophysiologically characterized as glia in the cerebral cortex of the cat., J. Comp. Neurol. 186: 173-188.
Trachtenberg, M.C. and Pollen, D.A., 1970, Neuroglia: biophysical properties and physiological function., Science 167: 1248-1252.
Varon S., and Somjen, G.G., 1979, Neuron-glia interactions., Neurosciences Research Program Bulletin 17:1-239.
Vern, B.A., Schuette, W.H. and Thibault, L.E., 1977, $[K^+]_o$ clearance in cortex: A new analytical model. J. Neurophysiol. 40: 1015-1023.
Villegas, J., 1978, Cholinergic properties of satellite cells in the peripheral nervous system., In: Schoffeniels et al., (eds). pp. 207-215.
Virchow, R., 1858, Cellularpathologie in ihre Bergrundung auf physiologische und pathologische Gewebelehre. Hirschwald, A., Berlin.
Vyklicky, L., Syková, E., Kříž, N., and Uječ, E., 1972, Post-stimulation changes of extracellular potassium concentration in the spinal cord of the rat., Brain Res. 45: 608-611.
Vyskočil, F., Kříž, N. and Bureš, J., 1972, Potassium-selective microelectrodes used for measuring the extracellular brain potassium during spreading depression and anoxic depolarization in rats., Brain Res. 39: 255-259.
Wolff, J., 1965, Elektronenmikroskopische Untersuchungen über Struktur und Gestalt von Astrozytenfortsätzen., Z. Zellforsch 66: 811-828.
Woodward, J.K., Bianchi, G.P., and Erulkar, S.D., 1969, Electrolyte distribution in rabbit superior cervical ganglion., J. Neurochem.16: 289-299.

Adv. Physiol. Sci. Vol. 3. Physiology of Non-excitable Cells
J. Salánki (ed.)

MODELS OF FLOW AND PRESSURE MODULATED ISOOSMOTIC REABSORPTION IN MAMMALIAN PROXIMAL TUBULES*

Donald J. Marsh
Department of Physiology and Biophysics, University of Southern California School of Medicine
Los Angeles, California 90033, USA

The proximal tubule reabsorbs tubular fluid isoosmotically under virtually all experimental conditions and over a wide range of rates. The ability of this tubular segment to adjust the rate of fluid reabsorption automatically gives rise to a functionally important load adaptive property often referred to as glomerulotubular balance.

There have been a number of successful attempts to explain isoosmotic reabsorption by epithelia. (Patlak et al.,1963, Diamond and Bossert, 1967, and Sackin & Boulpaep, 1975) These have all involved active transport of NaCl along basolateral cell membranes into lateral intercellular channels. Local accumulation of solute into these channels draws water from the cell by osmosis, and the resulting fluid moves across the basement membrane under a head of hydrostatic pressure. Each of these explanations has sought only to explain isoosmotic reabsorption at one rate. A greater challenge arises when the load adaptive property requires explanation.

Two phenomena are thought to underlie glomerulotubular balance: cotransport of Na^+ across apical cell membranes, and adjustments of interstitial hydrostatic pressure secondary to changes in hydrostatic or colloid osmotic pressure in peritubular capillaries.

Cotransport of Na^+ with glucose or amino acids is a well established process (Crane, 1962, Kinne et al., 1975). The rate of entry of Na^+ depends on the concentrations of organic molecules, and vice versa. If a higher concentration of organic molecule stimulates Na^+ entry, more Na^+ will be delivered to the Na-K-ATPase at the basolateral cell membranes, and the rates of salt and water transport will increase. An increase of glomerular filtration rate, for example, would increase the load of organic molecule delivered to the tubule, and might affect the downstream concentration profile of these molecules. A change in fluid reabsorption rate would also affect the concentration profile. Because of these interactions, it becomes difficult to evalute the quantitative impact of cotransport on glomerulotubular balance.

*Supported by NIH Research Grant AM15968

We therefore derived the following model to determine whether cotransport can explain glomerulotubular balance to any significant extent. The model is derived for the steady state, is based on local mass balance, and uses glucose for purposes of illustration.

In an element of volume along a tubule of radius, r, the difference in glucose mass flow along a distance, Δx is

(1) $\Delta c q = -2\pi r k_1 c \Delta x$

Where c is the glucose concentration, q the volume flow rate, and k_1 is a rate coefficient. This expression assumes that the Na^+ concentration remains constant. The rate of transport does, in fact, depend on the Na^+ concentration, but since it remains constant in vivo, this concentration can be incorporated into the coefficient.

The equation for volume flow rate Δq over the same distance is:

(2) $\Delta q = -2\pi r (k_2 c + k_3) \Delta x$

This expression assumes that Na^+ entry into the cell has two components, one dependent on the cotransport mechanism, and another that is not. This second pathway can represent more than one mechanism. Dividing both sides of Eq (2) by Δx and taking the limit yields:

(3) $$\frac{dq}{dx} = -2\pi r (k_2 c + k_3)$$

Dividing both sides of Eq (1) by Δx, taking the limit, separating dependent variables and inserting Eq (3) yields:

(4) $$\frac{dc}{dx} = -2\pi r \frac{c}{q}(k_2 c + k_1 + k_3)$$

The initial conditons can be specified as:

(5) $C(o) = Co$

and

(6) $q(o) = qo$

This derivation leads to a second order nonlinear initial value problem for which no analytic solution was found. The system was solved numberically with a variable step size routine that uses a fourth order Adams Moulton predictor corrector method to integrate the differential equations.

The accompanying figures show some results. As can be seen, glucose concentration drops to zero along the length of tubule, as it is known to, and fluid is reabsorbed. Reabsorption of fluid is flow or load dependent, and the concentration curves in the first figure explains this dependency; concentration does not drop as quickly at higher flow rates. Thus, a concentration difference at different flow rates affects the local rate of reabsorption. If there is no concentration difference, no difference in reabsorptive rates can occur. Unfortunately, while the curves of Fig. 1 show flow dependent reabsorption, they also show a concentration profile that differs substantially from experimental results (Deetjen and

FIGURE 1. Simulated glucose concentrations and volume flow rates, with a set of parameters that achieves good glomerulotubular balance.

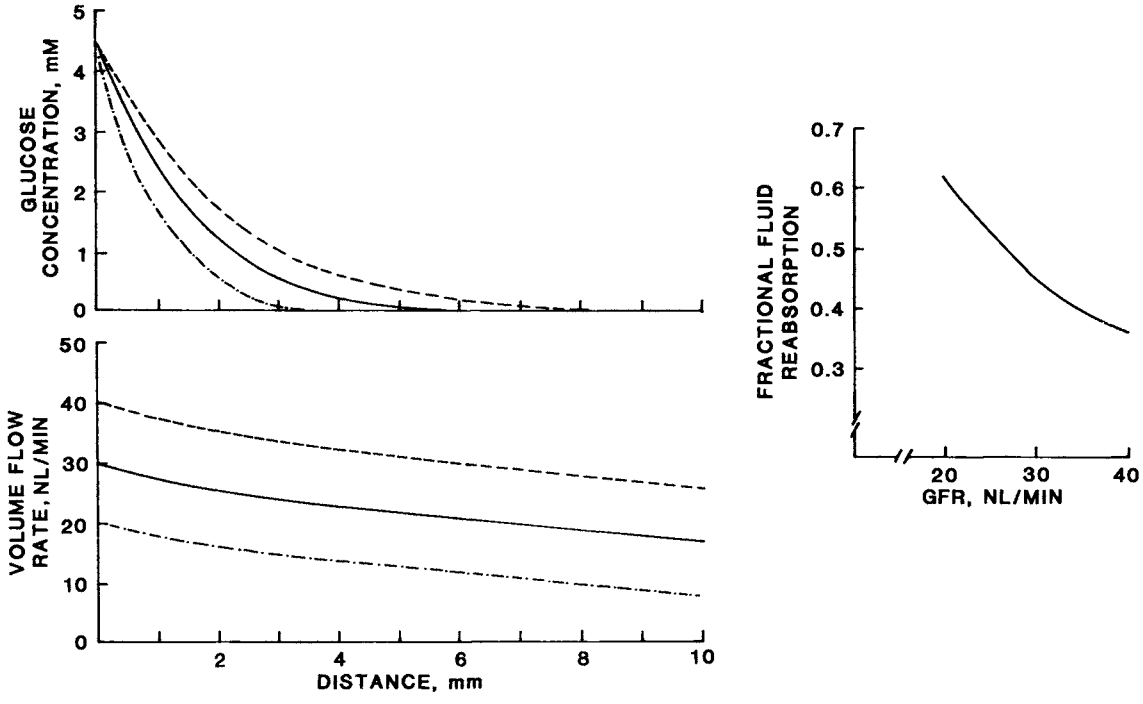

FIGURE 2. Simulated glucose concentrations and volume flow rates with a set of parameters that predicts glucose concentration curves similar to those found experimentally.

GLOSSARY OF SYMBOLS .

A	channel cross-section area, cm^2
A_{max}	maximum channel cross-section area, cm^2
α	volume flow rate, dimensionless
b	NaCl concentration gradient, (mOsm cm^{-4}) × 10^{-3}
β	NaCl concentration gradient, dimensionless
C	NaCl concentration, (mOsm cm^{-3}) × 10^{-3}
$\bar{C}$	arithmetic mean NaCl concentration, (mOsm cm^{-3}) × 10^{-3}
γ	NaCl concentration, dimensionless
D	channel NaCl diffusion coefficient, $cm^2\ sec^{-1}$
E	emergent osmolality, (mOsm cm^{-3}) × 10^{-3}
k_1	channel wall hydraulic permeability, dimensionless
k_2	NaCl active transport rate, dimensionless
k_3	basement membrane hydraulic permeability, dimensionless
k_4	tight junction hydraulic permeability, dimensionless
k_5	basement membrane NaCl permeability, dimensionless
k_6	tight junction NaCl permeability, dimensionless
k_7	NaCl reflection coefficient, tight junction, dimensionless
k_8	NaCl reflection coefficient, basement membrane, dimensionless
L	hydraulic permeability, cm sec^{-1} mm Hg^{-1} or NaCl permeability, cm sec^{-1}
λ	distance, dimensionless
N	NaCl active transport rate, mOsm $cm^{-2}\ sec^{-1}$
ξ	compliance parameter, mm Hg^{-1}
p	hydrostatic pressure, mm Hg
$\bar{p}$	cell hydrostatic pressure, mm Hg
Π	osmotic pressure, mm Hg
q	volume flow rate, $cm^3\ sec^{-1}$
R	universal gas constant, mm Hg T^{-1} mol^{-1}
r	A/A_{max}, dimensionless
S	channel circumference, cm
σ	NaCl reflection coefficient
T	absolute temperature, °K
Φ	hydrostatic pressure, dimensionless
X	channel length, cm
x	distance, cm
z	pump distribution, dimensionless

Subscripts

B	basement membrane
BS	basement membrane, NaCl
IS	interstitial space
L	lumen
o	isotonic
T	tight junction
TS	tight junction, NaCl

TABLE 2. Dimensionless parameters

$$k_1 = \Pi_o(SLX)\Big/\left(\frac{A_{max}D}{X}\right). \tag{8}$$

$$k_2 = \left(\frac{N_0}{C_0}\right)\Big/\left(\frac{A_{max}D}{X}\right). \tag{9}$$

$$k_3 = L_B/(SLX). \tag{10}$$

$$k_4 = L_T/(SLX) \tag{11}$$

$$k_5 = L_{BS}\Big/\left(\frac{A_{max}D}{X}\right) \tag{12}$$

$$k_6 = L_{TS}\Big/\left(\frac{A_{max}D}{X}\right) \tag{13}$$

$$k_7 = \sigma. \tag{14}$$

$$k_8 = \sigma_B. \tag{15}$$

$$r = A/A_{max}. \tag{16}$$

Boylan, 1968). These curves show glucose concentration falling more gradually than has been found in micropuncture experiments. When the coefficient, k_1 is adjusted to bring the predicted concentration profile into agreement with experimental results, the flow dependence of reabsorption is altered, because the concentration differences experienced over the length of the tubule become smaller. Since glomerulotubular balance can achieve a virtual constancy of fractional fluid reabsorption, this study suggests that cotransport related adaptations cannot play a major role, although they can contribute to the overall effect.

The second proposed cause of glomerulotubular balance is an effect of changing determinants of peritubular capillary fluid exchange. There is already a substantial body of evidence showing that proximal tubule reabsorption is dependent on hydrostatic and colloid osmotic pressure in the capillary. Recently we showed a correlation of proximal reabsorption with net interstitial pressure, providing further confirmation of the theory (Quinn and Marsh, 1979).

The major challenge created by this hypothesis is that it requires modulation of fluid reabsorption rates without apparent chemical signalling; the hydrostatic pressure difference across the basement membrane controls the rate of fluid flow despite the apparent constancy of the rate of active transport. It has been assumed that back flux through the tight junction is the controlled variable.

To test this idea we derived a model of the tight junction-intercellular channel-basement membrane pathway. The derivation is given elsewhere (Huss and Marsh, 1975), the system equations are in Tables (1-3). Table 4 shows the behavior of the system as interstitial hydrostatic pressure is varied, using a set of parameters established by trial and error testing. Figures 3 and 4 show NaCl concentration and flow as functions of distance along the channel at two intersititial pressures. Several conclusions can be drawn:

TABLE 1. *A*) System equations

$$\frac{dq}{dx} = SL_1[(\tilde{p} - p) + (\Pi(x) - \Pi_\alpha)],\ 0 \leq x \leq X. \tag{1}$$

$$\frac{dC}{dx} = b(x). \tag{2}$$

$$\frac{db}{dx} = \frac{1}{AD}q(x)b(x) + \frac{SLC(x)}{AD}[(\tilde{p} - p) + (\Pi(x) - \Pi_\alpha)] - \frac{S}{AD}N(x). \tag{3}$$

B) Boundary conditions

$$q(0) = L_T[(p_L - p) + \sigma(\Pi(0) - \Pi_L)]. \tag{4}$$

$$q(0)C(0) - ADb(0) = q(0)\tilde{C}_T(1 - \sigma) + L_{TS}[C_L - C(0)]. \tag{5}$$

$$q(X) = L_B[(p - p_{IS}) + \sigma_B(\Pi_{IS} - \Pi(X))]. \tag{6}$$

$$q(X)C(X) - ADb(X) = q(X)\tilde{C}_B(1 - \sigma_B) + L_{BS}[C(X) - C_{IS}]. \tag{7}$$

TABLE 3. *A*) Dimensionless system equations

$$\frac{d\alpha}{d\lambda} = \gamma(\lambda) + (\Phi - \Phi). \tag{17}$$

$$\frac{d\gamma}{d\lambda} = \beta(\lambda). \tag{18}$$

$$\frac{d\beta}{d\lambda} = \frac{k_1}{r}\{\alpha(\lambda)\beta(\lambda) + [1 + \gamma(\lambda)][\gamma(\lambda) + (\Phi - \Phi)]\} - \frac{k_2}{r}z(\lambda). \tag{19}$$

where

$$z(\lambda) = 1,\ 0 \leqq \lambda \leqq 1 \tag{20}$$

B) Dimensionless boundary conditions

$$\alpha(0) = k_4[\Phi_L - \Phi + k_7\gamma(0)] \tag{21}$$

$$\frac{k_1}{r}\alpha(0)\left[k_7 + (1 + k_7)\frac{\gamma(0)}{2}\right] - \beta(0) = -\frac{k_8}{r}\gamma(0). \tag{22}$$

$$\alpha(1) = k_3[\Phi - \Phi_{IS} - k_9\gamma(1)]. \tag{23}$$

$$\frac{k_1}{r}\alpha(1)\left[k_8 + (1 + k_8)\frac{\gamma(1)}{2}\right] - \beta(1) = \frac{k_5}{r}\gamma(1). \tag{24}$$

TABLE 4. Pressure-modulated reabsorption

Transmural pressure (mm Hg)	Flow (ml/sec)	Emergent osmolality (osm)	Channel pressure (mm Hg)	Channel area (relative)
0	2.83×10^{-12}	0.301	16.2	0.63
10	3.35×10^{-12}	0.299	7.3	0.44
20	3.86×10^{-12}	0.298	−1.6	0.28
30	4.34×10^{-12}	0.296	−10.6	0.15
40	4.80×10^{-12}	0.296	−19.7	0.08

$k_1 = 12.0, k_2 = 0.03, k_3 = 0.1, k_4 = 0.05, k_5 = 1.0, k_7 = 0.3, k_8 = 0.005, k_9 = 0.083.$

1. Using a reasonable set of parameters, this model predicts isoosmotic transport.
2. Over a range of interstitial pressures typical of those found in experimental circumstances, the model predicts that reabsorption rate varies with interstitial pressure. The modulation is consistent with experimental results, and is the result of variable flux of NaCl across the tight junction; active transport rate remains constant by assumption. Pressure dependent changes in tight junction or basement membrane permeability are not needed and in fact exert a deleterious effect on sensitivity to pressure- a rather counterintuitive result.
3. NaCl concentration in the channel varies very little from isotonic. If the concentration were to exceed isoosmotic to any significant extent, the hydrostatic pressure in the channel would arise, and the sensitivity of reasorption to pressure would disappear.
4. To obtain the curves shown in Figures 3 and 4, it was necessary to set the tight junction solute permeability to a value 20 times the basement membrane value. This relationship is not what one might expect. When the relationships between these parameters was reversed, pressure dependent isoosmotic reabsorption remained, but 60% of the fluid flow was through the tight junction pathway, and only 40% through the basolateral cell membranes.

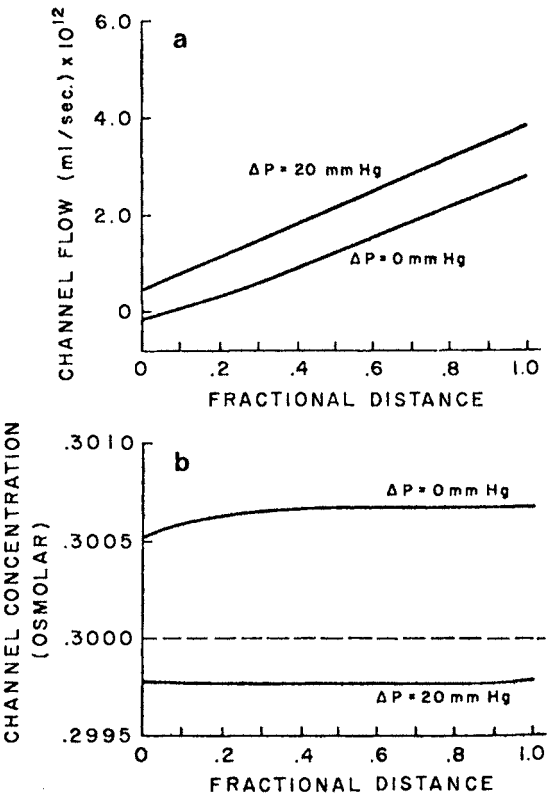

Figure 4. *a*) Fluid flow rate as a function of distance along the intercellular channel, for two values of the transmural pressure gradient. *b*) Osmolar concentration as a function of distance, for two values of the transmural pressure gradient.

This prediction awaits experimental verification.

The results of this study suggest that pressure modulation of isoosmotic reabsorption is an effective mechanism for controlling proximal tubule reabsorption. Thus, when a change in glomerular filtration rate changes filtration fraction, this mechanism becomes an effective one for achieving glomerulotubular balance. When filtration rate changes without affecting peritubular capillary variables, cotransport dependent phenomena are not likely to provide much adaptability.

REFERENCES

Crane, R.K. Hypothesis for mechanism of intestinal active transport of sugars. Fed. Proc. 21:891-895, 1962.

Deetjen, P. and J.W. Boylan. Glucose reabsorption in the rat kidney. Pflügers Archiv. 299:19-29, 1968.

Diamond, J. and W. Bossert. Standing-gradient osmotic flow; a mechanism for coupling of water and solute transport in epithelia. J. Gen. Physiol. 50:2061-2083, 1967.

Huss, R.E. and D.J. Marsh. A model of NaCl and water flow through paracellular pathways of renal proximal tubules. J. Membr. Physiol. 23:305-347, 1975.

Kinne, R., H. Murer, E. Kinne-Saffran, M. Thees, and G. Sachs. Sugar transport by renal plasma membrane vesicles. J. Membr. Biol. 27:375, 1975.

Quinn, M. and D.J. Marsh. Peritubular control of proximal tubule reabsorption in the rat. Am. J. Physiol. F478-F487, 1979.

Sackin, H. and E.L. Boulpaep. Models for coupling of salt and water transport. J. Gen. Physiol. 66:671-733, 1975.

Ullrich, K.J., G. Rumrich, and S. Kloess. Specificity and Na dependence of the active sugar transport in the proximal convolution of the rat kidney. Pfluegers. Archiv. 351:35-48, 1974.

Patlak, C.S., D.A. Goldstein, and J.F. Hoffman. The flow of solute and solvent across a two-membrane system. J. Theor. Biol. 5:426-442, 1963.

Adv. Physiol. Sci. Vol. 3. Physiology of Non-excitable Cells
J. Salánki (ed.)

CELL CONFIGURATION AS A FACTOR IN ISO-OSMOTIC TRANSPORT IN THE NEPHRON

Daniel J. Welling and Larry W. Welling
Research Service, Veterans Administration Medical Center, Kansas City, Missouri and Departments of Pathology and Physiology, University of Kansas Medical Center, Kansas City, Kansas, USA

In the past several years we have determined a quantitative stereological picture of cells in epithelia known to be iso-osmotic transporters (1,2,3). Our studies focused initially on the proximal convoluted tubule (PCT) and proximal straight tubule (PST) of the rabbit, nephron segments which are copious transporters of water and solute and which appear to be typical examples of iso-osmotic transporters. In this discussion we will consider those segments again and also will consider other nephron segments known to have different transport characteristics. In this way we will explore the possibility that a pattern exists between the shape of cells in an epithelium and the osmolality of the transported solutions.

Shown in Figure 1 are cell shapes obtained by morphometric analysis of transmission electron micrographs. To the left and superimposed on hexagons of average cell size are the outlines of a cell as might be seen in five equally spaced planes from cell apex to base. To the right is a 3-dimensional model obtained by stacking the cross-sections on the left. The model represents the average cell configuration in proximal nephron of adult rabbit and its accuracy has been confirmed recently by the

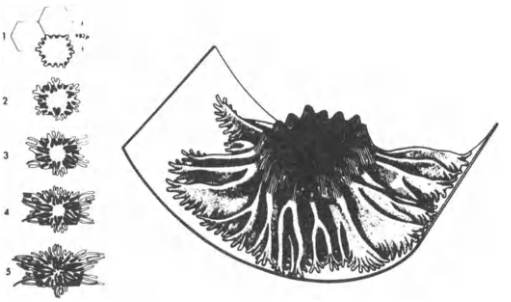

Fig. 1. Artist's rendition of cell shape in proximal renal tubule (right) as constructed by stacking of morphometrically determined cell outlines (left) in 5 equally spaced planes from cell apex to base. Reproduced from Ref. 2.

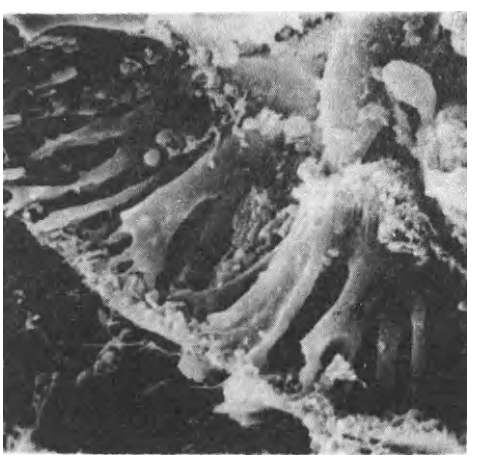

Fig. 2. Scanning electron micrograph of rabbit proximal renal tubule. Reproduced from Ref. 4.

scanning electron microscopy studies of Dr. Andrew Evan (4). A typical micrograph in Figure 2 shows the broken end of a rabbit proximal convoluted tubule. As in the stereologic model, one is able to see clearly the apical brush border, the drapery-like folding of major and minor lateral cells processes, and the so-called basal villi. The quantative morphometric studies also bring to light several other interesting features, namely:

1) The area of the brush border is equal to that of the lateral cell surfaces in both the convoluted and the straight tubule segments and is quite large, about 3×10^6 μm^2 per mm tubule length or about 3×10^3 μm^2 per cell.

2) If water moves through the cells at the observed rate of transepithelial volume absorption, about 1 nl/min/mm in convoluted tubule and 0.5 nl/min/mm in straight tubule, the cell volumes are turned over about once per minute. Such a rapid exchange rate could be accomplished by the large surface to volume rations.

3) The shape of the spaces between the cells, the lateral intercellular channels, is much more complicated than a simple "cylinder" or a set of parallel plates, geometries which were used in the initial modeling of iso-osmotic transport by Curran and MacIntosh (5), by Diamond and Bossert (6), and later by others.

Shown on the left in Figure 3 is a very simplified representation of an intercellular channel in proximal nephron. On the right is an infinitesimal slice of that channel where dimension x is measured in the direction from cell apex to base. One now can seen that nature has provided the channel with two curious features. First, the circumferential distance around the cells, and therefore the peripheral dimension S(x) of the channel, increases greatly with x. Second, the dis-

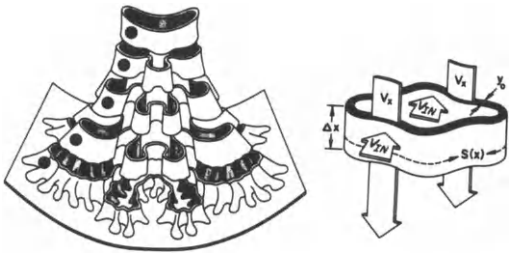

Fig. 3. Model of an intercellular space surrounding a simplified proximal tubule cell (left). On the right is an infinitesimal slice, x, of the intercellular space showing the components of fluid velocity into the channel, V_{in}, and along the channel, V_x. Cell separation distance is y_o and cell circumference is S(x).

tance between the two channel walls, y, is approximately constant from apex to base. That distance frequently is reported to be about 300 Å. Thus, the cross-sectional area of the channel increases rapidly from apex to base because of increasing cell circumference and not because of increasing cell separation. This space geometry has several important implications with regard to the pathway taken by the absorbate. It is generally accepted that absorbate ultimately passes via the intercellular channels. However, it may enter those channels by a paracellular route via junctional complexes at their apical ends, by a transcellular route across the apical and lateral cell surfaces, or by a combination of both routes. While there is no direct experimental evidence to date

which allows us to make a choice among these possibilities, the peculiar configuration of the channels does allow one to make the following statements:

1) If water is moving entirely by a paracellular path then its speed must decrease sharply from apex to base as the crosssectional area of the intercellular channel increases. A Poiseuille resistor of these dimensions would require a pressure drop of about 15 cm H_2O to produce the observed volume flow.

2) If water is moving entirely by a transcellular path then the ever increasing channel cross-section could accommodate the progressively accumulating volume of fluid. Such a system would require a very small pressure drop along the channel, less than 1 cm H_2O, and the speed of the fluid would remain relatively constant.

In light of these statments, we have found some indirect evidence which might distinguish between paracellular and transcellular flows. Specifically, we know from the work of Welling and Grantham (7) that transepithelial pressure in the renal tubule is taken up across the tubule basement membrane and that the cells act as direct pressure communicators. We also know that isolated cells from renal tubules are very highly deformable and can be drawn into small pipets by pressure differences less than 1 cm H_2O (8). Thus, we are led to the logical assumption that the cell membranes which constitute the intercellular channels are highly deformable and that they are sensitive to pressure drops (9). This means simply that points of high pressure cannot build up in the intercellular channel, that pressure from point to point along the channel is approximately balanced and, therefore, that water speed down the channel must also be approximately constant. On this bases, and given the type of

morphology observed in proximal renal tubules, we conclude that the transcellular flow option is the more likely. That is, for water flow to be steady along the channels of that epithelium, water must be accumulating from movement across the lateral cell walls.

As an aside, it is perhaps important to point out that proximal tubule cells with their interdigitating, pleated walls are by no means a universal type of cell shape. We recently have found that the cell circumference in rabbit gallbladder is effectively enlarged by microvilli within the lateral intercellular channels but that no appreciable change occurs in cell circumference in passing from cell apex to base. In this case the cross-sectional area of the channels increases by enlarging the separation distancy y and not by the enlargement of the circumferential dimension S(x) as occurs in the proximal tubule. The important point is that the channel cross-sectional area does increase and, on the basis of deformable walls, indicates that in the different cell types water is conducted at least partly across the lateral cells walls. At this time it is not clear just why these different cell types choose to increase their channel areas in these separate ways.

On the basis of the hypothesis of deformable channel walls, the following deductions now can be made:

1) Increasing cross-sectional area of intercellular channels, caused either by increasing cell circumference or by increasing cell separation or both, indicates transcellular fluid movement.

2) The variation of channel cross-sectional area is an indication of the rate of water movement into the channels across the cell walls. Therefore, it also is an indication of the size but (not the type) of the forces required for that water transport.

Referring again to the infinitesimal slice of intercellular channel shown in Figure 3, we can define the explicit mathematical relationship of structure to function by using the mass balance equation for the intercellular space,

$$V_x \; y \; S(x) = V_x(o) \; y(o) \; S(o) \; + \; 2 \int_o^x V_{in} \; S(x) \; dx,$$

where y is the separation distance between cells, S is the channel circumference, V_x is the stream velocity down the channel, and V_{in} is the velocity of fluid movement across the channel walls. If we now include the deformability hypothesis, that is, the approximation that V_x is a constant, the mass balance equation can be differentiated so that the change in geometry is a function of the flow across the lateral cell membranes (9):

$$y \; d\ln S/dx + dy/dx = 2 \; V_{in}/V_x.$$

For example, in the rabbit proximal convoluted and straight tubules, y is approximately constant so that $dy/dx = 0$ and $d\ln S/dx$ is proportional to V_{in}. On the other hand, in gallbladder, S is approximately constant, $d\ln S/dx = 0$, and it is dy/dx which is proportional to V_{in}. In either case, the changing cross-sectional area of the channel can be used for a direct calculation of the speed V_{in} of the water entering the channels.

It is now instructive to look at the details of iso-osmotic transporters, such as PCT and PST, and compare them to a hypertonic reabsorber as exemplified by the cortical thick ascending limb of Henle (TALH). In Figure 4 is plotted the log of the cell circumferences S in these segments versus the distance x as measured from cell apex to base. We see that in all cases ln S increases faster than linear. Given that the lateral cell walls are deformable, these curves indicate that V_{in} increases from cell apex to base. This brings us to a consideration of the forces causing water transport across these epithelia. The classical

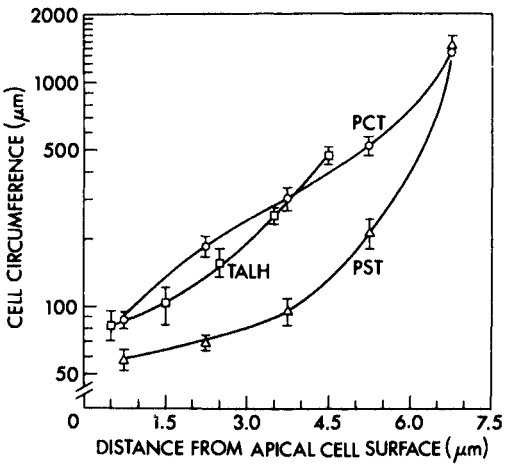

Fig. 4. Logarithms of cell circumference in proximal convoluted tubule (PCT), proximal straight tubule (PST), and cortical thick ascending limb of Henle (TALH) plotted versus distance from cell apex to base.

supposition has been that water movement is driven by an osmotic difference between the intra- and intercellular spaces, a difference supplied by the active transport of sodium into the intercellular channel. For iso-osmotic transporters this force must be very small (i.e. small osmotic difference) so that the emerging fluid is just barely hypertonic and not distinguishable from isotonic by our current measuring techniques. The question is, how can this nearly isotonic driving force be accomplished. There are two possibilities:

1) Active transport pumps might be localized upstream, near the apical end of the channel, so that the dilution of the hypertonic solution by transcellular water is practically complete by the time the fluid exists at the basal slit (the position taken by Diamond and

Bossert (6)), or

2) Transport might take place evenly along the channel but so close to isotonicity as to escape detection.

There are two compelling reasons for believing that the latter possibility is the correct one. First, the intercellular channel length is so short in the nephron (about 5 to 7.5 microns) that diffusing ions would distribute themselves evenly within the channel. In a 7.5 micron distance the diffusion front is more than an order of magnitude faster than the bulk flow speed as determined by the flow rate and the exit geometry in these epithelia. This point has been made some years ago by Drs. Emile Boulpaep and Henry Sackin and by us.

The second reason for accepting an evenly distributed, nearly isotonic transport mechanism is that the measured lateral surface areas are very large in relation to volume. Therefore, with hydraulic conductivities in the physiologic range of erythrocytes, volume flows of the measured amounts can take place with only very small forces. In other words, with osmotic differences too close to isotonicity to be detected experimentally. Stated another way, a trickle of water driven by a small force over an immense area adds up to a large amount of flow.

Now, if the active transport and associated forces are relatively uniform down the channel, we still need to explain the non-linear increase in the log of the cell circumference as shown in Figure 4. We have asked, therefore, whether a force in addition to active transport might be responsible for isosmotic volume flow in these segments? We think the answer is yes and the force is provided by serum protein.

It has been known for some time that serum protein in the bathing solutions has large effects on volume absorption in renal tubules (10). This effect could be due to the large surface areas which exist because

of the complicated foot processes at the base of the cells. That is, if protein can diffuse up stream, and there is evidence for that (11), then it can produce an osmotic effect across a very large area. If we speculate that the additional force is in fact due to protein diffusing from the bath we then can compute the hydraulic conductivity of the cell which would be necessary to inact this force. The answer comes out that the hydraulic conductivity needs to be only a little greater than in red cells to produce volume flow consistent with the cell circumference curves and the cell wall deformability considerations. Since the cell circumference curves are related to the standing diffusion for protein, the structure data can be used as separate estimate on the fluid speed in the channel. Using this data, a comparison of convoluted, straight, and thick ascending limb segments bares out the relationship that if net transport in the convoluted segment is 1 nl/min/mm, then in the straight it is 1/2 and in the thick limb it is 1/10.

The problems of ion transport across or between epithelial cells are more complex than those of water flow because of the variety of different mechanism available for the transport of ions in biological systems. To gain preliminary insight into the ion transport in nephron we recently have modeled the results of a series of experiments on collapsed renal tubules started some years ago by Drs. Jared Grantham and Mark Dellasaga (12) and continued more recently by Dr. Michael Linshaw (13). Their preparation is such that when tubules are collapsed and are then made to swell in hypotonic medium, observed changes in tubule volume indicate water and ion movement across the basal-lateral surfaces of the cells. Information then is obtained for flows across one of the epithelial series membranes and the characteristics of half of the problem of transepithelial transport can be ascertained. The usefulness of these findings depends, of course, on the tacit assumption that flow is conducted along similar

routes when the lumen is open and ordinary transcellular movement is taking place. If the tubules are exposed to a bath made hypotonic by a sudden reduction in NaCl, the cells swell in less than one minute to about 60% above their initial volume but then regulate to near their initial volume in less than 7 minutes. Curiously, if active transport pumps are incapacitated by ouabain, or if the basement membrane is removed by collagenase, the cells do not regulate in hypotonic medium until the bathing medium protein concentration is greatly increased. We have shown recently that these observations can be understood if the membrane through which water and ions are conducted is heteroporous, that is, if the membrane contains populations of pores having both high and low reflection coefficients for the permeable solutes. Thus, while water enters the cells driven by the osmotic pressure due to permeable solutes across small highly reflective pores, it is drawn out of the cells across the low reflection large pores by hydrostatic and oncotic pressure. Ions then are entrained on the water streams through the low reflection pores and the cells can relieve themselves of an osmotic burden.

Could this concept of a heteroporous membrane contribute to the solution of the iso-osmotic transport puzzle? Perhaps. It is obvious that if both small and large pores exist in the apical and basal-lateral membranes, water might be entrained across the larger pores and transport, by definition, would be isosmotic. The problem is then, what is the driving force for the water across the larger pores? Certainly, if the cells are truly deformable, the effect of hydrostatic pressure on fluid movement across the tubule would be highly rectified and not very efficient. This is confirmed by experiment. On the other hand, intracellular and extracellular impermeant solutes such as protein could be important

for driving water, particularly considering the large surface areas available in the proximal tubule.

If one models the apical and basal-lateral membranes as heteroporous it is possible to compute the ion and water flows across the series membranes by using known renal intracellular ionic concentrations. We have found recently that if the apical and basolateral membranes are as large as in the proximal tubule, calculations show that water and the passive anion chloride move at nearly the same rate. This indicates that the transport is nearly isosmotic. If the membranes are made more homoporous, that is, with less possibility for entrained ion flow, the need for a separate co-transport facility or paracellular leak for chloride is increased.

What then is the effect of different apical and basal-lateral membrane areas on the tonicity of the transported fluid? Remember first that in the convoluted and straight segments the apical and lateral surface areas are equal while in thick limb the lateral surface area is 10 times larger than the apical and the total area is only about 1/3 that in the convolute. Secondly, for the membrane areas to be important in osmotic transport, a certain degree of decoupling between ions and water is necessary. Therefore, to compare the iso-osmotic transporters such as proximal tubule to the hypertonic transporters such as thick limb, on the basis of membrane areas, we considered a constant co-transport of chloride in these segments and asked whether the effects of the smaller apical and lateral areas in thick limb were sufficient to explain hypertonic transport in that segment. The answer was that the consequent computed ratio of chloride to water movement was about 3 to 1 and indicates that the high resistance water route of the thick limb contributes significantly to the hypertonic transport in that segment. Obviously, other mechanisms such as increased co-transport in this segment could

also account for the hypertonicity of the absorbate but this simple analysis points out that cell structure is certainly disposed to support the tonicity of reabsorbate in the nephron.

In conclusion, we believe that the peculiar cellular configurations and surface areas of the diverse segments of the nephron indicate significant means to alter the tonicity of the transported solutions. Furthermore, iso-osmotic transport takes place when large water movement occurs through large membranes areas across which relatively modest osmotic gradients serve as driving forces.

REFERENCES

1. Welling, L. W. and D. J. Welling. Surface areas of brush border and lateral cell walls in the rabbit proximal nephron. Kidney Int. 8: 343-348, 1975.
2. Welling, L. W. and D. J. Welling. Shape of epithelial cells and intercellular channels in the rabbit proximal nephron. Kidney Int. 9:385-394, 1976.
3. Welling, L W., D. J. Welling, and J. J. Hill. Shape of cells and intercellular channels in rabbit thick ascending limb of Henle. Kidney Int. 13:144-151, 1978.
4. Evan, A. P., Jr., D. A. Hay, and W. G. Dail. SEM of the proximal tubule of the adult rabbit kidney. Anat. Rec. 19:397-414, 1978.
5. Curran, P. F. and J. R. MacIntosh. A model system for biological water transport. Nature (London) 193:347, 1962.
6. Diamond J. M. and W. H. Bossert. Standing-gradient osmotic flow. A mechanism for coupling of water and solute transport in epithelia. J. Gen. Physiol. 50:2061-2083, 1967.

7. Welling, L. W. and J. J.Grantham. Physical properties of isolated perfused renal tubules and tubular basement membranes. J. Clin. Invest. 51:1063-1075, 1972.

8. Grantham, J. J. Vasopraessin: effect on deformability of urinary surface of collecting duct cells. Science 168:1093-1095, 1970.

9. Welling D. J., L. W. Welling, and J. J. Hill. Phenomenological model relating cell shape to water reabsorption in proximal nephron. Am. J. Physiol. 234:F308-F317, 1978.

10. Grantham, J. J., P. B. Qualizza, and L. W. Welling. Influence of serum proteins on net fluid reabsorption of isolated proximal tubules. Kidney Int. 2:66-75, 1972.

11. Tisher, C. C. and J. P. Kokko. Relationship between peritubular oncotic pressure gradients and morphology in isolated proximal tubules. Kidney Int. 6:146-156, 1974.

12. Dellasega, M. and J. J. Grantham. Regulation of renal tubule cell volume in hypotonic media. Am. J. Physiol. 224:1288-1294, 1973.

13. Linshaw, M. A. and J. J. Grantham. Effect of collagenase and ouabain on renal cell volume in hypotonic media. Am. J. Physiol. 238:F491-498, 1980.

Adv. Physiol. Sci. Vol. 3. Physiology of Non-excitable Cells
J. Salánki (ed.)

SENSITIVITY AND INSTABILITY IN STANDING GRADIENT FLOW

Isaak Rubinstein and Lee A. Segel
Department of Applied Mathematics, Weizmann Institute, Rehovot, Israel

1. Introduction and formulation

This paper is concerned with the simplest form of standing gradient flow, essentially as originally proposed by Diamond and Bossert (1967). Two new points are brought out, that the flow is very sensitive to one of the boundary conditions and that under certain circumstances the flow is unstable.

Consider a straight channel of length L, cross-sectional area a and circumference c. Let x^* measure distance along the channel, starting from its closed end $x^* = 0$. Assume that solute is actively pumped across the channel walls at rate $N^*(x^*)$. An internal solute concentration different from the fixed concentration C_0 outside the tube induces water flow across the bounding membrane of permeability P.

Mathematical formulation of the problem requires equations of solute and water balance for the velocity v^* and the solute concentration C^* as functions of x^* and the time t^*. We shall write the equations in terms of the following dimensionless variables:

$$x = \frac{x^*}{\delta},\quad t = \frac{t^*}{(aC_0/cN_0)},\quad C = \frac{C^*}{C_0},\quad v = \frac{v^*}{cN_0\delta/aC_0},\quad N = \frac{N^*}{N_0}. \tag{1.1}$$

Here δ is a 'typical' length and N_0 is a typical solute pumping rate; these parameters will be specified later. The equations are

$$C = 1 + \nu v_x,\quad C_t = N - (vC - \eta C_x)_x, \tag{1.2a,b}$$

in terms of the dimensionless parameters

$$\nu = \frac{N_0}{PC_0^2},\quad \eta = \frac{aC_0D}{cN_0\delta^2}. \tag{1.3a,b,c}$$

Here D denotes solute diffusivity and subscripts x and t imply partial differentiation.

These equations are essentially identical with those employed by Diamond and Bossert (1967) except that the possibility of time variation has been taken into account. Diamond and Bossert (1967) assumed that the solute concentration at the open end ($x^*=L$) was C_0. To be more accurate (as was pointed by Weinbaum and Goldgraben, 1972) one should match the concentration at the open end with the concentration determined by solving a suitable problem for solute and water concentration in the lumen into which the tube in question empties. Much of the effect of this generalization can be seen by taking the boundary condition at the open end to be $C^* = C_1$, where C_1 is to be regarded as a positive parameter. The other boundary conditions will be the traditional ones associated with a closed end at $x^* = 0$. In dimensionless form, the boundary conditions are

$$\text{at } x = 0\text{: } v = 0,\ C_x = 0; \qquad \text{at } x = \lambda\text{: } C = C_1/C_0. \quad (1.4a,b,c)$$

Here $\lambda = L/\delta$.

Diamond and Bossert (1967) assumed that active solute transport was confined to a region near the closed end of the tube, and modelled this by the assumption

$$N^*(x^*) = N_0,\ 0 \leq x^* \leq \delta;\ N^*(x^*) = 0,\ \delta < x^* \leq L;$$

i.e.

$$N(x) = 1,\ 0 \leq x < 1;\ N(x) = 0,\ 1 < x \leq \lambda. \quad (1.5)$$

Segel(1970) observed that in almost all the numerical results of Diamond and Bossert (1967) the parameter ν could be regarded as small, while η could be written in the form

$$\eta = \lambda^2/(\nu\kappa^2)\ [\text{so } \kappa^2 \equiv cPC_0L^2/(aD)], \quad (1.6)$$

and κ could be assumed to be of order of magnitude unity. Perturbation methods (explained more fully in the chapter on standing gradient flow by Lin and Segel, 1974) could then be employed to obtain an approximate expression for a dimensionless version of the emergent osmolarity Os, where

$$Os = \frac{Os^*}{C_0} = \frac{(cN_0\delta/a)}{C_0v^*(L)} = \frac{1}{v(\lambda)}. \quad (1.7)$$

A steady situation ($\partial/\partial t = 0$) was assumed. For the case

$$C(\lambda) = 1 \quad (1.8)$$

considered by Diamond and Bossert (1967), Segel (1970) obtained the approximate formula

$$Os = \frac{\cosh \kappa}{\cosh \kappa - 1}, \quad (1.9)$$

after making the further assumption that λ was large. This formula was in excellent agreement with almost all of the numerical results of Diamond and Bossert (1967), and has been used by several authors as a starting point for comparison of the Diamond-Bossert theory with experimental data.

A major benefit that flows from the analysis of a simple model is the identification and interpretation of important dimensionless parameters. The qualitative role that these parameters play will often be retained when complicating effects are considered.

In the present case, three dimensionless parameters govern the problem -- λ, κ, and ν. The first of these is obviously a measure of the extent to which active solute pumping is confined to the closed end of the channel. The results show little sensitivity to λ -- for example, quite similar graphs of emergent osmolarity as a function of λ are obtained for $\lambda = 2$ and $\lambda = \infty$ (Segel, 1970).

To discern the meaning of κ, we write

$$\kappa^2 = \frac{[c(C_a - C_0)PL]C_0}{aD[(C_b - C_0)/L]} \cdot \frac{C_b - C_0}{C_a - C_0}. \tag{1.10}$$

Here C_a is a solute concentration chosen so that the square-bracketed factor in the numerator is the rate of water flow into the channel across its boundaries. The concentration C_b is selected so that the square-bracketed factor in the denominator equals the solute gradient at the channel exit, thus insuring that aD times this bracket equals the diffusive flux (F^*_{diff}) of solute out of the channel. Since the rate at which water emerges from the channel equals the rate at which water permeates the channel walls, the convective efflux of solute (F^*_{conv}) equals the product of the concentration C_0 at the open end times the square-bracketed factor in the numerator of Eq. (1.10). Consequently

$$\kappa^2 = \frac{F^*_{conv}}{F^*_{diff}} \phi, \text{ where } \phi \equiv \frac{C_b - C_0}{C_a - C_0}. \tag{1.11}$$

The factor ϕ in (1.11) is generally expected to be of magnitude unity. The interpretation of κ^2 is thus given by

$$\kappa^2 \approx F^*_{conv}/F^*_{diff}. \tag{1.12}$$

We remark that by its definition

$$Os = (F^*_{conv} + F^*_{diff})/(F^*_{conv}). \tag{1.13}$$

Comparing Eqs. (1.11) and (1.13) we infer that a rough approximation to Os should be given by

$$Os = 1 + \phi\kappa^{-2} \tag{1.14}$$

where ϕ is a factor that normally is of magnitude unity. As is pointed out by Segel (1970) if Eq. (1.9) is approximated for the case κ^2 small, then agreement with (1.14) is obtained if $\phi = 2$. For large κ^2, Os approaches zero as indicated by (1.14). And indeed, the formula

$$Os = 1 + 2\kappa^{-2} \tag{1.15}$$

provides a rough match to Eq. (1.9) for all values of κ^2. For present purposes, this is important only as a check on the reasoning which led to the principal point we wish to make here, that the dimensionless parameter κ^2 should be interpreted as describing the relative importance of solute convection and diffusion, in the form of the ratio of convective to diffusive emergent solute transport.

In an attempt to provide a better interpretation than we have heretofore for ν, we begin by asking what volume of water w must be added to an existing volume V to keep constant concentration, if an amount of solute m is added to the initial amount M. From $(M + m)/(V + w) = M/V$ we find $w = mV/M$. If we consider a unit time, in the case under consideration $M = aLC_0$, $m = N_0 c\delta$, $V = aL$, so an amount of water

$$w = N_0 c\delta / C_0 \tag{1.16}$$

should be added per unit time to maintain a constant solute concentration in the face of solute pumping at rate N_0 per unit area. On the other hand, the actual rate of water inflow is $PcL(C_a - C_0)$. The ratio of the two rates is

$$\frac{N_0}{PC_0^2} \cdot \frac{\delta}{L} \cdot \frac{C_0}{C_a - C_0} = \nu \cdot \frac{1}{\lambda} \cdot \frac{1}{(C_a/C_0) - 1}. \tag{1.17}$$

The last two factors tend to cancel, so that ν can be regarded as estimating the ratio between the water inflow rate required to keep solute concentration from building up and the actual inflow rate. Although this ratio seems small in physiological situations, there is some solute build-up because of spatial inhomogeneities. On the other hand, a small value of ν explains the observation that the concentration of secreted fluid seems virtually independent of the rate of active transport. To summarize

$$\kappa^2 \approx \frac{\text{convective solute flux}}{\text{diffusive solute flux}}, \quad \nu \approx \frac{\text{iso-osmotic water inflow (well-stirred)}}{\text{actual water inflow}}.$$

2. The effects of a slight change in the lumen solute concentration

We now wish to consider a generalization of the analytic results to the case wherein boundary condition (1.8) is replaced by

$$C(\lambda) = 1 + \beta\nu, \ \beta \text{ a constant.} \tag{2.1}$$

Since ν is a small parameter and β is assumed to be of magnitude unity, the new problem differs only by a slight change in the imposed concentration at the open end of the tube. The calculations proceed as before with the assumptions

$$C(x;\nu) = C^{(0)}(x) + \nu C^{(1)}(x) + \ldots, \quad v(x;\nu) = v_0(x) + \nu v_1(x) + \ldots \tag{2.2a,b}$$

The only difference is that the former boundary condition $C^{(1)}(\lambda) = 0$ becomes

$$C^{(1)}(\lambda) = \beta. \tag{2.3}$$

The results are

$$C^{(0)} \equiv 1, \ C^{(1)} = v_x^{(0)} \tag{2.4}$$

$$v^{(0)} = x - K_1 \sinh(\kappa\lambda^{-1}x) \text{ for } 0 \leq x \leq 1; \tag{2.5}$$

$$v^{(0)} = 1 - K_2 \cosh\kappa(1-\lambda^{-1}x) - (\beta\lambda\kappa^{-1})\sinh\kappa(1-\lambda^{-1}x) \text{ for } 1 < x \leq \lambda.$$

As before, we assume for simplicity that λ is large. Then

$$K_1 = \frac{\lambda}{\kappa}\,\frac{\cosh\kappa-\beta}{\cosh\kappa}, \quad K_2 = \frac{1-\beta\cosh\kappa-\beta\lambda\kappa^{-1}\sinh\kappa}{\cosh\kappa}, \tag{2.6a,b}$$

and (1.9) is generalized to

$$Os = \frac{\cosh\kappa}{(1-\beta)\cosh\kappa - 1 + \beta\lambda\kappa^{-1}\sinh\kappa}. \tag{2.7}$$

Interpretation of this result is facilitated if we write it in the form

$$Os = \frac{1}{[\overline{Os}(\kappa)]^{-1} + \beta(\lambda\kappa^{-1}\tanh\kappa - 1)}, \tag{2.8}$$

where $\overline{Os}(\kappa)$ is the dimensionless osmolarity obtained in Eq. (1.9) when $\beta = 0$ (the "classical" result). For illustrative purposes, consider a situation in which measured permeabilities are so small that κ has the value 0.1. From Eq. (1.9)

$$\overline{Os}(\kappa) \simeq (\kappa^2/2)^{-1} = 200,$$

so that the "classical" analysis would lead to an osmolarity that is an unacceptable two orders of magnitude larger than the ambient solute concentration. But if $\beta \approx 5$ and $\lambda \approx 10$, say, then Eq. (2.8) gives $Os \approx 0.02$, a drastically lower value.

And if ν is small as assumed, this drastic change has been obtained merely by the small concentration alteration $C^* = C_0 \rightarrow C^* = (1+5\nu)C_0$ at the open end.

Putting the matter more generally, we have shown analytically that the flow modelled by Diamond and Bossert (1967) can change markedly if the concentration at the exit is altered slightly from C_0. This sensitivity has been previously noted in one form or another by Weinbaum and Goldgraben (1972), Huss et al (1976), Andreoli and Schafer (1978), and Weinstein and Stephenson (1979). What is novel here is the particularly simple context in which the result appears.

One concludes that there is a certain inappropriateness in the controversy (see for example Hill, 1975, and Diamond, 1977) as to whether Eq. (1.9) is in accord with experiments. It appears that an almost immeasurable factor can have a strong quantitative effect, so that there is little point in a detailed comparison between experiments and the osmolarity predicted by the classical standing gradient model. The physical reason for the effect seems to be that with relatively large permeability ($\nu << 1$) a small increase in the exit concentration will draw in a large compensating water flow.

3. Possible instability of absorbing standing gradient flow

Let us now consider a general absorbing tubule in which $N^*(x^*)$ is any negative function with (for definiteness in defining the dimensionless variables) a maximum magnitude N_0. Let us choose the length scale equal to L. We eliminate C by substituting Eq. (1.2a) into (1.2b). We then integrate with respect to x, with lower limit $x = 0$, and apply the boundary condition (1.4b) in the form $v_{xx} = 0$. The result is

$$\nu v_t = \nu\eta v_{xx} - v - \nu v v_x + M;\ v(0) = 0,\ v_x(1) = 0, \quad (3.1a,b,c)$$

where

$$M(x) = \int_0^x N(s)\,ds. \quad (3.2)$$

Boundary condition (3.1c) follows from the classical form $C = 1$ of the original boundary condition (1.4c). The equations of (3.1) thus constitute a rearranged version of the standard standing gradient flow problem.

Let $\bar{v}(x)$ be a time independent solution of (3.1), so that

$$\nu\eta\bar{v}_{xx} - \bar{v} - \nu\bar{v}\bar{v}_x + M = 0;\ \bar{v}(0) = 0,\ \bar{v}_x(1) = 0. \quad (3.3a,b,c)$$

The purpose of this section is to show that under certain conditions $\bar{v}(x)$ is an unstable solution, in that small perturbations from this solution will grow in the course of time. To show this we introduce the perturbation $v'(x,t)$:

$$v(x,t) = \bar{v}(x) + v'(x,t). \tag{3.4}$$

Upon substituting Eq. (3.4) into Eqs. (3.3) and deleting nonlinear terms on the assumption that v' is small, we obtain

$$\nu v'_t = \nu\eta v'_{xx} - v' - \nu(v'\bar{v})_x. \tag{3.5}$$

Continuing the standard practices of linear stability theory we seek a solution of the form

$$v' = u(x)\exp(\sigma t), \sigma \text{ a constant.} \tag{3.6}$$

The equation for u is obtained by substituting Eq. (3.6) into Eq. (3.5). We simplify this equation by restricting ourselves to situations wherein ν is large (situations of opposite character to those considered in the Segel (1970) analytic approximations). With this assumption we obtain

$$u_{xx} + (wu)_x = \bar{\sigma}u;\ u(0) = 0,\ u_x(1) = 0, \tag{3.7a,b,c}$$

where we have made the definitions

$$\bar{\sigma} = \sigma/\eta,\ w(x) = -\bar{v}(x)/\eta. \tag{3.8a,b}$$

The equations of (3.7) constitute an eigenvalue problem of a well-studied form. Nontrivial solutions u exist only for certain values of $\bar{\sigma}$, and these eigenvalues can be shown to be real numbers. Since $\bar{\sigma}$ is proportional to the growth rate σ of Eq. (3.6), small perturbations will grow exponentially in time if and only if there is a positive eigenvalue $\bar{\sigma}$. Perturbations will decay exponentially if all the $\bar{\sigma}$ are negative. We will now demonstrate that the "marginal" case $\bar{\sigma} = 0$ that divides instability from stability, is a possible eigenvalue for a broad class of steady solutions $\bar{v}(x)$. One would then conjecture that there is a class of modifications of $\bar{v}$, obtainable by modifications of the integrated transport M(x), that would push the zero eigenvalue into the positive domain, and thereby would destabilize the system. We will quote a theorem to this effect.

Turning then to the marginal situation, we denote by $r(x)$ the solution to Eqs. (3.7) when $\bar{\sigma} = 0$. Elementary integration methods show that the solution to Eq. (3.7a) and boundary condition (3.7b) is

$$r = A \exp[-\int_0^x w(\xi)d\xi]\int_0^x \exp[\int_0^\theta w(\xi)d\xi]d\theta, \tag{3.9}$$

for any constant A. Imposition of boundary condition (3.7c) leads to the result that a nontrivial solution ($A \neq 0$) exists if the following "neutral stability" condition holds:

$$w(1)\int_0^1 \exp[-\int_\theta^1 w(\xi)d\xi]d\theta = 1. \tag{3.10}$$

Note from Eq. (3.10) that a necessary condition for neutral stability is $w(1) > 0$. This means that in the steady solution the velocity $\bar{v}$ must be directed inwards at the mouth of the tube, a characteristic of absorbing flow.

To show that Eq. (3.10) can be satisfied with a physically plausible choice of w(x), consider the possibility

$$w(x) = \alpha \tanh kx, \tag{3.11}$$

which is of the general form found by Diamond and Bossert (1968) in their study of absorbing flows. Substitution of Eq. (3.11) into Eq. (3.10) yields

$$I(\alpha,k) = 1, \text{ where } I(\alpha,k) = \alpha \tanh k \int_0^1 \left[\frac{\cosh k\theta}{\cosh k}\right]^{\alpha/k} d\theta. \tag{3.12}$$

Table I gives values of I for several choices of the parameters α and k.

Table 1. Values of the integral I for various values of the parameters k and α defined in Eq. (3.11).

α	k	I	α	k	I
0.2	1	0.14	1	10	0.63
1		0.58	5		1.01
5		1.18	10		1.12
0.2	2	0.18	1	20	0.63
1		0.65	10		1.12
5		1.08			
0.2	5	0.18			
1		0.64			
5		1.01			
10		1.12			
20		1.71			
40		3.33			

It is clear that the neutral stability condition (3.11) can be satisfied by reasonable choices of the parameters.

We have shown that the marginal state can be attained for a broad class of functions w and hence for a corresponding class of transport functions M or N. We now indicate briefly how to conclude the existence of truly unstable flow. To this end it is helpful to introduce the change of variable

$$u = y \exp[-\frac{1}{2}\int_0^x w(\xi)\, d\xi] \tag{3.13}$$

with which Eqs. (3.7) take the standard form

$$y_{xx} + (\tfrac{1}{2}w_x - \tfrac{1}{4}w^2)y = \bar{\sigma}y;\ y(0) = 0,\ y_x(1) - \tfrac{1}{2}w(1)y(1) = 0. \tag{3.14}$$

Having demonstrated that there exists a nontrivial solution of Eqs. (3.14) with $\bar{\sigma} = 0$, we conclude that if $w(x)$ is replaced by a different function $W(x)$ then there are nontrivial solutions to Eqs. (3.14) with positive $\bar{\sigma}$, provided that

$$w_x - \tfrac{1}{2}w^2 > W_x - \tfrac{1}{2}W^2,\ w(1) > W(1).$$

This result follows from comparison theorems for ordinary differential equations: see in particular Birkhoff and Rota (1969), Chapter 10, Section 8.

The physical reason for the possible instability is not difficult to discern. Consider an imaginary slice of fluid bounded by the tubule walls and two parallel faces. In an absorbing tubule under steady-state conditions, convection into the slice is greater than convection out -- with solute accumulation being prevented by outward transport through the lateral walls. If a perturbation should result in a cloud of concentration increase, convection tends to concentrate the solute further, but this tendency toward instability will triumph only if it outweighs the contrary effects of diffusion. In a secreting tubule, on the other hand, less solute enters through one face than leaves through the opposite face; here convection and diffusion both act to disperse solute increases, so that instability is impossible.

The general argument just given shows that instability probably occurs generally in absorbing tubules for sufficiently small diffusivities, even though our demonstration has been carried out under the assumption that ν is large. (Such an assumption is not physiologically unreasonable. The data on parameters collected by Diamond and Bossert (1967) for example, permits a value of ν as high as 100.)

To conclude, calculations backed up by physical reasoning suggest that small perturbations could destabilize the standard standing gradient flow in situations where solute diffusivity is small and velocity variation is rapid. Determination of the ultimate form of the solution must be left to future work, but one can at least suggest that it might be worth looking for unusual features in strongly absorbing channels.

ACKNOWLEDGEMENT. The work of Lee A. Segel was partially supported by NSF Grant MCS79-03548 -- to Rensselaer Polytechnic Institute, where he is a Research Professor.

Any opinions, findings, and conclusions or recommendations expressed in this publication are those of the authors and do not necessarily reflect the views of the National Science Foundation.

REFERENCES

Andreoli, T. E. and Schafer, J. A. (1978). Volume absorption in the pars recta. III. Luminal hypotonicity as a driving force for isotonic volume absorption. Am. J. Physiol. 234, F349-F355.

Birkhoff, G. and Rota, G-C (1969). Ordinary Differential Equations (2nd ed.) Blaisdell, Waltham.

Diamond, J. M. (1977). The epithelial junction: bridge, gate, and fence. The Physiologist 20, 10-18.

Diamond, J. M. and Bossert, W. H. (1967). Standing-gradient osmotic flow: a mechanism for solute-linked water transport in epithelia. J. Gen. Physiol. 50 2061-83.

Diamond, J. M. and Bossert, W. J. (1968). Functional consequences of ultrastructural geometry in "backwards" fluid transporting epithelia. J. Cell Biol. 37, 694-702.

Hill, A. E. (1975). Solute-solvent coupling in epithelia: a critical examination of the standing-gradient osmotic flow theory. Proc. R. Soc. Lond. B. 190, 99-114.

Huss, R. E., Stephenson, J. L., and Marsh, D. J. (1976). Mathematical model of proximal tubule solute and water transport. Physiologist 19, 236 (abstract).

Lin, C. C. and Segel. L. A. (1974). Mathematics Applied to Deterministic Problems in the Natural Sciences, Macmillan, New York.

Segel, L. A. (1970). Standing-gradient flows driven by active solute transport. J. Theoret. Biol. 29, 233-50.

Weinbaum, S. and Goldgraben, J. R. (1972). On the movement of water and solute in extracellular channels with filtration, osmosis, and active transport. J. Fluid Mech 53, 481-512.

Weinstein, A. M. and Stephenson, J. L. (1979). Electrolyte transport across a simple epithelium. Biophys. J. 27, 165-186.

Adv. Physiol. Sci. Vol. 3. Physiology of Non-excitable Cells
J. Salánki (ed.)

ULTRASTRUCTURE OF EPITHELIA AS RELATED TO MODELS OF ISO-OSMOTIC TRANSPORT

Arvid B. Maunsbach
Department of Cell Biology, Institute of Anatomy, University of Aarhus, Denmark

INTRODUCTION

Structural parameters are important in most models of epithelial fluid transport. The structural parameters may concern general characteristics of the epithelia, such as the organization of intracellular structures, intercellular junctions and sub-epithelial compartments, or they may relate to quantitative characteristics e.g. of surface areas of epithelial cells and dimensions of transport pathways.

The aim of this presentation is to relate some recent ultrastructural observations on kidney epithelia to models and mechanisms proposed for iso-osmotic epithelial transport. Emphasis is placed on quantitative information derived from stereological analysis and the interpretation of qualitative observations.

ULTRASTRUCTURE AND DIMENSIONS OF THE LATERAL INTERCELLULAR SPACE

On the basis of electrophysiological studies Boulpaep (1971) demonstrated the existence of a paracellular pathway in the renal proximal tubule. There is now much evidence that the paracellular pathway or shunt plays an important role in epithelial salt and fluid transport. At the ultrastructural level the paracellular pathway consists of the tight junction and the lateral intercellular space (LIS). In several models of epithelial salt and fluid transport the structural parameters of the lateral intercellular space are important (Diamond and Bossert, 1967; Sackin and Boulpaep, 1975; Welling et al., 1978). To provide a basis for further correlations between the structure and the function of the lateral intercellular space in a physiologically well-characterized epithelium, an ultrastructural study was carried out on the Necturus proximal tubule using serial sectioning and stereological analysis (Maunsbach and Boulpaep, 1980a, 1980b).

The three-dimensional organisation of the lateral intercellular space of the Necturus proximal tubule and, in particular, the lateral cell membrane, was analysed by serial sectioning. The ultrathin sections (average section thickness 350 Å) were cut at right angle to the axis of proximal tubules from control animals. Analysis of the serial sections revealed that the cell membrane projections observed in single sections were true folds of the cell membranes and rarely finger-like projections (Maunsbach and Boulpaep, 1980b). The folds were usually oriented parallel to the basement mem-

brane in contrast to most folds of mammalian proximal tubule cells (Maunsbach, 1973). Folds from adjacent Necturus cells often interdigitated extensively and therefore increased the path depth (luminal-peritubular depth) of the paracellular shunt. However, when the lateral intercellular spaces were dilated the folds did not interdigitate and the path depth became shorter. Thus, the width of the LIS in the Necturus proximal tubule influenced the path depth of the LIS.

Serial sectioning also showed that the regions of LIS with interdigitating cell membranes and long LIS path depth were located adjacent to regions where there were no or few folds and where the path depth was short. The latter regions therefore served as luminal-peritubular channels or shunts within the lateral intercellular space. This heterogeneity in interspace geometry complicates the development of detailed models describing the transport properties of the interspace.

The stereological analysis was carried out on complete cross-sections of Necturus proximal tubules which were oriented with their axis perpendicular to the section (Maunsbach and Boulpaep, 1980a). The areas of the cell membranes and the dimensions of the lateral intercellular space were analysed in free-flow tubules and in tubules with experimentally increased or decreased intraluminal pressures. The surface densities of the cell surfaces were determined stereologically and used to calculate the absolute cell surfaces/mm length of tubule. The surface density of the luminal cell surface (excluding the microvilli) and of the basal cell surface, both of which were assumed to be oriented perpendicular to the section, was determined from $S_V = \frac{\pi}{2} \cdot N_i/L_T$, where N_i is the number of intersections between the surface and the test lines and L_T is the total length of the test lines. Randomly oriented surfaces (lateral intercellular spaces in complete tubular cross-sections) were determined using the formula $S_V = 2 \cdot N_i/L_T$. The brush border surface area was calculated from the density of microvilli on the luminal cell surface (N_S, in microvilli/μm^2) and the length and diameter of the microvilli. The density of microvilli was determined from the formula $N_S = N_l/(m+t)$ where N_l is the number of microvilli projecting from a measured length of luminal cell surface, m the diameter of the microvilli and t the section thickness (Gundersen, personal communication).

Table 1. Cell membrane areas in Necturus proximal tubule

	$10^6 \mu m^2$/mm tubule	ratio
Luminal cell surface		
Excluding microvilli	0.207	1
Including microvilli	3.81	18.4
Lateral cell surface	2.00	9.7
Basal cell surface	0.340	1.6

The absolute and relative areas of the cell surfaces of Necturus proximal tubule cells in control animals are shown in Table 1. The area of the luminal cell surface, including the microvilli, is somewhat larger than the combined area of the lateral and peritubular cell membrane and the area of the lateral cell membrane facing the lateral intercellular space is much greater than the area of the peritubular (basal) cell surface. In the rabbit proximal tubule the luminal surface and the baso-lateral cell surfaces are equal in area (Welling and Welling, 1975). The microvilli enlarged the luminal cell surface of Necturus cells by a factor of about 18 which is less than half the enlargement caused by the microvilli in the first convoluted segment (S1) of the rat proximal tubule (Maunsbach, 1973).

The dimensions of the lateral intercellular space were calculated from the volume of the lateral intercellular space and the length of the tight junction and the peritubular opening of the interspace. The path depth of the lateral intercellular space (d) was calculated both for the condition when the path is assumed to follow all the folds of the lateral cell membranes and for the condition when the pathway does not follow the small folds of the membrane, such as when the lateral intercellular spaces are dilated. When the path depth of LIS is maximal the width (w) is at its minimum value and at the minimum path depth the width of the lateral intercellular space is maximal (Table 2). Since the lateral cell membranes in free-flow control tubules were only in part parallel the values for path depth and intercellular space width in control tubules fall between the maximum and minimum values.

Table 2. Dimensions of paracellular pathway in Necturus proximal tubule

Tight junction length, mm/mm tubule length	19.2
Peritubular length of LIS, mm/mm tubule length	33.5
Volume density of LIS, $10^{-2}\mu m^3/\mu m^3$	2.78
Path depth of LIS (d), min.-max. in μm	23.2-41.2
Width of LIS (w), min.-max. in nm	178-300

The minimum path depth of the lateral intercellular space (23.2 μ) is only slightly longer than the height of the cell (19.5 μ) and even the maximum path depth (41.2 μ), which assumes complete interdigitation of all lateral folds of the cell membrane is only about twice the cell height (Table 2). The expression $d^2/(w/2)$ (or d^2/r for a cylindrical channel with radius r and channel length d), which includes the structural parameters that determine the emerging concentration of the absorbate in the standing gradient theory (Segel, 1970), shows minimum-maximum values of 3.6-19.1 mm with the observed dimensions of the lateral intercellular space in free-flow tubules of control animals. However, these values are more than one or two orders of magnitude lower than the value of 500 mm calculated by Hill (1975) as a minimum value for iso-osmotic transport according to the standing gradient theory. Thus, the present quantitative observations are not compatible with iso-osmotic transport according to the standing gradient theory in the Necturus proximal tubule.

The circumference of the proximal tubule cells at the level of the basement membrane is approximately 1.7 times the circumference at the level of the tight junction (peritubular length of LIS/length of tight junction, Table 2). In comparison, the circumference of the proximal tubule cell of the rabbit kidney increased by a factor of 15.7 from a zone adjacent to the tight junction to the zone close to the peritubular basement membrane (Welling and Welling, 1976). In the rabbit proximal tubule it has been suggested that the forces required for water flow in the lateral intercellular space show a relationship to the cell shape, in particular the circumference of the cell at each distance from the tight junction (Welling et al., 1978). It is not known whether a similar relationship exists in the Necturus tubule, but the present observation of only a small increase in cell circumference from cell apex to cell base in Necturus is compatible with this possibility since the rate of fluid absorption in the proximal tubule is considerably lower in Necturus than in the rat.

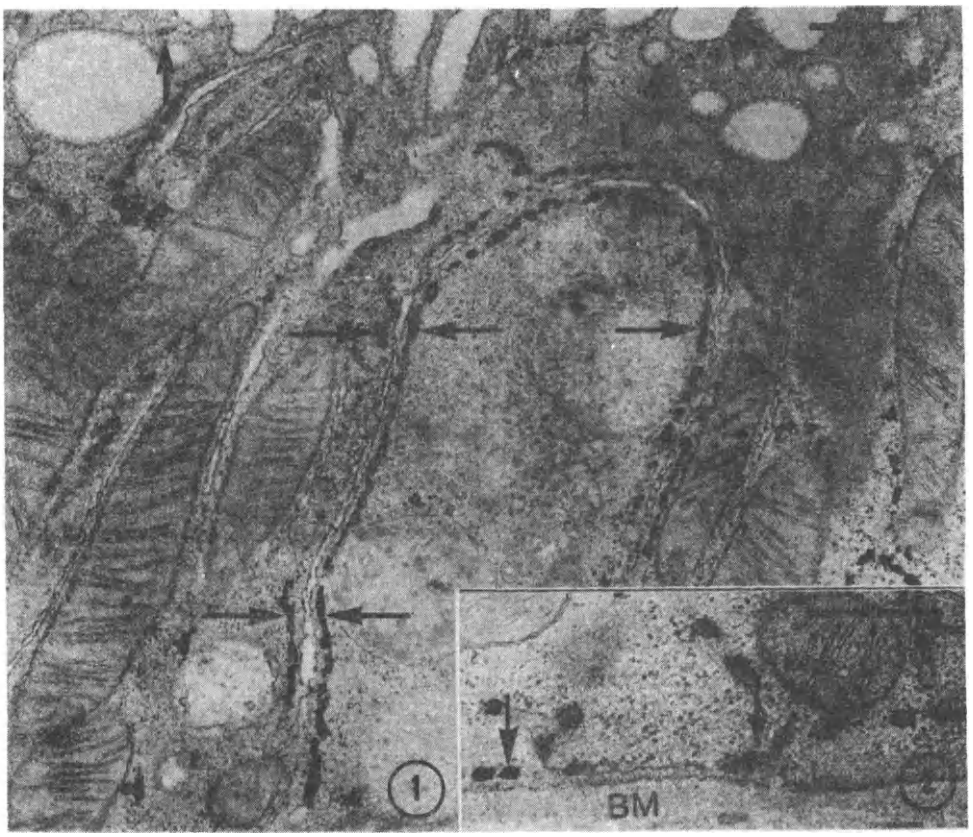

Fig. 1. Localisation of glucose-6-phosphatase activity in the paramembranous endoplasmic reticulum (PER) of rat proximal tubule. The PER is located close to the lateral cell membranes (horizontal arrows) and the luminal cell membranes (vertical arrows). Bar, 0.5 μm. Fig. 2. Localisation of glucose-6-phosphatase in PER adjacent to the peritubular cell membrane of rat proximal tubule cell (arrows). BM, basement membrane. Bar,0.5 μm.

THE PARAMEMBRANOUS ENDOPLASMIC RETICULUM (PER) - A TRANSCELLULAR PATHWAY?

In 1964 Ericsson showed that part of the endoplasmic reticulum in rat proximal tubule cells is located close to the lateral cell membrane and suggested that this part of the endoplasmic reticulum, which he called the paramembranous tubular system, might be involved in transport functions in these cells (Ericsson, 1964). The system has since been further studied by means of different ultrastructural methods (Jacobsen and Jørgensen, 1973; Møllgård and Rostgaard, 1978; Rostgaard amd Møllgård, 1980). It consists of anastomosing tubules and flattened cisternae located close to the apical cell surface and the lateral and basal cell membranes. It has been referred to as the tubulo-cisternal endoplasmic reticulum (TER) and speculative terms such as transport-functioning ER or transcellular ER have been discussed (see Møllgård and Rostgaard, 1978). We prefer the term paramembranous ER (PER), since it is a neutral term emphasizing the close relation-

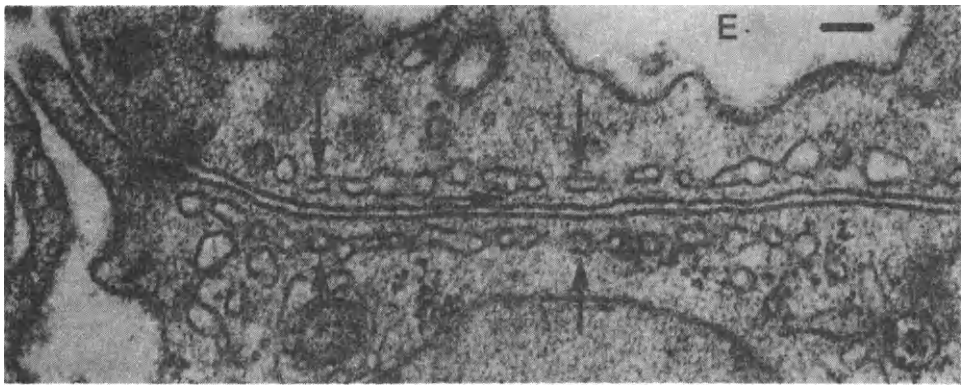

Fig. 3. Paramembranous endoplasmic reticulum (PER) located close to the lateral cell membranes of proximal tubule cells in the rat kidney (vertical arrows). There is no contact between the PER and the lateral cell membranes. In places an electron dense material forms a layer in between the PER and the lateral cell membrane (horizontal arrow). E, endocytic vacuole; TJ, tight junction; MV, microvilli. Bar, 0.1 µm.

ship of the system to the cell membrane and that it is part of the endoplasmic reticulum.

It is a crucial question in epithelial physiology whether or not there are also transcellular (transepithelial) channels through epithelia, in addition to the paracellular pathway. Such channels could be expected to dramatically influence the functional properties of an epithelium and would have to be included in models of iso-osmotic epithelial transport. Since the PER system is located close to both the luminal cell membrane and the baso-lateral cell membrane, and apparently forms a continuous system within the proximal tubule cells, it is necessary to critically examine the possibility that it forms transepithelial channels. We have therefore examined the proximal tubule cells of the rat kidney in ultrathin section by high resolution electron microscopy and determined the ultrastructural localisation of glucose-6-phosphatase and Na,K-ATPase, cytochemical markers of the endoplasmic reticulum (Ericsson and Jakobsson, 1968) and the baso-lateral membrane, respectively.

Glucose-6-phosphatase was located by the method of Teutsch (1978) and observed in the PER system as well as the other parts of the endoplasmic reticulum (Figs. 1 and 2). Enzyme positive components were observed close to the luminal (Fig. 1) as well as the peritubular cell membranes (Fig. 2). The lateral cell membranes were often followed by components of PER that were glucose-6-phosphatase positive. This enzyme activity, however, was never observed in the baso-lateral cell membrane. Na,K-ATPase, located through its potassium-stimulated p-nitrophenylphosphatase activity by the one-step procedure of Mayahara et al. (1980), was located in the baso-lateral cell membrane, but was never associated with the PER system or other cytoplasmic membranes. These cytochemical observations do not provide evidence for a continuity between the cell membrane and the membranes of the PER. Furthermore, careful study of ultrathin sections of proximal tubule cells, following glutaraldehyde and/or osmium tetroxide fixation and dif-

ferent combinations of en bloc staining and section staining with uranyl acetate and lead citrate, showed that the lateral cell membrane was not in direct continuity or contact with the PER system (Fig. 3).

It is noteworthy that a variety of tracers, demonstrable by electron microscopy have been used to locate transport pathways in the proximal tubular epithelium, both from the luminal and the peritubular side. However, in no case have tracers been observed in a location corresponding to the PER. Microperoxidase (mol. wt. about 1700) was also excluded from this system (Horster and Larsson, 1976). It is concluded that there is presently no ultrastructural evidence in proximal tubule cells, where the PER system has been most extensively investigated, that the paramembranous endoplasmic reticulum forms transcellular (transepithelial) channels.

SUB-EPITHELIAL TRANSPORT BARRIERS

The iso-osmotic transport pathway in the proximal tubule extends from the tubule lumen to the peritubular capillary. As a consequence the pathway is in part intraepithelial and in part subepithelial. Sackin and Boulpaep (1975) included subepithelial compartments and barriers in their model of iso-osmotic transport. However, in many models of iso-osmotic transport in kidney or other epithelia the subepithelial part of the pathway has been neglected even though it may include large subepithelial compartments with complex barriers.

The necessity of considering subepithelial structures and compartments when analysing transport pathways through epithelia was recently stressed by Pedersen et al. (1978, 1980), who quantitatively studied the relationship between tubules and peritubular capillaries in the rat renal cortex. The peritubular cortical interstitium was divided into the narrow interstitium, which is located where the capillary wall is in immediate contact with the peritubular surface, and the wide interstitium, which contains the interstitial cells (Fig. 4). The narrow interstitium primarily contains the tubular and capillary basement membranes and represents 0.7% of the volume of the renal cortex (Pedersen et al., 1980). The wide interstitium corresponds to 6.0% of the cortical volume and the interstitial cells constitute almost half of that volume. The peritubular surface of the proximal tubule is to a larger extent in contact with the wide interstitium (57.5%) than it is with the narrow interstitium (42.4%). The total thickness of the narrow interstitium, from the peritubular cell membranes to the capillary endothelium, is somewhat variable, but in many regions less than 2000 Å. However, the distance between the peritubular capillary and many regions on the peritubular surface in the wide interstitium may be up to several µm. Thus, the transport pathways through the interstitium vary considerably with respect to length (Fig. 4). The ultrastructure of the capillary wall varies also in relation to the narrow and the wide interstitium. Not only does a major part (59.6%) of the capillary surface face the narrow interstitium around proximal tubules, but 67.9% of the surface is characterized by endothelial fenestrae. In contrast, a minor part of the capillary surface, which faces the wide interstitium, has fenestrae within only 37.1% of its area.

These ultrastructural observations on the peritubular interstitium in the rat kidney suggest the existence of at least two pathways between the tubule lumen and the peritubular capillaries: a short pathway passing through the narrow interstitium and a richly fenestrated endothelium and a long

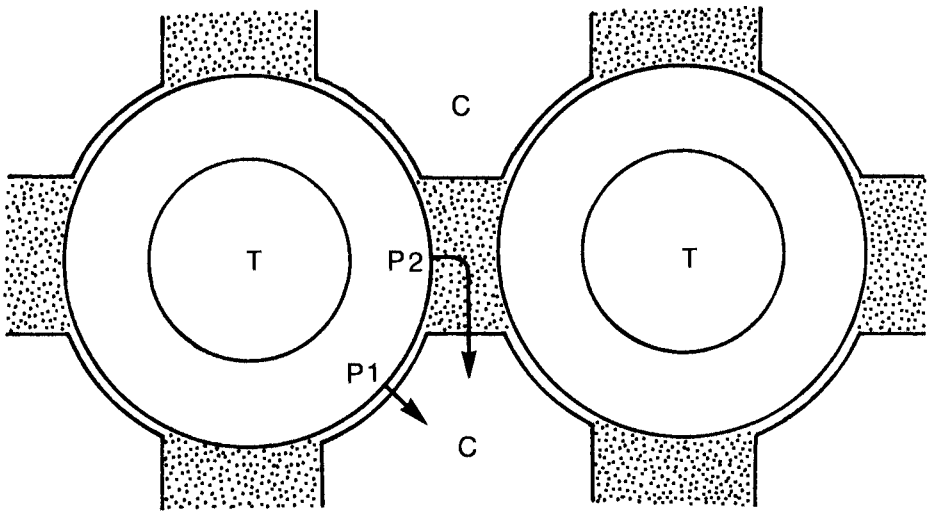

Fig. 4. Schematic drawing of the peritubular interstitium based on the ultrastructural observations by Pedersen, Persson and Maunsbach (1980). Tubules (T) and capillaries (C) are separated either by the wide interstitium (dotted) or the narrow interstitium. The arrows mark possible pathways through the narrow (P1) and the wide interstitium (P2).

pathway passing through the wide interstitium and a less fenestrated endothelium (Fig. 4). Since the content of the narrow interstitium may be more readily exchanged than that of the wide interstitium it is suggested that the two compartments have different roles in the mechanism and regulation of tubular salt and fluid transport.

ACKNOWLEDGEMENT

This work was supported by The Danish Medical Research Council and by USPHS Grant AM-13844 and AM-17433 from the National Institutes of Arthritis, Metabolic and Digestive Diseases.

REFERENCES

Boulpaep, E.L. (1971). Electrophysiological properties of the proximal tubule: Importance of cellular and intercellular transport pathways. In Electrophysiology of Epithelial Cells (G. Giebisch, ed.), F.K. Schattauer Verlag, Stuttgart, New York, pp. 91-118.
Diamond, J.M. and Bossert, W.H. (1967). Standing-gradient osmotic flow: A mechanism for coupling of water and solute transport in epithelia. J. Gen. Physiol. 50, 2061-2083.
Ericsson, J.L.E. (1964). Absorption and decomposition of homologous hemoglobin in renal proximal tubular cells. An experimental light and electron microscopic study. Acta pathol. microbiol. scand. Suppl. 168, 1-121.
Ericsson, J.L.E., Jakobsson, S. (1968). Fine structural localization of glucose-6-phosphatase in renal proximal tubules. Proc. Intern. Congr. Histochem. Cytochem., 3rd, New York, p. 53-54.
Hill, A.E. (1975). Solute-solvent coupling in epithelia: a critical examination of the standing gradient osmotic flow theory.Proc.R.Soc.190, 99-114.

Horster, M. and Larsson, L. (1976). Mechanisms of fluid absorption during proximal tubule development. Kidney Int. 10, 348-363.
Jacobsen, N.O. and Jørgensen, F. (1973). Ultrastructural observations on the pars descendens of the proximal tubule in the kidney of the male rat. Z. Zellforsch. Mikrosk. Anat. 136, 479-499.
Maunsbach, A.B. (1973). Ultrastructure of the proximal tubule. Chapter 2 in Handbook of Physiology, Section 8: Renal Physiology (J. Orloff and R.W. Berliner, eds.), American Physiological Society, Washington D.C., pp. 31-79.
Maunsbach, A.B. and Boulpaep, E.L. (1980a). Hydrostatic pressure changes related to paracellular shunt ultrastructure in proximal tubule. Kidney Int. 17, 732-748.
Maunsbach, A.B. and Boulpaep, E.L. (1980b). Influence of hydrostatic pressure changes on paracellular shunt ultrastructure in proximal tubule. In Functional Ultrastructure of the Kidney (A.B. Maunsbach, T.S. Olsen and E.I. Christensen, eds.), Academic Press, London, pp. 443-456.
Mayahara, H., Fujimoto, K., Ando, T. and Ogawa, K. (1980). A new one-step method for the cytochemical localization of ouabain-sensitive, potassium-dependent p-nitrophenylphosphatase activity. Histochemistry 67, 125-138.
Møllgård, K. and Rostgaard, J. (1978). Morphological aspects of some sodium transporting epithelia suggesting a transcellular pathway via elements of endoplasmic reticulum. J. Membrane Biol. 40, 71-89.
Pedersen, J.C., Persson, A.E.G. and Maunsbach, A.B. (1978). Ultrastructure and quantitative characterization of compartments in renal cortical interstitium. In Proceedings of an International Symposium on Correlation of Renal Ultrastructure and Function, University of Aarhus, Aarhus, p. 56.
Pedersen, J.C., Persson, A.E.G. and Maunsbach, A.B. (1980). Ultrastructure and quantitative characterization of the cortical interstitium in the rat kidney. In Functional Ultrastructure of the Kidney (A.B. Maunsbach, T.S. Olsen and E.I. Christensen, eds.), Academic Press, London, pp. 443-456.
Rostgaard, J. and Møllgård, K. (1980). Morphologic evidence for a transcellular pathway via elements of endoplasmic reticulum in rat proximal tubules. In Functional Ultrastructure of the Kidney (A.B. Maunsbach, T.S. Olsen and E.I. Christensen, eds.), Academic Press, London, pp. 250-266.
Sackin, H. and Boulpaep, E.L. (1975). Models for coupling of salt and water transport. Proximal tubular reabsorption in Necturus kidney. J. Gen. Physiol. 66, 671-733.
Segel, L.A. (1970). Standing-gradient flows driven by active solute transport. J. Theor. Biol. 29, 233-250.
Teutsch, H.F. (1978). Improved method for the histochemical demonstration of glucose-6-phosphatase activity. Histochemistry 57, 107-117.
Welling, L.W. and Welling, D.J. (1975). Surface areas of brush border and lateral cell walls in the rabbit proximal nephron. Kidney Int. 8, 343-348.
Welling, L.W. and Welling, D.J. (1976). Shape of epithelial cells and intercellular channels in the rabbit proximal nephron. Kidney Int. 9, 385-394.
Welling, D.J., Welling, L.W. and Hill, J.J. (1978). Phenomenological model relating cell shape to water reabsorption in proximal nephron. Am. J. Physiol. 234, F308-F317.

Adv. Physiol. Sci. Vol. 3. Physiology of Non-excitable Cells
J. Salánki (ed.)

QUASI-ISOTONIC FLOWS: APPROXIMATE SOLUTIONS BASED UPON THE QUASI-ISOTONIC CONVECTION APPROXIMATION

J. A. King-Hele
Department of Mathematics, University of Manchester, Oxford Road, Manchester M13 9PL, England

1. INTRODUCTION

The purpose of this paper is to describe briefly some recent developments in the theory of solute and water transport in intercellular spaces. There is strongly physiological evidence that there are relatively large water velocities in the intercellular spaces. It is generally believed that these large flows are driven by the osmotic gradients which are generated when Sodium is actively pumped into the intercellular spaces, the Chloride ions following passively. In many physiological situations the water velocities are so slow that diffusion of solute dominates the convection of solute in the bulk of the fluid. However when the flow is confined to a long narrow channel much larger velocities can be generated which convect a significant amount of solute and so have physiological significance.

The problem of coupling of water and solute in an intercellular space is an interesting one for the theoretician because it appears that the same basic mechanism could be important in a wide variety of physiological situations where the membrane parameters and geometrical dimensions differ by orders of magnitude. In such situations the dimensionless parameters which determine the nature of the solution are of particular significance for it is then possible to determine rapidly the relative importance of convection and diffusion, say, by evaluating a single dimensionless parameter. The equations which govern the flow are non-linear ordinary differential equations. These can be solved numerically in any given case, but the significance of the results so obtained is not always evident. This is especially true when speculative values of the membrane parameters are used in the calculation. Under such circumstances an approximate analytical solution, provided it is not too complicated, could be of more value than a mass of computation.

The task then is to seek approximate analytical solutions of the governing equations in dimensionless form. The most widely used approximation is called the quasi-isotonic convection approximation (Segal 1970). It is known that in many situations the solute concentration in the cell, the intercellular space and the capillary differ from one another by less than ten percent. This must often be the case since otherwise large osmotic forces would operate to reduce the concentration differences. The quasi-isotonic convection approximation in its simplest form states that we can put $c = c_c$ everywhere in the equations except where concentration

differences multiplied by permeability or diffusion coefficients occur, where c_c is the mean concentration usually taken as the cell concentration. In practice c often differs from c_c by less than about ten percent, so that this can be a good approximation. The effect of this approximation is to make the governing equations and boundary conditions linear so that they can be solved analytically. This linearization also has another benefit because the various forcing effects such as active transport, oncotic pressure gradients or applied hydrostatic pressure gradients are then uncoupled and may be treated separately. Their combined effect can be found by simple addition.

Some of these ideas are illustrated in section 2 by some special cases. However the model can be made more realistic, and more complicated.

2. THE GOVERNING EQUATIONS

Consider one dimensional flow of a single electrically neutral solute through an intercellular channel of constant width W_i and length L (see Fig.1). Let the tight junction be situated at x = 0, and the basement membrane at x = L, and let v(x) and c(x) be the mean velocity and concentration respectively at station x. Then the conservation equation for water and solute may be written in the form

$$\frac{dv}{dx} = \frac{4L_p^{\beta}RT}{W_i}(c(x)-c_c) \tag{1}$$

$$\frac{d}{dx}(cv-D\frac{dc}{dx}) = \frac{2}{W_i}(2\omega_s^{\beta}RT(c_c-c(x))+N\ n(x/L)) \tag{2}$$

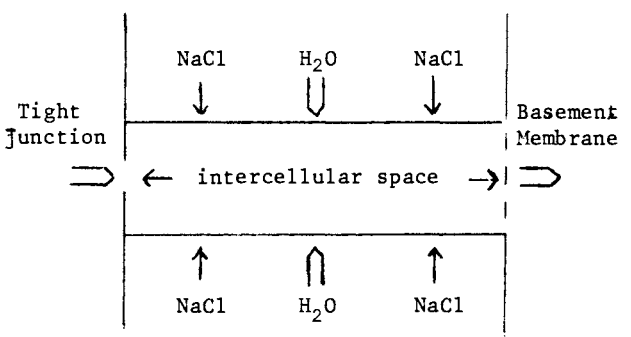

Fig.1. Diagramatic representation of water and solute flow in an intercellular space.

In these equations c_c is the cell concentration, L_p^{β} and ω_s^{β} are the permeability and diffusion coefficient of the lateral membrane respectively, N is a constant which gives the magnitude of the solute transport per unit area across the lateral membrane,, D is the constant diffusion coefficient, R is the gas constant and T is the absolute temperature. We have also assumed that the reflection coefficient $\sigma_s^{\beta} = 1$. The function n(x/L) describes the variation of active transport along the space.

As the flow is very slow, there is a close balance between the pressure gradient force driving the flow down the intercellular space and the

retarding viscous force so that there is Poiseuille flow. In this two dimensional situation it may be shown that

$$\frac{dp}{dx} = \frac{-12\eta}{W_i^2} v(x) \tag{3}$$

where $p(x)$ is the pressure at station x and η is the coefficient of viscosity.

Equations (1)-(3) are three coupled non-linear differential equations for the three unknown functions $v(x)$, $c(x)$ and $p(x)$. The non-linearity arises in Eq(2) because of the product cv. As discussed in the introduction, this linear term may be approximated by $c_c v$ where c_c is the cell concentration. It would of course be incorrect to put $c(x) = c_c$ in Eq(1) since it is the small concentration difference multiplied by a large permeability which is driving the flow. It will be seen later that this key approximation is valid if

$$\varepsilon = \frac{N}{2c_c^2 d^2 L_p^\beta RT} << 1 \tag{4}$$

where $d = 1+\omega_s^\beta/c_c L_p^\beta$. In the case of Necturus $\varepsilon \simeq 0.1$ and the analytical approximations obtained agree well with the exact numerical results obtained by Boulpaep and Sackin (1975). It should be noted here that the value of ε is independent if the geometry of the intercellular space and depends only upon the size of the active transport and the properties of the lateral membrane.

In order to solve Eqs(1)-(3) we need to specify boundary conditions at $x = 0,L$. In the standing gradient model (Bossert and Diamond (1967)) it was assumed that $c = c_c$ at $x = L$. However for the values of the parameters which are now thought to be realistic, (Hill, 1975), the application of this boundary condition leads to an emergent osmolarity c_{em} greatly in excess of c_c, where

$$c_{em} = \frac{\left[cv - D\frac{dc}{dx}\right]_{x=L}}{v(L)} \tag{5}$$

The reason is that the diffusion term in Eq(5) is then comparable to the convective term. This was not the case for the parameters chosen by Bossert and Diamond (1967). A different boundary condition was employed by Boulpaep and Sackin (1975). They used a simple model of a capillary, and in effect chose $c = c_c$ in the capillary, a more realistic assumption. However it was shown in King-Hele (1979) that for their model the emergent fluid was isotonic to order ε. Assuming that there is no significant water or solute flux through the back of the cell, the emergent osmolarity of the fluid entering the capillary must be equal to the emergent osmolarity of the fluid crossing the basement membrane $x = L$. Hence in seeking approximate solutions of the equations using the isotonic convection approximation, which involves an error of order ε, it is sufficient to assume that, with the same error, the emergent fluid at $x = L$ is isotonic to the cell concentration. The advantage of applying this boundary condition at $x = L$ is that we do not have to model the capillaries or the basement membrane. This condition is, from Eq(5),

$$D\frac{dc}{dx} = (c(L)-c_c)v(L) \text{ at } x = L \tag{6}$$

We shall also assume that the pressure is given at x = L i.e.

$$p = p(L) \text{ at } x = L. \tag{7}$$

We shall treat the tight junction x = 0 as a semi-permeable membrane of width W_t, permeability L_p^α, reflection coefficient σ_s^α and diffusion coefficient ω_s^α. Then the fluxes of water and solute across the tight junction are

$$W_t J_v(o) = W_t L_p^\alpha [p_o - p(o) - 2\sigma_s^\alpha RT(c_o - c(o))] \tag{8}$$

$$W_t J_s(o) = W_t [2\bar{\omega}_s^\alpha RT(c_o - c(o)) + \tfrac{1}{2}(c_o + c(o))(1-\sigma_s^\alpha)L_p^\alpha(p_o - p(o))] \tag{9}$$

where p_o and c_o are the given pressure and concentration in the tubule and p(o) and c(o) are the pressure and concentration in the intercellular space at x = 0 respectively. We have defined here an 'effective' diffusion coefficient $\bar{\omega}_s^\alpha$ by

$$\bar{\omega}_s^\alpha = \omega_s^\alpha - \frac{\sigma_s^\alpha}{2}(1-\sigma_s^\alpha)(c_o + c(o)) \tag{10}$$

It should be noted that $\bar{\omega}_s^\alpha$ can be positive or negative unlike ω_s^α which is always positive. This is because $\bar{\omega}_s^\alpha$ incorporates in it some effect of convection through the tight junction due to osmotic effects which act in the opposite direction to pure diffusion. Now the flux of water and solute is continuous at the tight junction and hence

$$W_t J_v(o) = W_i v(o) \tag{11}$$

$$W_t J_s(o) = W_i \left[cv - D\frac{dc}{dx}\right]_{x=0} \tag{12}$$

These conditions, together with Eqs(8)-(10) determine sufficient boundary conditions at x = 0.

It is convenient now to write the equations and boundary conditions in dimensionless terms. We define a non-dimensional length y and velocity U(y) by

$$y = x/L, \qquad U(y) = (dW_i c_c/2NL)v(x) \tag{13}$$

where $d = 1+\omega_s^\beta/c_c L_p^\beta$. We also define a dimensionless concentration difference C(y) and pressure difference P(y) by

$$C(y) = (2dL_p^\beta RTc_c/N)(c(x)-c_c) \tag{14}$$

$$P(y) = (dW_i^3 c_c/24\eta L^2 N)(p(x)-p(L)) \tag{15}$$

It should be explained here that the scale of the velocity chosen above was determined by balancing the active transport term with the convective term in Eq(1), taking into account the back diffusion term. Hence provided the

term Ddc/dx in Eq(1) is of a similar magnitude the dimensionless velocity U(y) will be order unity, as will C(y) and P(y). Using Eqs(13)-(15), Eqs (1)-(3) become

$$\frac{dU}{dy} = C \tag{16}$$

$$\frac{d}{dy}(U(1+\varepsilon C) - \frac{1}{k^2}\frac{dC}{dy}) = n(y) \tag{17}$$

$$\frac{dP}{dy} = -U \tag{18}$$

where the important dimensionless parameters k and ε are given by

$$k^2 = \frac{4L_p^{\beta}RTc_c dL^2}{DW_i}, \quad \varepsilon = \frac{N}{2c_c^2 d^2 L_p^{\beta} RT} \tag{19}$$

It can be seen from Eq(17) that k^2 is a measure of the ratio of the convection of solute (allowing for the effect of back diffusion) to diffusion of solute in the x-direction. When convection dominates $k^2 >> 1$, and when diffusion dominates $k^2 << 1$. For Necturus k^2 is of order unity, but for the Bossert and Diamond (1967) parameters $k^2 >> 1$. It can be seen that the value of k^2 is most sensitive to the value of L, although at present there is most controversy about the value of L_p^{β}.

Before writing down the boundary conditions at x = 0, L in dimensionless form we shall make the simplifying assumption that osmotic forces dominate the pressure gradient forces in the tight junction i.e. from Eq(8)

$$[p_o - p(o)] << [2\sigma_s^{\alpha}RT(c_o - c(o))] \tag{20}$$

This assumption can be justified a'postiori for Necturus. The effect of this assumption is to remove the coupling between the pressure given by Eq(18) and the remaining Eqs(16)-(17). The velocity and concentration equations can be solved first, and the pressure field determined afterwards.

Using Eq(20), the boundary conditions given by Eqs(6)-(12) can be written in the dimensionless form

$$\frac{dC}{dy} = \varepsilon k^2 UC, \quad P = 0, \text{ at } y = 1 \tag{21}$$

$$C = aU - \Delta C, \quad \varepsilon UC - \frac{1}{k^2}\frac{dC}{dy} = -bU \text{ at } y = 0 \tag{22}$$

where the dimensionless constants a, b and ΔC are given by

$$a = \frac{2L_p^{\beta}L}{L_p^{\alpha}\sigma_s^{\alpha}W_t}, \quad b = \frac{1}{d}(1 + \frac{\bar{\omega}_s^{\alpha}}{c_c\sigma_s^{\alpha}L_p^{\alpha}}), \quad \Delta C = \frac{2L_p^{\beta}RTc_d(c_c - c_o)}{N} \tag{23}$$

We note that ΔC is a dimensionless form of the concentration difference between the cell and the tubule. The parameter a is a measure of the influence of the tight junction on the water flow in the intercellular

space. Its value is determined by properties of the tight junction and lateral membrane. If for example the tight junction is almost closed i.e. W_t or L_p^α are 'small', then the parameter a is large. The parameter b is a measure of the diffusion and convection of solute through the tight junction and its value depends upon the properties of the tight junction alone. If bd > 1 i.e. $\omega_s^\alpha > 0$ there is a net flux of solute through the tight junction from the intercellular space.

It may now easily be seen that the non-linear terms which arise in Eq(17), and in the boundary condition Eqs(21)-(22) are all proportional to ε defined in Eq(19). Hence if ε is small the equations are approximately linear. It can also be seen from Eq(14) which can be written in the form

$$c(x)-c_c = \varepsilon d c_c C(y) \tag{24}$$

that if ε is small c(x) is close to c_c provided d and C(y) are of order unity. Successively better approximations to the equations and boundary conditions can be obtained by assuming that U(y), C(y) and P(y) can be expanded as power series in ε with coefficients which are functions of y. These better approximations are easily obtained for the case when the tight junction is closed and n(y) $\equiv$ 1, but are algebraically complicated in the general case. For this reason we shall only give the more accurate approximation for the former case.

To illustrate the theory we shall use some data for Necturus given by Boulpaep and Sackin (1975). We take $L = 2.5\times10^{-3}$ cm, $W_i = 5\times10^{-6}$ cm, $W_t = 2.5\times10^{-7}$ cm, c_c = 100mM, $L_p^\beta = 2.8\times10^{-10}$ cm $s^{-1}(cm\ H_2O)^{-1}$, $L_p^\alpha = 6.1\times10^{-6}$ cm $s^{-1}(cm H_2O)^{-1}$, $RT = 2.5\times10^4$ (cm H_2O)$cm^3 mmol^{-1}$, $D = 1.5\times10^{-5}$ $cm^2 s^{-1}$, $\omega_s^\beta = 3\times10^{-11}$ cm s^{-1}mmol$cm^{-3}(cmH_2O)^{-1}$, $\omega_s^\alpha = 4.6\times10^{-7}$cm s^{-1}mmol cm^{-3} (cm H_2O), $N = 4\times10^{-8}$ mmol $cm^{-2}s^{-1}$, $\eta = 10^{-5}(cm\ H_2O)s^{-1}$. Then

$$\varepsilon = 0.06,\ k = 0.70,\ a = 1.31,\ b = 0.86.$$

The mathematical methods used in solving these equations are straightforward, and the details will not be given here. We shall now consider some special cases.

Case 1. Tight Junction Closed. Uniform Active Transport in $0 < x < L$ ($n(y) \equiv 1$)

In this case we solve Eqs(16)-(18) with the boundary conditions Eq(21) and

$$U = \frac{dC}{dy} = 0 \quad \text{at} \quad y = 0 \tag{25}$$

These latter conditions may be derived formally from Eqs(22) by letting $W_t \to 0$ i.e. $a \to \infty$. The relevant approximate solution is

$$U(y) = y + \varepsilon\left(\frac{\sinh ky}{\sinh k} - y\right) \tag{26}$$

$$C(y) = 1 + \varepsilon\left(\frac{k\cosh ky}{\sinh k} - 1\right) \tag{27}$$

$$P(y) = \tfrac{1}{2}(1-y^2) - \frac{\varepsilon}{k}\left[\frac{\cosh ky-\cosh k}{\sinh k} + \frac{k}{2}(1-y^2)\right] \tag{28}$$

with an error of order ε^2. Hence if $\varepsilon = 0.06$ the error is about 0.36 percent. The dimensional quantities v(x), c(x) and p(x) can now be obtained by substituting for U(y), C(y) and P(y) into Eqs(13)-(15). Using the numerical data given earlier, we find that the dimensional form of Eqs(26)-(28) is using Eqs(13)-(15),

$$v(x) = 1.93\times10^{-4}\left[\frac{x}{L} + 0.06\left(1.32\sinh\frac{kx}{L} - \frac{x}{L}\right)\right] \text{cms}^{-1} \tag{29}$$

$$c(x) = 112 - 0.06\left[1 - 0.92\cosh\frac{kx}{L}\right] \text{mM} \tag{30}$$

$$p(x) = p(L) + 1.09\left(1 - \frac{x^2}{L^2}\right) - 0.11\left[\cosh\frac{kx}{L} - \cosh k\right] \text{cm } H_2O \tag{31}$$

Notice that for these values of the parameters the pressure difference between the tight junction and the basement membrane is

$$p(o)-p(L) = 1.12 \text{ cm } H_2O. \tag{32}$$

This is the pressure difference required to drive fluid down the intercellular space against the effect of viscosity. It is worth noting here that the magnitude of this pressure difference is particularly sensitive to W_i and L since from Eq(15), the scale of the pressure difference is proportional to L^2/W_i^3. Thus if for example W_i is reduced by a factor of two there will have to be an eight-fold increase in the pressure difference p(o)-p(L). This sensitive dependence on W_i comes partly from the effect of a reduction of W_i on the viscous stress and partly from the fact that if W_i is reduced the velocity of the flow must increase.

Case 2. Tight Junction Closed: Active Transport limited to $0 < x < \gamma L$

In this case we assume that the same total transport is uniformly distributed over the interval $0 < x < \gamma L$. Then the distribution function introduced in Eq(2) is

$$n(y) = \begin{cases} 1/\gamma, & 0 < y < \gamma \\ 0 & \gamma < y < 1 \end{cases} \tag{33}$$

For $0 < y < \gamma$ the solution, with an error of order ε, is

$$U(y) = \frac{y}{\gamma} - \frac{\sinh k(1-\gamma)\sinh ky}{\gamma k \sinh k} \tag{34}$$

$$C(y) = \frac{1}{\gamma} - \frac{\sinh k(1-\gamma)\cosh ky}{\gamma \sinh k} \tag{35}$$

$$P(y) = P(\gamma) + \frac{1}{2\gamma}(\gamma^2-y^2) - \frac{\sinh k(1-\gamma)}{\gamma k^2 \sinh k}(\cosh k\gamma - \cosh ky) \tag{36}$$

For $\gamma \leq y \leq 1$

$$U(y) = 1 - \frac{\sinh k\gamma \sinh k(1-y)}{\gamma k \sinh k} \tag{37}$$

$$C(y) = \frac{\sinh k\gamma \cosh k(1-y)}{\gamma \sinh k} \tag{38}$$

$$P(y) = (1-y) - \frac{\sinh k\gamma}{\gamma k^2 \sinh k}(\cosh k(1-y)-1) \tag{39}$$

One not unexpected property of this solution is that dc/dy is negative so that the concentration decreases as c increases. However if for example $k = 0.7$ and $\gamma = 0.5$ we find that $C(0)-C(1) = 0.12$ so that the gradient is quite small. If however k is large Eq(38) becomes approximately, for $\gamma < y \lesssim 1$

$$C(y) = \frac{1}{2\gamma} e^{-k(y-\gamma)}$$

which shows that in this case the difference between c(L) and c_c is exponentially small. This was essentially the case discussed by Bossert and Diamond (1967). Another feature to note is that for all values of γ, $U(1) = 1$. It follows that, to order ε, the water flux through the basement membrane is independent of γ if the total active transport is the same. Since from Eq(16), $dU/dy = C$, it follows that the mean value of C between $y = 0$ and $y = 1$ is independent of γ, so that larger values of $C(y) > 1$ near $y = 0$ are balanced by smaller values of $C < 1$ elsewhere.

It may now be seen that the essential requirement of the standing gradient theory that $c(x)-c_c$ be very small in a significant length of intercellular space near $x = L$ can only be satisfied if $k^2 >> 1$ and there is a significant region near $x = L$ where no active transport occurs. The definition of k^2 shows that $k^2 >> 1$ when L or L_p^β is 'large' or W_i is 'small'.

The approximation used here is based upon $\varepsilon \to 0$ for k fixed. If however k is large and ε is not very small, a different approach may be required.

Case 3. Tight Junction Open: Uniform Active Transport in $0 < x < L$ $(n(y) \equiv 1)$

In this more complicated case we shall again give the solution with an error of order ε. Higher approximations can be obtained but they are algebraically complicated. Then neglecting terms multiplied by ε in the equations and boundary conditions we find

$$U(y) = y+(1+\Delta C)\left(\frac{b \sinh k(1-y)+(1-b)\sinh k}{bk \cosh k+a \sinh k}\right) \tag{40}$$

$$C(y) = 1-(1+\Delta C)\frac{kb \cosh k(1-y)}{bk \cosh k+a \sinh k} \tag{41}$$

$$P(y) = \tfrac{1}{2}(1-y^2)+(1+\Delta C)\left(\frac{b(\cosh k(1-y)-\cosh k)+k(1-b)(1-y)\sinh k}{k(bk \cosh k+a \sinh k}\right) \tag{42}$$

These results are to be compared with the first terms in Eqs(26)-(29). The extra terms in Eqs(40)-(42) reflect the influence of the tight junction, and tend to zero as $W_t \to 0$ i.e. as $a \to \infty$. As before the variables v(x), c(x) and p(x) can now be found from Eqs(13)-(15).

This solution has several interesting properties.

(1) The structure of the solution depends on five dimensionless parameters, a, b, d, k and ΔC. The process of forming dimensionless groups has led to great simplification, since these five parameters involve no less than thirteen independent dimensional variables, all of which may change from one physiological situation to another.

(2) The solute concentration increases down the channel, and has zero gradient at y = 1. As in the previous case the gradient is small if k = 0.70. The graph of C(y) against y for this and the previous cases is shown in Fig.2.

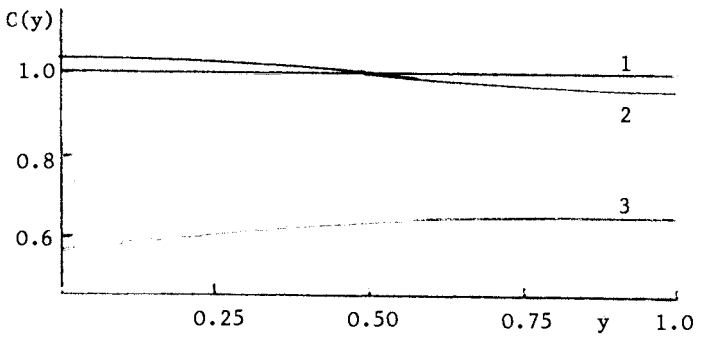

Fig.2. Graph of C(y) against y for the three cases considered in this paper. We have taken $\gamma = 0.5$ for case 2 and neglected the term proportional to ε in case 1. For Necturus $c(x) \simeq 100+12C(y)$ mM.

(3) The solution illustrates the fact that since the equations are linear when ε is small, the solution will depend linearly on the forcing terms which in this case are the active transport N and the concentration difference $c_c - c_o$. Of course N does not appear explicitly in the solution because it has been scaled out, but it will appear in the corresponding dimensional form. The relative effect of the difference $c_c - c_o$ and N is clearly measured by ΔC defined in Eq(23). For the values of the parameters given earlier we find that $\Delta C \ll 1$ provided $c_c - c_c \ll 12.4$mM, which suggests that this forcing effect may not be negligible.

(4) We can readily determine the effect of the tight junction on the flow. For Necturus we find that, if $\Delta C = 0$, $U(0) = 0.43$, $U(1) = 1+(1-b)U(0) = 1.06$, $C(0) = a\,U(0) = 0.56$, $C(1) = 1-kbU(0)\,\mathrm{cosech}\,k = 0.66$. The most obvious feature of these results is that despite a significant flux of water into the intercellular space via the tight junction, the flux of water through the basement membrane is only six percent more than that for the case of the closed tight junction (for which U(1) = 1). The reason for this is that the concentration differences between the cell and the intercellular space is about half the corresponding value for the case when the tight junction is closed (C(0) = C(1) = 1 in that case, with an error of order ε). This is due to the leakage of solute through the tight junction from the intercellular space. The solute balance has to take account of the fluxes through the tight junction and basement membrane, the active transport, and the back diffusion through the lateral membrane. We find that the ratio of the solute flux through the basement membrane to the net flux through the lateral membrane is

$$\frac{U(1)}{d-(d-1)(U(1)-U(0))} = 0.76 \tag{43}$$

Thus in this case the flux of solute through the tight junction into the tubule is about one third of the flux of solute through the basement membrane.

It remains only to determine the conditions under which the pressure gradient force across the tight junction is small compared with the osmotic pressure gradient force i.e. from Eq(20)

$$|p_o - p(o)| \ll |2\sigma_s^{\alpha} RT(c_o - c(o))| \tag{44}$$

We have seen that in this numerical example C(0) = 0.56, and consequently from Eq(14)

$$|c_o - c(o)| = \varepsilon dc_c C(o) = 6.9\text{mM}. \tag{4.5}$$

Hence the theory is self consistent if

$$|p_o - p(o)| \ll 241 \text{ cm } H_2O \tag{46}$$

which is almost certainly satisfied.

3. SUMMARY

We have found simple approximate analytic solutions of the equations which govern the flow of a single electrically neutral solute through an intercellular space using the quasi-isotonic convection approximation ($\varepsilon \ll 1$). The dimensionless parameter ε is a measure of the difference between the cell concentration and the typical concentration in the intercellular space and is often small. For Necturus $\varepsilon \simeq 0.06$. If ε is small, the analytic solution is completely determined by five dimensionless parameters k, a, b, d and ΔC, which between them involve fourteen dimensional parameters many of which could vary substantially from one physiological situation to another. The parameter ΔC is a measure of the ratio of the forcing effect due to an imposed concentration difference between the cell and the tubule and the active transport.

The analytical results have been applied to Necturus. It is shown in particular that about forty percent of the water which passes through the basement membrane has to come through the tight junction. About one third of the solute which enters the intercellular space from the cell leaks back through the tight junction.

The theory presented here has made no assumptions about the properties of the basement membrane or the capillary walls. If these properties are known it is possible to extend the theory.

References

Bossert, W.H. and Diamond, J.M. (1967). J. gen. Physiol. 50, 2061.
Boulpaep, E. and Sackin, H. (1975). J. gen. Physiol. 66, 671.
Hill, A.E. (1975). Proc. R. Soc. Lond. B. 190, 99.
King-Hele, J.A. (1979). J. theor. Biol. 80, 451.
Segal, L.A. (1970). J. theor. Biol. 29, 233.

Adv. Physiol. Sci. Vol. 3. Physiology of Non-excitable Cells
J. Salánki (ed.)

EPITHELIAL TRANSPORT. INTRODUCTION

Hans H. Ussing
Institute of Biological Chemistry A, August Krogh Institute, University of Copenhagen
13 Universitetsparken, DK-2100 Copenhagen Ø, Denmark

This Congress symposium is called "Epithelial Transport" in the programme. You will notice, however, that only a few epithelial organs are going to be discussed, and that most of the time will be devoted to frog skin and toad urinary bladder. Considering the amount of excellent transport studies being performed on numerous other epithelia one might of course wonder why the two "classical epithelia" should have nearly all the limelight.

When planning the symposium I felt, however, that it would be timely to find out where we stand with respect to the fundamental model which is used for the majority of studies of epithelial transport. I am thinking here of the two-membrane model for the origin of the frog skin potential which we presented for the first time at the 20th International Congress of Physiological Sciences in Brussels in 1956 (Ussing and Koefoed-Johnsen, 1956; Koefoed-Johnsen and Ussing, 1958). As it is well known the essential assumptions are that the apical end of the transporting cell is passively, but selectively permeable to sodium and tight for potassium whereas the inward-facing membrane is permeable for potassium, but lacks passive sodium permeability. The sodium-potassium exchange pump is supposed to be located exclusively in the inward-facing membrane. The model was later suplemented with a paracellular shunt path (Ussing and Windhager, 1964).

This model served well as a basis for the development of hypothesis which explains the more involved behaviour of other

epithelial organs like kidney tubule and intestine where the primary transport processes are assumed to drive others via co-transport and counter-transport.

But no chain is stronger than the weakest link. Thus the theme of this symposium should be:"How sure are we that the basic model is correct, and how can we describe the individual steps involved." For such studies no preparations seem to serve better than frog skin and toad urinary bladder.

The applicability of the latter preparation is quite apparent. The toad urinary bladder has a single-layered epithelium consisting of cylindrical cells connected by tight seals. Thus histologically it has an attractive visual likeness to the model.

At first sight the frog skin has very little similarity to the theoretical model. It is a multilayered structure with inserted skin glands and covered by a layer of cornified cells. Actually, however, the skin works beautifully in accord with the model. Several fortunate features contribute to this end-result: 1) The cornified layer is very thin and very permeable to ions. 2) The glands, except when stimulated with adrenaline, are electrically silent and do not conduct ions. 3) The living epithelial cells are connected in three dimensions by conducting junctions, so as to form a syncytium-like entity, the outward-facing membrane of which is sodium selective, whereas the basolateral surfaces correspond to the inward-facing membrane of the model. The coupling was first proposed independently by Farquhar and Palade (1964), and Ussing and Windhager (1964), but it is the work with the electron probe (Rick et al., 1978) which has given firm evidence that most or all of the cell layers must allow rapid equilibration of potassium and sodium between neighbouring cells.

The analysis of ion transport in frog skin and toad bladder is comparatively easy, not only because so few species are being transported but also because the conductance of the paracellular shunt pathways is usually quite small.

In many other epithelia, especially the "leaky" ones the

paracellular pathway becomes much more important. Methods which can serve to characterize the alternative pathways for each ionic species are needed in the future.

I shall briefly mention a new principle which may be of use in this context.

We have shown (Sten-Knudsen and Ussing, in preparation, see also Ussing, 1978)that for any species the ratio of pre-steady state fluxes is equal to the steady state flux ratio: $j^{(12)}(t)/j^{(21)}(t) = J^{(12)}/J^{(21)}$. This is true from the moment of first passage of the isotopes if only one pathway is available and if conditions along the path remain constant. This thesis is correct independent of the mechanism responsible for the transport. Thus it is correct whether we are dealing with electrodiffusion or active transport. The derivation is carried through for an arbitrary number of layers with arbitrary properties placed in series. Unstirred layers are included as additional series barriers. The two bathing solutions should, however, be well stirred and of constant composition.

If, nevertheless, the isotope experiment shows that the flux ratio is changing with time it can only mean that more than one pathway is available for the ion in question. In fact, the pathways must differ with respect to mean passage time as well as to flux ratio.

We have tested the principle by studying the behaviour of sodium fluxes through frog skin (Ussing, Eskesen and Lim, in press). Influx and efflux of sodium were measured at two minute intervals on symmetrical skin samples from the same frog.

In a typical experiment (Ringer solution on both sides, open circuit) the flux ratio was initially much lower than one but increased over a period of 20 minutes to about 3.5. This behaviour can be explained by the existence of two pathways for sodium: A rapid shunt path where sodium moves by electrodiffusion, and a slower cellular pathway where sodium is subject to active transport.

If one assumes the existence of only two pathways it is possible to resolve the measured fluxes in two pairs, one characteristic for the fast and the other for the slow pathway.

REFERENCES

Farquhar, M.G. and Palade, G.E. (1964): Functional organization of amphibian skin. Proc. Nat. Acad. Sci. 51: 569-77.

Koefoed-Johnsen, V. and Ussing, H.H. (1958): The nature of the frog skin potential. Acta physiol. scand. 42: 298-308.

Rick, R., Dörge, A., von Arnim, E. and Thurau, K. (1978): Electron microprobe analysis of frog skin epithelium: Evidence for a syncytial sodium transport compartment. J. Membrane Biol. 39: 313-31.

Sten-Knudsen, O. and Ussing, H.H. (in preparation): The flux ratio equation under non-steady state conditions.

Ussing, H.H. (1978): Interpretation of tracer fluxes. In: Membrane Transport in Biology, vol. I: 115-40. Springer-Verlag, Berlin, Heidelberg, New York.

Ussing, H.H. and Koefoed-Johnsen, V. (1956): Nature of frog skin potential. Abstr. Comm. 20th Intern. Physiol. Congr., Brussels.

Ussing, H.H. and Windhager, E.E. (1964): Nature of shunt path and active sodium transport path through frog skin epithelium. Acta physiol. scand. 61: 484-504.

Ussing, H.H., Eskesen, K. and Lim, J. (in press): The flux ratio transient as a tool for separating transport pathsays in epithelia.

Adv. Physiol. Sci. Vol. 3. Physiology of Non-excitable Cells
J. Salánki (ed.)

IONIC TRANSPORT PROPERTIES OF THE ISOLATED URINARY BLADDER OF THE TOAD

Alexander Leaf
Departments of Medicine, Harvard Medical School, Massachusetts General Hospital, Boston Massachusetts, 02114 USA

The urinary bladder of the toad Bufo marinus has proven a useful experimental model for the study of transepithelial transport of sodium, nonionic solutes and water. It transports only sodium ions actively from mucosal to serosal media. Sodium transport is specifically enhanced by the mineralocorticoid, aldosterone. Sodium, nonionic solutes, and water transport are all increased by vasopressin, though each moves across the rate limiting permeability barriers independently. In these functions the toad bladder mimics those of the collecting ducts of mammalian kidneys.

Histologically the urinary bladder of the toad consists of a layer of mucosal epithelial cells, responsible for all the transport activities, which is supported by a submucosa of loose connective tissue, bundles of smooth muscles and capillaries. A serosa covers the contramucosal surface. The tissue is transparently thin and highly distensible. The mucosal layer consists of granular cells (85%), mitochondrial-rich cells (5%), and basal cells (10%). There are occasional scattered mucous cells. However, each cell that abuts on the mucosal surface has at least a foot process on the basement membrane (1). Thus, the transepithelial transport process involves the transport across only a single layer of cells. The mucosal layer of cells may be removed essentially intact from the underlying submucosa simply by scraping with a glass microscope slide (2). Separate analysis of scraped mucosa and submucosa indicates that only one-fifth to one-tenth of the water, sodium, potassium and chloride content of the tissue is contained within the mucosal layer of epithelial cells (3).

Viewing the bladder surface by phase contrast miscroscopy, it is evident that the granular cells provide a pavement-like surface structure occupying over 98% of the surface. Mitochondrial-rich cells which are bottle-shaped have only a very small exposure to the mucosal surface. The latter are much more frequent in bladders from Colombian toads than in those from the Dominican Republic (4). Since the granular but not the mitochondrial-rich cells bind tritiated ouabain in large amounts on their baso-lateral plasma membranes (5), it is the former that are engaged in transepithelial sodium transport - a transcellular process. The role for the mitochondrial-rich cells is not clear though their content of carbonic anhydrase suggests a role in hydrogen ion secretion (6). The much greater numbers of mitochondrial-rich cells in bladders of Colombian toads than in those from Dominican toads is consistent with the demonstrable hydrogen ion

secretion by the former (7,8) but lack of acid secretion by the latter (9).

The adjacent cells at the luminal margins are joined by tight or limiting junctions. It is now appreciated that passive ion movement across the bladder wall traverses these tight junctures and follows a paracellular pathway across the tissue. There is little ion specificity in this pathway and it has been shown that the flux of labeled sodium from serosa to mucosa is unaffected by amiloride which blocks transcellular transport of sodium (10). Civan and DiBona (11) have demonstrated that the paracellular, intercellular pathway varies in its permeability over the physiologic range of sodium concentrations to which its luminal surfaces is exposed. As urinary solute concentration falls, the permeability decreases thus preventing back diffusion of sodium from body fluids into urine and sustaining large sodium concentration gradients across the tissue.

The apical plasma membranes of the mucosal layer of cells are essentially impermeable to potassium and to chloride ions. This has been demonstrated for potassium by Robinson and Macknight (12) who showed that even with prolonged incubation of toad bladders with ^{42}K in the mucosal bathing medium less than 1% of the tissue potassium had equilibrated with that in the mucosal medium.

Vasopressin stimulates transepithelial sodium transport (13) and increases the intracellular sodium content (noninulin space sodium content) of scraped epithelial cells (14). But the gain of intracellular sodium must be balanced by an equal gain of anionic charges within the cell to preserve electrical neutrality. This occurs by a gain in intracellular chloride that equals the increase in cellular sodium. However, in contrast to the sodium increase which occurs following vasopressin by increased permeability of the luminal surface to sodium and by entry of sodium from the mucosal bathing solution into the cell, the chloride increase results from a gain of intracellular chloride from the serosal bathing medium; the luminal plasma membrane is impermeable to chloride(15).

That sodium transported actively across the epithelium, moves via a transcellular route is indicated by several lines of indirect evidence. As mentioned, the Na, K-dependent adenosinetriphosphatase is located in the basolateral plasma membranes of the mucosal cells, as demonstrated by ouabain binding to the transport enzyme (5). Furthermore, the intracellular content of sodium in the scraped epithelial cells varies as it should if it were the intracellular pool of sodium involved in transepithelial transport. With amiloride blocking entry of sodium into the cells or with sodium-free mucosal bathing medium the intracellular sodium content falls (16) as would be expected if no sodium could enter the cells to be available to be extruded from the cells by the transport enzyme at their basolateral plasma membranes. Contrariwise, when the transport enzyme is blocked by ouabain sodium content within the cells increases markedly (17). When sodium is removed from the mucosal medium the ouabain affects only a minor change in intracellular sodium content whereas removal of sodium from the serosal medium does not affect the large gain of cell sodium produced by ouabain. Thus, the sodium within the cells arises from sodium in the mucosal bathing medium and little, if any, sodium has access to the cell from the serosal medium. Metabolic studies likewise

confirm a very low or absent rate of sodium penetration from serosal medium into cell (18,19). The traffic of sodium across the basolateral plasma membranes occurs only via the active transport sites (sodium pumps) and is unidirectional from cell interior to serosal medium.

The most valid data of intracellular ion content comes from measurements made by means of electron microprobe analyses (20) which confirms the data reported above. Essentially, it was shown that the intracellular concentration of sodium is some 12 to 16 mM and unaffected by removing all sodium from the serosal medium, i.e. dependent solely on the entry of sodium into the cells from the mucosal medium. Addition of ouabain (10^{-3}M) to the serosal medium causes a large gain of intracellular sodium with chloride and loss of cellular potassium. Removing sodium from the mucosal medium prevented the intracellular ionic changes with ouabain, again indicating that only sodium of mucosal origin has access to the cells.

To date, there has been reported no successful measurements of intracellular electrical potentials of toad bladder cells because the small size of these cells make impalement difficult and accentuates the artefacts of membrane potential measurements. If one applies the membrane potentials and resistances obtained by Higgins and Frömter for urinary bladder of Necturus (21) to the toad bladder and the ionic concentrations measured by the electron microprobe, one can construct a reasonable ionic and electrical profile across the transporting mucosal cells of the toad bladder. This is shown in Figure 1A and 1B. Figure 1A depicts the profiles in a short-circuited bladder. The electrical profile is of the "well" type with cell interior -90 mV negative to the bathing medium and symmetrical because the tissue is short-circuited. The sodium concentration of the Ringer's solution is 120 mM and of the cell interior some 12mM. Sodium is depicted as moving into the cells passively across the apical plasma membrane with the concentration gradient (10 to 1) and electrical gradient (-90 mV) providing a driving force for sodium entry equivalent to 148 mV. At the basolateral membrane the sodium must be extruded against the same electrochemical gradient by the active transport mechanism.

Figure B shows the electrical and ionic profile of sodium in an open-circuited bladder with transepithelial potential of +70 mV (serosa positive to mucosa). Because of the low conductance of the apical membrane compared with that of the basolateral membrane (1 to 13), a 70 mV potential across the tissue is partitioned so that (13/14) or 65 mV will be added to the potential at the apical membrane making this -25 mV and 5 mV will be added to the basolateral membrane potential making this +95 mV. The measured net sodium transport with the tissue short-circuited was J_{Na}= 5.6 ± 0.6 (mg d.w.)$^{-1}$ n moles (mg d.w.)$^{-1}$(min)$^{-1}$ and with a transepithelial potential of +70 mV, J_{Na} was reduced to 3.2 n mole (mg d.w.)$^{-1}$(min)$^{-1}$. The intracellular sodium concentration may be calculated as:

$$\frac{J_o}{J_{+70}} = \frac{RT/zf \ln Na_m/Na_{c(o)} + \psi_m - \psi_{c(o)}}{RT/zF \ln Na_m/Na_{c(+70)} + \psi_m - \psi_{c(+70)}}$$

From such a calculation an intracellular concentration of 11.6 mM is obtained at transepithelial potential, Δ - +70 mV (22).

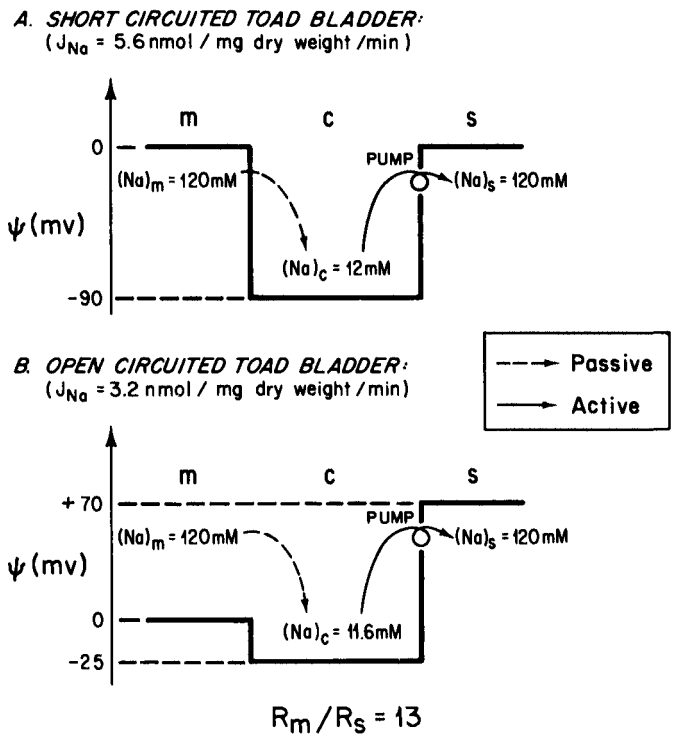

Figure 1. The electrical profile and sodium concentrations in the short-circuited (A) and open-circuited (B) toad bladder. The ordinate is the membrane potential, ψ, in mV. M,C, and S are the three compartments considered: mucosal medium, intracellular compartment, and serosal medium, respectively. In the short-circuited tissue (A) the intracellular potential is depicted as -90 mV and symmetrical at the two cell membranes. When bathed with 120 mM sodium Ringer's solution the intracellular sodium concentration was 12 mM. In the open-circuited preparation (B) a transepithelial electrical potential of +70 mV is shown. Because the conductance of the apical membranes is only 1/13 that of the basolateral plasma membrane, an asymmetric potential profile results. This is associated with only a minor decrease of intracellular sodium concentration and increase in serosal membrane potential (22).

The very high resistance of the apical plasma membrane to that of the basolateral membrane indicates that it is the rate limiting step in transepithelial transport and that any significant increase in transport induced by hormones such as vasopressin and aldosterone must entail an increase in permeability of the apical plasma membrane by the hormone to

sodium entry. Also the relative high resistance of apical to basolateral plasma membranes effectively buffers the work required of the active transport mechanism at the basolateral surface from changes in transepithelial potential. Any change in transepithelial potential is distributed largely across the apical surface perturbing, thereby, the electro-chemical gradients at the basolateral surface against which sodium must be actively transported only to a very minor degree. The major effect of imposing transepithelial electrical potential gradients is to modify the driving force and hence the rate of sodium transport into the cell at its apical surface. Hyperpolarizing potentials will reduce sodium transport while hypo - polarizing or depolarizing transepithelial electrical gradients accelerate entry of sodium into the cell but affect very little the work of sodium extrusion across the basolateral cell membrane. This presumably accounts for the constancy of stoichiometry of sodium ions transported to supra-basal carbon dioxide produced over a range of imposed transepithelial potentials of -50 to +70 mV (23).

In summary, the transport of sodium across the isolated urinary bladder of the toad Bufo marinus has been reviewed. The tissue consists of a single layer of transporting epithelial cells supported by a submucosa which does not participate in the transport process. Sodium is transported transcellularly crossing two major permeability barriers, the apical or luminal and the basolateral plasma membranes of the predominant granular cell. Entry into the cell across the luminal membrane is a passive but specific process exhibiting saturation kinetics. This is the major permeability barrier in the tissue. Once within the cell the sodium mixes with the intracellular sodium which constitutes the "active transport pool". At the basolateral surface the sodium ion is extruded by an energy requiring process, the Na,K-dependent adenosine triphosphatase, into the serosal medium. Other ions such as chloride and potassium traverse the bladder passively via the paracellular pathway. The apical plasma membrane is essentially impermeable to these ions which, however, readily enter the cells across the basolateral plasma membrane. This membrane, however, has a very low permeability for sodium except through the active transport pathway so little recycling of sodium occurs across the basolateral cell surface. From analogy with the bladder of Necturus the intracellular electrical potential is assumed to be some 90 mV negative to the serosal bathing medium. Electron microprobe studies indicate that the intracellular sodium concentration is some 12 to 16 mM and varies according to the functional state of the tissue and the concentration of sodium in the mucosal medium. Hormones that stimulate sodium transport have as their major effect an enhancement of the permeability of the luminal surface to sodium.

Acknowledgement

Results reported in this paper were in part supported by a grant HE 06664 from the National Heart, Lung and Blood Institute, National Institutes of Health, U.S.A.

References

1. DiBona, D.R., Civan, M.M. and Leaf, A. : The anatomic site of the transepithelial permeability barriers of toad bladder. J. Cell. Biol. 40: 1-7, 1969.

2. Gatzy, J.T. and Berndt, W.O.: Isolated epithelial cells of the toad bladder. Their preparation, oxygen consumption, and electrolyte content. J. Gen. Physiol. 51:770-784, 1968.

3. Macknight, A.D.C., Civan, M.M. and Leaf, A.: The sodium transport pool in toad urinary bladder epithelial cells. J. Membrane Biol. 20:365-386, 1975.

4. DiBona, D.R.: Direct visualization of epithelial morphology in the living amphibian urinary bladder. J. Membrane Biol. 40(special issue): 45-70, 1978.

5. DiBona, D.R. and Mills, J.W.: Distribution of Na^+-pump sites in transporting epithelia. Fed. Proc. 38:134-143,1979.

6. Rosen, S., Oliver, J.A. and Steinmetz, P.R.: Urinary acidification and carbonic anhydrase distribution in bladders of Dominican and Colombian toads. J. Membrane Biol. 15:193-205, 1974.

7. Frazier, L.W.: Interrelationship of H^+ excretion and Na^+ reabsorbtion in the toad urinary bladder. J. Membrane Biol. 19:267-276,1974.

8. Ludens, J.H. and Fanestil, D.D.: Acidification of urine by the isolated urinary bladder of the toad. Am. J. Physiol. 233:1338-1344, 1972.

9. Leaf, A.: Transepithelial transport and its hormonal control in the toad bladder. Ergebnisse der Physiologie 56:216-263, 1965.

10. Saito, T., Lief, P.D. and Essig, A.: Conductance of active and passive pathways in the toad bladder. Am. J. Physiol. 226:1265-1271, 1974.

11. Civan, M.M. and DiBona, D.R.: Pathways for movement of ions and water across toad urinary bladder. III. Physiologic significance of the paracellular pathway. J. Membrane Biol. 38:359-386,1978.

12. Robinson, B.A. and Macknight, A.D.C.: Relationships between serosal medium potassium concentration and sodium transport in toad urinary bladder. J. Membrane Biol., 26:269-286, 1976.

13. Leaf, A.: Some actions of neurohypophyseal hormones on a living membrane. J. Gen. Physiol. 43:175-189, 1960.

14. Macknight, A.D.C., Leaf, A. and Civan, M.M.: Effects of vasopressin on the water and ionic composition of toad bladder epithelial cells. J. Membrane Biol. 6:127-137, 1971.

15. Macknight, A.D.C.: Contribution of mucosal chloride to chloride in toad bladder epithelial cells. J. Membrane Biol. 36:55-63,1977.

16. Macknight, A.D.C. and Leaf, A.: The sodium transport pool. Am. J. Physiol. 234(1)F1-F9, 1978.

17. Macknight, A.D.C., Civan, M.M. and Leaf, A.: Some effects of ouabain on cellular ions and water in epithelial cells of toad urinary bladder. J. Membrane Biol. 20:387-401,1975.

18. Canessa, M., Labarca, P. and Leaf, A.: Metabolic evidence that serosal sodium does not recycle through the active transepithelial transport pathway of toad bladder. J. Membrane Biol. 30:65-77,1976.

19. Macknight, A.D.C. and McLaughlin, C.W.: Transepithelial sodium transport and CO_2 production by the toad urinary bladder in the absence of serosal sodium. J. Physiol. London, 269:767-776,1977.

20. Rick, R., Dörge, A., Macknight, A.D.C., Leaf, A. and Thurau, K.: Electron microprobe analysis of the different epithelial cells of toad urinary bladder. J. Membrane Biol. 39:257-271, 1978.

21. Higgins, J.T.,Jr., Gebler, B. and Frömter, E.: Electrical properties of amphibian urinary bladder. II. The cell potential profile of in Necturus maculosus. Pflugers Arch. 371:87-97,1977.

22. Leaf, A., Chu, G. and Schultz, S.: The significance of relative membrane resistances in determining the work of transport across epithelia. Proc. Symposium on Epithelial Ion and Water Transport. Dunedin, New Zealand, Raven Press,1980.

23. Canessa, M., Labarca, D.R., DiBona, D.R. and Leaf, A.: Energetics of sodium transport in toad urinary bladder. Proc. Natl. Acad. Sci. U.S.A. 75:4591-4595,1978.

Adv. Physiol. Sci. Vol. 3. Physiology of Non-excitable Cells
J. Salánki (ed.)

COMPUTER MODEL OF TRANSPORTING EPITHELIAL CELLS. ANALYSIS OF CURRENT-VOLTAGE AND CURRENT-TIME CURVES

E. Hviid Larsen, Bjørn E. Rasmussen and Niels Willumsen
Zoophysiological Lab. A, Universitetsparken 13, DK-2100 Ø, Denmark

It has for long been a tradition to work with the short-circuited and symmetrically bathed multicellular membrane. This technique is excellent for singling out active pathways and for providing a precise measure of active ion transport. On the other hand, measurements of passive ionic currents require non-zero transmembrane electrochemical potential differences. Unravelling characteristics of passive pathways implies examination of how their currents vary with membrane potential and ionic composition of the bathing solutions. The theme of the present paper is the origin of non-linear current-voltage curves of multicellular membranes, the toad skin epithelium serving as experimental model. For theoretical treatment a simple version of the Koefoed-Johnsen-Ussing two-membrane-model is constructed for computer analysis. The predictions made are compared with experimental data. This approach enables us to pin-point shortcomings and to propose extentions to meet the requirement of experimental findings. Previous examination of steady-state features (Larsen & Kristensen 1978, Larsen 1978) is here extended to cover also non-steady-state behaviour. In his discussion of the interdependence of membrane conductances, Na-currents and intracellular potentials in frog skin Lindemann (1977a, b) used a similar approach. The first comprehensive treatment of non-steady-state behaviour of the model is that of Lew, Ferreira and Moura (1979). We think their papers should be consulted to fully appreciate the strength of computer assisted analysis of epithelial membrane models.

1. The non-linear current-voltage curve in toad skin

The experimental protocol involves three types of measurements.
1. Steady-state transepithelial currents as function of transepithelial

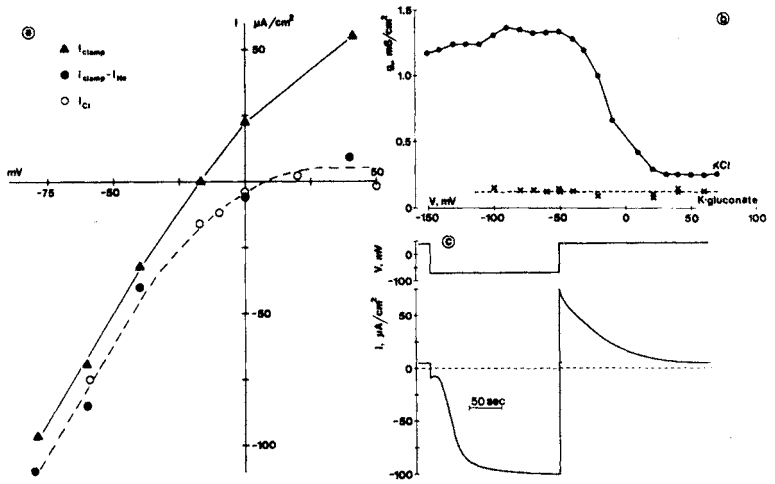

Fig. 1. Toad skin, NaCl-Ringer on the inside. a. *Steady-state I-V and I(Cl)-V curves with NaCl-Ringer on the outside. (Bruus et al. 1976).* b. *Steady-state g-V relation with KCl- or K-Gluconate Ringer on the outside.* c. *Record of current response to a change in V from +40 mV to -70 mV and back. V-program on top. KCl-Ringer on the outside.*

voltage (I-V relations), *2.* steady-state transepithelial conductances as function of V (g-V relations), and *3.* current-time courses following a step-wise change of V (I-t curves).

1. In this type of experiments V* is clamped long enough at each value to secure a time-independent current. By simultaneous measurements of transepithelial unidirectional ^{22}Na- and ^{36}Cl-fluxes the currents are split up into their ionic components. From Fig. 1a it is seen that the toad skin most easily passes steady-state currents in outward direction (outward-going rectification). These outward currents obtained by hyperpolarization of the skin are carried by an inward movement of chloride ions. The contribution of I_{Cl} to the clamping currents at reversed V is small. In this voltage region the currents are almost identical to the inward-going I_{Na}. The upward-going curvature of the I_{Cl} -V graph illustrates a strong voltage dependence of the steady-state transepithelial Cl-conductance (Bruus *et al.* 1976).

2. The g-V relation is typically S-shaped with its steepest region near -20 mV and its maximum plateau below -70 mV (Larsen & Kristensen 1978). Figure 1b shows an example obtained with KCl-Ringer outside. It can also be

*) V is expressed as the potential of external (corneal) bath minus that of internal (serosal) bath. Inward currents are taken as positive.

seen that with Cl-free external solution g is independent of V. This is another way of illustrating that the transepithelial chloride pathway is to be found with a high conductance at values of V below -70 mV and a low conductance when the skin is clamped to positive values of V.

3. The time course of conductance changes is shown in Fig. 1c. Pulsing V from a holding value of +40 mV to -70 mV leads to a small instantaneous current response. After a brief delay the outward-going current slowly increases reaching its steady-state in the course of 100 sec. After full activation the voltage is stepped back to its initial holding value. This leads to a large inward current, *i.e.* the activated conductance does not rectify. In turn, the current decreases towards its initial low steady-state level illustrating the full reversibility of the conductance change.

In considering the nature of the above Cl-current rectification two types of theoretical framework present themselves.

A. The unidirectional fluxes through the activated pathway obey the flux-ratio equation (Larsen 1980). This provides evidence that a traditional electro-diffusive process governs the movement of Cl across the rate limiting membranes. Thus, a certain degree of rectification is expected from a trivial voltage dependence of membrane conductances (Goldman 1944, Hodgkin & Katz 1949). If, in addition, the cellular Cl-concentration increases with an inward-going flux of Cl, the Cl-conductances of the outward and inward facing membranes are expected to increase as well. With a cell water volume of about 1 $\mu l/cm^2$ non-steady-state currents associated with these accumulation/depletion processes might well have half-times in the order of 10 sec.

B. The g-V relations and time-dependent currents in excitable membranes are best explained by assuming voltage-controlled permeability changes to the ion involved (Hodgkin & Huxley 1952). Although the time course of cation current activation in nerve cells is 4 orders of magnitude faster than that of the above Cl-current activation there is evidence that gating processes may be slowed down 4 orders of magnitude by increasing the oxidized cholesterol content of the lipid membrane in which the channel precursers are embedded (Baumann & Mueller 1974).

The two-membrane-model of Koefoed-Johnsen and Ussing (1958) supplied with a paracellular shunt (Ussing & Windhager 1964) serves as basis for a closer examination of the first mentioned possibility (Fig. 2). Although not explicitly stated by this models, *we* shall assume that passive currents

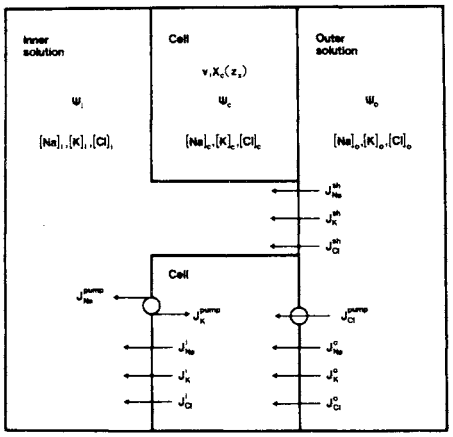

Fig. 2. The two-membrane-model with a paracellular shunt and an active Cl-pump. Inner membrane, P(K)>>P(Na). Outer membrane, P(Na)>>P(K). The Cl-pump is not in operation in the calculations below.

are described by the integrated form of the Nernst-Planck electrodiffusion equations with constant (*i.e.* voltage and concentration independent) permeabilities. Na-concentration dependence of the inner membrane Na/K-pump is taken from a previous study (Larsen *et al.* 1979). The aim is to find out how much this most simple version of the model can explain.

2. Outline of the model

In this section we briefly outline the mathematical formulation of the model and the computational methods used. The model calculations yield as their primary outcome the ionic currents through the epithelium in the voltage clamp mode. Steady-state as well as non-steady-state currents are calculated.

To compute fluxes across the inner and outer membrane, intracellular potential and intracellular ionic concentrations must be known. Considering three permeable ions this adds up to ten unknown variables linked by six flux equations. In a steady-state, inner and outer membrane fluxes must be equal for each ionic species yielding three more equations. The remaining equation stems from the electroneutrality condition.

Cell volume regulation has been allowed for by assuming the existence of a fixed amount of impermeable intracellular anions. The concentration of these enters the electroneutrality condition, thereby adding cell volume to the list of unknown variables. The assumption of isosmolarity between the serosal and the cellular compartment provides the extra condition.

At steady-state the computing strategy is the following. A value of the

cellular potential is guessed. Cellular concentrations of the permeable ions are found from equations expressing vanishing ionic net fluxes into the cell. The concentration of the impermeable anion is found from the isosmolarity condition, and the net charge in the cell is computed. This sequence of computations is repeated with a corrected value of the cellular potential until the net charge becomes zero. As this condition is met, the steady-state has been found. Fluxes, currents, etc are calculated, and added to the paracellular contributions to get the total transepithelial quantities.

To solve the non-steady-state some modifications are needed, since inner and outer membrane fluxes of one particular ionic species are no longer equal. Their difference (the net flux) equals the rate of change of intracellular amount of substance. This gives three continuity equations in replacement of the three "zero netflux" equations used at steady-state. The intracellular concentrations at some particular time no longer belong to the set of unknown variables, but are replaced by the corresponding concentration changes within a certain time interval. We are, therefore, still left with eleven unknown variables and eleven equations, three of them now forming a set of coupled 1. order non-linear differential equations.

This leads to the following line of computations. After a sudden pertubation of the transepithelial potential, cellular concentrations and volume are instantaneously unchanged. The intracellular amounts of ionic species are computed. Given at a certain time these amounts, the volume is computed from the isosmolarity condition, and with an initial guess of the intracellular potential the total electric currents across the two cell membranes are computed. The value of the intracellular potential is now iteratively corrected until the two electric currents become equal, since this is necessary to ensure electroneutrality in the cellular compartment at all times. Next, net fluxes into the cell are computed, and the three continuity equations are integrated using a fourth order Runge-Kutta method to give the intracellular amounts of permeable ions at the end of a small time interval. This procedure is repeated until the final steady-state is reached adding, of course, at all times the paracellular, and the transcellular contributions to get the total current.

3. I-V curves of the model epithelium with constant permeabilities

The relative permeabilities of outer and inner membrane conductors are chosen such as to obtain a ratio of the outer and inner membrane resistance

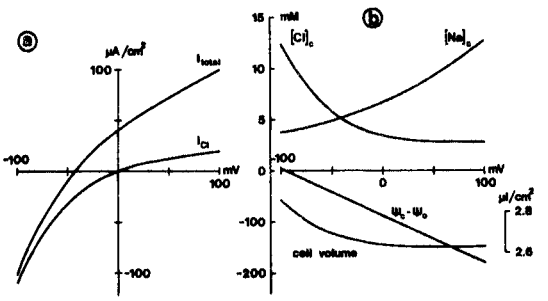

Fig. 3. Model analysis, NaCl-Ringer in the outer and inner compartments. a. *Steady-state I-V and I(Cl)-V curves of model-epithelium with an anion-selective outward facing membrane (P(Cl)/P(Na) = 10).* b. *Variation of steady-state intracellular concentrations, potential, and volume with transepithelial potential difference.*

above 0.7 in accordance with experimental findings (Lindemann & Thorns 1967, Nagel 1976, Helman & Fisher 1977). This implies that the overall rectification is determined by the ion selectivity of the outer membrane. Thus, if the outer membrane Na-permeability (P^o_{Na}) is larger than the outer membrane Cl-permeability (P^o_{Cl}) steady-state as well as instantaneous I-V curves are non-linear and concave towards the I-axis. This situation might well prevail in the skin of *Rana pipiens* which shows inwardgoing rectification (Helman & Fisher 1977). With $P^o_{Na}<P^o_{Cl}$ the model epithelium behaves like an outwardgoing rectifier closely resembling the toad skin (Fig. 3a). This steady-state rectification is due partly to changes in the intracellular Cl-concentration (Fig. 3b), but the instantaneous voltage dependence of the (outer membrane) Cl-conductance contributes significantly as well (see Fig. 4b).

It is noteworthy that significant curvatures in the steady-state I-V diagrams are obtained with changes of intracellular ion concentrations which probably are tolerated by the living tissue, and that the cell water volume varies but a few percent as function of the transcellular potential between ±100 mV (Fig. 3b). In this voltage range the active Na-transport varies an order of magnitude (between 80 and 10 μA/cm²), illustrating a considerable stability of the intracellular ion and water content of the model cell.

4. I-t curves of accumulation/depletion processes

The time course of non-steady-state currents following a stepwise change of V from a holding potential of 0 mV is shown in Fig. 4a. In the model cell clamped to 0 mV (I_{SC} = 40.4 μA/cm²) Cl is distributed in electrochemical equilibrium across both membranes at an intracellular potential of -89.4 mV. Changing V to -100 mV, instantaneously leads to a significant change in the outer membrane potential difference to -15.0 mV and a change in the inner

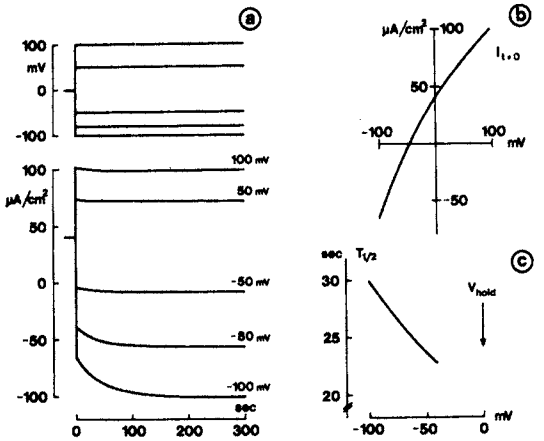

Fig. 4. Model analysis (cont.). a. *Current responses to voltage clamping. Voltage clamp program on top.* b. *Instantaneous I-V curve from a holding potential of 0 mV.* c. *Half-times of transient currents as function of transepithelial clamping potential.*

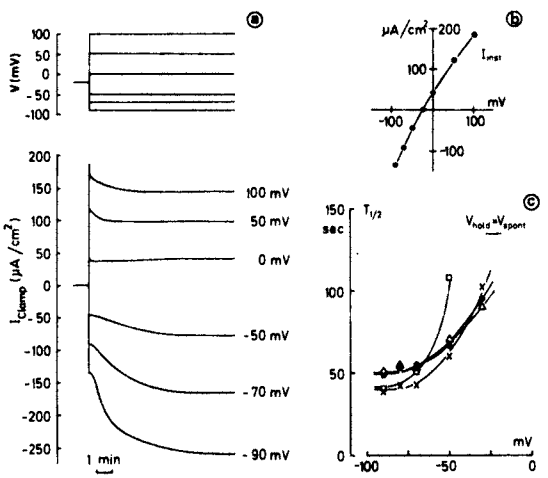

Fig. 5. Toad skin, NaCl-Ringer on both sides. a. *Current responses to stepwise changes in V. Voltage clamp program on top.* b. *"Instantaneous" I-V curve. Currents read 500 msec after pulsing V from the spontaneous potential.* c. *Half-times of transient currents as function of transepithelial clamping potential. Different symbols indicate data from 4 preparations. (Larsen & Kristensen 1978).*

membrane potential difference to -115.0 mV.

The current carried by a passive pathway is given by

$$I_j^m = g_j^m \, (V^m - E_j^m), \qquad (1)$$

where g_j^m is the integral conductance of the pathway involved, V^m is the membrane potential, and E_j^m is the equilibrium potential (j = Na, Cl or K, and m = *o*uter, *i*nner or *sh*unt membrane). Due to the voltage dependence of g_j^m (see f.ex. Finkelstein & Mauro 1963, Sten-Knudsen 1979) the above changes in membrane potentials result in an increase in g_{Cl}^o (as well as in

g^o_K and g^i_{Na}) and a decrease in g^o_{Na}, g^i_K, and g^i_{Cl}. Thus, the currents are disturbed instantaneously owing to changes in their driving force as well as in their conductance (g^{sh}_j remains constant because of identical composition of the inner and outer bathing solution). Immediately, this starts a cellular accumulation of Cl (derived from the external solution) and K (derived from the inner solution) and a cellular depletion of Na via the inner membrane Na/K pump. The transient component of the clamping current is the sum of these accumulation/depletion currents. The current becomes time independent as the individual ion fluxes across the inward and outward facing membrane match again. With the above example (V = -100 mV) the new steady-state is characterized by an inner membrane potential of -96.0 mV, and the following cellular concentrations (mM), K_c = 113.8 (increased from 110.3), Na_c = 3.68 (decreased from 6.73), and Cl_c = 12.4 (increased from 3.38).

The transient currents decay almost monoexponentially with time. Their time constants, however, depend on the potential difference imposed across the epithelium. This becomes clear by inspection of Fig. 4c, showing that - in the interval -40 mV to -100 mV - $T_{\frac{1}{2}}$ *increases* with the amplitude of the voltage displacement from the holding value.

5. I-t curves in toad skin epithelium

Figure 5a shows a family of I-t curves in a toad skin preparation exposed to NaCl-Ringer at its inner and outer surface. To facilitate comparison with computer calculations (Fig. 4) the same protocol was applied at the computer terminal and in the laboratory. In the experiment the spontaneous potential defines the initial steady-state (V = -22 to -24 mV, I = 0 $\mu A/cm^2$).

Voltage clamping leads to a non-linear instantaneous I-V graph, concave towards the I-axis (Fig. 5b). This is compatible with the hypothesis that an outward-facing membrane with $P^o_{Cl} > P^o_{Na}$ rules the clamping currents (compare with Fig. 4b).

The subsequent slow time-dependent currents have two features which are incompatible with I-t curves of the model epithelium. *1.* Following hyperpolarization, the currents increase along an *S-shaped curve*. *2.* Their half-times *decrease* with increasing hyperpolarizing voltage pulse (Fig. 5c).

Thus, the predictions made by the most simple version of the two-membrane-model do not fully explain our experimental data.

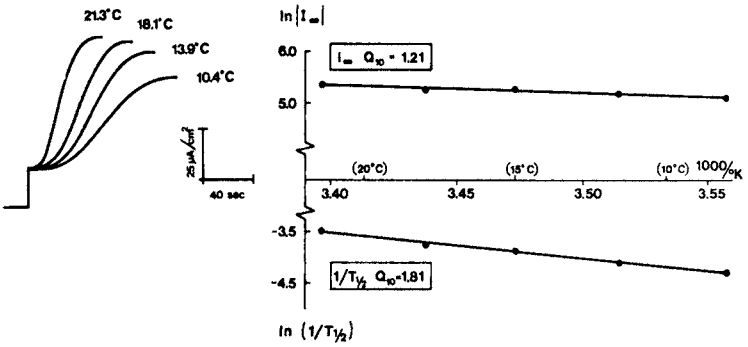

Fig. 6. Toad skin, NaCl-Ringer on the inside, KCl-Ringer on the outside. Left. *Current responses to change in V from +40 mV to -80 mV at ambient temperatures indicated on the records.* Right. *Arrhenius diagrams. I^{∞} is the fully activated steady-state current. $T-\frac{1}{2}$ is the half-time of the current transient.*

6. Identification of two types of membrane processes by means of their temperature dependence

In the above treatment of voltage clamp data it is assumed that the time dependent conductance changes rely on membrane currents carrying ions into or out of an intraepithelial compartment. In this type of model it is the currents flowing through the membranes which control the slow conductance changes. The deviations between predictions made from this model and experimental findings suggest the involvement of a more complex type of membrane process, which is separated from the translocation of ions through the membrane. The rate at which this hypothetical process brings the system from one steady-state to another varies as a decreasing function of the voltage pulse imposed across the skin*. This taken together with the delay of current activation suggested to us that a Hodgkin-Huxley gate type mechanism rules the conductance activation (Larsen & Kristensen 1978).

Hodgkin, Huxley & Katz (1952) showed that in the squid axon the temperature coefficient of the current activation is considerably larger than that of steady-state conductances, in accordance with the view that a gating reaction controls the time-dependent currents. Results of this type

*) This applies to the voltage interval investigated above. In agreement with simple H-H kinetics, $T_{\frac{1}{2}}$ varies as a bell-shaped function of V with its maximum value between -20 and 0 mV (Larsen 1980).

of experiment are shown in Fig. 6. The toad skin was exposed to KCl-Ringer on its outside and to NaCl-Ringer at its serosal surface. Full activation of the Cl-conductance was brought about by stepping V from a holding value of +40 mV to -80 mV. It is clear that a decrease in ambient temperature affects both the steady-state current at V = -80 mV and the rise time of current activation. In the temperature interval investigated the Arrhenius plots depict straight lines from which temperature coefficients (Q_{10}) can be calculated. The low temperature coefficient of the fully activated steady-state current corresponds to that of cation currents in excitable tissues. The significantly higher temperature coefficient of the current activation is in agreement with the hypothesis that a membrane process operating independent of ion translocation controls the rate at which the membrane conductance is brought from one steady-state to another.

7. Flux-ratio analysis

As an independent way of characterizing the nature of the Cl-conductance we have carried out a flux-ratio analysis (Larsen 1980). In absence of bulk flow of solvent a simpel passive transport obeys the Ussing flux-ratio equation (Ussing 1949),

$$\frac{J_{Cl}^{in}}{J_{Cl}^{out}} = \frac{(Cl)_o}{(Cl)_i} \exp(-FV/(RT)), \qquad (2)$$

where J_{Cl}^{in} and J_{Cl}^{out} are inward-going and outward-going unidirectional fluxes, $(Cl)_o$ and $(Cl)_i$ the chemical activities in the outer and inner bathing solution, V the transepithelial potential difference, and F, R, and T have their usual meanings. After logarithmic transformation and introduction of E_{Cl} by the Nernst-equation, we get

$$\text{Log}_{10} \frac{J_{Cl}^{in}}{J_{Cl}^{out}} = -(V-E_{Cl})/58 \text{ mV} \qquad (3)$$

From Fig. 7 it can be seen that for -100 mV $\leq$ V < 0 mV, and with 114.6 mM Cl on each side of the skin good agreement between theoretical (full line) and experimental (o-symbols) flux-ratios is obtained. In this potential region, therefore, Cl-transport takes place along a simple passive pathway. At reversed potential differences (V>0 mV) the experimental fluxratios are up to three orders of magnitude larger than expected for simple passive

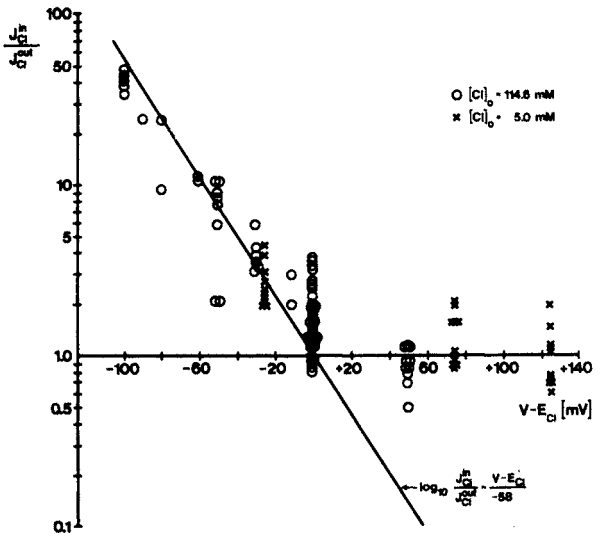

Fig. 7. Flux-ratio analysis of steady-state unidirectional Cl-fluxes across toad skin epithelium (Larsen 1980).

transport. Here, the experimental flux-ratios are *independent* of the driving force and always close to unity, which means that the net charge transfer is close to zero. This is true whether the driving force is manipulated by voltage clamping (o-symbols) or by lowering the external Cl-activity (x-symbols), thus giving compelling evidence that a 1:1 Cl-exchange pathway rules the Cl-transport for V>0 mV. In other words, closure of a conductive pathway takes place as V is changed from below the spontaneous potential difference to values above zero mV.

CONCLUSION

In the above analysis of the mechanism of Cl-current rectification in toad skin epithelium we have dealt with three different approaches.

1. Computer model analysis showing that the observed time course of Cl-current activation is incompatible with current transients associated with simple accumulation/depletion processes.

2. Investigation of the temperature dependence of the fully activated Cl-current and the time constant of Cl-current activation, revealing a significant difference in their temperature coefficients.

3. Flux-ratio analysis disclosing disappearance of a conductive pathway as the transepithelial potential difference is reversed.

We think that taken together, these findings give sufficient evidence for proposing that the strong Cl-current rectification in this tissue is due to a potential dependent Cl-permeability change.

ACKNOWLEDGEMENTS

One of us (EHL) wishes to thank Dr. Poul Kristensen for his collaboration in much of the experimental work discussed in this paper. It is a pleasure to thank Lone Pedersen for art work and Lis Nielsen for typing the manuscript. The project is supported with grants from the Danish State Research Council (511-7120, 511-20276) and from the Novo Foundation.

REFERENCES

Baumann, G. & P. Mueller (1974). A molecular model of membrane excitability. *J. Supramol. Struct.* 2, *538-558*.

Bruus, K. P. Kristensen & E. Hviid Larsen (1976). Pathways for chloride and sodium transport across toad skin. *Acta physiol. scand.* 97, *31-47*.

Finkelstein, A. & A. Mauro (1963). Equivalent circuits as related to ionic systems. *Biophys. J.* 3, *215-237*.

Goldman, D.E. (1943). Potential, impedance, and rectification in membranes *J. gen. Physiol.* 27, *37-60*.

Helman, S.I. & R.S. Fisher (1977). Microeletrode studies of the active Na-transport pathway of frog skin. *J. Gen. Physiol.* 69, *571-604*.

Hodgkin, A.L. & A.F. Huxley (1952). A quantitative description of membrane current and its application to conduction and excitation in nerve. *J. Physiol. (London)* 117, *500-544*.

Hodgkin, A.L. & B. Katz (1949). The effect of sodium ions on the electrical activity of the giant axon of the squid. *J. Physiol. (London)* 108, *37-77*.

Hodgkin, A.L., A.F. Huxley & B. Katz (1952). Measurement of current-voltage relations in the membrane of the giant axon of *Loligo*. *J. Physiol. (London)* 116, *424-448*.

Koefoed-Johnsen, V. & H.H. Ussing (1958). The nature of the frog skin potential. *Acta physiol. scand.* 42, *298-308*.

Larsen, E. Hviid (1978). Computed steady-state ion concentrations and volume of epithelial cells. Dependence on transcellular Na^+ transport. In *Osmotic and Volume Regulation,* C. Barker Jørgensen and E. Skadhauge (eds.) *438-456. Alfred Benzon Symposium XI. Munksgaard, Copenhagen.*

Larsen, E. Hviid (1980).Chloride current rectification in toad skin epithelium. *Federation Proc. (in press).*

Larsen, E. Hviid & P. Kristensen (1978). Properties of a conductive cellular chloride pathway in the skin of the toad *(Bufo bufo). Acta physiol. scand.* 102, *1-21.*

Larsen, E. Hviid, W. Fuchs & B. Lindemann (1979). Dependence of Na-pump flux on intracellular Na-activity in frog skin epithelium (R. Esculenta) *Eur. J. Physiol. Suppl. 382, R 13.*

Lew, V.L., H.G. Ferreira & T. Moura (1979). The behaviour of transporting epithelial cells. I. Computer analysis of a basic model. *Proc. R. Soc. Lond.* B 206, *53-83.*

Lindemann, B. (1977a). Circuit analysis of epithelial ion transport I: derivation of network equations. *Bioelectrochem. & Bioenerg.* 4, *275-286.*

Lindemann, B. (1977b). Circuit analysis of epithelial ion transport II: concentration- and voltage-dependent conductance. *Bioelectrochem. & Bioenerg.* 4, *287-297.*

Lindemann, B. & U. Thorns. Fast potential spike of frog skin generated at the outer surface of the epithelium. *Science,* 3807, *1473-1477.*

Nagel, W. (1976). Intracellular electrical potential difference of frog skin epithelium. *Pflügers Arch. ges. Physiol.* 365, *135-143.*

Sten-Knudsen, O. (1979). Passive transport processes. In *Membrane Transport in Biology,* G. Giebisch, D.C. Tosteson & H.H. Ussing (eds.) *5-113. Springer-Verlag, Berlin-Heidelberg-New York.*

Ussing, H.H. (1949). The distinction by means of tracers between active transport and diffusion. *Acta physiol. scand.* 19, *43-56.*

Ussing, H. H. & E.E. Windhager (1964). Nature of shunt path and active sodium transport path through frog skin epithelium. *Acta physiol. scand.* 61, *484-503.*

Adv. Physiol. Sci. Vol. 3. Physiology of Non-excitable Cells
J. Salánki (ed.)

EFFECT OF ADH ON THE CAPACITANCE OF APICAL EPITHELIAL MEMBRANES

J. Warncke and B. Lindemann
2nd Department of Physiology, 6650 Homburg/Saar, FRG

Recent experiments [1] have shown that ADH stimulates the Na-uptake of toad urinary bladder by increasing the number of channels available for Na-transport through the apical membrane. Is this recruitment achieved by unmasking of channels already in the membrane or, for instance, by fusion with the membrane of vesicles containing new channels? To investigate the possibility of recruitment by fusion we have recorded the apical membrane capacitance in response to ADH-stimulation. If fusion is involved a small increase in membrane area my be expected and cause an increase in membrane capacitance.

MATERIALS and METHODS

The experimental set-up is shown in Fig. 1. We use the non-invasive method of high precision impedance analysis. Sinusoidal voltage displacements of 5 mV or less are input to the voltage clamp, ranging from 1600 to .1 Hz in decrements of 4 or 6 per octave. Bursts consist of 3 to 10 periods and the total sweep needs about 8 times the time of the longest period. The recorded current is analysed by correlation, yielding amplitude and phase at each frequency. The data are plotted as impedance spectrum with amplitude and phase or as Nyquist or Cole plots (Fig. 1 mid left). A non-linear regression will give the optimal rational function with complex coefficients called transfer function

$$H(w) = (1 + c_1 jw + c_2 (jw)^2)/(c_3 + c_4 jw + c_5 (jw)^2)$$

j = imaginary unit, $w = 2\pi f$.

The quality of the fit is checked by comparing the data with the modelled values and the error is usually in the range of 1 - 2 %. Splitting the coefficients of the function as specified by the model results in values for the apical and latero basal resistances and capacitances and the series resistance

of bath and supporting tissue. The non specific shunt conductance is determined separately by blocking the Na-specific pathway with amiloride.

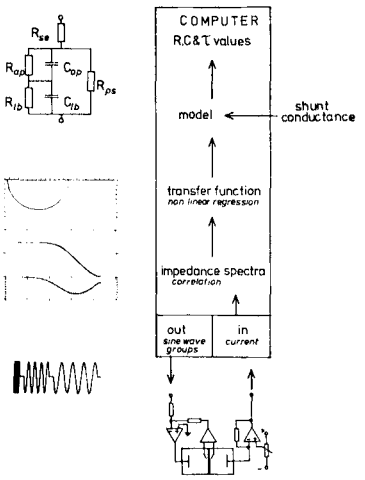

Fig.1: Protocol for impedance measurements
An on-line-computer (Nova or Z80-based microprocessor) generates fully programable sine-wave bursts used as input to a voltage clamp. The current signal is correlated with the input to yield phase and amplitude, which are plotted (mid left). Mathematical treatment will lead to values of the model constants (upper left). The shunt R_{ps} has to be measured separately.

The accuracy of the measurement is checked with known RC-dummy networks.
The abdominal skin of Rana esculenta and the urinary bladder of the toad Bufo marinus are used in these experiments. Mucosal solutions are always sulfate-Ringer and serosal solutions are sulfate-Ringer if possible. Set-up and solution are described elsewhere [2].

RESULTS

ADH influences both membranes

Fig. 2 demonstrates that the application of ADH influences both membranes in the absence of an osmotic transepithelian gradient. Both semicircles of the Nyquist or Cole plot of the toad bladder impedance are changed. The agreement of the model calculation and the data points is good, even in those cases where 2 time constants show systematic deviations (control curve A1, large R-side), 3constants will fit with the usual precision (ADH curve A2). Expressing this additional time constant as parallel RC network leads to values of 600 Ohm and 1000 µF. Ignoring this process and fitting the remaining curve does not change the calculated constants.

The apical capacitance is always the smaller as can be demonstrated by depolarization with high serosal K, where 1 membrane disappears electrically, or with different Na concentrations on the mucosal side, which affects mostly the apical membrane.

The fact that ADH acts in normal and depolarized membranes can be used to get reliable measurements even in those cases where the Cole plots do not separate, by simply depolarizing the epithel.

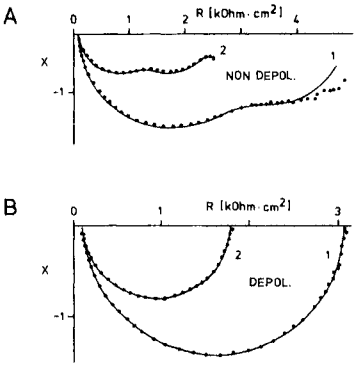

Fig. 2:Cole-plot of normal (A) and depolarized (B)toad bladder with 20 mU/ml ADH (2)and without (1). The solid line is calculated according to the model.

ADH increases the apical capacitance

The time dependence of the membrane parameters can be seen in Fig. 3. The apical capacitance increases in normal and depolarized membranes after adding 20 mU ADH. In the normal epithel also the latero-basal capacitance increases. Simultaneously all resistances decrease and short circuit current increases, too. For higher doses of ADH the apical resistance might be much smaller as the latero-basal resistance as was reported by Nagel [3].Measurements during the initial fast response are hardly possible because the method depends on relative stable parameters during the measurement.

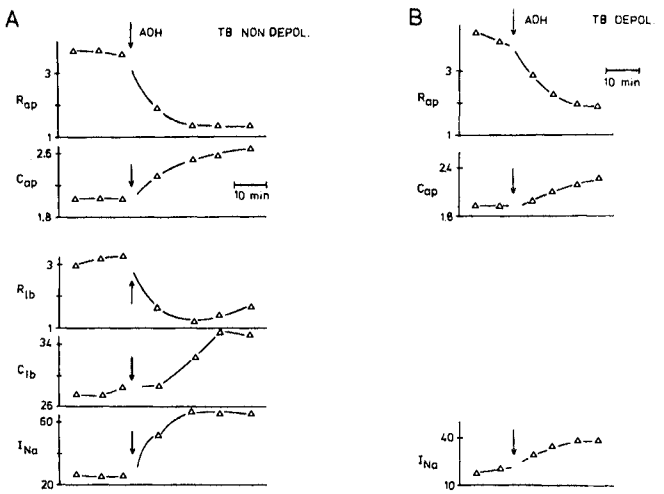

Fig. 3: Time dependence of membrane parameters treated with ADH. Same bladder as in Fig. 2. Normal (A) and depolarized (B). ADH increases the capacitances and decreases all resistances. Units are kOhm and μFarad for 1 cm^2, current in μA.

It is noteworthy that the latero-basal membrane has a ten-fold larger capacitance as the apical membrane and taking this as indication of the real surface means that this membrane is very tight, about 100 kOhm for 1 cm^2.

Na-permeability increasing drugs do not increase the capacitance

Treating frog skin with 2 mM benzimidazolguanidine (BIG) or toad bladder with 2 mM p-chloromercury-phenyl sulfonic acid (PCMPS) does not change the membrane capacitance while reducing the apical resistance to half of the control value. Furthermore, imposing an osmotic gradient in the presence or absence of ADH did not increase the capacitance. In both cases there might be a small decrease of the apical capacitance (Table 1).

Influence of various agents on the apical membrane:

% of CONTROL R_{ap}	% of CONTROL C_{ap}			
76	108	FS	ADH_{20}	(3)
45	123	TB	ADH_{20}	(3)
77	113	TB	ADH_5	(8)
43	97	FS	BIG	(4)
47	98	TB	PCMPS	(4)
-	88	FS	1/10 RINGER	(2)

Table 1: ADH 20 mU/ml or 5 mU/ml increased the capacitance in frog skin (FS) and toad bladder (TB), sodium permeability changing drugs did not. The osmotic gradient was done under full amiloride block.

DISCUSSION

There is little morphological change of the apical surface of bladders if ADH is supplied and no osmotic gradient is present or if a gradient is imposed on controls [4]. However, application of ADH in the presence of an osmotic gradient reduces the amount of microvilli, and causes swelling. Therefore, the finding that swelling does not increase the effective surface area is unexpected. Neither unmasking existing channels (e.g. by BIG) nor osmotic effects change the surface area.Only ADH, which "recruits" new channels, increases the surface.This indicates that there might be a pool of channel rich membranes (vesicles) which get incorporated into the apical membrane via the action of ADH.

REFERENCES

1. J.H.-Y.Li, L.G.Palmer, I.S.Edelman, B.Lindemann, Pflügers Arch. 382: R13 (1979)
2. W.Fuchs, E.H.Larsen, B.Lindemann, J.Physiol. 267: 137-166 (1977)
3. W.Nagel, J. Membrane Biol. 42: 99-122 (1978)
4. F.Spinelli, A.Grosso, R.C.de Sousa, J. Membrane Biol. 23: 139-156 (1975)

Support was received from the DFG through SFB 38, project C1

Adv. Physiol. Sci. Vol. 3. Physiology of Non-excitable Cells
J. Salánki (ed.)

DETERMINATION OF THE COUPLING RATIO OF THE Na-K PUMP RESPONSIBLE FOR TRANSEPITHELIAL Na TRANSPORT BY BLOCKADE OF K CHANNELS

Robert Nielsen
with technical assistance of Birgit Hasman
University of Copenhagen, Institute of Biological Chemistry A, 13 Universitetsparken, DK-2100 Copenhagen Ø, Denmark

According to the two-membrane hypothesis (Koefoed-Johnsen and Ussing, 1958) the origin of the electrical potential across the isolated frog skin) can be explained by the fact that the frog skin is composed of an outward-facing membrane which is selectively permeable for Na^+-ions, but impermeable for K^+-ions and permeable for small anions like Cl^-. The inward-facing membrane is permeable to K^+ and small anions, but impermeable to free Na^+. The high intracellular K^+ concentration and the active transcellular Na^+ transport are according to this model accomplished by the same mechanism, namely, a coupled Na-K pump located at the inward facing membrane. This hypothesis predicts that there should be a correlation between the $^{39}K^+$-$^{42}K^+$ exchange across the inward facing membrane and the active transepithelial Na^+ transport. However, measurement of the $^{39}K^+$-$^{42}K^+$ exchange across the inward facing membrane have failed to show any clear coupling stoichiometry between the transepithelial Na^+ transport and $^{39}K^+$-$^{42}K^+$ exchange (for ref. see Nielsen 1979a). A different approach was therefore sought.

According to the two-membrane hypothesis (Fig. 6A) one would expect that addition of a component which makes the outward facing membrane permeable to K^+ should result in an active outward transport of K^+. Polyene antibiotics increase the permeability of cell membranes for K^+ and other ions. Addition of the polyene antibiotics (filipin and amphotericin B) to the outside bathing solution of the isolated frog skin resulted in an active outward transport of K^+ (Nielsen 1971, Nielsen 1972; Bakhteeva and Natochin 1975). In a recent paper (Nielsen 1979a) it is shown that the filipin induced active outward K^+ transport is coupled to the active inward Na^+ transport.

According to the two membrane hypothesis it should also be possible to determine coupling ratio of the Na-K pump by repressing the passive K^+ current across the inward facing membrane. If the active transepithelial Na^+ transport is carried out by a Na-K pump with a coupling ratio of *e.g.* 1.5 (3Na/2K), then according to the two membrane hypothesis (Fig. 6A), 2/3 of the SCC across the inward facing membrane is carried by K^+ via the K^+-"channel" and 1/3 by Na^+ ions via the Na-K pump. Addition of a component which completely hamper the K^+ flux through the K^+ channel, should therefore initially reduce the SCC by 2/3 because the current carried by the K^+ ions via the K^+ channel is switched off.

The passive net K^+ flux via the K^+ channel from the cells to the inside bathing solution (IBS) should decrease if the K^+ concentration in the IBS is increased. Furthermore Ba^{++} has been shown to reduce the K^+ conductance in frog heart (Hermsmeyer and Sperelakis 1970), in frog muscle (Henderson 1974), and in frog skin (Nagel 1979, Nielsen 1979a). In order to investigate whether it was possible to determine the coupling ratio of the Na-K pump by blocking the K^+ channel, the effect of Ba^{++} and K^+ on the SCC were investigated.

From the experiments presented here it is concluded that Ba^{++} can be used as a tool to determine the coupling ratio (β) of the Na-K pump, and β was found to be 1.5.

MATERIALS AND METHODS

The experiments were performed on male and female frogs (Rana temporaria and Rana esculenta). The skins were mounted in perspex chambers (area 3.14 cm^2) and bathed in stirred Ringer's solution. Cl^- Ringer's solution was composed of (in mM): Na^+, 115; K^+, 2.5; Ca^{++}, 1.0; HCO_3^-, 2.5; Cl^-, 117; pH = 8.2. The gluconate Ringer's solution was hypotonic since it was found that isotonic gluconate Ringer's solution caused a pronounced inhibitions of the SCC. The gluconate Ringer's solution was composed of (in mM): Na^+, 74.7; K^+, 2.5; Ca^{++}, 1.0; TRIS-gluconate, 5.0; HCO_3^-, 2.5; gluconate, 76.7; pH = 8.2. The 10 mM, 25 mM and 50 mM KCl and K^+ gluconate Ringer's solution was produced by substituting Na^+ by K^+. The short circuit experiments were performed according to the method by Ussing and Zerahn (1951).

Addition of Ba^{++} to the IBS of the isolated frog skin resulted in an inhibition of the SCC and in an increase in the transepithelial resistance (Fig. 1 and Fig. 5A). 2-5 min after the addition of Ba^{++} the SCC started to recover and the resistance started to decrease. The recovery phase was completed 20-90 min. after the addition of Ba^{++}. The recovery varied from 30% to 150%, thus, in some cases prolonged incubation with Ba^{++} resulted in an activation of the SCC. The replacement of the IBS by Cl^{-} Ringer's solution without Ba^{++} resulted in a further transient increase in the SCC (Fig. 1 wash).

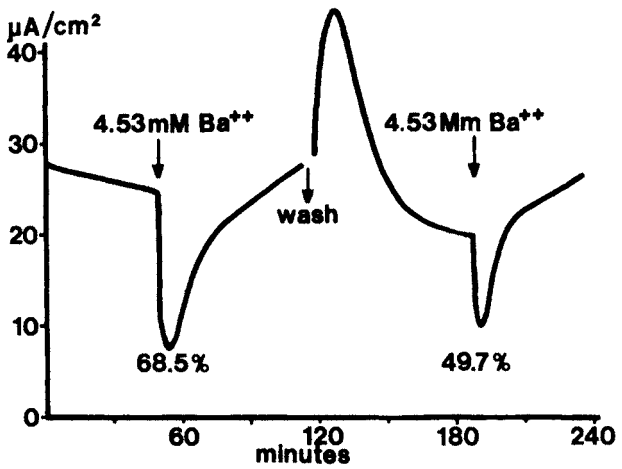

Fig. 1. Effect of 4.53 mM Ba^{++} on the short-circuit current across isolated frog skin. At the first arrow Ba^{++} is added to the inside bathing solution. At the arrow "wash" the inside bathing solution was replaced by a solution without Ba^{++}. At the third arrow Ba^{++} is added to the inside bathing solution again.

The initial decrease in SCC and increase in resistance is in agreement with the notion that Ba^{++} blocks the K^{+} channel. However, the observed spontaneous recovery indicates that presence of Ba^{++} in the IBS results in the formation of a Ba^{++} insensitive K^{+} channel.

If Ba^{++} was added to the IBS a second time after the wash out of Ba^{++} from the IBS, a transient inhibition followed by the recovery was observed, but the percentage reduction in the SCC was always smaller. In the experiment shown in Fig. 1, the inhibition obtained after the first

addition of Ba^{++} was 68.5%, whereas the inhibition obtained at the second addition of Ba^{++} was 49.7%. Thus, the effect of Ba^{++} was only partially reversible.

When Ba^{++} is added to the IBS of isolated epithelium the same result is obtained as in whole skin (Nielsen 1979b), but the inhibition is faster, because the thickness of the unstirred layer on the inside has been reduced by removal of the connective tissue. The primary inhibitory effect of Ba^{++} is faster than the secondary effect (the recovery), so the two effects are separated in time (Nielsen 1979b). Therefore it is possible to measure the Ba^{++} induced initial inhibition without getting to much interference from the subsequent recovery. The initial Ba^{++} induced inhibition (measured on whole skins) is plotted against the Ba^{++} concentration in the IBS (Fig. 2), the Ba^{++} induced inhibition of the SCC increases with increasing Ba^{++} concentration until a maximum inhibition is reached.

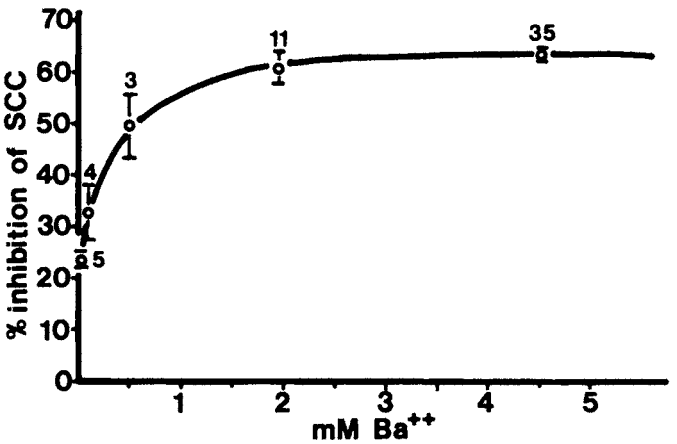

Fig. 2. Maximum pertentage reduction of the short-circuit current elicited by various concentrations of Ba^{++}. Values are the mean ±S.E.

The maximum inhibition obtained with 4.53 mM Ba^{++} (Fig. 2) was 63.7 ±1.0%, in another series (Nielsen 1979b) the mean was found to be 65.0 ±1.9% (n = 10).

The fact that the initial inhibition of the SCC found after the addition of Ba^{++} shows saturation, and the maximum inhibition is close to 66.6% indicates that the coupling ratio of the Na-K pump is 1.5.

Effect of K^+

If the initial Ba^{++} induced inhibition of the SCC is caused by an inhibition of the K^+-current across the inward facing membrane, one would expect that an increase in the K^+ concentration in the IBS also should result in an inhibition of the SCC. The calculated percentage inhibition of the steady state SCC caused by an increase in the K-concentration is shown in Fig. 4 (broken line). The percentage inhibition is calculated on basis of a computer programme (Hviid Larsen and Kristensen 1978); in the calculations it is assumed that the Na^+, K^+ and Cl^- permeabilities of the membranes stay constant before and after the increase of the K^+ content in the IBS.

The change from Ringer's solution with 2.5 mM K^+ to Ringer's solution with 25 mM K^+ resulted as the addition of Ba^{++} in a transcient inhibition of the SCC followed by a spontaneous activation (Fig. 3).

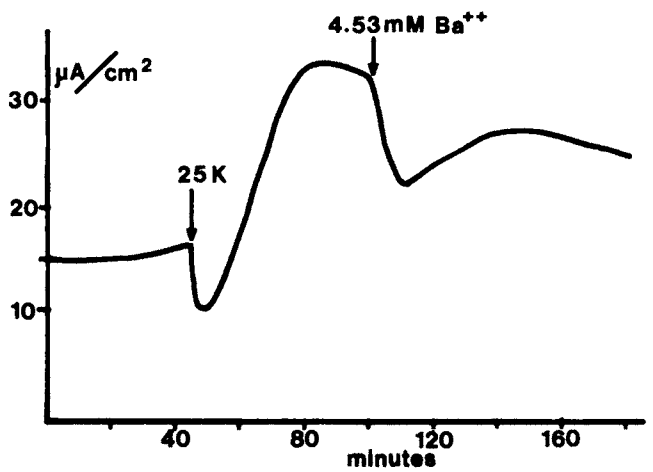

Fig. 3. Effect of 25 mM K^+ on the short-circuit current in Cl^- Ringer's solution. At the arrow 25 K, the K^+ concentration in the inside bathing solution was changed from 2.5 mM to 25 mM. At the arrow Ba^{++}, 4.53 mM Ba^{++} was added to the inside bathing solution.

After about 20 min. incubation with 25 mM K^+ in the IBS the SCC is higher than in the control period (Fig. 3, 0-40 min.) thus prolonged incubation with 25 mM K^+ in the IBS results in an activation of the SCC, and not in an inhibition as the computer programme predicts (Fig. 4). This indicates that the permeability coefficients for Na^+ and K^+ do not remain constant.

In order to explain the observed increase in the SCC we have to assume that both the K^+ permeability of the inner membrane (P^i_K) and the Na^+ permeability of the outer membrane (P^o_{Na}) increases. Activation of the SCC caused by the presence of high K^+-concentration in the IBS has also been observed by Ussing *et al.* (1965).

After the SCC had reached a new steady state during the incubation with 25 mM K^+ in the IBS, Ba^{++} (4.53 mM) was added. The maximal initial inhibition found after addition of Ba^{++} in the presence of 25 mM K^+ in the IBS was 31.5% (Fig. 3). In the presence of 2.5 mM K^+ in the IBS the addition of 4.53 mM Ba^{++} resulted in about 65% reduction of the SCC (Fig.2)

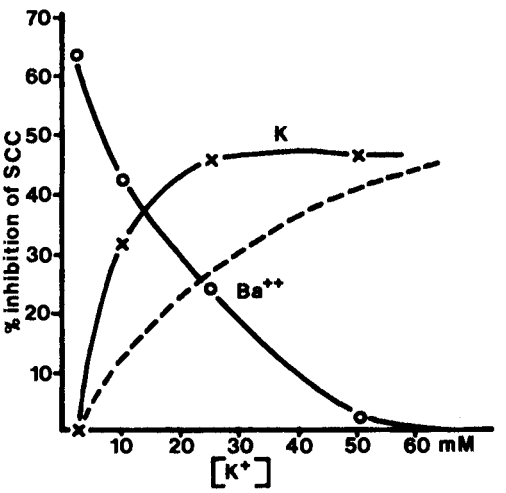

Fig. 4. The broken line shows the calculated steady state percentage inhibition of the short-circuit current caused by an increase of the K^+ concentration in the inside bathing solution (IBS). The line labelled K shows the maximum initial inhibition caused by an increase in the K^+ concentration of the IBS. The line labelled Ba^{++} shows the maximal initial inbibition obtained by the addition of 4.53 mM Ba^{++} to the IBS at different K^+ concentrations.

Fig. 4 shows the maximal initial inhibition found by increasing the K^+ concentration in the IBS from 2.5 mM to 10 mM, from 2.5 to 25 mM and from 2.5 mM to 50 mM, the initial reduction in the SCC increased by increasing the K^+ concentration in the IBS, but the K^+ induced inhibition was in all cases transient (as shown in Fig. 3). After the SCC had reached a new

steady level Ba^{++} (4.53 mM) was added. From Fig. 4 it is seen that the effect of 4.53 mM Ba^{++} decreases with increased K^+ concentration in the IBS, and in the presence of 50 mM K^+ in the IBS the inhibitory effect of Ba^{++} was abolished. This indicates: (i) that Ba^{++} and K^+ compete for the same site in the K^+ channel, or (ii) the presence of high K^+ in the IBS might result in the formation of a Ba^{++} insensitive K^+ pathway in the inward facing membrane.

Effect of Ba^{++} and K^+ in the presence of non permeating anions.

The two membrane hypothesis predicts that a decrease in P_K^i or an increase in the K^+ concentration in the IBS should result in a swelling of the cells. It has been shown by MacRobbie and Ussing 1961 that an increase in the K^+ concentration in the IBS result in a swelling of the cells in frog skin epithelia. Furthermore, a swelling of the frog skin epithelium gives rise to increased active Na^+ transport (Ussing 1965).

In order to investigate whether swelling of the cells should be involved in the recovery of the SCC observed after addition of Ba^{++}, the effect of Ba^{++} and K^+ in the presence of a very slow permeating anion was investigated. As impermeable anion gluconate was chosen.

The effect of Ba^{++} on the SCC and the transepithelial resistance in gluconate- and Cl^-Ringer's solution is shown in Fig. 5. The maximal initial inhibition found in Cl^- Ringer's solution was 64.8 ±1.5% and in gluconate Ringer's solution 55.4 ±4.0% (n = 4). In Cl^- Ringer's solution the usual recovery of the SCC was observed whereas no or only a very slow recovery of SCC was observed in gluconate Ringer's solution. Both in gluconate and Cl^- Ringer's solution the addition of Ba^{++} resulted in an increase in the transepithelial resistance, but in Cl^- Ringer's solution the increase in resistance was transient whereas in gluconate Ringer's solution the resistance remained high. The replacement of the IBS by a Ringer's solution containing 25 mM K^+ and 4.53 mM Ba^{++} resulted in the gluconate experiment in a fast increase in the SCC and in a decrease in the transepithelial resistance (Fig. 5A). This indicates that Ba^{++} and K^+ compete for the same site in the "K^+-channel".

In Cl^- Ringer's solution the changes in SCC and resistance were much smaller when the IBS was replaced by a Ringer's solution containing 25 mM K^+ and 4.53 mM Ba^{++} (comp. Figs. 5A and 5B), this was mainly due to the spontaneous recovery in SCC and resistance which take place in Cl Ringer's

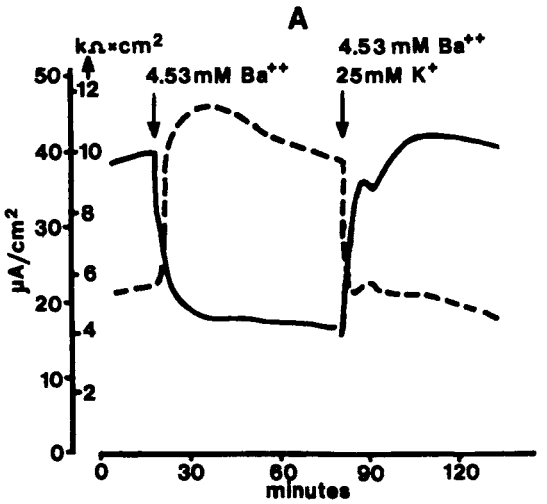

Fig. 5A. Effect of 4.53 mM Ba^{++} on the short-circuit current and the transepithelial resistance. The exp. was carried out in gluconate Ringer's solution. At the arrow 25 K^{+}, 4.53 Ba^{++} the inside bathing solution was changed to a Ringer's solution containing 25 mM K^{+} and 4.53 mM Ba^{++}.

_____ *Short-circuit current µA/cm²*

—— *Transepithelial resistance kΩx cm².*

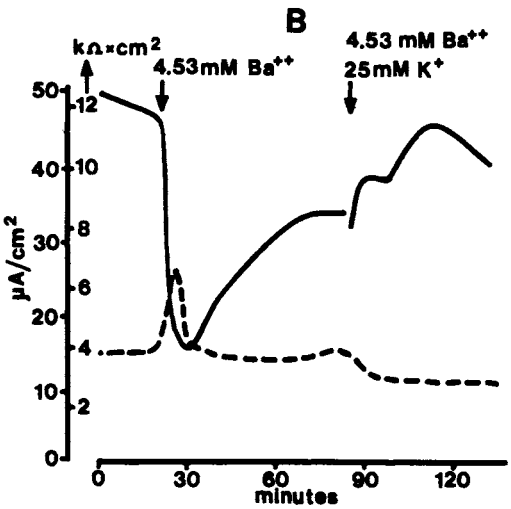

Fig. 5B. The same as Fig. 5A, but the exp. was carried out in Cl^{-} Ringer's solution.

solution. Thus, this experiment supports the notion that the spontaneous recovery at least partially is due to the formation of Ba^{++} insensitive K^+ "pathway" in the inward facing membrane.

DISCUSSION

The polyene antibiotic filipin makes the outward facing membrane of the isolated frog skin permeable for K^+ which results in an active outward transport of K^+. The addition of Ba^{++} to the IBS under these conditions (the presence of filipin) activate the active outward K^+ transport and reduces the active transepithelial Na^+ transport (Nielsen 1979b). A decrease in the K^+ permeability of the inward facing membrane can, according to the two membrane hypothesis, explain these observations. A decrease in the K^+ permeability should result in (i) a decrease in the SCC and (ii) in an increase in the transepithelial resistance and (iii) a depolarization of electric potential of the cells; addition of Ba^{++} to the IBS causes these changes, see Fig. 5B and Nagel (1979). From these observations and the finding that there is a competition between K^+ and Ba^{++} (Figs. 4 and 5) it is concluded that Ba^{++} reduces the K^+ permeability of the inward facing membrane.

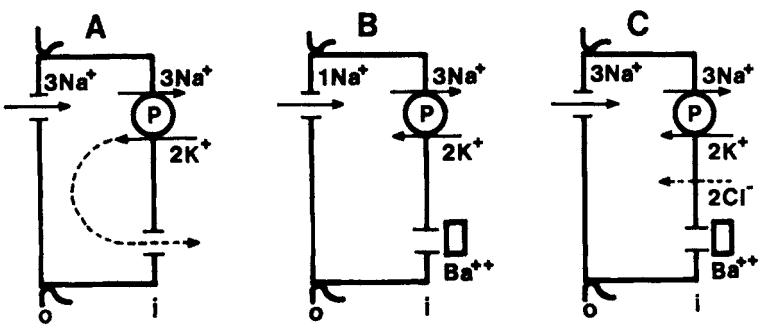

Fig. 6 A.B.C. The two membrane hypothesis. P Na-K pump with a coupling ratio of 1.5 (3Na/2K).

i inward facing membrane.

0 outward facing membrane.

The fact that the initial inhibition of the SCC after the addition of Ba^{++} shows saturation and that the maximum inhibition is close to 66.6% can be explained by the following model which is based on the two membrane hypothesis (Fig. 6A). The active transepithelial Na^+-transport is carried out by a Na-K pump with a coupling ratio of 1.5, consequently addition of a component (Ba^{++}) which completely blocks the K^+ channel would initially reduce the SCC by 2/3, because the current carried by the K^+ ions across the inward facing membrane is switched off. The recovery is due to secondary changes in the cells which results in the formation of Ba^{++} insensitive K^+ channels in the inward facing membrane and in an increase in P^0_{Na}, the last statement is based on the observation that the recovery after Ba^{++} in some cases is higher than 100%. Just after the K^+ channels are blocked the cellular Na^+ concentration is unchanged, therefore the Na-K pump will operate at the same rate, as before the addition of Ba^{++}, for a short period (thus, the Na^+ influx remains unchanged for a short period). In order to maintain electroneutrality in the cells, in this short period, the net Na^+ flux across the outward facing membrane has to be reduced by the amount of K^+ which is pumped into the cells (Fig. 6B), or the cells has to expel an equvivalent amount of other cations *e.g.* H^+ and Ca^{++}. If the cells expel other ions than Na^+ *e.g.* H^+ and Ca^{++} the initial inhibition would be less than 66.6%. The cells are also able to maintain electroneutrality by an uptake of anions *e.g.* Cl^- or HCO_3^- (Fig. 6C) in this situation the cells would swell. Thus, the formation of the Ba^{++} insensitive pathway might be caused by a changes in (i) cellular pH, or (ii) in a change in cellular Ca^{++} concentration or (iii) or it might be released by the swelling of the cells.

The amount of H^+ and Ca^{++} which can be extruded from the cells in this situation (blockade of the K^+ channel) is small compared with the net Na^+ flux, therefore the blockade of the K^+ channels should (if no changes took place in P^i_K or in the Na-K pump) result in a complete inhibition of the SCC if the model Fig. 6B was operating, or in a destruction of the cells because of the swelling if the model Fig. 6C was operating.

That the swelling of the cells or the uptake of KCl in some way are involved in the recovery apperars from the fact, that in the presence of the very slow permeating anion gluconate no or only a very slow recovery was observed. In gluconate Ringer's solution the initial Ba^{++} induced

inhibition was 55.4 ±4.0% whereas the initial inhibition in the corresponding controls in Cl^- Ringer's solution was 65.8 ±1.5%, this indicates that other cations *e.g.* H^+ or Ca^{++} are extruded from the cells to the IBS in gluconate Ringer's solution, therefore it can not be excluded that changes in cellular pH and Ca^{++} concentration also have an effect on the formation of the Ba^{++} insensitive K^+ channels.

CONCLUSION.

The data presented here shows that Ba^{++} blocks the K^+ channels in the isolated frog skin, and Ba^{++} and K^+ compete for the same site in the K^+ channel. Immediately after the blockade of the K^+ channel the cells forms or activate a Ba^{++} insensitive K^+ channel in the inward facing membrane. Furthermore the data presented here indicates that it is possible to estimate the coupling ratio of the Na-K pump by measureing the initial decrease in the SCC caused by the blockade of the K^+ channels.

Acknowledgments

I wish to thank Mrs. Lis Nielsen and Mrs. Inge Windfeld for typing the manuscript, Mr. Poul Hansen for making the drawings and Mr. Peter Korsgård for producing most of the apparatus used in this investigation.

REFERENCES

Bakhteeva, V.T., Natochin, Y.V. 1975. The passive and active elements of potassium secretion system in frog skin. *Lechenow Physiol. J. USSR.* 61: *1242.*

Henderson, E.C. 1974. Strophanthidin sensitive electrogenic mechanisms in frog sartorius muscle exposed to barium. *Pfluegers Arch.* 350: *81.*

Hermsmeyer, K., Sperelakis, N. 1970. Decrease in K^+ conductance and depolarization of frog cardiac muscle produced by Ba^{++}. *Am.J.Physiol.* 219: *1108.*

Koefoed-Johnsen, V., Ussing, H.H. 1958. The nature of the frog skin potential. *Acta Physiol. Scand.* 42: *298.*

Hviid Larsen, E., Kristensen, P. 1978. Properties of a conductive cellular chloride pathway in the skin of the toad (Bufo bufo). *Acta Physiol. scand.* 102: *1*

MacRobbie, E.A.C., Ussing, H.H. 1961. Osmotic behaviour of the epithelial cells of frog skin. *Acta physiol. scand.* 53: *348.*

Nagel, W. 1979. Inhibition of potassium conductance by barium in frog skin epithelium. *Biochim. Biophys. Acta* 552: *346.*

Nielsen, R. 1971. Effect of amphotericin B on the frog skin in vitro. Evidence for outwards active potassium transport across the epithelium. *Acta Physiol. Scand.* 83: *106.*

Nielsen, R. 1972. The effect of polyene antibiotics on the aldosterone induced changes in sodium transport across the isolated frog skin. *J. Steroid Biochem.* 3: *121.*

Nielsen, R. 1979. Coupled transepithelial sodium and potassium transport across isolated frog skin: Effect of ouabain, amiloride and the polyene antibiotic filipin. *J. Membrane Biol.* 51: *161.*

Nielsen, R. 1979. A 3 to 2 coupling of the Na-K pump responsible for the transepithelial Na transport in frog skin disclosed by the effect of Ba^{++} *Acta Physiol. Scand.* 107: *189.*

Ussing, H.H., Zerahn, K. 1951. Active transport of sodium as the source of electric current in the short-circuited isolated frog skin. *Acta Physiol. Scand.* 23: *110.*

Ussing, H.H., Biber, T.U.L., Bricker, N.S. 1965. Exposure of the isolated frog skin to high potassium concentrations at the internal surface. II. Changes in epithelial cell volume, resistance and response to antidiuretic hormone. *J. Gen. Physiol.* 48: *3-425.*

Ussing, H.H. 1965. Relationship between osmotic reactions and active sodium transport in the frog skin epithelium. *Acta physiol. scand.* 63: *141.*

Adv. Physiol. Sci. Vol. 3. Physiology of Non-excitable Cells
J. Salánki (ed.)

EFFECTS OF $HgCl_2$ ON THE APICAL MEMBRANE AND ION TRANSPORT PROCESSES IN TURTLE BLADDER

Thaddeus Wilczewski, Wolfram Nagel, William A. Brodsky and John Durham

Mount Sinai School of Medicine/CUNY, N.Y., N.Y., USA and University of Munich, Munich, FRG

The isolated, short-circuited bladder of Pseudemys scripta has been shown to possess active transport mechanisms for the reabsorption of Na, Cl, and HCO_3 (1-3). When such turtle bladder preparations are bathed on both surfaces by identical Na-rich media containing HCO_3 and Cl, mucosal additions of $HgCl_2$ (final conc. 10^{-5}M) are followed by monotonic decreases in Isc and PD (half-time of decay, 10 min) which reach 10% of the control levels after 10 min. During this period, the transepithelial resistance (Rt) reaches twice the control level, then decreases to half the control level between 60 and 240 min after $HgCl_2$ addition. The early Hg-induced increase in Rt was not detected by Schwartz and Flamenbaum in their studies of $HgCl_2$ effects on ion transport in this tissue (4). (Figure 1).

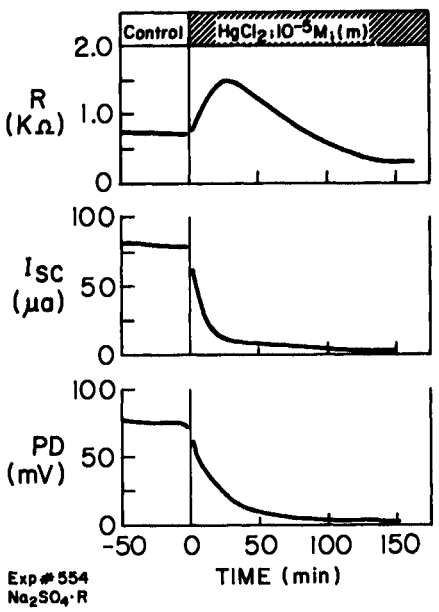

Figure 1. Effect of mucosally-added $HgCl_2$ (10^{-5}M) on R, Isc, and PD of bladders in Na-rich media. (Serosal additions of 10^{-4}M $HgCl_2$ produced no changes).

Microelectrode impalements under these conditions, reveal a $HgCl_2$-induced increase in the electronegativity of cell fluid with respect to mucosal fluid and an increase in the fractional resistance of the apical membrane (Ra/Rt) which also doubles in the first 30 min after $HgCl_2$ addition. It is of interest to note that these $HgCl_2$-induced changes in the apical membrane are similar to, though somewhat slower than those induced by the mucosal addition of amiloride (10^{-5}M) (Figure 2).

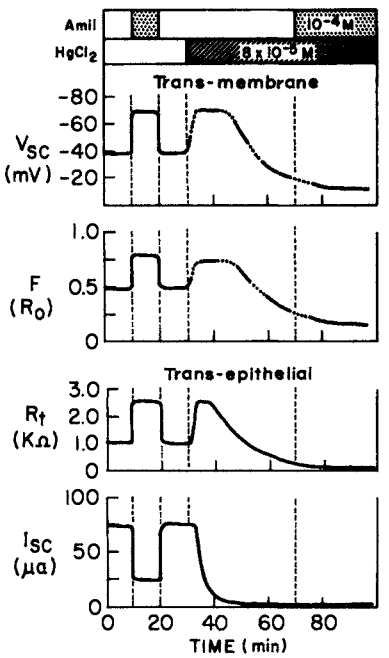

Figure 2. Similarity of effects of $HgCl_2$ and amiloride on: the transapical membrane of potential Vsc; fractional resistance of apical membrane (FRo); transepithelial resistance (Rt), and Isc. Bladders in Na-rich media.

Mucosal additions of $HgCl_2$ (final conc. 10^{-5}M) to ouabain-treated bladders bathed on both surfaces by identical Na-free media containing HCO_3 and Cl are followed by monotonic decreases in the transepithelial PD and Isc, which reach near-zero levels after 30-45 min while Rt first increases by ca. 25% and then decreases to below control levels. The concomitant forward flux (I^{Cl}_{ms}) and back flux (I^{Cl}_{sm}) of chloride increase while the transepithelial conductance ($Gt = 1/Rt$) increases; but the conductance of the half bladder across which I^{Cl}_{ms} is measured does not increase to the same extent as that of the mated half bladder across which I^{Cl}_{sm} is measured (Figure 3).

However the unidirectional chloride flux per unit of transepithelial conductance in the one half-bladder (I^{Cl}_{ms}/Gt) becomes and remains equal to that in the paired half bladder (I^{Cl}_{sm}/Gt), which means that the net "isoconductive" chloride reabsorption reaches zero during the second hour after $HgCl_2$ addition (Figure 4).

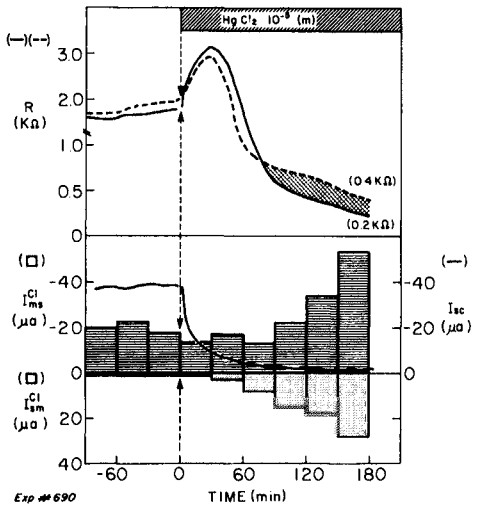

Figure 3. Effect of $HgCl_2$ on R, Isc, and unidirectional Cl flux (ms and sm) across each one of a mated pair of hemibladders containing HCO_3 and Cl.

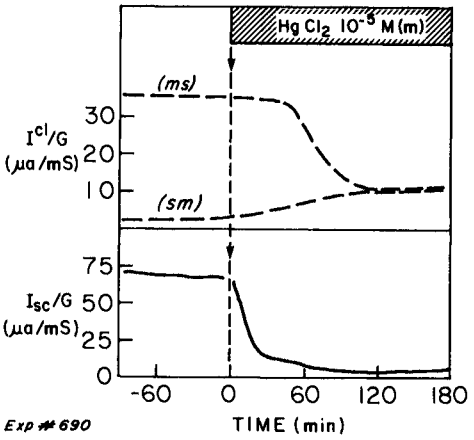

Figure 4. Same experiment as that depicted in Fig. 3, with Cl fluxes (ms and sm) and Isc normalized to the corresponding conductance (1/R) of each hemibladder.

The mercurial-induced effects on the Na transport-related Isc are reversed by: (1) removal of the $HgCl_2$-containing mucosal fluid after 30-40 min of exposure to the $HgCl_2$ or while Rt is still at twice the control level; and (ii) the addition of DTT (10^{-4}M) or amiloride (10^{-5}M) either before or during the first half hour after exposure to $HgCl_2$. The addition of amiloride followed by that of $HgCl_2$ protects the bladder against the toxic effects of mercuric ions for as long as two hours; then the removal of bothe the $HgCl_2$ and amiloride is followed by a restoration of Isc, PD and Rt to control levels. (Figures 5 and 6).

Conclusions. Mercuric ions added to the mucosal fluid first (within 30 min) block the Na paths in the apical membrane to suppress Na reabsorption. The subsequent ($1\frac{1}{2}$-2 hrs) increase in bladder conductance (Gt) with nullification of net isoconductive reabsorption could be due to a Hg-induced loosening of the tight junctions.

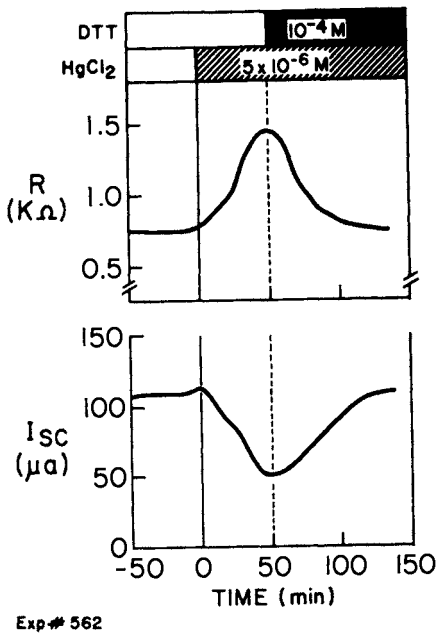

Figure 5. Reversal of Hg-induced changes in R and Isc by mucosal addition of DTT; Na-rich media.

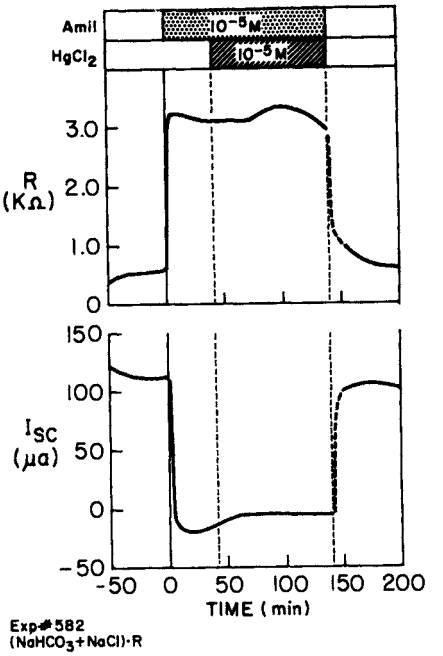

Figure 6. Two hour period of protection against $HgCl_2$-induced changes in R and Isc by the presence of mucosal amiloride; Na-rich media.

REFERENCES

1. Gonzalez, C.F., Y.E. Shamoo, H.R. Wyssbrod, R.E. Solinger, and W.A. Brodsky. Electrical nature of sodium transport across the isolated turtle bladder. Amer. J. Physiol. 213:333-340, 1967.

2. Gonzalez, C.F., Y.E. Shamoo and W.A. Brodsky. Electrical nature of active chloride transport across short-circuited turtle bladders. Amer. J. Physiol. 212:641-650, 1967

3. Schilb, T.P. and W.A. Brodsky. CO_2 gradients and acidification by transport of HCO_3 in turtle bladders. Amer. J. Physiol. 222:272-281, 1972.

4. Schwartz, J.H. and W. Flammenbaum. Heavy metal-induced alterations in ion transport by turtle urinary bladder. Amer. J. Physiol. 230:1582-1589, 1976.

Acknowledgments. Grant-in-aid support from: NIH (AM-16928-04A2) and NSF (PCM-76-02344). Invaluable technical help from Ms. Christina Matons.

Adv. Physiol. Sci. Vol. 3. Physiology of Non-excitable Cells
J. Salánki (ed.)

pH DEPENDENCE OF APICAL Na-TRANSPORT IN FROG SKIN

J. H.-Y. Li and B. Lindemann
SFB 38, C1, 2nd Department of Physiology, 6650 Homburg, FRG

Lowering the pH of the solution bathing the outward-facing membrane of frog skin (Rana esculenta and ridibunda) from 7.5 to 5.5 has been shown to increase the apical Na permeability [1,2]. To investigate further the nature of this natriferic stimulation by protons, we have analysed the amiloride-induced fluctuations of the short circuit current to determine whether or not the increase of Na permeability is the result of an increased single channel current. Such an increase may be expected from changes in the intra-membraneous electrical potential following the removal of negative fixed charges.

Skins with exposed area of 3 cm^2 were depolarized at their basolateral membranes in a serosal medium containing 58.3 mM K_2SO_4, buffered at pH 7.3. Their outer surface was in contact with 54.44 mM Na_2SO_4 and 1 mM $CaSO_4$ buffered by phosphate. When a reversible stimulation of I_{Na} by lowering outer solution pH had been demonstrated, further measurements of fluctuations were taken serially in 6 submaximal amiloride concentrations from 0 to 7.2 µM in the outer solution. The procedure was then repeated with the same set of amiloride concentrations at a lower pH value.

The Na current power density in the absence of amiloride increases at all frequencies used as the pH is lowered and I_{Na} increased (data not shown). Upon addition of submaximal concentrations of amiloride to the outer solution, Lorentzian spectral components appear. Their plateaus for a given amiloride concentration $(A)_o$ increase with the lowering of pH while the corner frequencies show little changes (Fig. 1). Thus, the microscopic rate constants derived from the chemical rate vs. $(A)_o$ plot show only insignificant changes at these pH values. When the inverse of Na permeability (P_{Na}), approximated here by $(Na)_o/I_{Na}$, is plotted against $(A)_o$, a regression line can be drawn to yield an apparent macroscopic Michaelis constant for the amiloride block (Fig. 2). In contrast to the absence of pH dependence of the microscopic rate constants, lowering the outer pH increases not only the Na permeability in the absence of amiloride (reduced ordinate intercept) but also the apparent affinity of the amiloride block (shifted abscissa intercept to the right). On the right

of Fig. 2 these values from individual experiments are assembled; the values from the same skin are connected by straight lines. The apparent Michaelis constant of Na-selfinhibition K_N was calculated based on the model of competitive inhibition between Na and amiloride. The calculated values for the single channel current i and the open channel density N_o are shown in Fig. 3. While i shows little pH dependence, N_o increases by pH stimulation. To obtain the total channel density, we evaluated an occupancy plot in the form of $(N_o + N_2)^{-1}$ vs. $(1 + (A)_o/K_A)^{-1}$ as shown in Fig. 4, where N_2 is the density of channels blocked by amiloride. The inverse of the extrapolated ordinate intercept in this plot corresponds to the total density of amiloride blockable channels.

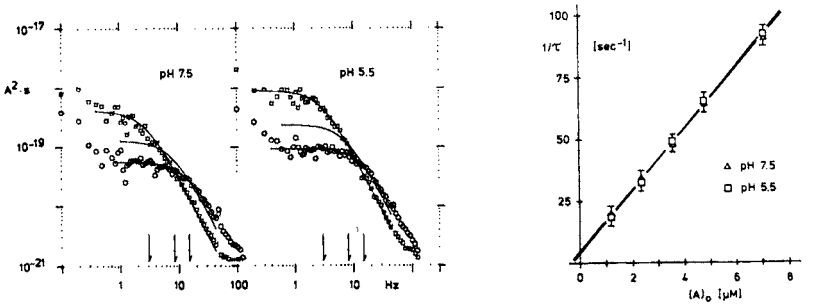

Fig. 1: Amiloride spectra at pH 7.5 and 5.5: $(A)_o$'s are 1.2, 3.6 and 7.2 μM. The curves are fitted Lorentzians. Right: the rate $1/\tau = 2\pi f_c$ vs. $(A)_o$ plot is for the mean corner frequencies from 5 skins.

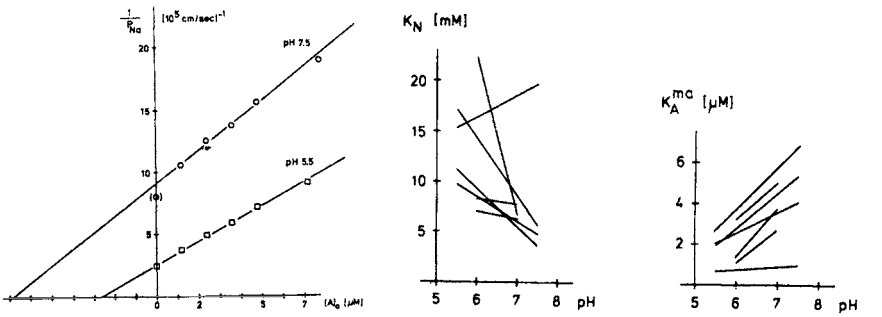

Fig. 2: Effects of acidification on the macroscopic Na permeability and the apparent amiloride affinity; lines drawn from the least square fit. Right: macroscopic apparent Michaelis constants of amiloride block and of Na-selfinhibition at different pH; lines connecting values from the same skin.

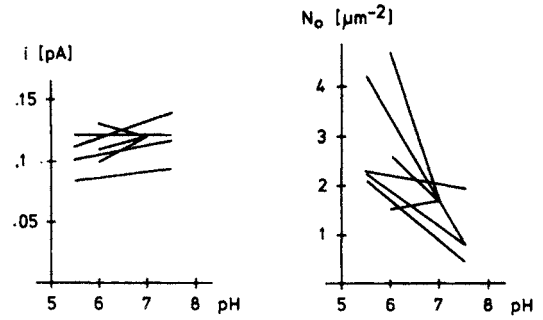

Fig.3: Single channel current (i) and open channel density (N_O) at different pH; lines connecting values from the same skin.

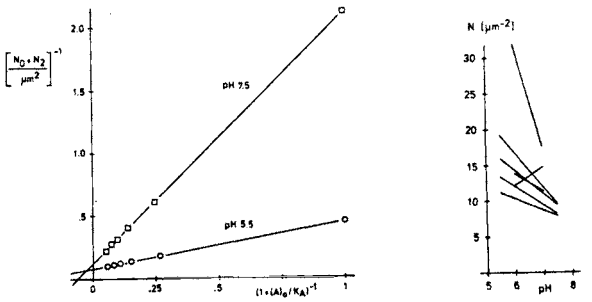

Fig.4: An occupancy plot: N_O, open; N_2, amiloride-blocked channels. The inverse of ordinate intercept gives total channel density N. Right: variation of N in different skins at different pH.

The stimulatory effect of acidification of the outer bathing medium in the pH range studied here has been shown also for the urinary bladder of the toad (Bufo marinus) [3]. In the frog skin of other species the effect of acidification, if any, is merely inhibitory [4,5,6]. The stimulatory natriferic pH effect is found here to be accompanied by an increase of the apparent macroscopic affinity of the amiloride block. Although it has been known that the protonated form of amiloride is responsible for the blocking of apical Na channels [5], the change in the concentration of protonated amiloride in our pH range for amiloride with pK = 8.7 is too small to account for the observed apparent affinity change. The lack of parallel in the pH dependence of the micro- and macro-behaviour of the amiloride block stands in contrast to the change in the blocking potency resulting from a modification on the amiloride structure [7]. There the change of the macroscopic affinity is accompanied by a similar change in the blocking potency as measured by the ease with which the blocker can reach and leave the site to effectuate a block. With the use of an impermeant buffer we observe that the response to the pH stimulation is in the order of seconds; therefore, the immediate effect of the added protons will be on the apical membrane. The possibility of a pH induced dissociation of polyvalent cations from some anionic sites in the membrane and a subsequent increase of P_{Na} in the toad bladder has been dismissed for lack of positive experimental evidence [3]. It also seems unlikely from the

present experimental data, because a change in the membrane fixed charges would change the intramembraneous electric field and cause changes in the single channel current. Although we have not yet examined the effect of apical electrical potential difference on the single channel current, we have observed consistently that a depolarized preparation has a single channel current 1.5 to 2 times smaller than that of its non-depolarized control. However, our evaluation of the values of the single channel current shows that this quantity is rather insensitive to the change of pH. The change of the Na activity near the apical membrane after the pH change is also unlikely; Van Driessche and Lindemann have demonstrated that the channel current is a linear function of the apical Na concentration [8], but in our pH experiments this quantity remains unchanged.

When the pH of the outer solution is lowered further, an inhibitory effect of proton on the P_{Na} develops. A competitive nature of proton with Na in this blockage has been suggested [2,4] . In the present study this type of blockage is not yet apparent as we have not used values of pH below 5.5. Therefore, macroscopically we achieved a sustained stimulation, and microscopically we found no change in the apparent on-rate constant of the amiloride blocking action. The latter finding suggests further that when proton and Na indeed competitively inhibit P_{Na} the apparent Michaelis constant of the proton blockage must be an order of magnitude larger than the proton concentrations used in our study; otherwise, a decrease in the apparent on-rate constant of the amiloride block should become noticeable at pH 5.5 [9] . This is in accord with the previous dose-response finding that the pK for the pH block is in the vicinity of 4 [2] .

In summary, the stimulatory action of acidification is due to an increase in the open channel density and a large fraction of the increase comes from the diminuition of the Na-self-inhibition effect. Indeed, the rapidity of the P_{Na} response is comparable to that induced by other external chemical reagents like para-chloromercuriphenylsulfonate and benzoylimidazole guanidine, which have been shown to increase P_{Na} also by removing the Na-selfinhibition without changing the magnitude of the single channel current [9].

References

1. Zeiske, W., Lindemann, B.: Blockage of Na-channels in frog skin by titration with proton and by chemical modification of COO^--groups. Pflügers Arch. 355: R71 (1975)
2. Lindemann, B., Voûte, C.: Structure and function of the epidermis. In: Frog Neurobiology, ed.R.Llinás and W.Precht, pp. 169-210. Springer Verlag, Berlin (1976)
3. Leaf, A., Keller, A., Dempsey, F.E.: Stimulation of sodium transport in toad bladder by acidification of mucosal membrane. Am.J.Physiol. 207: 547-552 (1964)

4. Schoffeniels, E.: Influence du pH sur le transport actif de sodium a travers la peau de grenouille. Arch.Insternat.de Physiologie et de Biochemie 63: 513-530 (1955)
5. Cuthbert, A.W.: Importance of guanidinium groups for blocking sodium channels in epithelia. Mol.Pharm.12:945-957 (1976)
6. Mandel, L.J.: Effects of pH, Ca, ADH, and theophylline on kinetics of Na entry in frog skin. Am.J.Physiol. 235: C35-C48 (1978)
7. Li, J.H.-Y., Lindemann, B.: Blockage of epithelial Na-channels by amiloride-analogues. Dependence of rate constants on drug structure. Pflügers Arch.379: R18 (1979)
8. Van Driessche, W., Lindemann, B.: Concentration-dependence of currents through single sodium-selective pores in frog skin. Nature 282: 519 (1979)
9. Li, J.H.-Y., Lindemann, B.: The mechanism of chemical stimulation of amiloride-sensitive Na-channels. Pflügers Arch. 384: R7 (1980)

Adv. Physiol. Sci. Vol. 3. Physiology of Non-excitable Cells
J. Salánki (ed.)

ON THE SITE OF ACTION OF PROSTAGLANDIN E_1 (PGE_1) AND OXYTOCIN IN A SODIUM TRANSPORTING EPITHELIUM

J. L. Reyes and J. Aceves
Pharmacology and Physiology Departments, Centro de Investigación del IPN, México 14, D. F. Mexico

INTRODUCTION.

Prostaglandins (PGs) stimulate epithelial Na^+ transport in epithelia such as frog skin (Lote et al. 1974, Barry et al. 1975) and renal tubules (Fülgraff & Meiforth, 1971). Ussing's model for Na^+ transport assumes that Na^+ enters the epithelium through the mucosal surface by a passive step and is transferred to the serosal side by an active process (Na^+ pump). The entry step appears to be the rate limiting step.

There is convincing evidence indicating that C-AMP mediates the stimulatory effect of neurohypophyseal hormones on Na^+ transport (Sapirstein & Scott 1973, Aceves 1977). Because PGs stimulate also C-AMP formation (Hall & O'Donoghue 1976), one would be inclined to conclude that both groups of hormones share a common site (or sites) of action. Therefore we thought interesting to study comparatively the effect of PGs and neurohypophyseal hormones on Na^+ transport in the isolated epithelium of the frog skin.

METHODS.

Transepithelial sodium transport.

It was estimated by measuring the short circuit current (SCC) as described by Ussing and Zehran (Ussing & Zehran 1951). Paired pieces frog skin (Rana pipiens) were mounted in perpex chambers. The inner or serosal side was bathed with normal Ringer (composition mM/L: NaCl 115, $NaHCO_3$ 2.4, KCl 5, $CaCl_2$ 1, $MgCl_2$ 2, glucose 10), while the outer or mucosal side was bathed with a low sodium-choline Ringer (NaCl 0.3, choline chloride 115, choline bicarbonate 2.5, KCl 5, $MgCl_2$ 2, glucose 10 mM/L, pH 7.4). Either oxytocin (50 mU/ml) or PGE_1 ($5x10^{-6}$M, kindly donated by Dr. J.E. Pike, Upjohn Co.), were added to the Ringer bathing the inner chamber.

Isolated frog skin bathed with very low Na^+ concentration on the mucosal side have in most cases (Morel & Bastide 1965) a negative going SCC (outward going Na^+ net flux). Therefore one would expect that an increase in the Na^+ permeability of the mucosal barrier would be accompanied by an increase in the negative SCC. We tried by this experimental approach to measure the possible increase in Na^+ permeability induced by the hormones.

Sodium extrusion.

Na^+ extrusion was measured as described by Aceves (1977) Epithelia isolated by the action of collagenase and hydrostatic pressure (Aceves &

Erlij, 1971), were loaded with Na^+ by exposure to cold (2-4°C), K^+-free solutions. Then, the epithelial pieces were transferred to Ringer solutions containing 0.25 mM K. In this rather low K concentrations the rate of Na^+ pumping is decreased and any stimulatory effect of the hormones is more easily determined.

To determine the magnitude of the Na^+ extrusion, the intracellular Na^+ content of the epithelia recovering with and without the hormones, was subtracted from the Na^+ content found in the epithelia at the end of the incubation period in K^+-free solutions. Extracellular Na^+ was washed out, shaking the epithelia in ice-cold isotonic mannitol (Aceves, 1977). Na^+ was measured by flame photometry.

Ouabain binding.

Ouabain binding was measured in isolated paired epithelia. Each epithelium was mounted in a perspex chamber. After one hour equilibration, oxytocin (50 mU/ml) was added to the inner side of one epithelium. At the peak of the stimulation of the SCC (after 1/2 hour of hormone addition), the Ringer of the inner chamber was replaced with one containing the same concentration of hormone plus tritiated ouabain (0.5×10^{-6}M) diluted with "cold" ouabain (4.5×10^{-6}M). The Ringer of the inner chamber of the control epithelium was also replaced with Ringer containing the same concentration of labelled and cold ouabain, but without the hormones. After one hour of the ouabain addition, when SCC was practically abolished, the labelled solutions was withdrawed and after several washes with ice-cold Ringer, the epithelia were dismounted from their chambers and subjected to a further washing during two periods of 10 min. in 200 ml of ice-cold Ringer under magnetic stirring. After this, the epithelia were left overnight at 100°C and their dry weight determined. Finally they were solubilized (NCS, tissue solubilizer) and after addition of a scintillant (Bray's solution), they were counted in a Packard Tricarb Mod. 2405 Counter.

Inhibition of SCC by amiloride.

Increasing and cumulative concentrations of amiloride were added to the mucosal solution. The SCC remaining after 10^{-4}M amiloride was subtracted from the SCC value inmediately before the administration of the first amiloride concentration; the subtracted value was taked as 100 per cent inhibition. The inhibition of any other amiloride concentration was expressed as percentage of this value. After this dose-response curve, the external chamber was thoroughly washed, and once the SCC stabilized, a second dose-response curve was determined in the presence of PGE_1 (1×10^{-6}M).

RESULTS.

Effect of prostaglandin E_1 and oxytocin on SCC.

In spite of the low external Na^+ concentration, both PGE_1 and oxytocin increased SCC (Fig. 1). The increment for PGE_1 was from -23±29 to 111±23 $nEq \cdot h^{-1}cm^{-2}$ ($p<0.05$); this increment was inhibited after the addition of amiloride to -148±12 $nEq \cdot h^{-1}cm^{-2}$. Oxytocin enhanced Na^+ transport from -118±51 to 45±50 $nEq \cdot h^{-1}cm^{-2}$ ($p<0.05$); SCC was also inhibited by amiloride to -225±48 $nEq \cdot h^{-1}cm^{-2}$.

Effect of PGE_1 and oxytocin on Na^+ extrusion.

The effect of the hormones was tested simultaneously both on SCC and on Na^+ extrusion. The SCC was measured in the skin of the legs of the frogs from which, to measure Na^+ extrusion, the epithelium was isolated from the

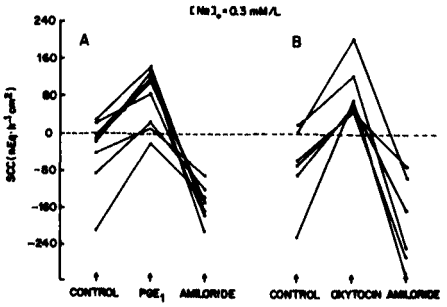

Fig. 1. A) Effect of PGE_1 ($5x10^{-6}M$) and amiloride ($1x10^{-5}M$) on SCC.

B) Effect of oxytocin (50 mU/ml and amiloride ($1x10^{-5}M$) on SCC.

Arrows show the control value of SCC and the effect after the addition of the tested compound.

abdominal skin. As can be observed (Table I) both hormones significantly stimulated SCC but only oxytocin increased Na^+ extrusion.

TABLE I.- EFFECT OF PGE_1 AND OXYTOCIN ON SCC AND Na EXTRUSION

	SCC ($\mu Eq/h^1cm^2$)		Sodium extrusion (Δ) ($\mu Eq/gm^1$ d.w.)	
	Before	After	Control	Experimental
Oxytocin (50mU/ml)	0.82±0.17	2.46±0.46*	1±14	33±10**
PGE_1 ($5x10^{-6}M$)	0.57±0.09	1.34±0.16*	1±14	2±11

*p<0.001 **p<0.02

Effect of oxytocin on ouabain binding.

The stimulation of Na^+ extrusion by oxytocin indicated that this hormone had an effect on the Na^+ pump of the serosal barrier of the epithelium. The stimulation of the Na^+ pumping could be due either to an increase in the number of pumping sites or to an increase in the turnover of the pump. As can be seem from figure 2, in spite that oxytocin more than double SCC, it did not modify the amount of ouabain bound to the serosal side of the epithelium.

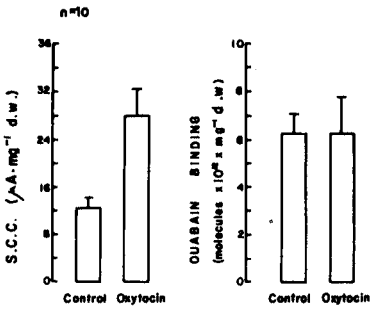

Fig. 2. Effect of oxytocin (50 mU/ml) on SCC and on ouabain binding, in paired isolated frog skin epithelia.

Effect of PGE_1 on amiloride affinity for inhibition of SCC.

Cuthbert and Shum (1974) found that antidiuretic hormone competitively antagonizes the inhibitory effect of amiloride on SCC. This effect constitutes additional evidence of the effect of the hormone on the Na^+ entry process across the mucosal barrier of the epithelium. To further assess the effect of PGE_1 on the Na^+ entry step, the effect of this hormone on the dose-response curve for amiloride inhibition of SCC was determined. As can be observed from figure 3, PGE_1 displaced the dose-response curve to the right. The apparent affinity constant was reduced from $5 \times 10^6 M^{-1}$ to $2.4 \times 10^6 M^{-1}$ by the hormone, which indicates that, as antidiuretic hormone, PGE_1 antagonizes the binding of amiloride to the Na^+ channels of the mucosal barrier of the epithelium.

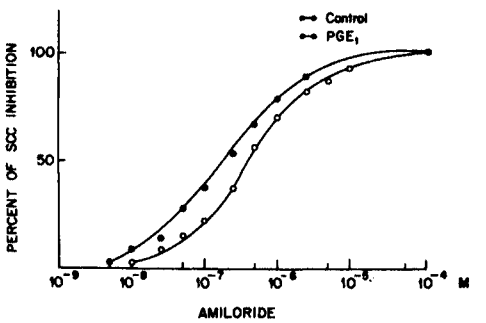

Fig. 3. Inhibition of SCC by amiloride. Cumulative dose-response curves, control (●—●) and after the addition of PGE_1 (o—o) to the solution bathing the serosal side of the frog skin ($p<0.05$)

DISCUSION.

The hormones that induce an stimulatory effect on the Na^+ transepithelial transport may act by any of three main mechanisms or by a combination of them: a) increasing Na^+ permeability; b) increasing the rate of Na^+ pumping or the number of Na^+ pumps; c) enhancing the available energy for the pumping process. Our results suggest that oxytocin stimulates transepithelial Na^+ transport by increasing the rate of Na^+ pumping at the serosal barrier (Fig. 2) and by increasing the entry of Na^+ across the mucosal barrier (Fig. 1). On the other hand, PGE_1 failed to show any effect on the Na^+ pumping at the serosal membrane (Table I) but showed a clear effect on the Na^+ entry step as judged by its antagonizing effect on amiloride inhibition of SCC (Fig. 3).

The stimulatory effect of PGE_1 on the transepithelial Na^+ transport in the presence of very low external Na^+ concentration might suggest that this increment is due to the presence of an active step located at the mucosal membrane as has been suggested for oxytocin by Morel and Bastide (1965). However without knowing the Na^+ electrochemical potential across the mucosal barrier in the presence of very low Na^+ concentrations in the mucosal solutions and in the presence of PGE_1, it is very difficult to decide whether the entry Na^+ in these conditions is a passive or an active process.

As noted before, both PGE_1 and oxytocin stimulates C-AMP formation in epithelia such as the frog skin, the nucleotide being the second messenger for the stimulatory effect of neurohypophyseal hormones on transepithelial Na^+ transport (Hall & O'Donoghue 1976). In line with this suggestion, exogenous C-AMP stimulates Na^+ extrusion in the isolated epithelium of the frog skin (Aceves, 1977). Therefore, a relevant question is to ask why PGE_1 does not show any effect on the Na^+ pump of the serosal barrier if its effect is

mediated also by C-AMP. The compartmentalization of C-AMP inside the epithelial cells has been invoked to explain different, sometimes antagonizing, effects of PGs of the E series and neurohypophyseal hormones.

BIBLIOGRAPHY.

Aceves, J. Sodium pump stimulation by oxytocin and cyclic AMP in the isolated epithelium of the frog skin. Pflügers Arch. 371: 211-216, 1977.

Aceves, J. & Erlij, D. Sodium transport across the isolated epithelium of the frog skin. J. Physiol. (Lond.) 212: 195-210, 1971.

Barry, E., Hall, W.J. & Martin, J.D.G. Prostaglandin E_1 and the movement of salt and water in frog skin (Rana temporaria) J. Gen. Pharmac. 6: 141-150, 1975.

Cuthbert, A.W., & Shum, W.K. Binding of amiloride to sodium channels in frog skin. Mol. Pharmacol. 10: 880-891, 1974.

Fülgraff, G. & Meiforth, A. Effects of prostaglandin E_2 on excretion and reabsorption of sodium and fluid in rat kidneys. Pflüggers Arch. 330: 243-256, 1971.

Hall, W.J. & O'Donoghue, J.P. Endogenous prostaglandins, adenosine 3':5'-monophosphate and sodium transport across isolated frog skin. J. Physiol. 258: 731-753, 1976.

Lote, C.J., Rider, J.B. & Thomas, S. The effect of prostaglandin E_1 on the short-circuit current and sodium, potassium, chloride and calcium movements across isolated frog (Rana temporaria) skin. Pflüggers Arch. 352: 145-153, 1974.

Morel, F. & Bastide, F. Action of l'ocytoxine sur la composante active du transport de sodium par la peau de grenouille. Biochim. Biophys. Acta, 94: 609-611, 1965.

Sapirstein, V.S. & Scott, W.N. Cyclic AMP and sodium transport. Quantitative and temporal relationships in toad urinary bladder. J. Clin. Invest. 52: 2379-2382, 1973.

Adv. Physiol. Sci. Vol. 3. Physiology of Non-excitable Cells
J. Salánki (ed.)

EFFECTS OF FUROSEMIDE AND ETHACRYNIC ACID ON SODIUM TRANSFER ACROSS THE PARIETAL PERITONEAL MEMBRANE

E. Feder and J. Knapowski
Department of Pathophysiology, Medical Academy, ul. Święckiego 6, 60-781 Poznań, Poland

In recent years, studies were conducted on the effect of various pharmacologic agents and hormones on the rate of substance transport in peritoneal dialysis as applied in animals as well as in humans /1,3/. Till now, however, the mechanisms of action of these compounds have not been clarified. The compounds in question include diuretic drugs which have been inducing variable effects on peritoneal sodium clearance during peritoneal dialysis /2,6/.

A series of studies on isolated fragments of parietal peritoneum has been performed in vitro to establish the effect of furosemide and ethacrynic acid on peritoneal transport of sodium ion.

MATERIALS AND METHODS

Parietal peritoneum fragments were isolated from the diaphragm and anterior abdominal wall of Wistar strain rats and mounted into an Ussing-type chamber according to the technique previously described /4,5/. In a few-hour-lasting experiment, in 30 min. intervals, bidirectional transfer of ^{22}Na was estimated.

RESULTS AND DISCUSSION

The results of a first series of experiments demonstrated a small but statistically significant difference between

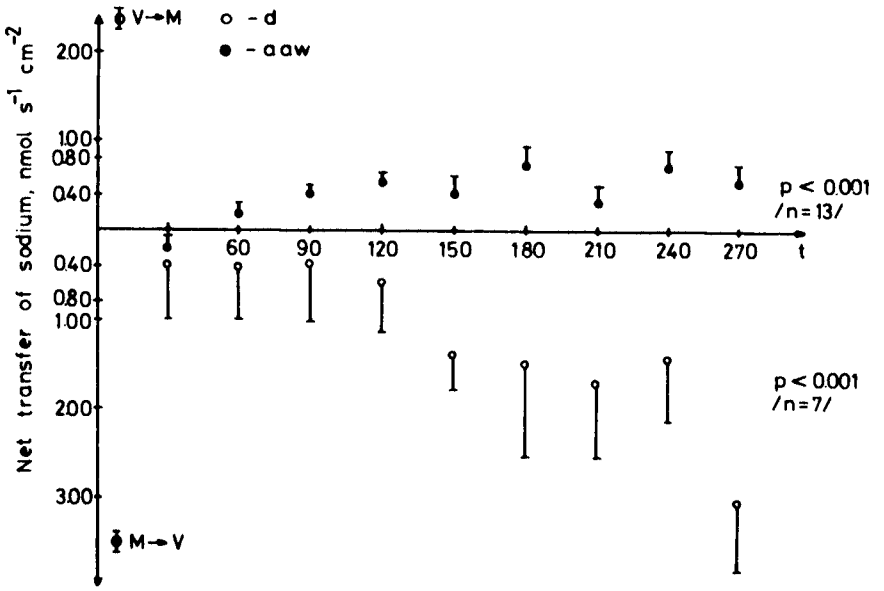

Fig.1. Net transfer of sodium across the peritoneal mesothelium of the diaphragm /o/ and anterior abdominal wall /●/ in 30 min. intervals /mean ± SE/ during the course of experiment. The resultant net transfer values /between 120th and 270 th min./ differ from zero significantly.

the two directions of sodium transfer through the membranes. In diaphragmatic peritoneum net sodium transfer from peritoneal mesothelium to muscular side was observed while in fragments of parietal peritoneum isolated from anterior abdominal wall net transfer in the opposite direction prevailed. The results suggest that, apart from passive diffusion, an active sodium ion transport may take place in mesothelial cells /Fig. 1/ .

In subsequent series of experiments the effect of furosemide and ethacrynic acid on bidirectional ^{22}Na transfer was examined. The compounds were added to medium bathing the mesothelial site of the membrane in two consecutive doses, yielding the final concentrations of 10^{-4}M or $5x10^{-4}$M, and 10^{-5}M or 10^{-3}M, for furosemide and ethacrynic acid, respectively. The effect of furosemide on bidirectional ^{22}Na transfer through

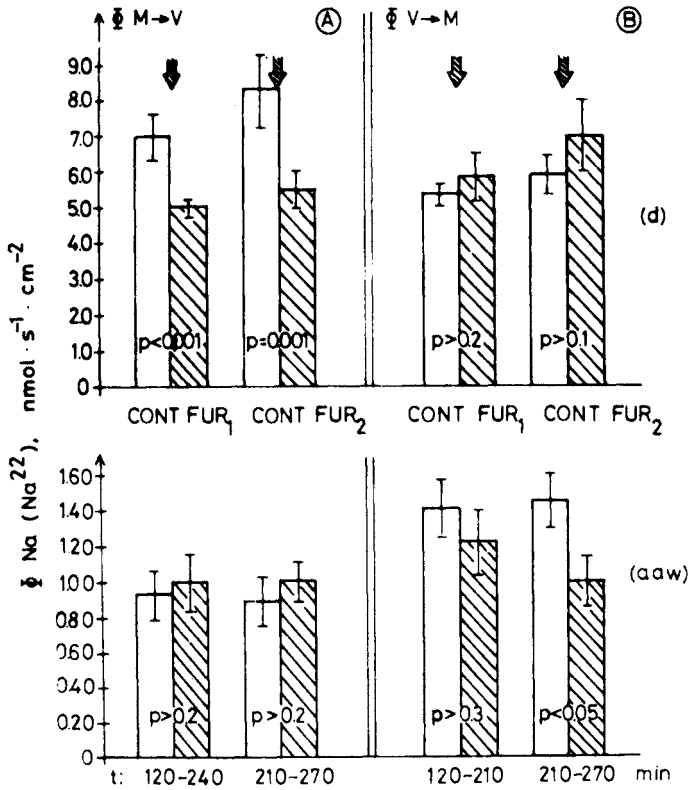

Fig.2. The effect of furosemide /$Fur_1=10^{-4}M$, $Fur_2=5x10^{-4}M$/ on bidirectional ^{22}Na transfer through diaphragmatic peritoneum /d/ and anterior abdominal wall peritoenum /aaw/. A - transfer from mesothelial to muscular side, B - transfer from muscular side to mesothelium.

diaphragmatic peritoneum and abdominal wall peritoneum is illustrated in Fig.2.

The experiments showed a diminshed sodium transfer through the membrane under the effect of furosemide. Only the direction of transfer which prevailed under normal conditions was affected by furosemide. Thus, in case of diaphragmatic peritoneum, the transfer from peritoneal cavity to vessels was affected while in abdominal wall peritoneum transfer in the opposite direction was decreased. Assuming that the enhanced sodium transfer through peritoneum resulted from an actively transporting mechanism and that furosemide action depressed

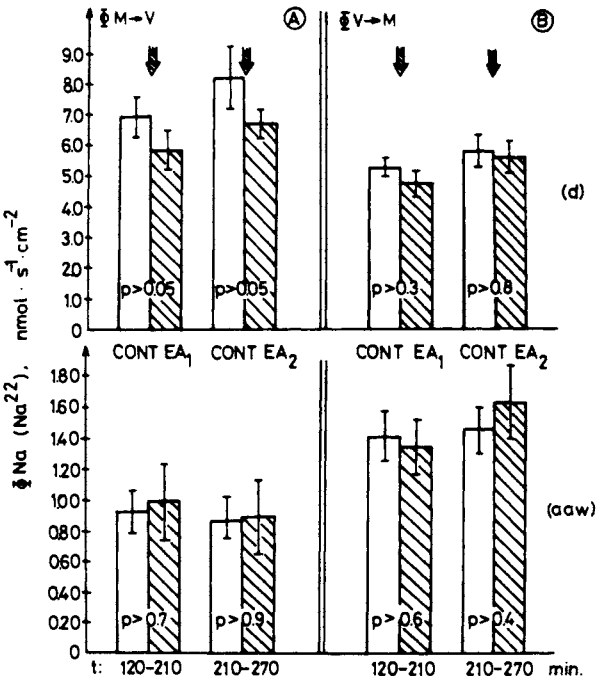

Fig.3. The effect of ethacrynic acid /$EA_1=10^{-5}M$, $EA_2=10^{-3}M$/ on bidirectional ^{22}NA transfer through diaphragmatic peritoneum /d/ and anterior abdominal wall peritoneum /aaw/. A - transfer from mesothelial to muscular side, B - transfer from muscular side to mesothelium.

the transfer to the level of transfer in the opposite direction one might suggest that the drug inhibited this active mechanism.

The effect of ethacrynic acid on bidirectional ^{22}Na transfer was estimated in peritoneal fragments also originating from the two anatomical sites. The series demonstrated no significant effect of ethacrynic acid on the transfer in either type of the membrane /Fig.3/.

CONCLUSIONS

1. Net sodium ion transfer in parietal peritoneum covering the diaphragm is directed from peritoneal cavity to the vascular side while in parietal peritoneum covering the anterior abdominal wall it shows the opposite direction.

2. Furosemide, when added to the mesothelial side of parietal peritoneum covering the diaphragm, significantly inhibits sodium ion flux toward the vascular space while in parietal peritoneum isolated from the anterior abdominal wall it inhibits sodium ion flux in the opposite direction.
3. Ethacrynic acid does not significantly affect bidirectional sodium ion transfer through parietal peritoneum covering diaphragm or anterior abdominal wall.
4. Mesothelial cells of parietal peritoneum react to pharmacological agents showing altered transport properties.

REFERENCES

1. Barbour, G.L.: The kinetics of peritoneal dialysis: a review /1979/ Dial.Transplant.8/1/; 1055-1060
2. Giordano, G., DeSanto, N.G., Capasso, G., Papa, A.: Peritoneal sodium diuresis induced by furosemide added to peritoneal dialysis fluid /1975/ Abstr.Am.Soc.Artif.Intern. Organs 4; 10
3. Gutman, R.A.: Toward enhancement of peritoneal clearance /1979/ Dial.Transplant.8/11/; 1072-1099
4. Knapowski, J., Feder, E., Simon, M., Zabel, M.: Evaluation of participation of parietal peritoneum in dialysis: Physiological, morphological and pharmacological data /1979/ Proc. Eur.Dial.Transpl.Assoc. /Amsterdam/ 16; 155-164
5. Knapowski, J., Simon, M., Feder, E.: Preparation of parietal peritoneum for measurements of in vitro permeability /1979/ Int.J.Artif.Organs 3/3/; 219-223
6. Maher, J.F., Hohnadel, D.C., Shea, C., Disanzo, F., Cassetta M.: Effect of intraperitoneal diuretics on solute transport during hypertonic dialysis /1977/ Clin.Nephrol. 7/3/;96-100

This work was supported by a grant N^{O} 623/VI from the Polish Academy of Sciences /Faculty of Medical Sciences/.

Adv. Physiol. Sci. Vol. 3. Physiology of Non-excitable Cells
J. Salánki (ed.)

EPITHELIAL TRANSPORT CONCLUDING REMARKS

Hans H. Ussing
Institute of Biological Chemistry A, August Krogh Institute, University of Copenhagen, 13 Universitetsparken, DK-2100 Copenhagen Ø, Denmark

The discussion served mainly to clarify the points made by the speakers, and no serious objections were made to their conclusions.

The overall impression left after the session was that the two-membrane theory of epithelial transport is now firmly established. In the cases of amphibian skin and toad urinary bladder the nature of the individual steps in the transport process has been further characterized.

1/ The passive entry of sodium is governed by a sodium selective channel rather than by a membrane carrier. The entry is modulated by the outside sodium concentration acting on the inhibitory site of the sodium channel.

2/ The transport pool for sodium is virtually the total cellular sodium pool, both in frog skin epithelium and in bladder epithelium. In frog skin, conducting cell junctions make the whole epithelium act like a cyncytium.

3/ At least in frog skin and toad urinary bladder the sodium pump is a sodium-potassium exchange pump, which is also electrogenic, because 3 sodium ions are pumped from cell lateral space for every two potassium ions pumped in the opposite direction.

4/ Passive chloride entry /at least in toad skin/ is regulated by a gating mechanism which is sensitive to the transepithelial potential. Thus the electrodiffusion of chloride completely stopped if the potential is reserved.

Several new approaches and techniques were discussed and especially the electric fluctuation analysis snows promise for the future.

Adv. Physiol. Sci. Vol. 3. Physiology of Non-excitable Cells
J. Salánki (ed.)

RELATIONSHIP BETWEEN MEMBRANE TRANSPORT AND METABOLISM INTRODUCTORY REMARKS

Arnost Kleinzeller
Department of Physiology, University of Pennsylvania, Philadelphia, PA 19104, USA

It is generally taken for granted that the transport of solutes across the cell membrane (and also across membranes of intracellular organelles) can play a role in the regulation of cellular metabolism. Several ways were considered (Kleinzeller and Kotyk, 1963) by which this may be accomplished:

1) The transported solute (sugars, amino acids, etc.) represents a substrate for cellular metabolism; the transport step may be rate-limiting.

2) The transported solute (e.g. mineral ions) affects the intracellular rate of metabolic processes.

3) The transport of a solute (against the chemical and/or electrochemical potential gradient) requires some portion of the available metabolic energy and thus may affect the energetic balance of the cell.

In the light of more recent knowledge the above may represent too narrow an approach to the subject. This is borne out by the recognition that the cell membrane is itself a structure displaying a considerable turnover of its components (e.g. phospolipids: Hokin and Hokin, 1967; proteins: Amos et al. 1977), and thus is subject to metabolic control including appropriate genetic control mechanisms.

In my introductory comments to this Symposium I wish to draw attention to some mechanisms by which the relationship between membrane transport and metabolism is achieved. I shall illustrate some of my points using data from our laboratory, mostly relating to transport and metabolism of sugars. Many facets of the broad subject of our Symposium will be considered in more detail in the Proceedings.

Control of cell metabolism by rate-limiting transport of a solute

The scheme shown in Fig. 1 represents the simplest conceivable mechanism of interrelationship between transport and metabolism.

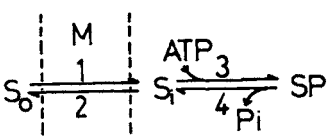

Fig. 1. Transport and cellular metabolism of solute S: Individual fluxes. M: Membrane; SP: Product of S; subscripts i and o indicate the respective intracellular and extracellular compartments; numbers indicate individual independent flux pathways.

In this scheme, the flux of each component step may be expressed by the Michaelis-Menten formalism. Under steady-state conditions the intracellular substrate concentration will be constant and therefore concentration S_i will be given by the algebraic sum of the respective fluxes into, and out of, the compartment of S_i. It follows that in the case of pathway 1 being rate-limiting, S_i will be considerably lower than the external concentration S_o. In accordance with such scheme the saturable, carrier-mediated glucose transport across the cell membrane was found to be the rate-limiting step (and thus S_i was practically zero) in muscle (Randle and Smith, 1958), yeast (Kleinzeller and Kotyk, 1963) or hepatoma - but not normal liver cells (Van Rossum et al. 1973). Furthermore, whenever specifically examined in the above examples, the apparent K_m of glucose utilization by the cells was several orders of magnitude higher than that of the first reaction for the entry of intracellular glucose into the metabolic pool, i.e. hexokinase.

Metabolic feed-back control of solute transport

The transport of glucose in the examples given above is mediated by a membrane carrier, but does not per se require metabolic energy since it does not proceed against a chemical potential gradient. Therefore, the uptake of glucose would not be expected to be affected by cellular metabolism. Contrary to such an assumption, it has been first shown by Randle and Smith (1958) that the muscle cell controls glucose uptake by

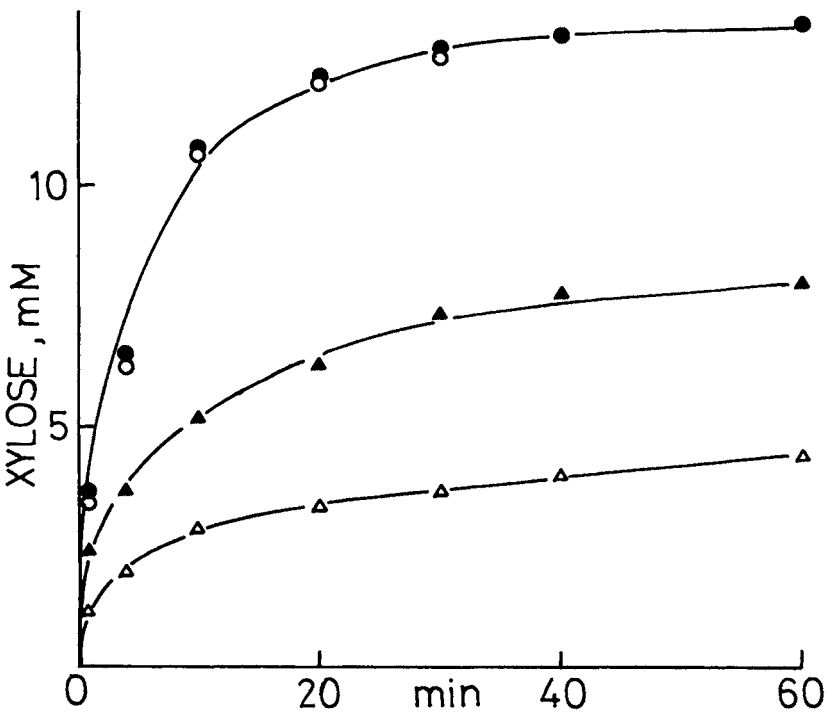

Fig. 2. The Pasteur effect and the uptake of D-xylose by Saccharomyces cerevisiae at 30 °C; air or N_2. D-Xylose-^{14}C, 14.3 mM; ○ ; xylose alone, air; ●,xylose alone, N_2; △ , xylose plus 2.7 mM glucose, air; ▲, xylose plus 2.7 mM glucose, N_2. Ordinate: intracellular xylose concentration, mM.

permitting a higher rate of membrane transport under anaerobic conditions than during aerobiosis.

The following experiments with yeast cells (Kleinzeller and Kotyk, 1963) have a bearing on the understanding of the control mechanism. Two sugars sharing the same transport system, D-xylose and D-glucose, were employed.

Since the intracellular glucose concentration in yeast is practically zero, under both aerobic and anaerobic conditions, the increased uptake anaerobically, characteristic of the Pasteur effect, implies an increased rate of substrate transport across the membrane. Fig. 2 shows that oxygen per se does not appear to affect the transport mechanism, as evidenced by identical rates of uptake of the non-metabolizable analog of glucose, D-xylose. However, in the presence of low concentrations of D-glucose the uptake of xylose was markedly depressed by the presence of oxygen independently of the competition of both sugars for the carrier. Such data lead to the conclusion that some metabolic product of glucose inhibits the membrane transport of xylose by a feed-back mechanism as indicated in Fig. 3.

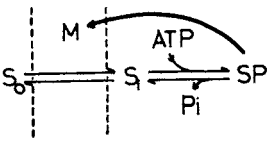

Fig. 3. Metabolic feed-back inhibition of solute influx. For symbols see Legend to Fig. 1.

The molecular nature of this feed-back control mechanism is so far unknown (see, e.g. Morgan and Whitfield, 1974). A kinetic analysis indicated that in yeast cells both the K_m and V_{max} of the glucose influx were affected by the change from anaerobic to aerobic conditions (Kotyk and Kleinzeller, 1967). It cannot be excluded that in addition to the postulated feed-back mechanism, the entry of glucose into cells is also controlled by the membrane transport of the phosphate anion (Racker, 1965): in ascites tumor cells, the intracellular concentration of Pi was shown to limit both glycolysis and respiration.

Consideration of the schemes given in Figs. 1 and 3 requires several comments:

First, the schemes are valid whatever the mechanisms of the component reactions. In particular, this applies to the nature of the transport pathways across the membrane. If any of these fluxes were active (being directly or indirectly coupled to metabolic energy and proceeding against the electrochemical potential gradient) this would express itself in the values of the respective kinetic parameters but would not affect the schemes. However, such a system would gain an additional characteristic: the appropriate flux would also be dependent on the cellular concentration of the immediate source of energy driving the active transport system.

Second, metabolic feed-back effects on the kinetic parameters of the membrane transport fluxes deserve some analysis. Changes of the affinity between the carrier and the transported solute (i.e. the transport constant of the Michaelis-Menten type) assume direct action on

the conformation of the carrier. On the other hand, changes of the transport capacity may be rather complex: not only the mobility of the carrier in the membrane (including the state of the membrane lipid environment) but also accessibility of membrane sites (structural, but also formation or repression) may be involved.

It is pertinent to substantiate the above statement by a summary of available information: cell growth appears to be associated with major changes in the transport parameters for various substrates. Two mechanisms have been proposed for the observations:
i) Alterations in membrane viscosity, monitored by measuring changes in fluorescence polarization (Collard et al. 1977); it will be shown below that changes in membrane fluidity are also held responsible for the insulin effect of membrane sugar transport. ii) Glucose starvation, which enhances by a complex feed-back mechanisms hexose transport and depresses the synthesis of two membrane proteins (Amos et al. 1977; Shu et al. 1977). It remains to be seen whether the loss of cellular metabolites which takes place during membrane fusion is in a similar way responsible for changes in membrane permeability (Pasternak and Micklem, 1973). Since membrane fusion is a key event including e.g. pinocytosis, phagocytosis, but also secretion of macromolecules, the observed phenomenon may well affect the cellular metabolism under a variety of physiological conditions. Finally, it ought to be mentioned here that it is still a matter of discussion whether transformation of cells to tumor cells is associated with an increase of sugar transport (cf. Hatanaka, 1976; Romano, 1976).

In the light of the schemes and comments we shall now proceed to examine some specific examples of interrelationship between transport and metabolism.

Some mechanisms of the relationship between transport and cell metabolism

Electrolyte transport and cell metabolism

It has been pointed out (Whittam and Willis, 1963) that a major portion of the cellular oxidative phosphorylation capacity is used for the operation of the Na-pump. Thus, the inhibition of the (Na-K)-activated ATPase produced an approx. 2/3 inhibition of the respiration of renal cells.

However, other mechanisms may also be operative here. First, it appears that in vascular smooth muscle, aerobic glycolysis is closely linked to Na and K transport, whereas ATP generated by oxidative phosphorylation is primarily coupled to contractile energy requirements (Paul et al. 1979). The localization of glycolytic enzymes in the cell membrane, found in erythrocytes (Fossel and Solomon, 1977), may represent a plausible model.

Secondly, the active transport of most amino acids (in many cells) and of sugars (in epithelia) is brought about by a carrier-mediated coupling between the substrate and the down-hill flux of Na (Schultz and Curran, 1970); the sink for the passive Na flux is produced by the operation of the Na-pump. Quantitatively, the extra amount of Na entering the cells in this way appears to represent only a minor fraction of the total Na influx and thus would not produce an additional drain on cell energy. However, recent studies (Murer and Hopfer, 1974; Beck and Sacktor, 1978) have shown that as opposed to previous views, the uphill

solute transport is brought about by the total of electrochemical ionic gradients across the membrane; thus, both the chemical potential of Na and $\Delta\psi$ may be the driving forces. This point has a bearing on the coupling between electrolyte transport and metabolism in that any mechanism affecting the electrical polarity of the cell membrane will also change the rate of entry of cellular substrates. Coupling between solute and proton fluxes have been found in some cells. Such coupling has been predicted by Mitchell (1966) and found to drive sugar transport in bacteria (West, 1970), algae (Komor and Tanner, 1974) and yeast (Eddy, 1978). Recently, a coupling between H^+ fluxes and metabolism in the toad urinary bladder has been reported by Kelly et al. 1980. In this acid secreting tissue the proton flux increased the oxidation of a variety of substrates; vice versa, the addition of substrate to starved cells enhanced the H^+ flux.

Finally, the transport of Na is also coupled to the transport of anions, e.g. phosphate, and Ca^{2+}. The cellular concentration of both these ionic species are believed to be determinants of metabolism. In particular the role of Ca^{2+} in the excitation-secretion coupling (Baker, 1974) has been emphasized.

Some hormonal effects on sugar transport and metabolism

Two types of experiments will be related herein demonstrating the effects cAMP and of insulin on sugar transport and metabolism in renal cells in order to demonstrate some aspects of the localization and mechanism of action of these agents.

It is now well established that sugars, including D-glucose, are actively transported into renal tubular cells by a brush-border localized, process coupled to the down-hill electrogenic Na flux (see above). α-Methyl-D-glucoside is a convenient non-metabolizable model sugar. Glucose can also enter the tubular cells by a Na-independent, phloretin sensitive transport system localized predominantly at the basal-lateral cell face (Kleinzeller et al. 1977). Fig. 4 shows that glucose oxidation by renal cortical cells is little affected by agents inhibiting the Na-dependent transport system, i.e. phlorizin, ouabain or absence of Na, whereas phloretin was a more powerful inhibitor (Kleinzeller and McAvoy, 1977). Such experiments indicate that it is glucose entering the cells at their antiluminal face which serves preponderantly as substrate for the nutritional requirements of the cells. Moreover, since only a minor fraction of the glucose which was transported into the cells at their brush border entered the metabolic pool, some cellular compartmentation of this physiological substrate is implied.

Fig. 5 shows the effect of dibutyryl-cyclic AMP (2 mM) on the renal handling of several model sugars (Kleinzeller and McAvoy, unpublished). It will be seen that cAMP activated the Na-dependent active transport of α-methyl-D-glucoside at the brush border, as already previously shown (see, e.g. Kippen et al. 1979), but actually inhibited glucose oxidation as well as the uptake of 2-deoxy-D-glucose, which shares with glucose the carrier at the basal-lateral cell face. The effect appears to be specific for cAMP; cGMP was ineffective. While the activation by cAMP of the Na-dependent transport pathway may be due to an increased influx of Na (R. Kinne, personal communication), the mechanism of the inhibitory action on the basal-lateral glucose transport system remains to be elucidated.

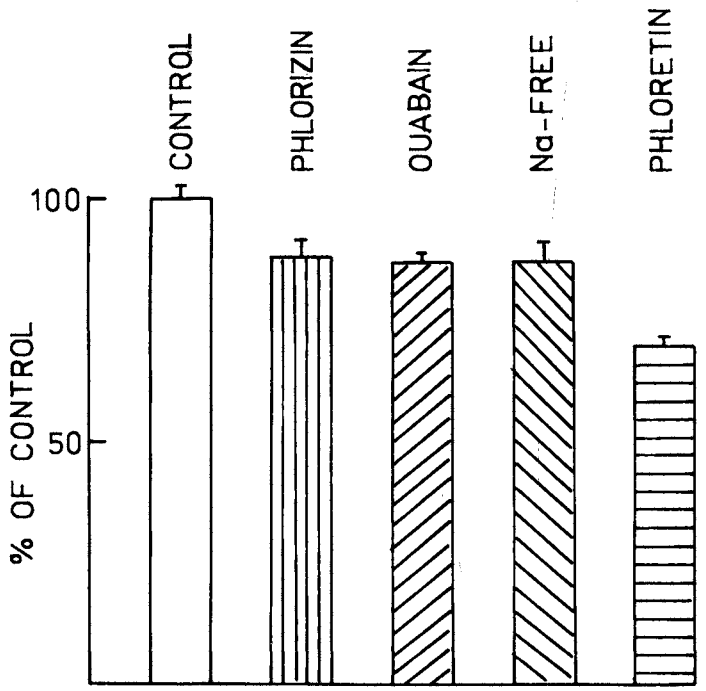

Fig. 4. Glucose oxidation by renal cortical cells and the effect of various inhibitors thereon. Rabbit renal cortical slices were used : 25 °C, O_2, 1 mM [U-^{14}C]-D-glucose (0.5 µCi/ml), 60 min incubation. Mean values ± S.E., (3 animals, 15-18 analyses).

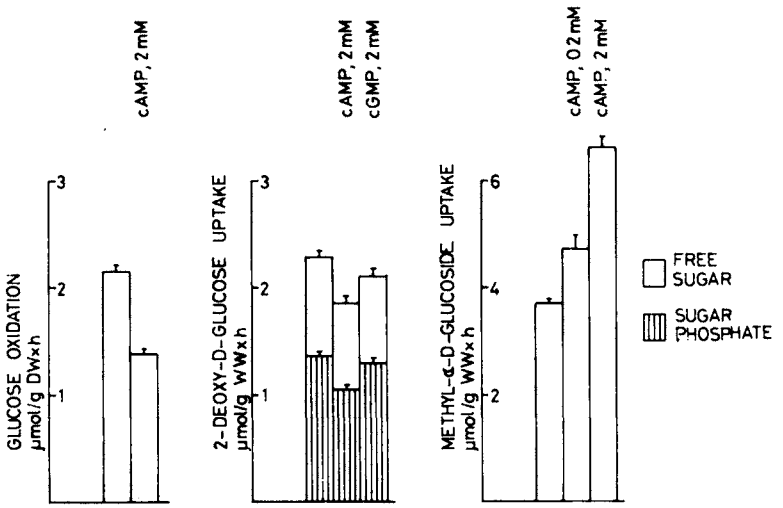

Fig. 5. Effect of dibutyryl cyclic AMP on the renal handling of various sugars in rabbit renal cortex. Slices of rabbit renal cortex were used:

25 °C, oxygen, 60 min incubation. The oxidation of glucose (μmol/g tissue dry weight (DW) x h, uptake of 2-deoxy-D-glucose and of α-methyl-D-glucoside (μmol per g tissue wet weight (WW) x h). Mean values ± S.E. of at least 12-18 analyses (2-3 animals).

Insulin activates the entry of sugars into a variety of cells, possibly by changing the fluidity of the cell membrane, thus affecting the transport capacity (Melchior and Czech, 1979). A similar activating effect of insulin has been reported for the uptake of glucose by renal cortical cells, (Mahler and Szabo, 1968). Fig. 6 (unpublished data) shows that hypoinsulinaemia, produced by treating rats with streptozotocin, affects both the affinity and transport capacity for glucose of the basal-lateral transport system in renal tubular cells. The molecular mechanism of insulin action remains to be elucidated.

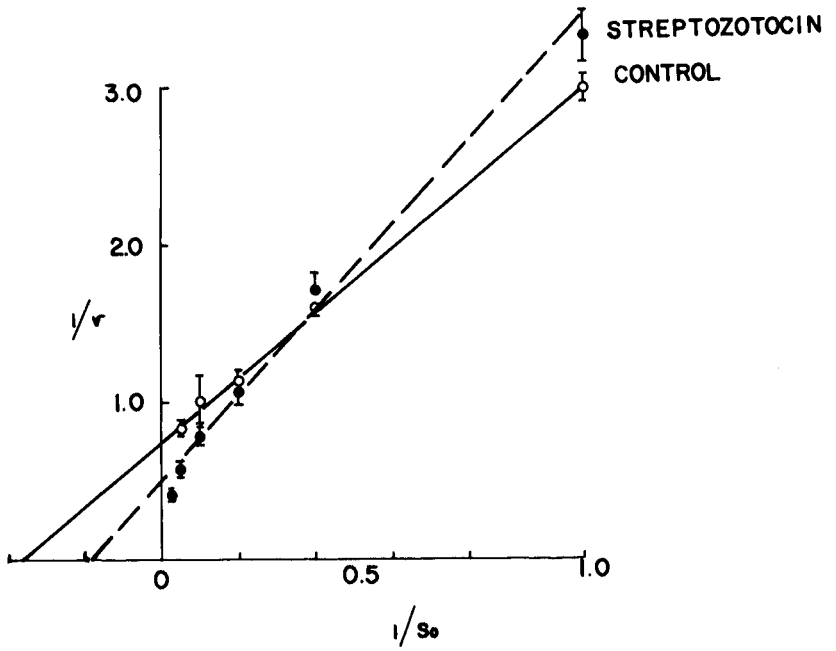

Fig. 6. Double reciprocal plot of the effect of glucose concentration on the oxidation of [U-^{14}C]-D-glucose by rat renal tubuli: effect of streptozotocin-induced hypoinsulinemia. All points are the means ± S.E. of at least 6 analyses (3 animals).

Several points arise from the above results: first, agents such as cAMP may differ widely in their action on different pathways of sugar transport. Second, insulin apparently acts on the transport and metabolism of glucose in a complex manner, affecting both the affinity and the transport capacity of the carrier. One additional element in the action of insulin relates to the fact that the membranes of renal cortical cells rapidly degrade the hormone (see Mahler and Szabo, 1968).

In all the above experiments, more information as to the molecular mechanisms involved in the interrelationship between transport and metabolism is desirable. I would like to conclude with the hope that the Proceedings of our Symposium will point the way to a better understanding of this interaction.

This work was supported in part by the U.S. Public Health Service Grant AM 12619.

References

Amos, H., Musliner, T.A., and Asdourian, H. (1977). Regulation of glucose carriers in chick fibroblasts. J. Supramol. Biol. 7: 499-513.

Baker, P.F. (1974). Excitation-secretion coupling. In recent advances in Physiology IX (Linden, R.J., ed.). pp. 51-86. Churchill Livingstone, London.

Beck, J.C., and Sacktor, B. (1978). The sodium electrochemical potential-mediated uphill transport of D-glucose in renal brush border membrane vesicles. J. Biol. Chem. 253: 5531-5535.

Collard, J.G., de Wildt, A., Oomen-Meulemans, E., Smeekens, J., Emmelot, P., and Inbar, M. (1977). Increase in fluidity of membrane lipids in lymphocytes, fibroblasts and liver cells stimulated for growth. FEBS Lett. 77: 173-178.

Czech, M.P. (1977). Molecular basis of insulin action. Ann. Rev. Biochem. 46: 359-384.

Eddy, A.A. (1978). Proton-dependent solute transport in microorganisms. Curr. Top Membr. Transp. 10, 280-360.

Fossel, E.T., and Solomon, A.K. (1977). Membrane-mediated link between ion transport and metabolism in human red cells. Biochim. Biophys. Acta 464: 82-92.

Hatanaka, M. (1976). Saturable and nonsaturable process of sugar uptake: effect of oncogenic transformation in transport and uptake of nutrients. J. Cell. Physiol. 89: 745-750.

Hokin, M., and Hokin, L.E. (1967). The formation and continuous turnover of a fraction of phosphatidic acid on stimulation of NaCl secretion by acetycholine in the salt gland. J. Gen. Physiol. 50: 793-811.

Kelly, S., Dixon, T.E., and Al-Awquati, Q. (1980). Metabolic pathways coupled to H^+ transport in turtle urinary bladder. J. Membrane Biol. 54: 237-243.

Kippen, I., Hirayama, B., Klinenberg, J.R., and Wright, E.M. (1979). Effects of dibutyrylcyclic AMP on the transport of α-methyl-D-glucoside and α-aminoisobutyric acid in separated tubules and brush border membranes from rabbit kidney. Biochim. Biophys. Acta 558: 126-135.

Kleinzeller, A., Dubyak, G.R., Griffin, P.M., McAvoy, E.M., Mullin, J.M., and Rittmaster, R. (1977). Renal sugar transport in the winter flounder. III. Two glucose transport systems. Am. J. Physiol. 232: F227-234.

Kleinzeller, A., and Kotyk, A. (1963). Transport of sugars into yeast cells and the regulation of metabolism. Colloque Internat. sur les Mécanismes de Regulation. Marseille, pp. 373-377.

Kleinzeller, A., and McAvoy, E.M. (1977). Transport and Metabolism of D-glucose in renal tubular cells. Abstr. of Comm., XXVIIth Internat. Congr. of Physiol. Sci., Paris, Abstr. No. 1153.

Komor, E., and Tanner, W. (1974). The hexose-proton cotransport system of Chlorella. J. Gen. Physiol. 64: 568-581.
Kotyk, A., and Kleinzeller, A. (1967). Affinity of the yeast membrane carrier for glucose and its role in the Pasteur effect. Biochim. Biophys. Acta 135: 106-111.
Mahler, R.J., and Szabo, O. (1968). Metabolic effects of insulin in rat kidney after inhibiting degradation of the hormone. Endocrinology 83: 1166-1172.
Melchior, D.L., and Czech, M.P. (1979). Sensitivity of the adipocyte D-glucose transport system to membrane fluidity in reconstituted vesicles. J. Biol. Chem. 254: 8744-8747.
Mitchell, P. (1966). Chemiosmotic coupling in oxidative and photosynthetic phosphorylation. Biol. Rev. Cambridge Phil. Soc. 41: 445-502.
Morgan, H.E., and Whitfield, C.F. (1973). Regulation of sugar transport in eukaryotic cells. Curr. Top. Membr. Transp. 4: 255-303.
Murer, H., and Hopfer, U. (1974). Demonstration of electrogenic Na^+-dependent D-glucose transport in intestinal brush border membranes, Proc. Natl. Acad. Sci. U.S.A. 71: 484-488.
Pasternak, C., and Micklem, K.J. (1973). Permeability changes during cell fusion. J. Membrane Biol. 14: 293-303.
Paul, R.J., Bauer, M., and Pease, W. (1979). Vascular smooth muscle: Aerobic glycolysis linked to sodium and potassium transport processes. Science 206: 1414-1416.
Racker, E. (1965). Mechanisms in Bioenergetics. Academic Press, New York and London.
Randle, P.J., and Smith, G.H. (1958). Regulation of glucose uptake by muscle. 2. The effects of insulin, anaerobiosis and cell poisons on the penetration of isolated rat diaphragm by sugars. Biochem. J. 70: 501-508.
Romano, A.H. (1976). Is glucose transport enhanced in virus-transformed mammalian cells ? A dissenting view. J. Cell. Physiol. 89: 737-744.
Schultz, S.G., and Curran, P.F. (1970). Coupled transport of sodium and organic solutes across cell membranes. Physiol. Rev. 50: 637-718.
Shu, R.P.C., Pouyasegur, J., and Pastan, L. (1977). Glucose depletion accounts for the induction of two transformation-sensitive membrane proteins in Rous sarcoma virus-transformed chick embryo fibroblasts. Proc. Natl. Acad. Sci. U.S.A. 74: 3840-3844.
Van Rossum, G.D.W., Galeotti, T., Palombini, G., and Morris, H.P. (1973). The control of anaerobic glycolysis by glucose transport and ouabain in slices of hepatoma 3924A. Biochim. Biophys. Acta 394: 267-280.
West, I.C. (1970). Lactose transport coupled to proton movements in Escherichia coli. Biochim. Biophys. Res. Comm. 41: 655-661.
Whittam, R., and Willis, J.C. (1964). Ion movements and O_2 consumption in kidney cortex slices. J. Physiol. 168: 158-177.

Adv. Physiol. Sci. Vol. 3. Physiology of Non-excitable Cells
J. Salánki (ed.)

RELATIONSHIP BETWEEN TRANSPORT AND METABOLISM AT THE SUBCELLULAR LEVEL*

Lars Ernster
Department of Biochemistry, Arrhenius Laboratory, University of Stockholm, S-106 91 Stockholm Sweden

Until about 25 years ago, the study of cellular membrane transport was focused almost exclusively on processes taking place across the cell membrane itself. These processes were thought to be linked to cellular energy metabolism mainly by way of group-translocation reactions, in which the solute to be transported underwent covalent chemical changes, e.g. by phosphorylation. Active transport of inorganic ions, e.g. Na^+, K^+ or Ca^{2+} was of course known to occur across the cell membrane, but the relationship of these processes to the transport of metabolites - such as sugars or amino acids - or to energy metabolism was not understood.

Research during the last 2 or 3 decades has led to a drastic change in this situation. Some of the most important developments were as follows:

1. The discovery of transport-ATPases, e.g. the Na^+K^+-ATPase and the Ca^{2+}-ATPase.
2. The discovery of H^+-pumping electron transport and ATPase, and the role of the proton-motive force as a link between electron transport and ATP synthesis in both respiring and photosynthetic cells.
3. The discovery that metabolite transport is linked to cation and H^+ transport, e.g. by way of Na^+- and H^+-linked sugar and amino-acid carriers, which seems to be the main mechanism - rather than that based on group translocation - for the transport of metabolites across cell membranes.
4. The discovery that ion- and metabolite-transport systems are not confined to the cell membrane, but occur in intracellular membranes as well, notably the inner membrane of mitochondria, the inner envelope membrane of chloroplasts, and the membranes of the endoplasmic reticulum.

Table I summarizes some of the known transport systems occurring in various biological membranes. The following is

*Abridged version of the survey lecture presented.

Table I: SOME ION- AND METABOLITE-TRANSPORT SYSTEMS OF BIOLOGICAL MEMBRANES

Cell type, membrane	Pumps	Cation channels	Anion and metabolite translocators
Eukaryotes			
Plasma membrane	Na^+K^+-ATPase H^+-ATPase (fungi) Ca^{2+}-ATPase H^+K^+-ATPase (gastr.muc.)	$Na^+ \rightleftharpoons K^+$ $Na^+ \rightleftharpoons Ca^{2+}$ (excit.membr.) $K^+ \rightleftharpoons Ca^{2+}$	Na^+-linked H^+-linked (fungi)
Mitochondrial inner membrane	H^+-ATPase H^+-pumping electron-transp.system	$H^+ \rightleftharpoons K^+$ $H^+ \rightleftharpoons Ca^{2+}$ $Na^+ \rightleftharpoons Ca^{2+}$ (excit.membr.)	H^+-linked
Chloroplast thylakoid membrane	H^+-ATPase H^+-pumping electron-transp.system	?	
" inner envelope membr.			H^+-linked
Endoplasmic reticulum	Ca^{2+}-ATPase	?	?
Prokaryotes			
Plasma membrane	H^+-ATPase H^+-pumping electron-transp.system(s) light-driven H^+ pump (halophil. bact.) light-driven Na^+ pump (halophil. bact.)	$H^+ \rightleftharpoons Na^+$ $H^+ \rightleftharpoons K^+$ $H^+ \rightleftharpoons Ca^{2+}$	Mostly H^+-, few Na^+- and PT*-linked (*E. coli*) Na^+-linked (halophilic and marine bact.)

*PT = phosphotransferase

an illustration of the metabolic function and some current knowledge of the chemistry of these systems. In particular, some recent aspects of these systems will be discussed, with reference to the literature cited below:

a) Metabolite-transport systems of mitochondria (Scarpa, 1979; Lin & Klingenberg, 1980).
b) Reaction mechanism of the mitochondrial ADP/ATP translocator (Klingenberg, 1979).
c) Mitochondrial calcium transport (Carafoli et al., 1980).
d) Comparative aspects of the cell-membrane transport--ATPases of animal and fungal cells (Malpartida & Serrano, 1980).
e) Structure of the dicyclohexylcarbodiimide-binding protein component of the H^+-translocating ATPase complex of mitochondria, chloroplasts and bacteria (Seebald et al., 1979).
f) Purification and reconstitution of the H^+-translocating mitochondrial nicotinamide nucleotide transhydrogenase (Rydström, 1979).
g) Structure and function of bacteriorhodopsin and related ion-transport systems of halobacteria (Ovchinnikov et al., 1979; Stoeckenius & Casadio, 1979; Luisi et al., 1980).

Summary

1. Cation-transport ATPases, including Na^+K^+-ATPases, Ca^{2+}-ATPases as well as proton-translocating ATPases, serve as the primary driving forces for various ion- and metabolite-transport systems in biological membranes.

2. Transmembrane proton gradients constitute a common link of energy transfer between electron transport, ATP synthesis and hydrolysis, and active ion and metabolite transport in both respiring and photosynthetic cells.

3. In eukaryotic cells, active transport of ions and metabolites is not confined to the cell membrane, but occurs also across intracellular organelle membranes and plays a vital role in metabolic regulation.

4. Membrane proteins involved in ion and metabolite transport are often oligomeric structures displaying cooperativity between the subunits of the protein.

5. There is growing information about the structure and reaction mechanism of membrane proteins involved in biological transport. The relationship between transport and metabolism is beginning to be understood at the molecular level.

References

Carafoli, E., Crompton, M., Caroni, P., Schwerzmann, K., and Roos, I. (1980). The cycling of Ca^{2+} across the inner mitochondrial membrane. In Frontiers of Bioorganic Chemistry and Molecular Biology (Ananchenko, S.N., ed.). Pergamon Press, Oxford, pp. 405-416.

Klingenberg, M. (1979). The ADP, ATP shuttle of the mitochondrion. TIBS Nov. 1979, 249-252.

Lin, C.S., and Klingenberg, M. (1980). Isolation of the uncoupling protein from brown adipose tissue mitochondria. FEBS Lett. 113: 299-303.

Luisi, B.F., Weber, H.J., and Lanyi, J.K. (1980). EBEC Reports Vol. I, Pâtron Editore, Bologna, pp. 289-290.

Malpartida, F., and Serrano, R. (1980). Purification of the yeast plasma membrane ATPase solubilized with a novel zwitter-ionic detergent. FEBS Lett. 111: 69-72.

Ovchinnikov, Yu. A., Abdulaev, N.G., Feigina, M. Yu., Kiselev, A.V., and Lobanov, N.A. (1979). The structural basis for the functioning of bacteriorhodopsin: An overview. FEBS Lett. 100: 219-224.

Rydström, J. (1979). Energy-linked nicotinamide nucleotide transhydrogenase. Properties of proton-translocating and ATP-driven transhydrogenase reconstituted from synthetic phospholipids and purified transhydrogenase from beef heart. J. Biol. Chem. 254: 8611-8619.

Scarpa, A. (1979). Transport across mitochondrial membranes. In: Membrane Transport in Biology (Giebisch, G., Tosteson, D.C., and Ussing, H.H., eds.). Vol. II, Springer-Verlag, Berlin, pp. 263-355.

Seebald, W., Hoppe, J. and Wachter, E. (1979). Amino acid sequence of the ATPase proteolipid from mitochondria, chloroplasts and bacteia (wild type and mutants). In Function and Molecular Aspects of Biomembrane Transport (Quagliariello, E., Palmieri, F., Papa, S., and Klingenberg, M., eds.). Elsevier/North Holland, Amsterdam, pp. 63-74.

Stoeckenius, W., and Casadio, R. (1979). Dissociation and reconstitution of purple membrane. In: Membrane Bioenergetics (Lee, C.P., Schatz, G., and Ernster L., eds.). Addison-Wesley, Reading, MA., pp. 229-254.

Adv. Physiol. Sci. Vol. 3. Physiology of Non-excitable Cells
J. Salánki (ed.)

THE COUPLING BETWEEN TRANSPORT AND METABOLISM: THERMODYNAMIC ASPECTS

S. Roy Caplan

Laboratory of Theoretical Biology, DCBD, National Cancer Institute, National Institutes of Health Bethesda, Md. 20205 and Department of Membrane Research, Weizmann Institute of Science Rehovot, Israel

SUMMARY

Studies of active sodium transport in epithelia, active proton extrusion in mitochondria, and of other examples of ion transport coupled to metabolism indicate that coupling in these systems is not necessarily completely tight (i.e., a fixed and integral stoichiometry is not always observed). An evaluation of the energetics of such processes using classical flux ratio considerations and/or equivalent circuit models may, as a consequence, be misleading. On the other hand, nonequilibrium thermodynamics (NET) provides a basis for systematic investigation of the factors determining transport under all circumstances. The formal description in terms of linear NET is essentially simple, yet it enables us to distinguish between effects on energetic as against kinetic factors - especially in relation to the mode of action of substances regulating transport. Tightness of coupling may be evaluated quantitatively and related to efficiency, and it can be shown that incomplete coupling is energetically advantageous in many systems. Although in general flows are non-linear functions of forces and the Onsager reciprocal relations are obeyed only very near equilibrium, it is possible experimentally, at least in certain cases, to constrain the forces to "proper" pathways (e.g., in concentration space) such that linearity obtains and the reciprocal relations hold far from equilibrium. Linear behavior has indeed been observed in a variety of studies in epithelial and other systems, enabling the affinity (or negative Gibbs free energy) of the metabolic reaction driving transport to be measured.

INTRODUCTION

Thermodynamics provides a basis for the systematic investigation of the kinetic and energetic factors determining transport under all circumstances. In approaching the study of epithelial active sodium transport from this point of view, two governing considerations have been kept in mind. (i) Studies in epithelial tissues are relevant to the study of active sodium transport in all the tissues in which it is observed; epithelial membranes serve as useful model systems for the thermodynamic analysis of transport since they permit the ready control of bath concentrations and electrical forces determining rates of transport and metabolism. (ii) The understanding of the energetics of active sodium transport must contribute to an understanding of the energetics of active transport processes in general.

It is useful to review the classical approaches still commonly used to evaluate the energetic and kinetic factors determining transport. Studies of energetics are frequently based on the use of the flux ratio; in analogy to passive transport in simple systems, it is presumed that the ratio of the unidirectional fluxes of a given species provides a measure of the forces promoting its transport. The fundamental flaws in this approach have been discussed in detail (Kedem and Essig, 1965): the flux ratio can evaluate energetic parameters only if the flows are entirely via the active pathway and if tracer flows are uninfluenced by flows of other isotopes or other chemical species. Another approach to these issues is based on the equivalent circuit model (Ussing and Zerahn, 1951), which comprises an active conductance, an electromotive force of sodium transport E_{Na}, and a parallel passive conductance. In this model the conductances are considered to represent the kinetic factors, whereas E_{Na} is commonly taken as the "driving force" for the transport process. However, theoretical considerations as well as experimental results indicate that E_{Na} incorporates both kinetic and energetic factors (Civan et al., 1966; Essig and Caplan, 1968; Hong and Essig, 1976). The classical point of view leads to certain generally accepted prejudices about the active transport process. By analogy with stoichiometric chemical reactions, it was long assumed that active sodium transport is associated with a unique ratio of sodium transported to oxygen consumed (Zerahn, 1956; Ussing, 1960). Again, both theoretical considerations and experimental results show this not to be the case (Essig and Caplan, 1968; Vieira et al., 1972a). Furthermore, it was considered that the energy available for transport can be evaluated by the "calorific value," i.e., the heat released in the oxidation of glucose in a bomb calorimeter (Zerahn, 1956; Ussing, 1960). However, the pertinent quantity is not the heat released (enthalpy) but rather the free energy of the reaction under in vivo conditions.

These difficulties may be avoided by adopting a point of view based on nonequilibrium thermodynamics (NET). This enables one to analyze the behavior of a tissue systematically under a wide variety of operating conditions, as well as the mode of action of substances regulating transport. In particular, it makes it possible to distinguish between effects on energetic as against kinetic factors.

THE NONEQUILIBRIUM THERMODYNAMIC (NET) APPROACH

In analyzing the energetics of active sodium transport, it is necessary to start with a simple model. In frog skins and toad bladders of appropriate species, there appears to be only one significant active transport process, that of sodium, and thus only one significant output for the thermodynamic system. It is assumed that one metabolic process "drives" active transport. This scheme is represented in Fig. 1. Here one input process, the metabolism of substrate, is linked to one output process, the transport of sodium. Since the active transport system transports only sodium ions, whereas the tissue as a whole reabsorbs sodium chloride, it is necessary for there to be a pathway across which chloride can move. This may be thought of as a simple passive channel in parallel with the active transport pathway, which is presumably accessible more or less to all of the ions in the bathing solutions.

Since active transport is here taken to be a two-flow process, there are two pertinent flow equations to be considered - one for sodium transport in the active pathway, represented by J^a_{Na}, and one for metabolic reaction,

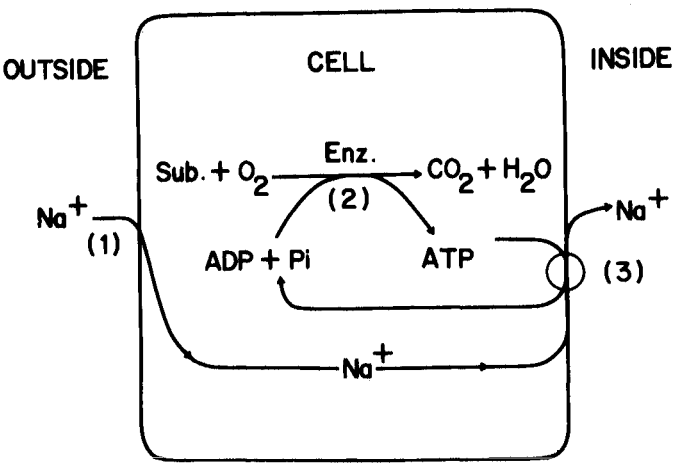

Fig. 1. Scheme for the active sodium transport system. (1) Apical passive entry of sodium, (2) mitochondrial oxidative phosphorylation, (3) basolateral sodium pump (after Essig, 1975).

represented by J_r:

$$J^a_{Na} = L_{Na}X_{Na} + L_{Nar}A \quad (1)$$

$$J_r = L_{Nar}X_{Na} + L_rA \quad (2)$$

Here X_{Na} is the negative electrochemical potential difference of sodium, and A is the affinity of a metabolic reaction which is driving sodium transport. The affinity is equivalent to the negative Gibbs free energy change $-\Delta G$ of the driving reaction, as yet undefined in biochemical terms. The L's are phenomenological coefficients. For simplicity linearity is assumed. J^a_{Na}, the rate of active sodium transport, is a function of the negative electrochemical potential difference, X_{Na}, but to the extent that it is coupled to metabolism it must also be a function of the affinity A. J_r, the rate of metabolism (here taken as suprabasal oxygen consumption) is a function of A, but to the extent that it is linked to transport it must also be a function of X_{Na}. By analogy with a variety of transport processes in non-living systems the validity of the Onsager reciprocal relation is assumed, i.e., the cross-coefficients in the two equations are set equal. The appropriateness of the simple linear thermodynamic formulation can be argued on various theoretical grounds, but instead it is instructive to consider the experimental evidence bearing on this point.

EXPERIMENTAL EVALUATION OF THE NET APPROACH

Stoichiometry

From a biochemical standpoint it is reasonable to expect that the trans-

port of a given quantity of sodium ion would be associated with the oxidation of substrate in a fixed stoichiometric ratio. From the viewpoint of NET, on the other hand, it is only necessary that the rate of input of metabolic energy exceed the rate of performance of electroosmotic work. Hence, in the short-circuited state (i.e., in the absence of either a concentration difference or an electrical potential difference across the membrane), on a priori thermodynamic grounds there is no limitation on Na/O_2 ratios, and these might differ in various tissues. Studies of oxygen consumption employing Clark electrodes with vigorous stirring have demonstrated suprabasal Na/O_2 ratios varying from 7.1 to 30.9 in short-circuited frog skins (Vieira et al., 1972a). Similarly, in determinations of CO_2 production in short-circuited toad bladders, Al-Awqati et al. (1975) found extensive variability of dJ_{Na}/dJ_{CO_2}. The relationships become still more complex with variation of the sodium concentration or electrical potential difference. Under these circumstances, the suprabasal Na/O_2 ratio will remain constant only if transport and metabolism are completely coupled (Essig and Caplan, 1968; Lahav et al., 1976; Lang et al., 1977).

Linearity

If the rate of active sodium transport is indeed a linear function of the forces promoting transport, one might expect to find linear current-voltage relationships. For this purpose it was important to study tissues in which transport via leak pathways was minimal. This was accomplished by carefully avoiding edge damage in mounting the tissues and by the use of tracer isotopes for the measurement of passive ion fluxes. This permitted the choice of those tissues in which a high fraction of total conductance was through the active pathway. The results of such studies in toad bladder (Saito et al., 1974) showed remarkable linearity in tissues in which about three-fifths of the total conductance was attributable to the active pathway. The finding of a steady-state linear current-voltage relationship in these tissues strongly indicates that the rate of active sodium transport J^a_{Na} was in these circumstances a linear function of the electrical potential difference.

Corresponding studies were carried out of the rate of metabolism, here taken as oxygen consumption. The initial experiments were carried out in the frog skin (Vieira et al., 1972b). Again there was striking linearity, with steady-state J_r a linear function of $\Delta\psi$ over a range of +160 to -160 mV. The finding of linearity of J_r in $\Delta\psi$ is consistent with the validity of Eq. (2) and again indicates constancy of phenomenological coefficients and invariance of the affinity with the perturbations of $\Delta\psi$ employed. Later studies showed similar behavior in the toad bladder (Lang et al., 1977). The conclusion that the dependence of the rate of oxygen consumption on the potential reflects the function of the active transport system is supported by the absence of such dependence following abolition of sodium transport by 10^{-3} M ouabain (Vieira et al., 1972b). Figure 2 illustrates a study by Lang et al. (1977) in which a simultaneous determination was made of the rates of active sodium transport J^a_{Na} and suprabasal oxygen consumption J^{sb}_r in toad urinary bladder. Both were linear functions of the electrical potential difference over a range of ± 80 mV.

The studies just described examined the influence of only electrical driving forces on transport and metabolism. Danisi and Vieira (1974) reported the effects of concentration driving forces. In studies of toad skins in which the transmembrane electrical potential difference was

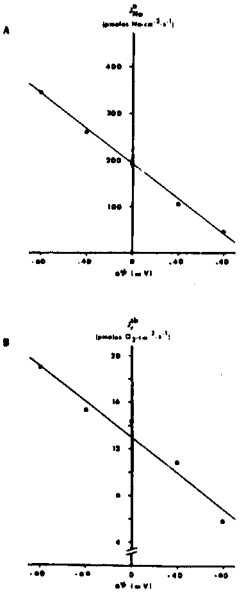

Fig. 2. Relationship between (A) J^a_{Na} and $\Delta\psi$, and (B) J^{sb}_r and $\Delta\psi$, in toad bladder (after Lang et al., 1977).

nullified, it was found that the rates of both active transport and oxygen consumption were linear functions of the chemical potential difference of sodium across the membranes. Similar studies of Beauwens and Al-Awqati (1976) in turtle urinary bladder under short-circuited conditions showed impressive linearity in the rates of proton secretion and glucose oxidation (measured as $^{14}CO_2$ production) as functions of mucosal pH at constant serosal pH. Thus, whatever the effects of external conditions on the intracellular concentration and electrical potential profiles, Eqs. (1) and (2) appear to be applicable.

The observation of linearity in the NET sense is not confined to epithelial membranes. Also impressive is the linearity of mitochondrial oxidative phosphorylation. In this system, in which both forces are subject to control, each flow is a linear function of each force, both when phosphorylating and under conditions of reverse electron transport (Rottenberg, 1973; Rottenberg and Gutman, 1977; Holian et al., 1977; Westerhoff and van Dam, 1979; Stucki, 1980). Results in mitochondria are consistent with Onsager reciprocity (Rottenberg, 1973; Stucki, 1980). Hence, although isolated chemical reactions are non-linear (unless the affinity A << RT), the elaborate regulatory mechanisms of biological systems evidently give rise to simpler behavior.

CHARACTERISTIC PARAMETERS OF THE NET APPROACH

Affinity

Given the above support for linear phenomenology, it seems reasonable to pursue the possibility that active transport in epithelial tissues might

show linearity not only in the electrochemical potential difference of sodium but also in the affinity of the metabolic driving reaction. If so, one can evaluate the affinity by use of the two phenomenological equations [Eqs. (1) and (2)]:

$$A = - I_o/(dJ_r/d\Delta\psi) \qquad \text{(A constant)} \tag{3}$$

Here the numerator represents the current measured in the absence of both an electrical potential difference and a concentration difference across the membrane, the short-circuit current, and the denominator is the slope of the plot relating the rate of metabolism J_r (oxygen consumption) to the electrical potential difference $\Delta\psi$. The affinity A represents the free-energy change (per mole of O_2) for a characteristic region of the metabolic chain for which A remains constant on perturbation of $\Delta\psi$. Clearly it is of physiological interest, since it must reflect the substrate-product concentration ratio in the metabolic pool which supports active transport. This is in contradistinction to mean cell concentration ratios of various substrates and products. Although attempts have been made to study the driving forces for transport by such measurements, mean concentration ratios may depend on tissue functions other than transepithelial transport. Attempts to evaluate cytopasmic ATP/(ADP x P_i) (Veech et al., 1970) also involve theoretical and experimental difficulties.

By relating the well-known equivalent circuit and NET representations, it is readily shown from Eq. (1) that

$$E_{Na} = (1/F)(L_{Nar}/L_{Na})A \tag{4}$$

Thus, in contrast to the thermodynamic affinity, the electromotive force of sodium transport comprises both permeability and energetic factors. This is confirmed by experimental findings.

Degree of coupling and efficiency

An advantage of the NET representation is that a dimensionless "degree of coupling" q can be defined, uniquely related to the maximum efficiency of the active transport system. This is given by (Kedem and Caplan, 1965)

$$q = L_{Nar}/\sqrt{L_{Na}L_r} \qquad (-1 \leq q \leq 1) \tag{5}$$

The efficiency, η, is defined as

$$\eta = \text{output/input} = -J^a_{Na}\, X_{Na}/J_r A \tag{6}$$

In the two limiting states of the pump, "static head" ($J^a_{Na} = 0$) and "level flow" ($X_{Na} = 0$), η is obviously zero with non-zero input. Between these states it passes through a maximum given by

$$\eta_{max} = q^2/(1 + \sqrt{1-q^2})^2 \tag{7}$$

This quantity can only be unity if coupling is complete ($q = \pm 1$); however in this case we have reversible equilibrium and the rates of both processes are zero. For this and other reasons Stucki (1980) has pointed out that complete coupling is not necessarily advantageous, and that the system may be optimized with regard to output in several ways, giving rise to certain

preferred or "distinguished" values of q.

CONDITIONS FOR LINEARITY FAR FROM EQUILIBRIUM

On a priori grounds Eqs. (1) and (2) hold close to equilibrium, but linearity would be expected to break down, in general, for forces of the magnitudes encountered under physiological conditions. However, the possibility of extended regions of linearity far from equilibrium is clearly indicated by the experimental results. An examination of this problem by means of the Hill diagram method (Hill, 1977) indicates that by applying appropriate constraints in the variation of the forces, "proper" pathways may be found such that in the close vicinity of some reference steady state linearity and reciprocity are achieved (Essig and Caplan, 1980). Furthermore, Rothschild et al. (1980) have recently shown, using the same method, that subject to two nonrestrictive conditions multidimensional inflection points, i.e. extended regions of linearity, characterize coupled systems. It may be demonstrated that such regions always exhibit reciprocity (Caplan, 1980). Although the phenomenological equations describing such regions each include an additive constant, one or both of these may become negligibly small in appropriate circumstances.

CONCLUSIONS

(1) Linear nonequilibrium thermodynamics (NET), although incompletely tested, appears to provide a valid framework for the design and analysis of experiments. In contrast to E_{Na}, the thermodynamic affinity A represents a purely energetic quantity.

(2) There is no unique stoichiometric ratio that relates the rates of active sodium transport and oxygen consumption under all circumstances.

(3) Rates of active sodium transport and oxygen consumption show the postulated linear dependence on the electrochemical potential difference of sodium. Although it has not yet been possible to test for linearity in A, various considerations suggest its likelihood.

(4) The NET approach should facilitate understanding of mechanisms altering sodium transport.

REFERENCES

Al-Awqati, Q., Beauwens, R., and Leaf, A. (1975) Coupling of sodium transport to respiration in the toad bladder. J. Membr. Biol. 22, 91-105.

Beauwens, R., and Al-Awqati, Q. (1976). Active H^+ transport in the turtle urinary bladder. J. Gen. Physiol. 68, 421-439.

Caplan, S. R. (1980). In preparation.

Civan, M. M., Kedem, O., and Leaf, A. (1966). Effect of vasopressin on toad bladder under conditions of zero net sodium transport. Am. J. Physiol. 211, 569-575.

Danisi, G., and Vieira, F. L. (1974). Nonequilibrium thermodynamic analysis of the coupling between active sodium transport and oxygen consumption. J. Gen. Physiol. 64, 372-391.

Essig, A. (1975). Energetics of active transport processes. Biophys. J. 15, 651-665.

Essig, A., and Caplan, S.R. (1968). Energetics of active transport processes. Biophys. J. 8, 1434-1457.

Essig, A., and Caplan, S.R. (1980). Active transport: conditions for linearity and symmetry far from equilibrium. Submitted for publication.

Hill, T.L. (1977). Free Energy Transduction in Biology (Academic Press, New York).

Holian, A., Owen, C.S., and Wilson, D.F. (1977). Control of respiration in isolated mitochondria: quantitative evaluation of the dependence of respiratory rates on [ATP], [ADP], and $[P_i]$. Arch. Biochem. Biophys. 181, 164-171.

Hong, C.D., and Essig, A. (1976). Effects of 2-deoxy-D-glucose, amiloride, vasopressin, and ouabain on active conductance and E_{Na} in the toad bladder. J. Membr. Biol. 28, 121-142.

Kedem, O., and Caplan, S.R. (1965). Degree of coupling and its relation to efficiency of energy conversion. Trans. Faraday Soc. 61, 1897-1911.

Kedem, O., and Essig, A. (1965). Isotope flows and flux ratios in biological membranes. J. Gen. Physiol. 48, 1047-1070.

Lahav, J., Essig, A., and Caplan, S.R. (1976). The thermodynamic degree of coupling between metabolism and sodium transport in frog skin. Biochim. Biophys. Acta 448, 389-392.

Lang, M.A., Caplan, S.R., and Essig, A. (1977). Sodium transport and oxygen consumption in toad bladder - a thermodynamic approach. Biochim. Biophys. Acta 464, 571-582.

Rothschild, K.J., Ellias, S.A., Essig, A., and Stanley, H.E. (1980). Non-equilibrium linear behavior of biological systems. Existence of enzyme-mediated multidimensional inflection points. Biophys. J. 30, 209-230.

Rottenberg, H. (1973). The thermodynamic description of enzyme-catalyzed reactions. Biophys. J. 13, 503-511.

Rottenberg, H., and Gutman, M. (1977). Control of the rate of reverse electron transport in submitochondrial particles by the free energy. Biochemistry 16, 3220-3227.

Saito, T., Lief, P.D., and Essig, A. (1974). Conductance of active and passive pathways in the toad bladder. Am. J. Physiol. 226, 1265-1271.

Stucki, J.W. (1980). The optimal efficiency and economic degrees of coupling of oxidative phosphorylation. Eur. J. Biochem. in press.

Ussing, H. H. (1960). The Alkali Metal Ions in Biology (Springer-Verlag, Berlin and New York).

Ussing, H.H., and Zerahn, K. (1951). Active transport of sodium as the source of electric current in the short-circuited isolated frog skin. Acta Physiol. Scand. 23, 110-127.

Veech, R.L., Raijam, L., and Krebs, H.A. (1970). Equilibrium relations between the cytoplasmic adenine nucleotide system and nicotinamide-adenine nucleotide system in rat liver. Biochem. J. 117, 499-503.

Vieira, F. L., Caplan, S.R., and Essig, A. (1972a). Energetics of sodium transport in frog skin. I. Oxygen consumption in the short-circuited state. J. Gen. Physiol. 59, 60-76.

Vieira, F.L., Caplan, S.R., and Essig, A. (1972b). Energetics of sodium transport in frog skin. II. The effects of electrical potential on oxygen consumption. J. Gen. Physiol. 59, 77-91.

Westerhoff, H.V., and van Dam, K. (1979). Irreversible thermodynamic description of energy transduction in biomembranes. In Current Topics in Bioenergetics, (ed.) Sanadi, D.R. (Academic Press, New York) 9, 2-62.

Zerahn, K. (1956). Oxygen consumption and active sodium transport in the isolated and short-circuited frog skin. Acta Physiol. Scand. 36, 300-318.

Adv. Physiol. Sci. Vol. 3. Physiology of Non-excitable Cells
J. Salánki (ed.)

GENETIC CONTROL OF CELLULAR TRANSPORT

David W. Jayme, Anne H. Dantzig, Edward A. Adelberg and Carolyn W. Slayman

Departments of Human Genetics and Physiology, Yale University School of Medicine
333 Cedar Street, New Haven, Connecticut 06510, USA

INTRODUCTION

It is now widely accepted that membrane transport proteins--like all other cellular proteins--are under genetic control. The most persuasive set of evidence comes from more than two decades of research on the lactose transport system of Escherichia coli. In 1956, Rickenberg, Cohen, Buttin, and Monod found that E. coli possesses an inducible transport system for lactose and structurally related sugars, and described a class of mutants (lacY) that could be induced for the enzymes of lactose metabolism but not for the transport system [1]. During the years that followed, additional lacY mutants were isolated, some lacking transport activity and others possessing qualitative abnormalities in transport [2-4]. Biochemical information began to appear in 1965, when Fox and Kennedy selectively labeled a membrane potein that had the properties expected of the lacY gene product: labeling was greatly decreased in non-induced cells and in most lacY mutants, while in temperature-sensitive mutants, it was suitably heat-labile [5,6]. Finally, early in 1980, definitive proof for the relationship between gene and protein came from the demonstration that the nucleotide sequence of the cloned lacY gene agrees with a partial amino acid sequence of the membrane protein [7,8].

During the same two decades, a large number of other transport mutants have been isolated in microorganisms and in cultured mammalian cells [9,10]. In addition, several well-known inherited disorders in animals and in man have been shown to result from alterations in membrane transport [11,12]. All of this evidence, taken together, points to the general existence of genetic control of membrane transport and to the fact that control can be exerted at a number of levels. Most directly, as in the case of lacY, mutations in the structural gene for a transport protein can lead to defects in amino acid sequence or can abolish the synthesis of the protein altogether. One can also imagine mutations that disrupt the post-translational modification (for example, glycosylation) of a transport protein or the synthesis of a required membrane lipid. And finally, at least in some instances, regulatory genes exist which control the timing and rate of transcription of the structural genes.

Given this array of possibilities, the membrane physiologist can make good use of genetic analysis. Methods can be devised in microorganisms and in cultured cells to select for transport mutants, and the mutants can be

employed to dissect transport mechanisms. The purpose of this review is to consider both the selection methods and the ways in which the resulting mutants can be exploited.

ISOLATION OF TRANSPORT MUTANTS

To isolate mutants of a cultured cell line, the standard procedure consists of mutagenesis (to increase the overall mutation rate), an intermediate period of growth (to allow mutant phenotypes to be expressed), a selection step (to enrich for the desired mutants), and screening (to identify the mutants). All of these procedures have been described in recent reviews [13,14], so we will focus here on selection and screening methods that have proved particularly valuable in the search for transport mutants.

Positive selection methods. Positive selection methods are the most straightforward kind, since conditions are chosen which prevent the growth of wild-type cells and allow only mutant clones to form. For example, cells might be plated in the presence of a drug that inhibits a particular transport system to select for drug-resistant mutants or in medium containing a toxic amino acid or sugar analogue to select for mutants unable to transport that analogue. Or cells can be plated in the presence of an abnormally low or abnormally high nutrient concentration, to suppress the growth of wild-type cells and to obtain mutants with altered transport pathways for the nutrient. Examples of mutants selected in these ways are listed in Table 1.

Table 1

Selection of Transport Mutants of Cultured Cells

Positive selection	
Drug resistance	Ouabain [15-17]
Resistance to toxic analogues	5-fluorotryptophan [18-19]
Ability to grow at a low nutrient concentration which does not support the growth of wild-type cells	K^+ [20]
Ability to grow at a high nutrient concentration which inhibits the growth of wild-type cells	phenylalanine [21] methionine [22]
Negative selection	
Inability to grow at a marginal nutrient concentration just sufficient for the growth of wild-type cells	K^+ [23] leucine [14, 24]
Tritium suicide	AIB [25] proline [14,24]

Negative selection methods. In negative selection methods, conditions are chosen to kill growing cells while permitting non-growing mutants to survive (Table 1). For example, mutagenized cells might be incubated in medium containing a required nutrient at a concentration just sufficient to support the growth of the wild type, but insufficient for the growth of transport-defective mutants. The wild-type cells are then killed by the use of a treatment that is lethal only to growing cells (uptake of [^{3}H]-thymidine; exposure to cytosine arabinoside or 5-fluorodeoxyuridine; uptake of 5-bromodeoxyuridine followed by irradiation with 310-nm light [13]).

All of the methods described up to this point require conditions where growth is dependent upon the functioning of a particular transport system. A useful alternative is a negative selection procedure called "tritium suicide", in which cells unable to transport a particular substrate are selected directly. In this procedure, mutagenized cells are exposed to [^{3}H]-substrate of high specific activity for a brief period and then stored at low temperature (typically, -100°C) for several weeks or months. Wild-type cells containing the [^{3}H]-labeled substrate are killed by internal radiation, while transport-defective mutants survive. An example of tritium suicide is described below.

Screening of putative mutants. Because no selection procedure is perfect, yielding only the desired mutants while suppressing the growth of all remaining wild-type cells, it is mandatory to screen the survivors in order to identify the ones with actual defects in transport. In many cases, this has been done by growing up the clones individually and measuring substrate influx by standard isotopic methods [15-23,25]. A rapid technique for screening large numbers of clones has recently become possible with the discovery by Esko and Raetz [26] that some cultured cells are capable of attaching to filter paper and of being replicated from one culture plate to another. Using a modification of this method, in which the filter paper replica was incubated with [^{14}C]-proline and subjected to autoradiography, we screened approximately 7000 clones for defects in proline uptake and identified 20 possible transport mutants [14].

USE OF MUTANTS TO STUDY TRANSPORT MECHANISMS

Once transport mutants have been isolated, they can be used to pose various kinds of questions about the mechanism of transport. The two examples that follow are drawn from recent work in our own laboratory, but we will also point out some of the ways in which similar approaches might be used to study other transport systems in other cell types.

Amino acid transport in cultured mouse lymphocytes. The work of Christensen and his colleagues has made it clear that mammalian cells possess multiple transport systems for amino acids [27]. For neutral amino acids alone, at least three major systems exist in most cells: the A system, which prefers alanine and other small, neutral amino acids; the L system, which prefers leucine and other amino acids with bulky, aliphatic side chains; and the ASC system, for alanine, serine, and cysteine (Fig. 1). Physiological and biochemical studies on these systems are complicated by overlapping substrate specificities. For example, alanine and methionine are taken up by all three routes; and even α-aminoisobutyric acid (AIB), often used as a specific substrate for the A system, is now known to be taken up in many cells by the ASC system as well [28]. For

this reason, it seemed that mutants lacking one or more of the systems might provide a more clearcut way to identify and characterize the system(s) that remain.

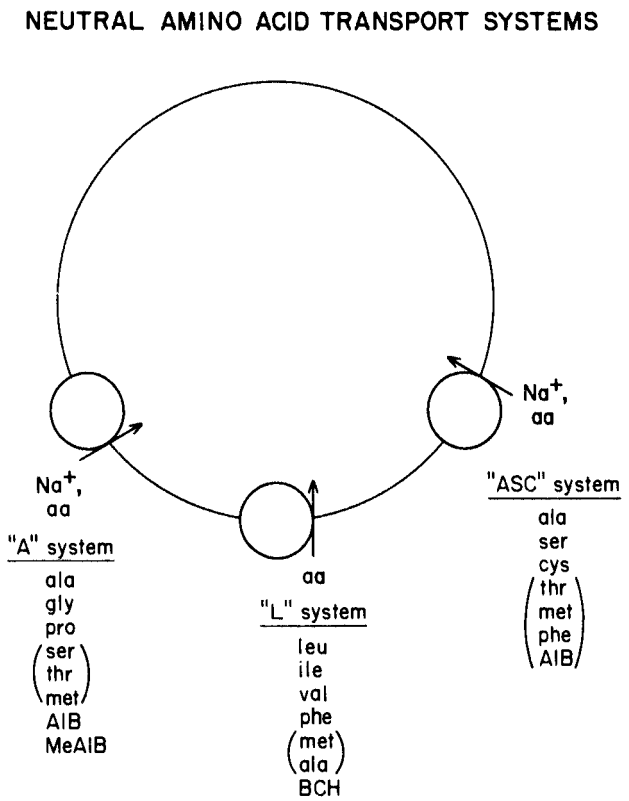

Fig. 1. Diagram of neutral amino acid transport systems and their substrate specificities, based on Christensen [27]. The A and ASC systems require Na^+; the L system is Na^+-independent. Abbreviations for model substrates: AIB, α-aminoisobutyric acid; MeAIB, α-methylaminoisobutyric acid; BCH, 2-aminonorbornyl-2-carboxylic acid.

Starting with GF-14, an established line of mouse lymphocytes, Finkelstein et al. [25] carried out tritium suicide with [^{3}H]-AIB, as diagrammed in Fig. 2. Of 200 surviving clones that were tested, two (GF-17 and GF-18) showed a 75-80% reduction in the V_{max} for AIB uptake via the A

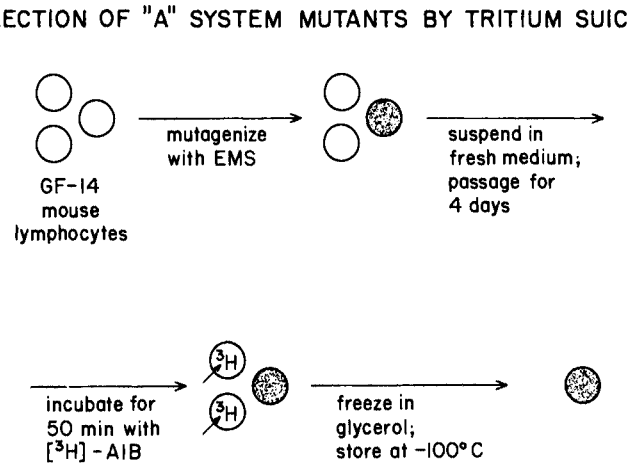

Fig. 2. Selection of "A" system mutants by tritium suicide, using [^{3}H]-AIB. Further details are given in ref. 25.

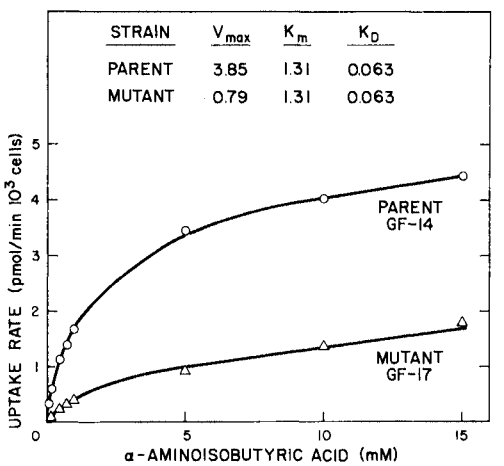

Fig. 3. Initial rate of AIB uptake in parental GF-14 lymphocytes and the GF-17 mutant as a function of AIB concentration. Data were fitted by computer, yielding values for V_{max} (pmol/10^3 cells·min), K_m (mM), and the diffusion constant, K_D (pmol/10^3 cells·min·mM). For further details, see ref. 30.

system (Fig. 3) [25,29]. Analysis of residual AIB transport in both mutants failed to reveal any abnormality in the pattern of competitive inhibition by other A system substrates, in sodium dependence, or in pH or temperature optimum, making it likely that the mutants synthesize fewer, but qualitatively normal, A transport sites [29].

One use for mutants lacking a particular transport system, as mentioned above, is to aid in the resolution of multiple transport systems with overlapping substrate specificities. In particular, preliminary uptake measurements with parental GF-14 lymphocytes had pointed to the existence of two uptake systems for L-glutamate: one (with high K_m and high V_{max}) corresponding to the A system and the other (with low K_m and low V_{max}) specific for L-glutamate. In GF-17 and GF-18, which had lost a major fraction of the A system, the specific system mediated a larger fraction of L-glutamate uptake (Fig. 4) and could be characterized more easily [30].

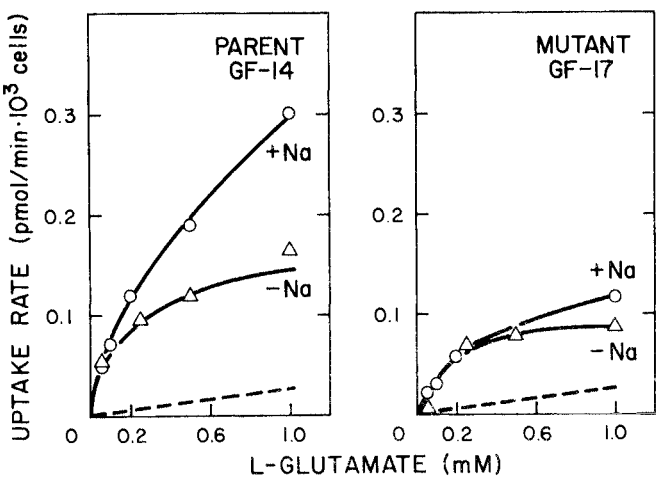

Fig. 4. Initial rate of L-glutamate uptake in parental GF-14 lymphocytes (left) and in the GF-17 mutant (right) as a function of L-glutamate concentration. The difference between the curves with and without Na^+ gives the contribution of the Na^+-dependent A system. The curve without Na^+ represents the Na^+-independent specific glutamate system plus a small contribution from diffusion (dotted line). See ref. 30.

Studies on mutants lacking a particular transport system can also shed light on the physiological role of that system. For example, the L system is the major route for uptake of several essential amino acids, so one

would expect its loss to be lethal. In such cases, genetic analysis is still possible, but one must search for conditionally lethal mutants (such as temperature-sensitive strains, in which a particular amino acid substitution has rendered the transport protein abnormally heat-labile; mutants of this kind cannot transport or grow at a high temperature but can be recovered at a low temperature where their transport proteins function normally). By contrast, the A system takes up only one essential amino acid--methionine, which is a substrate for the L and ASC systems as well--so one might expect the loss of the A system to result in slower growth but not to be lethal. In accordance with this prediction, the mutants GF-17 and GF-18 were found to grow quite well under standard conditions. Their generation times were 19.2 and 21.3 hrs, respectively, compared with 14.4 hrs for the parental strain GF-14 [25].

Future uses for GF-17 and GF-18 will be in the identification of the membrane protein(s) corresponding to the A system, in reconstitution experiments, and in studies on the regulation of amino acid transport.

Potassium transport in cultured mouse fibroblasts. A second example in which genetic analysis has been used to dissect a complex set of membrane transport systems is provided by recent work in our laboratory on potassium transport in cultured mouse fibroblasts. Just as mammalian cells possess multiple transport systems for amino acids, they also possess several pathways by which K^+ and Na^+ can cross the plasma membrane. Fig. 5 illustrates three of these pathways: (1) the classical ouabain-sensitive Na^+/K^+ pump; (2) a cotransport system for Na^+, K^+, and Cl^- which is sensitive to diuretics such as furosemide and bumetanide [31]; and (3) a Ca^{++}-activated K^+ channel [32]. Under normal circumstances, when cells are growing in culture medium containing 5 mM K^+ and 150 mM Na^+, they maintain a high internal K^+ concentration and a low internal Na^+ concentration relative to their environment. When cells are transferred to low-K^+ medium, however, influx no longer matches efflux; intracellular K^+ is lost; and the cells lyse.

This phenomenon has formed the basis for selecting a group of mutants altered in K^+ transport. Starting with a mutagenized suspension of LM(TK^-), a derivative of the mouse fibroblastic L cell line, Gargus et al. [20] plated the cells in medium containing a final K^+ concentration of 0.2 mM, too low to permit the growth of the parent cells. Clones that appeared (at a frequency of 1-10/10^7 cells plated) were isolated and characterized with respect to K^+ transport.

Based on the conditions under which they were selected, one might expect the mutants to possess either an increase in K^+ influx or a decrease in K^+ efflux. In the parental LM(TK^-) cells, the major route of K^+ influx at 0.2 mM K^+ is the ouabain-sensitive Na^+/K^+ pump [33]. None of the mutants proved to be altered in the V_{max}, the $K_{\frac{1}{2}}$ for extracellular potassium, or the ouabain sensitivity of this process [20,33]. Instead, one class of mutants (represented by LTK-5) showed reduced K^+ efflux through the diuretic-sensitive system (Fig. 6) [34], while another class of mutants (represented by LTK-1) appeared to be altered in a separate, diuretic-insensitive component of efflux (possibly the Ca^{++}-activated K^+ channel) [20].

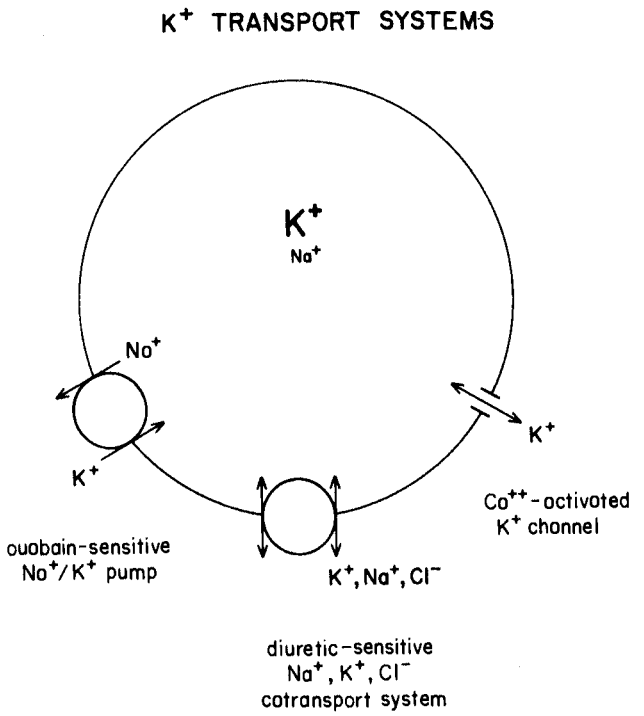

Fig. 5. Diagram of K^+ transport systems in cultured mouse fibroblasts, based on refs. 20, 33, and 34.

Further work will be needed to pinpoint the mutational defects in greater detail and to make use of the mutants in characterizing these pathways of K^+ transport. In the meantime, however, the LTK-5 mutant has already drawn our attention to an important physiological consequence of the diuretic-sensitive cotransport system: although it is often studied under conditions where it mediates net K^+ (and Na^+ and Cl^-) influx, the results illustrated in Fig. 6 suggest that it can serve as a significant "leak" pathway for potassium. Indeed, as shown in Fig. 7, blocking the cotransport system with diuretic actually permits the parental LM(TK$^-$) cells to grow at 0.2 mM K^+, while the ability of the LTK-5 mutant to grow is not altered [35].

CONCLUSIONS

In two separate situations, the isolation of transport mutants has contributed to the sorting out of multiple transport systems. In the case of amino acid transport in cultured mouse lymphocytes, mutants lacking the A system have supplemented knowledge gained from earlier experiments with model substrates and have permitted the detection of a new, Na^+-independent glutamate-specific transport system. In the case of K^+ transport in mouse

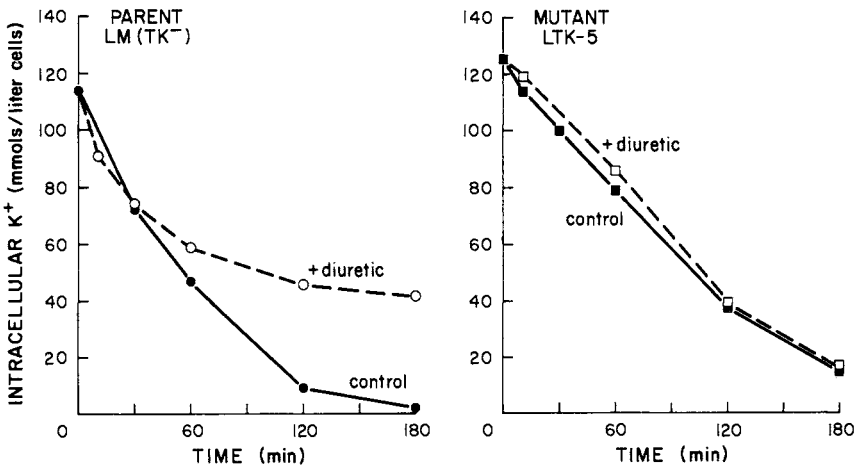

Fig. 6. Net K^+ efflux from parental LM(TK^-) cells (left) and the LTK-5 mutant (right) following resuspension in medium containing 0.2 mM K^+. Control flasks (closed circles) contained 1 mM ouabain to inhibit K^+ uptake via the Na^+/K^+ pump. The remaining flasks (open circles) contained ouabain plus the diuretic bumetanide (10μM) [34].

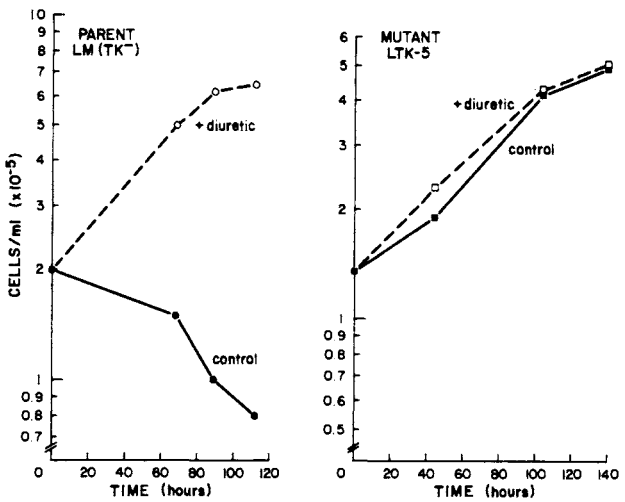

Fig. 7. Growth of parental LM(TK^-) cells (left) and the LTK-5 mutant (right) following resuspension in medium containing 0.2 mM K^+, with and without the diuretic furosemide (0.67 mM) [34].

fibroblasts, the LTK-1 and LTK-5 mutants promise to be useful in the study of two systems--the Na^+, K^+, Cl^- cotransport system and the Ca^{++}-activated K^+ channel--which are difficult to dissect unambiguously with the use of inhibitors alone. In the future, mutants of both kinds should be helpful in identifying membrane proteins corresponding to particular transport systems, in reconstitution experiments, and in studies on the physiological role of transport.

ACKNOWLEDGEMENTS

This work was supported by research grants GM20124 from the National Institutes of Health and PCM76-02818 from the National Science Foundation.

REFERENCES

[1] Rickenberg, H.V., Cohen, G.N., Buttin, G., and Monod, J. (1956). La galactoside-perméase d'Escherichia coli. Ann. Inst. Pasteur 91:829-857.

[2] Wilson, T.H., and Kusch, M. (1972). A mutant of Escherichia coli K12 energy-uncoupled for lactose transport. Biochim. Biophys. Acta 255: 786-797.

[3] West, I.C., and Wilson, T.H. (1973). Galactoside transport dissociated from proton movement in mutants of Escherichia coli. Biochem. Biophys. Res. Comm. 50:551-558.

[4] Kusch, M., and Wilson, T.H. (1973). Defective lactose utilization by a mutant of Escherichia coli energy-uncoupled for lactose transport. Biochim. Biophys. Acta 311:109-122.

[5] Fox, C.F., and Kennedy, E.P. (1965). Specific labeling and partial purification of the M protein, a component of the β-galactoside transport system of Escherichia coli. Proc. Natl. Acad. Sci. U.S.A. 54: 891-899.

[6] Fox, C.F., Carter, J.R., and Kennedy, E.P. (1967). Genetic control of the membrane protein component of the lactose transport system of Escherichia coli. Proc. Natl. Acad. Sci. U.S.A. 57:698-705.

[7] Ehring, R., Beyreuther, K., Wright, J.K., and Overath, P. (1980). In vitro and in vivo products of E. coli lactose permease gene are identical. Nature 283:537-540.

[8] Büchel, D.E., Gronenborn, B., and Müller-Hill, B. (1980). Sequence of the lactose permease gene. Nature 283:541-545.

[9] Slayman, C.W. (1978). Genetic determination of membrane transport; Chapter 7 in Membrane Transport in Biology (ed. Giebisch, G., Tosteson, D.C., and Ussing, H.H., Springer-Verlag, Berlin), pp. 239-257.

[10] Adelberg, E.A., and Slayman, C.W. (1978). Genes and membranes; Chapter 19 in Physiology of Membrane Disorders (ed. Andreoli, T.E., Hoffman, J.F., and Fanestil, D.D., Plenum, New York), pp. 357-367.

[11] Stanbury, J.B., Wyngaarden, J.B., and Fredrickson, D.S. (1978). The Metabolic Basis of Inherited Disease (McGraw-Hill, N.Y., 4th edition, Chapters 64-73), pp. 1526-1710.

[12] Lauf, P.K. (1975). Antigen-antibody reactions and cation transport in biomembranes: immuno physiological aspects. Biochim. Biophys. Acta 415:173-229.

[13] Adelberg, E.A. (1980). The induction of mutation in cultured cells; in Genetic Toxicology (ed. Rosenkranz, H.D., Zeiger, E., and DeSerres, F., Academic Press), in press.

[14] Adelberg, E.A., and Dantzig, A.H. (1979). Selection methods for membrane transport mutants, in Banbury Report 2, Mammalian Cell Mutagenesis (ed. Hsie, A.W., O'Neill, J.P., and McElheny, V.K., Cold Spring Harbor Laboratory), pp. 179-185.

[15] Baker, R.M., Brunette, D.M., Mankovitz, R., Thompson, L.H., Whitmore, G.F., Siminovitch, L., and Till, J.E. (1974). Ouabain-resistant mutants of mouse and hamster cells in culture. Cell 1:9-21.

[16] Mankovitz, R., Buchwald, M., and Baker, R.M. (1974). Isolation of ouabain-resistant human diploid fibroblasts. Cell 3:221-226.

[17] Robbins, A.R., and Baker, R.M. (1977). (Na,K)ATPase activity in membrane preparations of ouabain-resistant HeLa cells. Biochemistry 16:5163-5168.

[18] Taub, M., and Englesberg, E. (1976). Isolation and characterization of 5-fluorotryptophan-resistant mutants with altered L-tryptophan transport. Somatic Cell Genetics 2:441-452.

[19] Taub, M., and Englesberg, E. (1978). 5-fluorotryptophan resistant mutants affecting the A and L transport systems in the mouse L cell line A9. J. Cell. Physiol. 97:477-486.

[20] Gargus, J.J., Miller, I.L., Slayman, C.W. and Adelberg, E.A. (1978). Genetic alterations in potassium transport in L cells. Proc. Natl. Acad. Sci. U.S.A. 75:5589-5593.

[21] Englesberg, E., Bass, R., and Heiser, W. (1976). Inhibition of the growth of mammalian cells in culture by amino acids and the isolation and characterization of L-phenylalanine-resistant mutants modifying L-phenylalanine transport. Somatic Cell Genetics 2:411-428.

[22] Heiser, W., and Englesberg, E. (1979). Isolation and characterization of L-methionine-resistant mutants of SV40-transformed Balb 3T3 (SVT2) affecting L-methionine transport. Somatic Cell Genetics 5:345-361.

[23] Miller, I.L., Slayman, C.W., and Adelberg, E.A., unpublished results.

[24] Dantzig, A.H., Slayman, C.W., and Adelberg, E.A., unpublished results.

[25] Finkelstein, M.C., Slayman, C.W., and Adelberg, E.A. (1977). Tritium suicide selection of mammalian cell mutants defective in the transport of neutral amino acids. Proc. Natl. Acad. Sci. U.S.A. 74:4549-4551.

[26] Esko, J.D., and Raetz, C.R.H. (1978). Replica plating and *in situ* enzymatic assay of animal cell colonies established on filter paper. Proc. Natl. Acad. Sci. U.S.A. 75:1190-1194.

[27] Christensen, H.N. (1975). Biological Transport (2nd ed., W.A. Benjamin), pp. 514.

[28] Kilberg, M.S., Christensen, H.N., and Handlogten, M.E. (1979). Cysteine as a system-specific substrate for transport system ASC in rat hepatocytes. Biochem. Biophys. Res. Comm. 88:744-751.

[29] Dantzig, A.H., Adelberg, E.A., and Slayman, C.W. (1979). Properties of two mouse lymphocyte cell lines genetically defective in amino acid transport. J. Biol. Chem. 254: 8988-8993.

[30] Dantzig, A.H., Finkelstein, M.C., Adelberg, E.A. and Slayman, C.W. (1978). The uptake of L-glutamic acid in a normal mouse lymphocyte line and in a transport mutant. J. Biol. Chem. 253:5813-5819.

[31] Geck, P., Pietrzyk, C., Burckhardt, B.-C., Pfeiffer, B., and Heinz, E. (1980). Electrically silent cotransport of Na^+, K^+, and Cl^- in Ehrlich cells. Biochim. Biophys. Acta, in press.

[32] Lew, V.L., and Ferreira, H.G. (1978). Calcium transport and the properties of a calcium-activated potassium channel in red cell membranes. Curr. Topics in Membranes and Transport 10:217-277.

[33] Gargus, J.J., and Slayman, C.W. (1980). Mechanism and role of furosemide-sensitive K^+ transport in L cells: a genetic approach. J. Membrane Biol. 52:245-256.

[34] Jayme, D.W., Adelberg, E.A., and Slayman, C.W., manuscript in preparation.

[35] Jayme, D.W., Gargus, J.J., Slayman, C.W., and Adelberg, E.A. (1980). Effect of furosemide on Na^+ and K^+ fluxes in mouse L cells. J. Supramolec. Structure, Suppl. 4, p. 103.

Adv. Physiol. Sci. Vol. 3. Physiology of Non-excitable Cells
J. Salánki (ed.)

THE HORMONAL REGULATION OF ACTIVE ELECTROGENIC Na^+-K^+-TRANSPORT IN SKELETAL MUSCLE

T. Clausen
Institute of Physiology, University of Aarhus, 8000 Århaus C, Denmark

The active electrogenic transport of Na^+ and K^+ across the plasma membrane is essential for the maintenance of a wide variety of cellular properties and functions. Primarily, the Na^+-K^+-pump builds up a steady-state with a low intracellular Na^+/K^+-concentration ratio, which is controlled by the inherent kinetic properties of the membrane bound Na^+-K^+-activated ATPase. Secondary to this process, a membrane potential is generated and maintained with all what this implies for the passive distribution of charged particles across the plasma membrane as well as the propagation of electrical signals along the membrane.

Another important consequence of Na^+-K^+-pumping is related to the existence of Na^+-sensitive calcium transport processes in the plasma membrane (Ashley et al. 1974) and the mitochondria (Crompton et al. 1978). Due to these, the intracellular concentration of Na^+ ions may determine the cytoplasmic Ca^{++} ion level, which, in turn, is decisive for the control of the metabolism as well as the contractile performance of muscle cells.

Even though its effects on cellular functions are of indirect nature and sometimes slow in onset, the Na^+-K^+-pump is presumably the major regulatory transport structure in the plasma membrane. Therefore, it is natural to ask how its mode of operation is controlled in the cell and the organism. The biochemist would answer that the Na^+-K^+-pump is controlled by the local concentrations of Na^+, K^+, Mg^{++}, ATP, and a number of other compounds, not to mention vanadate. These proposals already give more than enough work for the transport physiologist studying intact cells. For a further understanding of the regulation of the active Na^+-K^+-transport in the intact organism, however, it is important to identify and describe the actions of the various hormones designed by Nature to coordinate the interplay between different cells and body compartments.

In the following, I shall try to summarize information obtained in studies of skeletal muscle. The presentation will be concentrated on three major questions:

1. Which hormonal effects can be detected on Na^+-K^+-transport, Na^+-K^+-contents, resting membrane potential (E_M), and ouabain binding in intact skeletal muscle?
2. Which receptors and cellular messengers are involved in these actions?
3. What is the significance of the hormonal control of the Na^+-K^+-pump in the regulation of metabolism, contractile performance and electrolyte distribution?

At least 3 different hormones seem to be involved in the control of active Na^+-K^+-transport in skeletal muscle: insulin, catecholamines, and thyroid hormones.

A. INSULIN

1. Effects:

It is well-documented that the hypokalemic effect of insulin can to a large extent be accounted for as the outcome of a stimulation of K^+-uptake in muscle (Kamminga et al. 1950; Zierler 1972).

In isolated muscles, insulin stimulates the uptake of ^{42}K. This effect is blocked by ouabain, but not by local anaesthetics, indicating that it reflects stimulation of the Na^+-K^+-pump (Clausen & Kohn 1977). Insulin also stimulates the efflux of labelled Na^+ from isolated muscles (Creese 1968; Moore 1973; Clausen & Kohn 1977; Kitasato et al. 1980). As a natural consequence of these effects, the continued exposure to the hormone leads to a decrease in the intracellular Na^+/K^+-concentration ratio.

Insulin induces hyperpolarization, both in vitro (Zierler 1957; Bolte & Lüderitz 1968; Otsuka & Ohtsuki 1970; Moore & Rabovsky 1979), and in vivo (Flatman & Clausen 1979). This effect is blocked by ouabain. The slow onset indicates that it is mainly the result of the redistribution of Na^+ and K^+ across the plasma membrane.

2. Mechanisms:

It should be emphasized that the above mentioned effects of insulin are selective in the sense that they are not modified by the omission of glucose or the addition of phlorizin (Clausen & Kohn 1977). Likewise, blocking the Na^+-K^+-pump does not interfere with the effect of insulin on glucose transport (Kohn & Clausen 1971). Thus, there is no direct relationship between the effects of the hormone on glucose transport and Na^+-K^+-pumping.

Whereas insulin does not increase the total number of Na^+-K^+-pumps, it increases the activity of the Na^+-K^+-activated ATPase (Brodal et al. 1974; Gavryck et al. 1975) and augments the rate of ^3H-ouabain binding (Clausen & Hansen 1977). These observations argue that the hormone acts specifically on the Na^+-K^+-pump so as to increase its turnover, perhaps by

increasing the affinity for Na^+ ions on the inner surface of the plasma membrane (Moore 1973; Kitasato et al. 1980). The observation that the effects of insulin on Na^+-K^+-transport, Na^+-K^+-contents and membrane potential (see Table 1) are additive to those exerted by adrenaline indicates that they are not mediated by a drop in the cytoplasmic concentration of cyclic AMP (Flatman & Clausen 1979).

Table 1: Combined effects of adrenaline and insulin on intracellular Na^+-K^+-concentrations and resting membrane potential (E_M) in rat soleus muscle.

The Na^+-K^+-concentrations of the tissue water space not available to ^{14}C-sucrose were determined and are expressed as mmol/l ± s.e. with the number of observations in parentheses. E_M was measured using conventional microelectrodes before and after the hormone-induced hyperpolarization was fully developed, i.e. for adrenaline, 7 min and for insulin, 15 min. The increase in E_M (ΔE_M) induced by the addition of adrenaline or insulin alone or adrenaline to insulin-treated muscles is shown with s.e. and the number of penetrations/muscles in parentheses (reproduced, with permission from "Nature" vol. 281, p. 580-581, 1979).

Additions	Intracellular Na^+-conc. (mmol/l)	Intracellular K^+-conc. (mmol/l)	ΔE_M (mV)
Control	22 ± 1 (7)	155 ± 2 (7)	
	p<0.001	p<0.001	
Insulin (100 mU/ml)	17 ± 1 (7)	170 ± 3 (7)	+3.5 ± 0.2 (199/5)
	p<0.001	p<0.005	p<0.001
Insulin (100 mU/ml) +Adrenaline (10^{-5}M)	7 ± 1 (6)	188 ± 3 (6)	+7.3 ± 0.3 (192/5)
	p<0.01	p<0.001	p>0.10
Adrenaline (10^{-5}M)	12 ± 1 (6)	168 ± 2 (6)	+7.4 ± 0.4 (194/5)

3. Significance:

Although insulin for more than 50 years has been the tool of choice in the treatment of hyperkalemic states, too little is known about its role in potassium homeostasis. It is well-established that physiological concentrations of insulin favour the transfer of K^+ from plasma into muscle cells (Andres et al. 1962), but the secretion of the hormone is only stimulated at extraordinarily high plasma K^+ levels (Cox et al. 1978; Clausen et al. 1980). On the other hand, lowered plasma insulin levels (as in diabetes mellitus) is associated with hyperkalemia and increased intracellular

Na^+-concentrations in muscle cells (Moore et al. 1979). In view of the muscular fatigue experienced by diabetic patients before they receive insulin treatment, it is of considerable interest to assess the consequences of insulin-induced Na^+-K^+-pump stimulation for the contractile performance of muscles. It was recently demonstrated that in isolated guinea pig muscles, insulin mimicks the action of adrenaline on the pattern of contraction (Holmberg & Waldeck 1980).

Even though insulin almost doubles the rate of active Na^+-K^+-transport, it only increases heat production and oxygen consumption by around 5% (Chinet & Clausen, unpublished observations). This agrees with earlier observations (for review, see Clausen 1975) and is in keeping with the relatively low energy requirement of the Na^+-K^+-pump in intact skeletal muscle (Chinet et al. 1977). The effect of insulin on the Na^+-K^+-pump is of little or no direct significance for its actions on glucose metabolism (Clausen 1975) or the Na^+-dependent uptake of amino acids in muscle (Goldman & Clausen, unpublished observations).

B. CATECHOLAMINES

1. Effects:

Although the hypokalemic effect of adrenaline has been known for almost 50 years (D'Silva 1934), it has not been made use of in clinical work. In fact, the stimulating effect of adrenaline on the Na^+-K^+-pump is more pronounced than that exerted by insulin, and specific beta-adrenoceptor agonists may be more convenient tools in the treatment of hyperkalemic states (Wang & Clausen, 1976; Rosa et al. 1980).

In isolated muscles, adrenaline and noradrenaline stimulate the uptake of ^{42}K as well as the efflux of ^{22}Na (Hays et al. 1974; Clausen & Flatman 1977). Both effects are blocked by ouabain, indicating that they reflect stimulation of the Na^+-K^+-pump. The hyperpolarizing effect of catecholamines on skeletal muscle cells (Tashiro 1973) is early in onset and to a large extent the direct outcome of acceleration of the electrogenic Na^+-K^+-pump (Clausen & Flatman 1977). During longer exposure to the hormones, the hyperpolarization is maintained, partly because the intracellular K^+-concentration is increased. Intracellular Na^+ may be decreased to around 1/3 of its normal level. The hyperpolarizing effect of adrenaline and beta-adrenoceptor agonists is perhaps even more pronounced in vivo (Flatman & Clausen 1979; Clausen & Flatman 1980).

2. Mechanisms:

Adrenaline does not increase the total number of Na^+-K^+-pumps, but, like insulin and Na^+-loading it increases the rate of ^3H-ouabain binding, indicating that the action is specifically exerted on the Na^+-K^+-pump (Clausen & Hansen 1977). These effects of catecholamines are mediated via $beta_2$-adrenoceptors (Clausen & Flatman 1980), and since they can be mimicked by **a**

combination of theophylline and dibutyryl cyclic AMP, they are probably the outcome of a stimulation of the adenylate cyclase.

3. Significance:

Under beta-adrenoceptor blockade, plasma K^+ is elevated, in particular during and after exercise (Carlsson et al. 1978). This may be of importance for the fatigue and reduced capacity for physical work experienced by patients receiving beta-blocking agents. Elevated plasma potassium was found to diminish the maximum working capacity (Bodil Nielsen, personal communication).

Catecholamines also influence the contractile pattern in skeletal muscle. It is well known that increased plasma catecholamine levels are associated with trembling or shaking. This is probably due to effects on the contractile pattern (Bowman 1980). Recent studies indicate that these phenomena can to a considerable extent be accounted for as the result of stimulation of the Na^+-K^+-pump (Tashiro 1973; Holmberg & Waldeck 1980).

In spite of the pronounced stimulating effect of beta-adrenoceptor agonists on the active Na^+-K^+-transport in soleus muscle, they only produce a modest rise in energy production. Thus, salbutamol (10^{-5}M) only gave a transient increase in heat production of 8% (as measured in a microcalorimeter) (Chinet et al. 1980).

The inhibitory effect of adrenaline on glucose transport in muscle (Walaas & Walaas 1950) has been related to a lowering of the intracellular Na^+-concentration (Bihler et al. 1978). As shown in Table 2 the $beta_2$-adrenoceptor agonist salbutamol (10^{-5}M) diminish the stimulating effect of submaximal concentrations of insulin (0.1 - 1 mU/ml) on the transport of ^{14}C-3-0-methylglucose in rat soleus muscles. This inhibitory effect is abolished by ouabain indicating that it is the outcome of a stimulation of the active Na^+-K^+-transport with ensuing lowering of the intracellular Na^+-concentration. Since the glucose transport system is activated by calcium, these effects may be related to a more efficient clearing of Ca^{++} ions when the cytoplasmic Na^+-concentration is lowered (see Bihler et al. 1978).

C. THYROID HORMONES

1. Effects:

It has repeatedly been demonstrated that pretreatment with thyroid hormones (T_3 & T_4) induces an increase in the activity of Na^+-K^+-activated ATPase in a variety of tissues (for review, see Smith & Edelman 1979). In skeletal muscle, the rate of Na^+-K^+-exchange is increased in proportion to the thyroid status (Asano 1978). Whereas the thyroid hormones have no immediate effect on Na^+-K^+-transport when added to isolated muscles in vitro, muscles prepared from hypothyroid, euthyroid

Table 2: Effect of beta-adrenoceptor agonists and ouabain on insulin-responsiveness of rat soleus muscle.

Intact soleus muscles were prepared from young rats (60-70 g) and loaded for 60 min with ^{14}C-3-Omethylglucose. They were then washed out in a series of tubes containing unlabelled buffer and the fraction of ^{14}C-activity lost from the muscles determined as described in detail elsewhere (Kohn & Clausen 1971). The fraction of ^{14}C-activity lost per min during the interval from 10 to 20 min after the addition of insulin is given ± s.e. with the number of observations in parentheses. Pretreatment with salbutamol, adrenaline or ouabain was initiated 90 min before the exposure to insulin.

Additions	Fraction of ^{14}C-3-O-methylglucose lost per min.	
Control	0.0033±0.0003 (4)	
Insulin (0.1 mU/ml)	0.0091±0.0019 (6)	p<0.05
Insulin (0.1 mU/ml) + Salbutamol (10^{-5}M)	0.0045±0.0003 (6)	
Insulin (1.0 mU/ml)	0.0218±0.0011 (19)	p<0.01
Insulin (1.0 mU/ml) + Salbutamol (10^{-5}M)	0.0166±0.0016 (8)	p<0.005
Insulin (1.0 mU/ml) + Adrenaline (10^{-6}M)	0.0121±0.0019 (5)	p<0.001
Insulin (1.0 mU/ml) + Adrenaline (10^{-5}M)	0.0108±0.0009 (5)	
Insulin (100 mU/ml)	0.0435±0.0035 (3)	p<0.80
Insulin (100 mU/ml) + Salbutamol (10^{-5}M)	0.0429±0.0015 (3)	
Insulin (1.0 mU/ml) + Ouabain (10^{-3}M)	0.0248±0.0016 (6)	p<0.60
Insulin (1.0 mU/ml) + Ouabain (10^{-3}M) + Salbutamol (10^{-5}M)	0.0265±0.0044 (3)	p<0.20
Insulin (1.0 mU/ml) + Ouabain (10^{-3}M) + Adrenaline (10^{-5}M)	0.0214±0.0024 (3)	

and hyperthyroid animals show progressive increase in the ouabain-suppressible ^{42}K-uptake in proportion to the thyroid status (Biron et al. 1979). Measurements of ^{3}H-ouabain binding indicate that this effect is accounted for by proportionate changes in the number of Na^+-K^+-pumps, the number of K^+ ions pumped per ouabain binding site remaining constant.

2. Mechanisms:

Studies with cell cultures have demonstrated that the number of Na^+-K^+-pumps is increased when the intracellular Na^+-concentration is maintained above the normal level. However, in muscles, the intracellular Na^+-concentration is not markedly altered with the thyroid status. Therefore, it is difficult to determine whether the primary action of thyroid hormones is to increase the Na-influx or rather exerted on other processes determining the rate of synthesis of new Na^+-K^+-pumps.

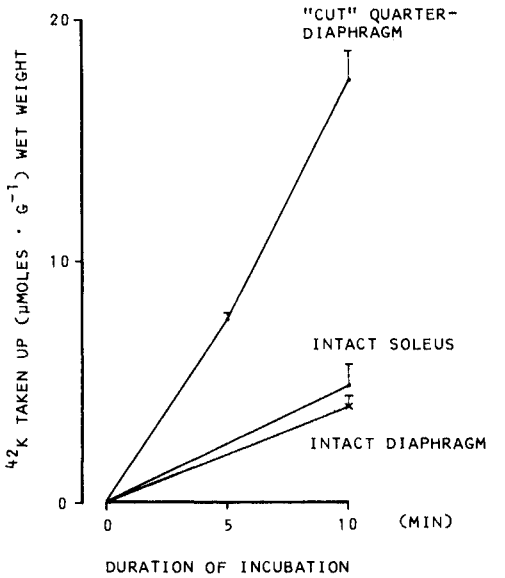

Fig. 1. Effect of tissue integrity on the ouabain-sensitive ^{42}K uptake in mouse muscle.

Quarterdiaphragms, intact soleus and diaphragm muscles from adult euthyroid mice were washed and preincubated for 15 min in Krebs-Ringer bicarbonate buffer (with 1·2 mM-Mg) with or without ouabain (10^{-3}M). They were then incubated for 5 or 10 min in the same buffer containing ^{42}K (0·1 μc/ml) with or without ouabain, blotted, freed from tendons and ribs and counted for ^{42}K. The results are given as the difference between the amount of ^{42}K taken up in the untreated and the ouabain-treated muscles. Each point represents the mean of four or five observations, with bars denoting s.e. (reproduced, with permission from J. Physiol. 297, 47-60 (1979)).

3. Significance:

Hyperthyroidism is sometimes associated with a tendency to develop attacks of hypokalemia. These attacks are preceded by a rise in serum insulin (IRI)(Shishiba et al. 1972). It is conceivable that the hypokalemia is related to an increased capacity for active Na^+-K^+-transport and enhanced response to the stimulating effect of insulin on the Na^+-K^+-pump in muscle.

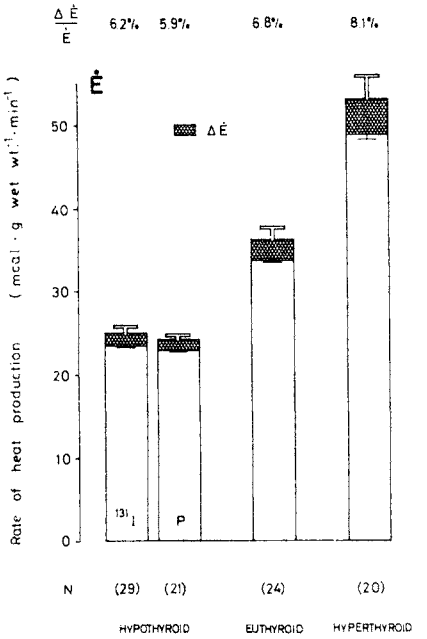

Fig. 2. Effects of thyroid status and ouabain on the steady state rate of heat production ($\dot{E}$) in intact mouse soleus.

$\dot{E}$ values of muscles obtained from hypothyroid (^{131}I-treated and perchlorate (P)-treated), euthyroid (control) and hyperthyroid (T_3-treated) mice are presented as columns with open bars above denoting s.e. The acute drop in $\dot{E}$ ($\Delta\dot{E}$) following exposure to ouabain ($10^{-3}M$) is indicated by the cross-hatched areas with thin bars below denoting s.e. The relative change in heat production ($\Delta\dot{E}/\dot{E}$) was less than 10% in all groups of (n) muscle pairs studied. All experiments were performed at 30° C, and the calorimeter chambers were perfused continuously with a bicarbonate-buffered Krebs-Ringer medium enriched with 10 mM-$MgCl_2$ replacing 15 mM-NaCl). The differences in $\dot{E}$ between hypothyroid, euthyroid and hyperthyroid groups are statistically significant ($P<0.0005$); so are the differences in absolute $\Delta\dot{E}$ values ($P<0.025$) (reproduced, with permission from J. Physiol. 297, 47-60 (1979).

It has been proposed that the changes in energy production associated with various thyroid states are for a major part due to changes in the rate of active Na^+-K^+-transport (for review, see Ismail-Beigi 1977). This idea was primarily based upon determinations of the ouabain-suppressible fraction of respiration in cut diaphragm preparations or tissue slices obtained from hypothyroid, euthyroid and hyperthyroid animals. However, in such preparations, the rate of active Na^+-K^+-transport is increased several fold, probably due to the excessive inward leak of Na^+ (see Fig. 1). Consequently, the ouabain-suppressible component of energy production is augmented far above the level which can be calculated and measured for intact tissue preparations. As shown in Fig. 2, the heat production in intact soleus muscles obtained from mice increase with the thyroid state. However, the ouabain-suppressible component is too small to account for the relatively large effects of the thyroid hormones. The acute exposure to either insulin or salbutamol in vitro leads to approximately the same increase in active Na^+-K^+-transport as pretreatment with thyroid hormones. In view of the modest rise in heat production induced by these agents, it is even more unlikely that the thermogenic effect of the thyroid hormones is the direct outcome of their effect on Na^+-K^+-pumping.

In summary, at least 3 different hormones are of physiological significance for the regulation of active Na^+-K^+-transport in skeletal muscle. This is essential for the Na^+-K^+-homeostasis of intra- and extracellular body compartments as well as the function of the motor apparatus. The metabolic consequences of this hormonal regulation seem to be of indirect nature and related to the Na^+-dependent control of the cytoplasmic Ca^{++} ion level, which in turn can determine glucose uptake as well as the rate of several steps in intermediary metabolism.

Table 3: Summary of hormone effects on soleus muscle.

	INSULIN	ADRENALINE	THYROID HORMONES
^{22}Na-EFFLUX	↑	↑↑	↑
^{22}Na-INFLUX	o	o	↑
^{42}K-INFLUX	↑	↑↑	↑
^{42}K-EFFLUX	o	o	↑
I.C. K/Na-RATIO	↑	↑↑	o
MEMBRANE POTENTIAL	↑	↑↑	o
^{3}H-OUABAIN BINDING	o	o	↑↑

REFERENCES:

Andres, R., Baltzan, M.A., Cader, G. and Zierler, K.L. (1962). Effect of insulin on carbohydrate metabolism and on potassium in the forearm of man. J. Clin. Invest. 41, 108-115.

Asano, Y. (1978). Increased cell membrane permeability to Na^+ and K^+ induced by thyroid hormone in rat skeletal muscle. Experientia Suppl. 32, 199-203.

Ashley, C.C., Ellory, J.C. and Hainaut, K. (1974). Calcium movements in single crustacean muscle fibres. J. Physiol. 242, 255-272.

Bihler, I., Sawh, P.C. and Sloan, I.G. (1978). Dual effect of adrenalin on sugar transport in rat diaphragm muscle. Biochim. Biophys. Acta 510, 349-360.

Biron, R., Burger, A., Chinet, A., Clausen, T. and Dubois-Ferrière, R. (1979). Thyroid hormones and the energetics in mammalian skeletal muscles. J. Physiol. 297, 47-60.

Bolte, H.-D. und Lüderitz, B. (1968). Einfluss von Insulin auf das Membranpotential bei alimentärem Kaliummangel. Pflügers Archiv 301, 254-258.

Bowman, W.C. (1980). Adrenergic activators and inhibitors. Handbook of exp. Pharmacology 54/ii, in press.

Brodal, B.P., Jebens, E., Öy, V. and Iversen, O.-J. (1974) Effect of insulin on (Na^+-K^+)-activated adenosine triphosphatase activity in rat muscle sarcolemma, Nature 249, 41-43.

Carlsson, E., Fellenius, E., Lundborg, P. and Svensson, L. (1978). β-adrenoceptor blockers, plasma-potassium, and exercise. The Lancet, August 19, 424-425.

Chinet, A., Clausen, T. and Girardier, L. (1977). Microcalorimetric determination of energy expenditure due to active sodium-potassium transport in the soleus muscle and brown adipose tissue of the rat. J. Physiol. 265, 43-61.

Chinet, A., Clausen, T. and Dubois-Ferrière, R. (1980). Secondary effects of stimulation and inhibition of active Na^+-K^+-transport on the heat production rate ($\dot{E}$) of mouse soleus muscle. Experientia, in press.

Clausen, T. (1975). Metabolic effects on muscular tissue. Handbook of Experimental Pharmacology XXXII/2.

Clausen, T. and Kohn, P.G. (1977). The effect of insulin on the transport of sodium and potassium in rat soleus muscle. J. Physiol. 265, 19-42.

Clausen, T. and Hansen, O. (1977). Active Na-K transport and the rate of ouabain binding. The effect of insulin and other stimuli on skeletal muscle and adipocytes. J. Physiol. 270, 415-430.

Clausen, T. and Flatman, J.A. (1977). The effect of catecholamines on Na-K transport and membrane potential in rat soleus muscle. J. Physiol. 270, 383-414.

Clausen, T., Wang, P., Ørskov, H. and Kristensen, O. (1980). Hyperkalemic periodic paralysis. Relationships between changes in plasma water, electrolytes, insulin and catecholamines during attacks. Scand. J. Clin. Lab. Invest. 40, 211-220.

Cox, M., Sterns, R.H. and Singer, I. (1978). The defense against hyperkalemia: The roles of insulin and aldosterone. N. Engl. J. Med. 299, 525-532.

Creese, R. (1968). Sodium fluxes in diaphragm muscle and the effects of insulin and serum proteins. J. Physiol. 197, 255-278.

Crompton, M., Moser, R., Lüdi, H. and Carafoli, E. (1978). The interrelations between the transport of sodium and calcium in mitochondria of various mammalian tissues. Eur. J. Biochem. 82, 25-31.

D'Silva, J.L. (1934). The action of adrenaline on serum potassium. J. Physiol. 82, 393-398.

Flatman, J.A. and Clausen, T. (1979). Combined effects of adrenaline and insulin on active electrogenic Na^+-K^+ transport in rat soleus muscle. Nature, 281, 580-581.

Gavryck, W.A., Moore, R.D. and Thompson, R.C. (1975). Effect of insulin upon membrane-bound (Na^+-K^+)-ATPase extracted from frog skeletal muscle. J. Physiol. 252, 43-58.

Hays, E.T., Dwyer, T.M., Horowicz, P. and Swift, J.G. (1974). Epinephrine action on sodium fluxes in frog striated muscle. Am. J. Physiol. 227, 1340-1347.

Holmberg, E. and Waldeck, B. (1980). On the possible role of K^+-ions in the action of terbutaline on skeletal muscle contractions. Acta Pharmacol. et toxicol. 46, 171-179.

Holmberg, E. and Waldeck, B. (1980). The effect of insulin on skeletal muscle contractions and its relation to the effect produced by beta-adrenoceptor stimulation. Acta Physiol. Scand., in press.

Ismail-Beigi, F. (1977). Thyroidal regulation of active sodium transport. Current Topics in Membranes and Transport, 9, 367-388.

Kamminga, C.E., Willebrands, A.F., Groen, J. and Blickman, J.R. (1950). Effect of insulin on the potassium and inorganic phosphate content of the medium in experiments with isolated rat diaphragms. Science 111, 30-31.

Kitasato, H., Sato, S., Murayama, K. and Nishio, K. (1980). The interaction between the effects of insulin and ouabain on the activity of Na transport system in frog skeletal muscle. Jap. J. Physiol. 30, 115-130.

Kohn, P.G. and Clausen, T. (1971). The relationship between the transport of glucose and cations across cell membranes in isolated tissues VI. Biochim. Biophys. Acta 225, 277-290.

Moore, R.D. and Rabovsky, J.L. (1979). Mechanism of insulin action on resting membrane potential of frog skeletal muscle. Am. J. Physiol. 236, 249-254.

Moore, R.D., Munford, J.W. and Popolizio, M. (1979). Effect of streptozotocin-induced diabetes upon intracellular sodium in rat skeletal muscle. FEBS LETTERS 106, 375-378.

Moore, R.D. (1973). Effect of insulin upon the sodium pump in frog skeletal muscle. J. Physiol. 232, 23-45.

Otsuka, M. and Ohtsuki, I. (1970). Mechanism of muscular paralysis by insulin with special reference to periodic paralysis. Am. J. Physiol. 219, 1178-1182.

Rosa, R.M., Silva, P., Young, J.B., Landsberg, L., Brown, R.S., Rowe, J.W. and Epstein, F.H. (1980). Adrenergic modulation of extrarenal potassium disposal. N. Engl. J. Med. 302,431-434.

Shishiba, Y., Shimizu, T., Saito, T. and Shizume, K. (1972). Elevated immunoreactive insulin concentration during spontaneous attacks in thyrotoxic periodic paralysis. Metabolism 21, 285-290.

Smith, T.J. and Edelman, I.S. (1979). The role of sodium transport in thyroid thermogenesis. Federation Proc. 38, 2150-2153.

Tashiro, N. (1973). Effects of isoprenaline on contractions of directly stimulated fast and slow skeletal muscles of the guinea-pig. Br. J. Pharmac. 48, 121-131.

Walaas, O. and Walaas, E. (1950). Effect of epinephrine on rat diaphragm. J. Biol. Chem. 187, 769-776.

Wang, P. and Clausen, T. (1976). Treatment of attacks in hyperkalæmic familial periodic paralysis by inhalation of salbutamol. THE LANCET, January 31, 221.

Zierler, K.L. (1957). Increase in resting membrane potential of skeletal muscle produced by insulin. Science 126, 1067-1068.

Zierler, K.L. (1972). Insulin, ions, and membrane potentials. Handbook of Physiology section 7: Endocrinology, Williams and Wilkins, Baltimore.

ACKNOWLEDGEMENT:

This investigation was supported by grants from Aarhus Universitets Forskningsfond and Statens Lægevidenskabelige Forskningsråd.

Adv. Physiol. Sci. Vol. 3. Physiology of Non-excitable Cells
J. Salánki (ed.)

THE REGULATION OF SUGAR TRANSPORT IN THE SQUID AXON AND GIANT BARNACLE MUSCLE FIBRE

A. Carruthers
Department of Physiology, University of London King's College, Strand, London WC2R 2LS, England

It has been recognised for more than thirty years that insulin accelerates hexose-transfer in mammalian muscle (Levine et al., 1949). A less well known observation is that metabolic poisons depress sugar transport in nerve (Diamond and Fishman, 1973). Although various studies have linked the control of membrane sugar permeability to alterations in intracellular ATP, cyclic nucleotide and ionised Ca levels, the mechanism of hexose-transfer regulation in nerve and muscle remains only poorly understood (Elbrink and Bihler, 1975; Czech, 1977). The possibility of a fundamentally different approach to solving the mechanism of sugar transport regulation is provided by the findings of experiments with the giant axon of the squid (Loligo forbesi) and giant muscle fibres of the barnacle (Balanus nubilis). As with hexose-transfer in mammalian nerve and muscle, sugar transport in the squid giant axon is depressed by cyanide (Carruthers, 1978) and transport in the giant barnacle muscle fibre is accelerated by insulin (Baker and Carruthers, 1980). The great advantage of working with these cells is their size. Using these giant cells it is not only possible to make measurements on a single cell but it is also possible to control the composition of the intracellular environment by internal dialysis (Brinley and Mullins, 1967).

The non-metabolised, but transported glucose analogue 3-O-methyl-glucose was used throughout. As with transport in mammalian nerve and muscle (Elbrink and Bihler, 1975), hexose-transfer in the squid axon and barnacle muscle fibre is mediated by a passive, selective, saturable, phloretin-sensitive, facilitated process.

Sugar uptake and exit in the dialysed squid axon are depressed when cytosolic ATP levels are lowered. As intracellular pCa and pH are clamped by use of buffers, these results suggest that ATP *per se* can modify hexose-transfer in the squid axon. This action of ATP is mimicked only by hydrolysable analogues of ATP; other naturally occurring nucleotides (ADP, AMP, cAMP, GTP) are without effect on transport. ATP_i seems to act by increasing the affinity of the transport system for sugar without altering the capacity (V_{max}) of the system. Changes in axoplasmic ionised Ca levels in the range 0.045-1.0 μM are also without effect on transport.

Insulin accelerates sugar transport in barnacle muscle by increasing the V_{max} of the transfer system (Baker and Carruthers, 1980). This increase in tissue sugar permeability appears to be preceeded by a fall in cytosolic cAMP and a rise in cGMP (see Figure 1).

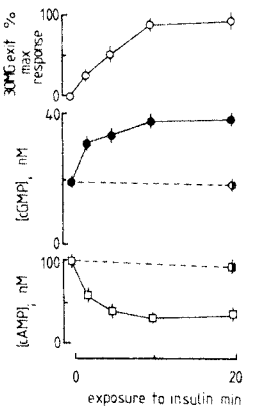

Figure 1 A-C The effects of insulin (5 $U.ml^{-1}$) on 3-O-methylglucose exit and tissue cyclic nucleotide levels in barnacle muscle.
A. Time-course of the stimulation of sugar exit in single muscle fibres on exposure to insulin. The fibres were bathed in sea water of composition (mM): NaCl, 442; KCl, 10; $MgCl_2$, 53; $CaCl_2$, 11; Tris, 10; pH, 7.6. Each point consists of 4 or more fibres. Mean fibre diameter, 1326 µm; temperature, 11^{o} C.
B. Time-course of the rise in cGMP levels caused by insulin. Each point consists of 6 or more seperate determinations. The concentration of cGMP following 20 min. incubation in insulin-free sea water is shown by the half-filled circle. Temperature, 12^{o} C.
C. Time-course of the fall in cAMP levels caused by insulin. Each point consists of 5 or 6 seperate determinations. cAMP levels corresponding to 20 min. incubation in insulin-free sea water are shown by the half-filled squares.
Cyclic nucleotide levels are expressed as $nMol.kg\ cell\ water^{-1}$.

These findings are not inconsistent with the view that insulin stimulates sugar transport by modifying cytosolic cAMP and cGMP levels.

Experiments with dialysed barnacle muscle fibres support this view. The results show that $cAMP_i$ inhibits sugar uptake half-maximally at a concentration of 1 µM and, provided the cytosolic ionised Ca level is greater than 0.1 µM, that $cGMP_i$ stimulates hexose-uptake. Calcium ions

appear to act by reducing the concentration of cGMP required to stimulate transport (see Figure 2).

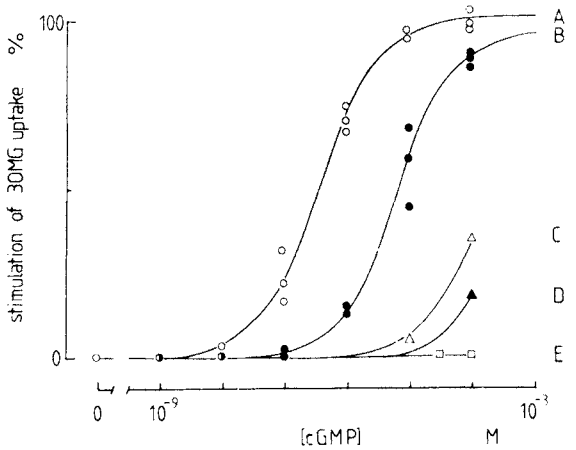

Figure 2 The effect of raised internal free Ca on the activation of 3-O-methylglucose uptake by cGMP in the dialysed muscle fibre. The data are pooled from 6 fibres. The fibres were dialysed with a solution of composition (mM): K aspartate, 150; NaCl, 32; $MgCl_2$, 10 (in excess of ATP); EGTA, 5; Hepes, 5; Pipes, 5; NaCN, 2; FCCP, 2 $\mu g.ml^{-1}$; phenol red, 2; pH, 7.0. Osmolality was adjusted to 975 mOsm with sucrose. ATP (2 mM) was added as Mg.ATP. The various ionised Ca levels were obtained by adding different amounts of $CaCl_2$ to the solution. The The different ionised Ca levels are 0.91, 0.5. 0.41, 0.27 and 0.11 μM for curves A-E respectively. Ordinate: % stimulation of sugar uptake from sea water containing 2 mM sugar. Abscissa: cGMP concentration in dialysis medium (M).

ATP must be present for both cAMP and cGMP to influence the rate of hexose-transfer although ATP-deplstion per se accelerates sugar uptake. These effects on hexose-transfer in barnacle muscle appear to be confined to changes in the capacity (V_{max}) of the transport system.

The results of experiments with the barnacle muscle fibre are consistent with the model outlined in Figure 3.

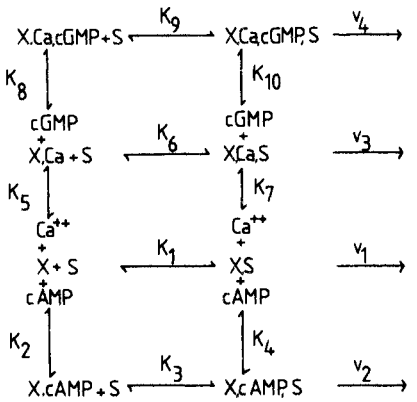

Figure 3 Model for the regulation of sugar transport in barnacle muscle. X represents carrier and S is sugar. K_1-K_{10} are dissociation constants and v_1-v_4 are rate constants proportional to the rate of transport across the membrane. The product of the reactions of carrier with intracellular control variable (Ca, cAMP, cGMP) e.g. X.cAMP, are shown only in schematic terms. ATP is present at saturating concentrations.

If $K_1 = K_3 = K_6 = K_9$ and $v_4 > v_1 = v_3 > v_2$, then cAMP will reduce the V_{max} for hexose transfer and calcium ions will increase the stimulation of transfer by cGMP (as shown in Figure 2).

REFERENCES

BAKER, P.F. & CARRUTHERS, A. (1980) Insulin stimulates sugar transport in the giant muscle fibres of the barnacle Balanus nubilis. Nature (in press).

BRINLEY, F.J.Jr. & MULLINS, L.J. (1967) Sodium extrusion by internally-dialysed squid axons. J. Gen. Physiol. 50 , 2303-2331.

CARRUTHERS, A. (1978) Glucose transport in squid axons. J. Physiol.(Lond) 281 , 19-20 P.

CZECH, M.P. (1977) Molecular basis of insulin action. Ann. Rev. Biochem. 46 , 359-384.

DIAMOND, I. & FISHMAN, R.A. (1973) High affinity transport and phosphorylation of 2-deoxy-D-glucose in synaptosomes. J. Neurochem. 20 , 1533-1542.

ELBRINK, J. & BIHLER, I. (1975) Membrane transport: its relation to cellular metabolic rates. Science 188 , 1177-1184.

LEVINE,R., GOLDSTEIN,M., KLEIN,S., & HUDDLESTUN, B. (1949) The action of insulin on the distribution of galactose in eviscerated, nephrectomised dogs. J. Biol. Chem. 179 , 985-986.

This work was supported by the MRC

Adv. Physiol. Sci. Vol. 3. Physiology of Non-excitable Cells
J. Salánki (ed.)

LIPOPROTEIN SYNTHESIS AND SECRETION BY RAT HEPATOCYTE CULTURES: STRUCTURAL-FUNCTIONAL INTERRELATIONSHIPS

Trudy Forte and Julia Bell-Quint
Donner Laboratory, University of California, Berkeley, CA 94720, USA

INTRODUCTION

In vitro studies with perfused rat livers [1,2] have shown that the liver is able to synthesize and secrete both nascent very low density lipoproteins (VLDL) and high density lipoprotein (HDL) particles. Studies on avian [3] and rat [4] liver parenchymal cells in monolayer culture have demonstrated that cultured hepatocytes secrete VLDL into the culture medium. We have recently shown that, in addition to VLDL, both low density lipoprotein (LDL) and HDL can be isolated from the culture medium of rat hepatocyte monolayers [5]. Moreover, we noted that the rate of lipoprotein secretion, particularly VLDL, show time-related changes. In the present report we correlate ultrastructural parameters of hepatocyte monolayer cultures with lipoprotein secretion as a function of time.

METHODS

Preparation of Monolayers: Parenchymal cells were isolated from the livers of male, WAG/rij rats by the method of Bissel et al. [6]. Isolated cells were first suspended in Leibovitz L-15 medium including 8.3 mM glucose, 32 mU/ml insulin, penicillin-streptomycin and 20% fetal calf serum. The latter was excluded after overnight attachment of cells to the petri dishes. Medium and cells were harvested separately and lipoproteins were isolated from the culture medium by means of preparative centrifugation techniques described by Lindgren [7]: VLDL were isolated at d < 1.006 g/ml, LDL at d 1.006-1.063 g/ml and HDL at d 1.063-1.21 g/ml.

Electron Microscopy: Isolated lipoproteins were visualized by negative staining techniques using 2% sodium phosphotungstate, pH 7.4. For ultrastructural studies on cells, hepatocyte cultures were fixed in situ with 2.5% glutaraldehyde in 0.15 M sodium cacodylate buffer, pH 7.4; postfixed in 1% osmium tetroxide in 0.15 M sodium cacodylate and en bloc stained with 2% uranyl acetate for 30 min. Cultures were subsequently embedded in Araldite.

RESULTS AND DISCUSSION

Rat hepatocyte cultures synthesize and secrete VLDL, LDL and HDL into the culture medium. As seen in Table 1, VLDL is the major lipoprotein isolated from the medium at early time points (up to 6.5 hr). With prolonged

incubation there is a notable decrease of VLDL so that after 48 hr VLDL concentration is reduced by 77%. Addition of sodium oleate to the medium resulted in the production of large quantities of VLDL (11.4 mg/g cell protein) during 48 hr incubation. Hence, fatty acids become rate limiting substrates for triglyceride (TG) synthesis during prolonged incubation in unsupplemented medium. At early incubations substantial quantities of LDL and HDL (Table 1) can also be isolated from the medium. Unlike VLDL, these lipoproteins do not show a loss of concentration during prolonged incubation. The HDL are 110 Å spherical particles similar to rat plasma HDL. The HDL fraction at short incubation periods consists of a single population of particles; these structures are approximately 296 Å diam and contain only apolipoprotein B. Their rapid appearance in the culture medium suggests that they are synthesized de novo. Prolonged incubation results in the appearance of larger structures (400-800 Å) in the LDL fraction; since TG also increases in this fraction with time, it suggests that degradation of VLDL has occurred thus producing an intermediate particle which is in the density range of LDL.

Table 1. Concentration of Lipoproteins Isolated from Rat Hepatocyte Culture Medium after 6.5 and 48 Hours of Incubation

	mg lipoprotein/g cell protein		
	VLDL	LDL	HDL
6.5 hours	4.6 ± 0.8	1.2 ± 0.1	1.6 ± 0.1
48.0 hours	1.1 ± 0.3	2.9 ± 0.5	3.8 ± 0.2

The ultrastructure of rat hepatocytes in monolayer culture is in many respects similar to that of the intact liver. After several hours in culture the cells form cord-like structures that assume the polarity normally seen in the liver. As in the intact liver, bile canaliculi with numerous short microvilli are present, Figure 1; Golgi complexes are found in close proximity to the bile canaliculus which is also their orientation in the liver. The lateral cell borders of adjacent hepatocytes are closely apposed and possess numerous interlocking filopdia; as seen in Figure 2, osmiophilic particles are frequently trapped within the intercellular space. These particles have a mean diam of 609 Å and are presumed to be VLDL. Their presence suggests that during short incubation periods the rate of VLDL secretion into the medium is underestimated.

The Golgi complex appears to undergo changes dependent on the metabolic state of the cells. At early incubation times the Golgi complex contains cisternae and smooth surfaced vesicles which enclose numerous VLDL particles 491 Å diam, range 300-883 Å, (Table 2 and Fig. 3). After 24 and 48 hr incubation periods only negligible amounts of VLDL are recovered in the medium; this is paralleled by a decrease in the number and size of particles found within the Golgi (Fig. 4). The small size, 306 Å of Golgi particles after prolonged incubation suggests that they are LDL (Table 2). This suggestion is strengthened by the fact that substantial quantities of LDL are isolated from the medium even after 48 hr. The presence of LDL within the Golgi and culture medium is evidence that the liver is able to synthesize and secrete LDL directly.

Table 2. Comparison of Electron Microscopic Size (Diam in Å ± S.D.) of Intracellular and Extracellular Lipoproteins

	6.5 hr	48 hr
Golgi Saccules	491 ± 111	309 ± 39
Intercellular Space	609 ± 165	N.D.*
Culture Medium VLDL	797 ± 219	N.D.
Culture Medium LDL	296 ± 29	248 ± 38**

* N.D. Not detectable.
**Approximately 20% of the total particles consist of structures, 631 ± 203 Å diameter.

As indicated earlier, at least part of the loss of VLDL from the medium after prolonged incubations can be explained by degradation of VLDL. VLDL disappearance may also be accounted for by receptor mediated uptake of particles into the cell; in fact, high affinity VLDL binding sites on hepatocytes have been described by Lakshmanan et al. [8]. Our ultrastructural

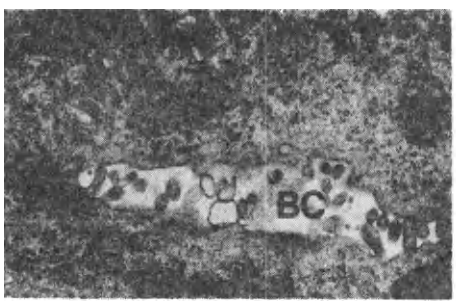

Fig. 1. Electron micrograph of a 6.5 hr hepatocyte culture. Bile canaliculus (BC) has been reformed. The Golgi (Go) is near the BC. Bar = 1μm.

Fig. 2. Intercellular (IC) region between two hepatocytes reveals the presence of numerous filopodia and trapped VLDL (arrows). A vesicle (V) transporting VLDL to the cell surface is also evident. Bar = 1 μm.

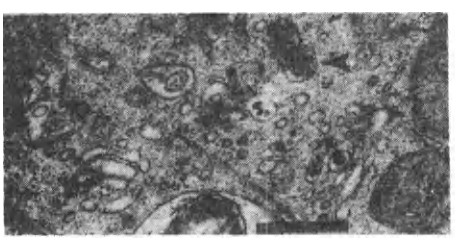

Fig. 3. Golgi region from a 6.5 hr culture. VLDL within Golgi saccules and vesicles are indicated by arrows. Bar = 0.5 μm.

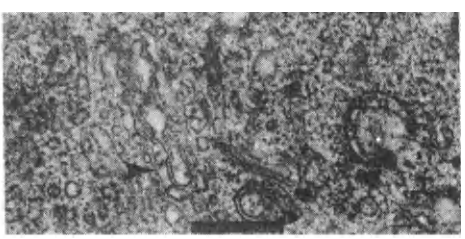

Fig. 4. Golgi region from a 48 hr culture. VLDL (arrow) are few in number and smaller than those of 6.5 hr incubation. Bar = 0.5 μm.

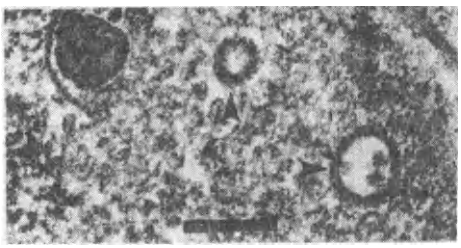

Fig. 5. Coated vesicles (arrows) within the cytoplasm of a cultured hepatocyte. VLDL particles are seen within one of the coated vesicles. Bar = 0.25 μm.

studies revealed the presence of VLDL containing coated vesicles (Fig. 5) in the apical portion of the hepatocytes. Similar coated pits have been associated with receptor mediated uptake of LDL by peripheral cells [9] thus it is likely that VLDL uptake and subsequent degradation steps are similar to those previously described for the LDL pathway.

ACKNOWLEDGEMENTS

This work was supported by NIH grant HL 18574 and by the Division of Biomedical and Environmental Research of the U.S. Department of Energy.

REFERENCES

1. Marsh, J.B. 1974. Lipoproteins of the Nonrecirculating Perfusate of Rat Liver. J. Lipid Res. 15: 544-550.
2. Hamilton, R.L., M.C. Williams, C.J. Fielding and R.J. Havel. 1976. Discoidal Bilayer Structure of Nascent High Density Lipoproteins from Perfused Rat Liver. J. Clin. Invest. 58: 667-680.
3. Tarlow, D.M., P.A. Watkins, R.E. Reed, R.S. Miller, E.E. Zwergel and M.D. Lane. 1977. Lipogenesis and the Synthesis and Secretion of Very Low Density Lipoprotein by Avian Liver Cells in Nonproliferating Monolayer Culture. J. Cell Biol. 73: 332-353.
4. Davis, R.A., S.C. Engelhorn, S.H. Pangburn, D.B. Weinstein and D. Steinberg. 1979. Very Low Density Lipoprotein Synthesis and Secretion by Cultured Rat Hepatocytes. J. Biol. Chem. 254: 2010-2016.
5. Bell-Quint, J. and T. Forte. 1979. Synthesis and Secretion of Lipoproteins by Cultured Rat Hepatocytes. J. Cell Biol. 83: 99a.
6. Bissel, D.M., L.E. Hammaker and U.A. Meyer. 1973. Parenchymal Cells from Adult Rat Liver in Nonproliferating Monolayer Culture. J. Cell Biol. 59: 722-734.
7. Lindgren, F.T. 1974. Serum Lipoproteins: Isolation and Analysis with the Preparative and Analytical Ultracentrifuge. In, Fundamentals of Lipid Chemistry (Burton, R.M. and Guerra, F.C., eds), Bi-Science Publications, Webster Grove, 475-510.
8. Lakshmanan, M.R., R.A. Muesing, G.A. Cook and R.L. Veech. 1977. Regulation of Lipogenesis of Isolated Hepatocytes by Triglyceride-rich Lipoproteins. J. Biol. Chem. 252:6581-6584.
9. Goldstein, J.L. and M.S. Brown. 1977. The Low-Density Lipoprotein Pathway and Its Relation to Atherosclerosis. Ann. Rev. Biochem. 46: 897-930.

Adv. Physiol. Sci. Vol. 3. Physiology of Non-excitable Cells
J. Salánki (ed.)

RELATIONSHIP BETWEEN MEMBRANE TRANSPORT AND METABOLISM CONCLUDING REMARKS

Arnost Kleinzeller
Department of Physiology, University of Pennsylvania, Philadelphia, PA 19104, USA

Our symposium summarized extensive evidence demonstrating various ways by which membrane transport and cellular metabolism are interrelated. The presented data clearly establish that no one single mechanism is involved: often, a cascade of events triggered by a defined experimental condition has to be postulated. However, several basic patterns are discernible and their recognition permitted to highlight pertinent problems by the invited speakers.

Three basic ionic pumps, i.e. the /Na^+-K^+/-activated ATPase, the proton pump and the Ca^{2+} pump appear to be operative in practically all eukaryotic and prokaryotic cells. These pumps are responsible for intracellular homoeostasis, and the electrochemical ionic gradients established across the cell membrane and membranes of intracellular organelles represent a direct link to cell metabolism as well as the driving force for cell function. The rapidly advancing knowledge of the molecular properties of these enzymes also enhances our understanding how the function of these membrane-bound enzymes may be regulated.

The application of nonequilibrium thermodynamics to active transport processes reveals some of the energetic aspects of coupling between transport and metabolism. We have seen that this coupling is not necessarily tight. This implies that the coupling mechanism/s/ may be a target of regulatory agents. Nonequilibrium thermodynamics has now become an important tool for the student of our field.

The interrelationship between transport processes and cell metabolism occurs at various levels of cell function. This was clearly demonstrated by evidence that the passive fluxes of cations across the membrane may be controlled by metabolism, thus directly affecting the physiology of the cell.

One of the most intriguing, yet complex, fields of interest concerns the action of hormones. Several pertinent examples were presented here indicating that hormonal agents may affect metabolism by 1. interfering directly or indirectly with the transport of electrolytes /including changes of intracellular ionic environment/, but also by 2. affecting cellular levels of cAMP and/or cGMP, or 3. possibly by a feedback mechanism changing the physical properties of the membrane, thus limiting the supply of metabolic substrates.

The membrane is in effect a cellular organelle with a rapid turnover of its constituents, permitting formation and repression of transport sites. The genetic approach, applied to study transport processes in mammalian cells grown in vitro, now emerges as a new, powerful tool for pinpointing individual transport pathways and thus simplifying our experimental attack on problems relating transport to metabolism.

At present our studies are only beginning to pass the phenomenological barrier. In order to define the relationship between membrane transport and metabolism in molecular terms, a more detailed understanding of the various facets of the processes is required. The tools of physiologists, geneticists and biophysicists, combined with a better insight into cell structure, will help to clarify the points of attack which eventually will have to be expressed in molecular biochemical terms. As so often in science, advances in a field are predicated by an integration of different concepts and experimental approaches.

Adv. Physiol. Sci. Vol. 3. Physiology of Non-excitable Cells
J. Salánki (ed.)

MACROMOLECULES MEDIATING CELL-CELL RECOGNITION

Max M. Burger, Gradimir N. Misevic, J. Jumblatt and Françoise J. Mir-Lechaire

Department of Biochemistry, Biocenter of the University of Basel, Klingelbergstrasse 70, CH 4056 Basel, Switzerland

Cell communication is a more general phenomenon than recognition. The latter can be a prerequisit for communication or it can also sometimes be the result of communication for instance. Recognition occurs in moving cells. Communication occurs both in moving as well as in immobilized cells in stable tissue organizations.

In some very specialized adult tissues single cells are moving around until they have found their target where highly differentiated surface structures are thought to mediate recognition. But even in the best known cases, namely the cytotoxic lymphocyte and its target as well as the sperm and its egg target, we know very little about the exact recognition structures, the recognition processes in molecular terms or the consequences, i.e. target cell lysis or the cortical egg reaction.

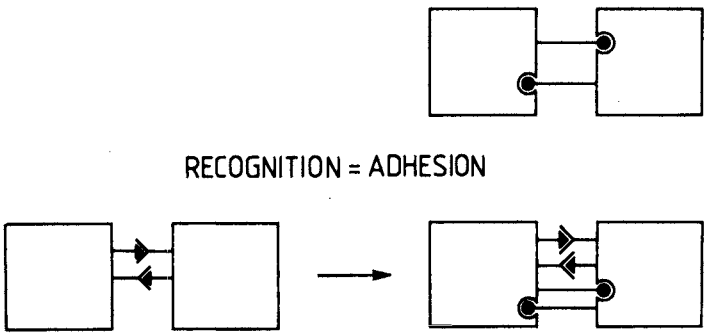

FIG. 1 - Two Models for Specific Cell-Cell Adhesion. In the first recognition molecules mediate adhesion directly. In the second recognition macromolecules induce secondary adhesion.

Intercellular recognition must be a key process in embryonic organ morphogenesis unless the entire blueprint is laid down in the extracellular matrix, a concept that would be quite difficult to sustain. Organ and tissue morphogenesis can be subdivided into 3 basic processes: movement of single cells or a tissue section from location A to B, recognition of B as the terminal location and thirdly fixation of that configuration

of the particular group of cells. Recognition occurs most likely already on the way from A to B because most of these movements do not produce the impression as they were random but generally a continous probing between the moving and the adjacent cells can be seen. This observation casts some doubts on purely chemotactic mechanisms which would be based on a gradient of molecules dispersed between the cells.

Several types of macromolecules have been isolated which promote either organ specific adhesion among dissociated embryonal cells or the sorting out of cells into structures simulating those occuring in vivo. It is one of the key questions in the field whether these macromolecular factors achieve their effect directly by mediating recognition and adhesion in one step or indirectly by the induction of secondary adhesions (Fig. 1).

While no definite answer is yet available for embryogenesis we would like to address this question to species-specific sponge cell recognition and aggregation which has already served much earlier as a model system for embryonic cell recognition.

SPONGE CELL RECOGNITION: A MODEL READY FOR AN ANALYSIS AT THE MOLECULAR LEVEL.

General Background: In many combinations where two batches of dissociated cells from two different sponge species are shaken together species specific sorting out into clumps of the original species can be observed. To what degree this occurs immediately and to what degree it occurs in a two step process where cells first adhere randomly and then only sort out into homospecific tissue clumps depends on the two species of sponges used but in some combinations the correct pairs seem to be formed quite early during reassociation processes.

The selective reaggregation of cells can be promoted with a surface component termed aggregation factor (AF) and isolated from the supernatant of sponge cells dissociated and washed in Ca^{++}- and Mg^{++}-free seawater. Such a factor requires Ca^{++} again in order to promote aggregation and it has been isolated only from a few species so far (1, 2, 3). The one from Microciona prolifera is a 2.1×10^7 dalton protein-polysaccharide complex with several thousand Ca^{++} binding sites. Spread for electronmicroscopy it appears as a ring of $\sim$ 800 Å diameter with 15-16 arms of 1'100 Å length (4, 5).

Isolation of an Active Subunit of the Factor which still Binds the Species Specific Receptor: Previous studies have shown Microciona aggregation factor to be irreversibly inactivated by EDTA, heat treatment, periodate and proteases (2, 4, 5), the first two without necessarily degrading the factor into smaller sized pieces. After labelling the factor complex with ^{125}I we found unexpectedly that pieces could be dissected out from the protoglycan complex with a heat, EDTA and 5 M urea treatment simultaneously. These labeled fragments still bound species specifically to their surface receptors (Figs. 2, 3). The fragments accumulating in the peak in Fig. 2 are in a size class of around 180 K dalton, an accurate measurement after polyacrylamide - SDS - electrophoresis being impossible due to the large carbohydrate content (over 50%). Preliminary further degradation with V-8 enzyme yielded binding fragments down to 10 K dalton and below.

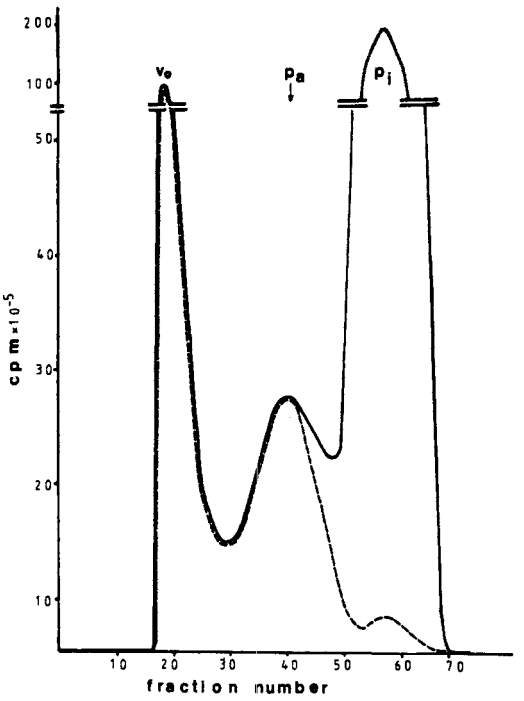

FIG. 2 - Dissociation of the Proteoglycan Aggregation Factor with Urea-EDTA-Heat and Separation on Sepharose 4 B. The supernatant of Microciona cells treated for 5 hours with Ca^{++}-, Mg^{++}-free seawater was spun at 1000 xg for 7 min, 3000 xg for 5 min, 20'000 xg for 20 min and precipitated with 30 mM $Ca\,Cl_2$ overnight. The pellet after 10'000 xg for 20 min was dissolved in Ca^{++}-CMF-Tris and repelleted for 3 hours at 100'000 xg. The pellet was dissolved in Ca-CMF-Tris and the excluded front of a 3000 Å glass bead column repelleted for 3 hours at 100'000 xg and dissolved in Ca-CMF-Tris. In a sucrose gradient of 10-30% the activity peak appeared after 3 hours at 39'000 rpm in the SV-41 rotor at 20%. The material was passed over a glass bead column in Ca-CMF-Tris and labeled with ^{125}I-chloramine-T at this stage or before the sucrose gradient. After treatment by the addition of 5 M urea and 40 mM EDTA to this Ca^{++} (2 mM)-CMF-Tris (20 mM, pH 7.4) buffer at 80° C for 4 hours the fragments were separated on a 28 x 1.6 cm Sepharose 4 B column in CMF or CMF-1.0 M urea. The column was loaded with 7.42 µg protein or 10.6 units and 34.1 X 10^6 cpm in 4 ml. The 1 ml fractions were counted before (——) and after dialysis (- - - -).

The Baseplate or Receptor Counterpart for the factor and a Possible Role for Calcium: After removing of the aggregation factor an inhibitor of aggregation can be isolated by a hypotonic shock (Fig. 4) which we called baseplate since its receptor functions are not yet clearly defined (6). Its surface location could recently be confirmed with immunofluorescent procedures (7). Although affinity chromatography methods in combination with neutral detergents yielded a highly purified inhibitor (over 1000 folds) as well, the exact nature of the two inhibitors and their identities are not yet resolved. Most likely it is a glycoprotein of about 40-60 K dalton.

One of the most basic questions was whether specificity for recognition is solely provided by interactions among the aggregation factor complexes or whether some specifity derives from an interaction between the factor and cell surface molecules. In order to investigate this question the two processes have to be assayed separately. It turned out that conditions for factor-surface binding did not require Ca^{++} while factor-factor binding did require just about that concentration known to be necessary for aggregation of the cells which incidently coincides also with

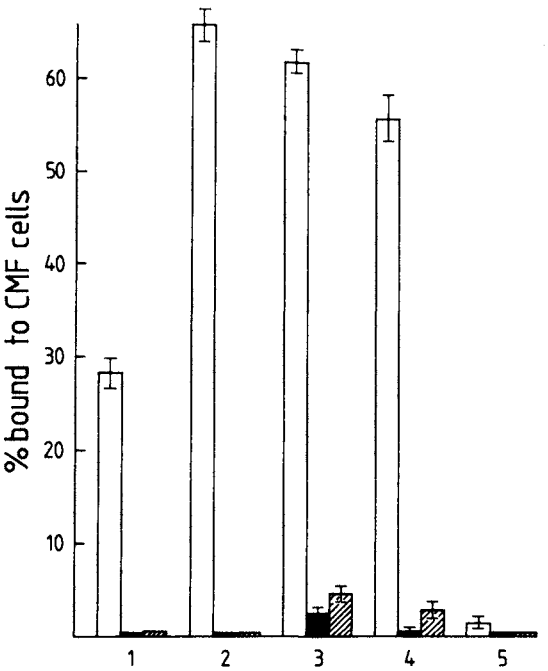

FIG. 3 - Maintenance of Species Specificity by the Urea-EDTA-Heat-Fragment.
In a binding experiment 0.70 μg protein were added to 4 x 10^6 cells (fixed or unfixed) in 0.4 ml for 20 min at R.T. To separate cells gently the sample was spun through 10% sucrose, 0.1% BSA for 5 min at 2000 xg and the total radioactivity was compared with that in the pellet and expressed in %.
First bar = Microciona, Second (black) bar = Mycale, Third (hatched) bar = Cliona. Sample numbers: 1 = undegraded Microcionafactor, 2 = Urea-EDTA-Heat treated factor before chromatography, 3 = Peak Vo, 4 = Peak Pa, 5 = Peak Pi (see Fig. 2).

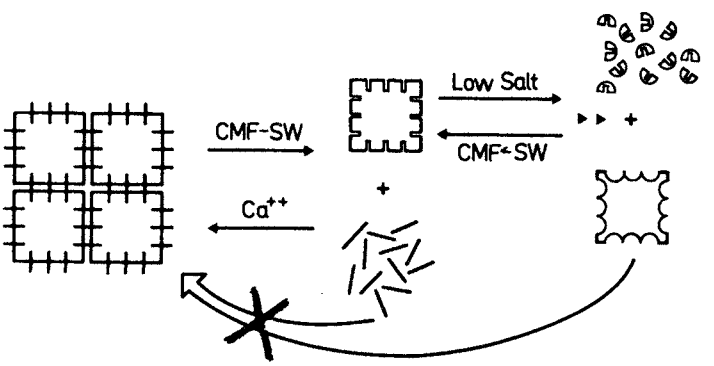

FIG. 4 - Isolation of Factor and Baseplate.
Ca^{++}-, Mg^{++}-free seawater (CMF-SW) releases the factor. Low salt releases the baseplate. Hypotonically treated cells do not aggregate with factor. If they are pretreated with baseplate they do however aggregate again. Baseplate inhibits factor-promotion of aggregation.

the Ca^{++} content of seawater (10 mM). Saturation of the surface sites in the absence of Ca^{++} occured at about 400 factor "molecules" per cell which turned out to be also just about the minimum amount of molecules bound, necessary for aggregation of the cells in the presence of Ca^{++} (8). Factor-cell binding in the absence of Ca^{++} retained the full species specificity (8). Factor-factor binding assayed with beads to which factor was previously covalently bound had essentially the same stability characteristics

as factor induced cell-cell aggregation (Table 1) which convincingly supports our older model that the force generating sites are Ca^{++}-mediated and are located inbetween factor molecules. At least a substantial part of the specificity is provided by interactions between the aggregation factor and the baseplate or other surface elements.

TABLE 1 - Factor-Cell Binding Sites Differ from Factor-Factor Binding Sites.

	Pretreatment of Microciona	Capability to aggregate cells or AF-beads	^{125}I-factor bound (cpm)
Microciona cells	none	++++	20'481
"	50°C, 10 min	+	18'024
"	10 mM EDTA, 30 min	+	31'473
"	5 mM periodate, 3 h.	-	15'358
"	baseplate 2.2 mg/ml	+	5'650
Cliona cells	none	-	2'162
"	10 mM EDTA, 30 min	-	1'642
AF-beads	none	++++	25'919
"	50°C, 10 min	+	8'381
"	10 mM EDTA, 30 min	+	9'014
"	5 mM periodate, 3 h.	+	5'501
"	baseplate, 2.2 mg/ml	+	5'965
BSA-beads	none	-	2'537

For experimental details see ref. 8. Any denaturing treatment that abolishes aggregating activities of the factor (AF) abolishes simultaneously factor-factor interaction as seen by binding of ^{125}I-AF to AF-conjugated beads. These treatments in particular the removing of Ca^{++} by EDTA did not abolish the species specific binding of factor to cells. Baseplate, the presumed receptor however prevents aggregation and binding. The inhibition of AF binding to AF-beads may steric explanations.

EFFICIENT AND FINAL SORTING OUT OF CELLS MAY REQUIRE AT LEAST A SECOND STEP.

We are not the only ones who have pointed out earlier that organ and tissue morphogenesis will most likely not solely depend on surface molecules which mediate recognition and adhesion in one step (9). It is true that glutaraldehyde fixed sponge cells can bind aggregation factor species specifically and can aggregate to some degree species specifically and that in this biochemical model system the two components baseplate and aggregation factor may be sufficient. Sponge cells which were not dissociated in Ca^{++}-, Mg^{++}-free seawater but were isolated still having their factor attached do clearly sort out however and our simple bimolecular model will require an additional process or component to explain that. One can assume that an easy dissociable dimer of the baseplate molecule mediates additional linkages between the factor molecules on the cell surface. Carbohydrate or fixed charge interactions providing weak specificities between subcomponents of the factor complexes are possible and are considered (Burkart and Burger, in preparation). However secondary surface contacts, still between factor complexes and baseplate molecules, now however on adjoing cells or between entirely different molecules may both increase the specificity as well as the tightness of the contact. We have

considered such a two step model earlier (see Fig 5) and would like to present two circumstantial experiments supporting it.

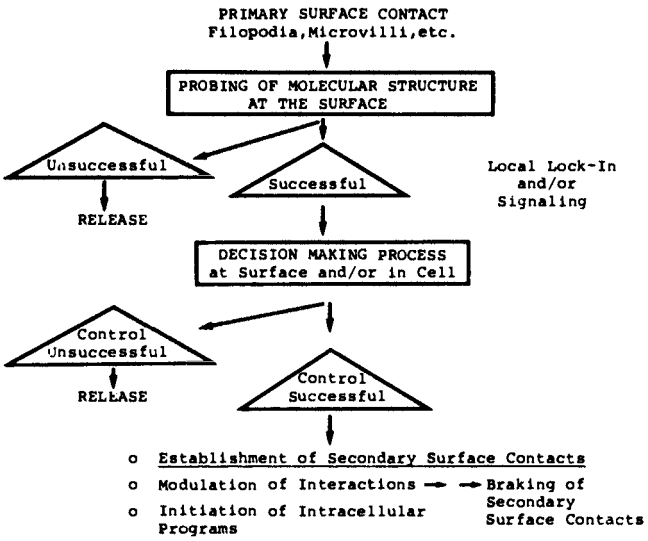

FIG. 5 - A Subdivision of the First Recognition Process During Cell Encounter. For more details see the Dahlem conference of ref. 10.

Freshly aggregated sponge cells can be redissociated only for a short time after initiation of the aggregation process. Then they suddenly enter a state in which disaggregation becomes much harder if not impossible. This sharp "transition state" depends on temperature (Fig. 6) as expected if a cellular event is involved. A more detailed temperature and time kinetic analysis may give some clues as to the nature of this secondary type of cell-cell interaction.

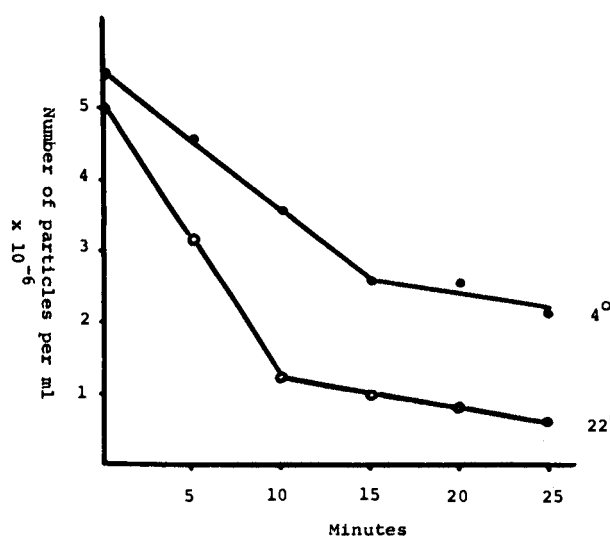

FIG. 6 - Two Step Aggregation. 1.2×10^7 dissociated Microciona cells per 0.6 ml were aggregated under standard conditions at R.T. for 10 min in a Linbro plate. Then the plate was tipped at an angle of 45° for the times indicated on the abscissa to allow collection of the cells at the bottom rim of the well for packing since they were not shaken. Then the supernatant was sucked off and replaced by Ca^{++}-, Mg^{++}-free seawater and the plate vigorously shaken

for 5 min. to dissociate the aggregates, which were monitored by counting the number of particles.

Molecular surface contacts may be a prerequisite for cellular communications and cellular communications may again be a prerequisite for more intimate and specific further secondary contacts. Evidence that the recognition and adhesion mediating sponge aggregation factor is a necessary prerequisite for communication comes from an earlier experiment carried out by Loewenstein (11).

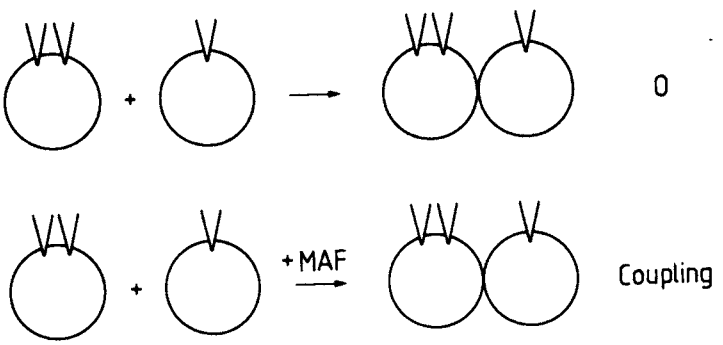

FIG. 7 - Aggregation Factor is a Prerequisite for Communication. Cells that have been mechanically dissociated and still retain their factor at the surface will develop a lower membrane resistance between them than towards the remainder of their surroundings, i.e. they couple (not shown). Cells which are stripped of their surface factor will not couple even if they are in closest appostion (upper line). If aggregation factor is added to the right species such cells will couple no later than 30 to 40 min. later. See Loewenstein ref. 11.

A further careful and detailed analysis of the surface macromolecules involved in primary contacts is as necessary as an analysis of those macromolecules involved in secondary contacts like for instance the so called gap junction subunits. Only after completion of such a study one can begin with more serious speculations on the processes that lead from the cellular probing observed during organ morphogenesis via recognition to fixation and maintenance of the correct tissue architecture.

We would like to acknowledge the collaboration and discussion with Drs. W. Burkart, W.J. Kuhns and T. Simpson. Supported by grant 3.513/79 from the Swiss National Science Foundation.

REFERENCES

(1) Humphreys, T. (1963). Chemical and *in vitro* reconstruction of sponge cell adhesion. I. Isolation and fuctional demonstration of the components involved. *Devel.Biol.* 8, 27-47.

(2) Moscona, A.A. (1968). Cell aggregation: Properties of specific cell ligands and their role in the formation of multicellular systems. *Devel. Biol.* 18, 250-277.

(3) Müller, W.E.G. and Zahn, R.K. (1973). Purification and characterization of a species-specific aggregation factor in sponges. *Exp. Cell Res.* 80, 95-104.

(4) Henkart, P.S., Humphreys, S. and Humphreys, T. (1973). Characterization of sponge aggregation factor: A unique proteoglycan complex. Biochemistry 12, 3045-3050.

(5) Humphreys, S., Humphreys, T. and Sano, J. (1977). Organization and Polysaccharides of sponge and aggregation factor. J. Supramol. Structure 7, 339-351.

(6) Weinbaum, G. and Burger, M.M. (1973). A two-component system for surface guided reassociation of animal cells. Nature, London 244, 510-512.

(7) Kuhns, W.J., Bramson, S., Simpson, T.L., Burkart, W., Jumblatt, J. and Burger, M.M. (1980). Fluorescent antibody localization of Microciona prolifera aggregation factor and its baseplate component. J. Embr. Morph., in print.

(8) Jumblatt, J., Schlup, V. and Burger M.M. (1980). Cell-cell recognition: Specific binding of Microciona sponge aggregation factor to homotypic cells and the role of calcium ions. Biochemistry 19, 1038-1042.

(9) Burger, M.M. (1977). Mechanisms of cell-cell recognition. Some comparison between lower organisms and vertebrates. In: Cell Interactions in Differentiation. Karkinen-Jääskeläinen,M., Saxén, L. and Weiss, L. (eds). Academic Press London, pp. 357-376.

(10) Burger, M.M. (1979). Early events of encounter at the cell surface. In: The Role of Intercellular Signals: Navigation, Encounter, Outcome. Nicholls, J.G. (ed.). Dahlem Konferenzen, Berlin, pp. 119-134.

(11) Loewenstein, W.R. (1967). On the genesis of cellular communication. Devel. Biol. 15, 503-520.

Adv. Physiol. Sci. Vol. 3. Physiology of Non-excitable Cells
J. Salánki (ed.)

CELL-TO-CELL COMMUNICATION VIA JUNCTIONAL MEMBRANE CHANNELS

Birgit Rose
Department of Physiology and Biophysics, University of Miami, School of Medicine, Miami, FL, USA

Adjoining cells of most tissues are interconnected by highly permeable membrane junctions providing direct pathways for the intercellular exchange of ions and molecules. The conduits for this direct cell-to-cell communication are aqueous channels contained in the cell junction — channels which span the width of both membranes of the adjacent cells, thereby in effect putting the neighbouring cells' cytoplasms in immediate communication with one another (Loewenstein, 1966). It is via these channels that currents spread rapidly and with little loss from cell to cell, a feature important for certain electrically excitable tissues such as heart, smooth muscle or electrotonically coupled nerve cells. But apart from the small inorganic ions also a wide range of larger molecules traverses these channels, making possible the intercellular transfer of a variety of physiologically important molecules. The permeability properties of cell-to-cell channels thus represent an important aspect of the general physiology of tissues or, for that matter, of any cell organization which functions by the concerted action of its cellular constituents.

CHANNEL SIZE or MOLECULAR SIZE LIMIT FOR CHANNEL PERMEATION

The actual or effective channel size is of great interest because it determines the molecular size limit to junction permeation. We probed channel permeability with several sets of fluorescent-labelled molecules which met the following requirements for useful channel permeability probes: water solubility, nontoxicity, impermeance of nonjunctional membrane, and conservation of integrity in cytoplasm (Simpson, Rose and Loewenstein, 1977). As a cell model system we used the insect salivary gland of Chironomus whose transparent and large (100-150 μm), polytaenic cells are particularly suitable for fluorescence and microinjection studies. For junction permeability tests, the tracers were injected into a cell and the cell-to-cell spread of fluorescence (or lack thereof) was noted. One set of tracers consisted of amino acids and linear peptides, labelled with dansyl chloride (DANS), fluorescein isothiocyanate (FITC), or Lissamine rhodamine B (LRB), and ranging from m.w. 380 to 4158. With these probes we found a molecular weight cutoff for junction permeation at about 2000. From measurements of spacefilling models of the largest permeating probes we inferred a lower-limit channel bore of 1.6 nm for accomodation of these molecules. Junctional transfer of the larger ($\gtrsim$2000 m.w.) nonpermeant peptides we tested presumably was blocked because these peptides can assume tertiary configurations stabilized by multiple intramolecular hydrogen bonding, producing

molecular shapes exceeding 1.6 nm in more than one dimension. This interpretation for the failure of these molecules' junction permeation is strengthened by the finding that certain peptides which, due to their amino acid compostion are unable to fold or to form helices, are junction permeant even at a m.w. of 3089-LRB(ProProGly)$_{10}$OH — the longest one of this kind that we tested. With all the larger peptides, a smaller one with different fluorescent label (and thus distinguishable) was coinjected into the same cell. Junctional transfer of the smaller tracer then indicated that the block to the larger molecule was not simply caused by channel closure due to cell injury.

Another set of channel probes consisted of linear and branched oligosaccharides. The unbranched oligosaccharides were all junction permeant, as would be expexted since their spacefilling models exceed 1.6 nm in only one dimension. Most revealing in terms of the actual dimension of the channel bore were the results obtained with 2 branched oligosaccharides (Schwarz mann, Wiegandt, Rose, Zimmerman & Loewenstein, unpublished data). One of the oligosaccharides, of m.w. 2975 (when labelled with FITC) or 3097 (when labelled with LRB) was junction impermeant. The other oligosaccharide, of m.w. 2327 (FITC), obtained by removing enzymatically the four terminal galactoses from the first oligosaccharide, on the other hand was junction permeant. The 2 largest dimensions are 3.0 nm and 4.5 nm for the larger and 2.1 and $\approx$4.0 nm for the smaller molecule, putting the channel bore at $\geqslant$2.1 nm, but certainly smaller than 3.0 nm. These oligosaccharide molecules are uncharged, both before and after enzyme treatment, and hence tell us the actual steric channel dimension.

In mammalian tissue culture cells the channels were found to be more restrictive with a cutoff to junctional permeation at $\approx$m.w. 800. These more restrictive channels also discriminate clearly against negative charges of the permeants, suggesting the presence of a fixed or an induced charge in these channels (Flagg-Newton, Simpson & Loewenstein, 1979).

REGULATION OF JUNCTIONAL CHANNEL PERMEABILITY

Loewenstein (1966) proposed that the cytoplasmic free Ca^{2+} concentration (Ca^{2+}_i) is a regulator of junctional permeability because various experimental conditions in which an increase in Ca^{2+}_i could have been expected, led to junctional uncoupling, that is to say to junctional channel closure. Using the Ca^{2+}-specific light-emitting protein aequorin as an indicator for Ca^{2+}_i, we showed that junctional coupling indeed decreased whenever Ca^{2+}_i rose at the junctional region (Rose and Loewenstein, 1976). In these experiments the spatial distribution of Ca^{2+}_i elevation was visualized with a TV camera-image intensifier system, and cell-to-cell coupling was measured electrically. Ca^{2+} injections, exposure to metabolic inhibitors or to Ca-ionophores all uncoupled cells when Ca^{2+}_i was seen to rise at the junction, supporting the hypothesis that Ca^{2+}_i mediates junctional uncoupling.

In several biological systems Ca and H ions hold close interrelationships. E.g. in energized mitochondria Ca-uptake releases H^+ (Bartley & Amoore, 1958) and vice versa (Åkerman, 1978), and Ca^{2+} and H^+ compete for binding sites on cell membrane (Carvalho, Sanui & Pace, 1963). Thus the question naturally arose whether H^+ can deputize Ca^{2+} in closing the channels or perhaps even mediate the Ca^{2+} action. The last point needed to be considered in particular when Meech and Thomas (1977) showed a decrease in intracellular pH (pH_i) during Ca-injection into snail neuron, and when Turin and Warner (1977) found that lowering pH_i of embryonic cells induced uncoupling.

In experimental terms the question is which of the two ions is suffici-

cient to uncouple cells. To in estigate this point, we monitored both Ca^{2+}_i and pH_i of Chironomus cells while experimentally inducing their uncoupling (Rose and Rick, 1978). We found that a pH_i decrease is not necessary for uncoupling; a Ca^{2+}_i elevation is sufficient: (1) Elevation of Ca^{2+}_i by treatment with cyanide produced uncoupling without significant change in pH_i. (2) Dinitrophenol did produce a significant fall in pH_i (0.4 pH units) but neither the onset of uncoupling nor of recoupling (DNP washout) correlated with the pH_i changes; in fact, a subsequent greater pH_i fall of the same cells (by exposure to 10% CO_2) did not affect coupling at all. (3) Injection of pH-buffered Ca-solution produced uncoupling just the same. (4) Uncoupling occurred even at alkaline pH_i ($\gtrsim$8.0), which also elevated Ca^{2+}_i e.g. when cells were exposed to NH_4Cl or, in one case, to ionophore A23187.

Whether a H^+ increase alone is sufficient to close junctional channels is not clear. Cell acidification caused uncoupling but also caused increase in Ca^{2+}_i; Injection of HCl invariably increased Ca^{2+}_i; exposure to 100% CO_2 did so detectably in 10 out of 25 cases, and the H^+ translocating ionophore Nigericin elevated Ca^{2+}_i, too. An increase in Ca^{2+}_i with 100% CO_2 was also seen in barnacle muscle (Lea and Ashley, 1978) and in Xenopus embryos (Rink, Tsien and Warner, 1980).

The Ca^{2+} mechanism of uncoupling has been demonstrated in other cell types as well. Heart cells, as De Mello (1975) has shown, are uncoupled by Ca injections. Dahl and Isenberg (1980) found in Purkinje fibers that rise in Ca^{2+}_i, measured with Ca-electrodes, is associated with uncoupling, and Petersen and Iwatsuki (1978) uncoupled cells of the pancreas by Ca^{2+} injections. Furthermore, the permeability of the junctions in mammalian tissue culture cells is reduced by treatments which increase Ca^{2+}_i (Flagg-Newton and Loewenstein, 1979).

GRADED CHANGES IN CHANNEL SIZE ?

To date, nothing at all is known at the molecular level about how the cell-to-cell channels are rendered closed. The simplest model would have Ca^{2+} interact directly with a channel moiety and thereby block its permeability (Loewenstein, 1967) — but our lack of information at that level permits quite unrestricted speculation. We posed one question however, and approached it experimentally (Rose, Simpson and Loewenstein, 1977): Do the individual channels close in a graded or in an all-or-none fashion, or to state it in different terms, do the channels have more than one stable state of openness? In the latter case, cells would have a fine control at their disposal: By varying the channels' aperture, the size limit to permeant molecules would be changed, allowing e.g. the exchange of ions but not of metabolites or larger molecules between cells at certain times of the cells' life.

To try to answer this question of graded channel closure, we coinjected pairs of molecules of different size and different label in control condition, or together with Ca^{2+} to modify channel permeability. The transfer velocities of the individual members of each tracer pair were determined in each case. When Ca was coinjected, the transfer velocity of the larger molecule of each pair was reduced much more severely — sometimes to the point of complete blockage of transfer — than the transfer velocity of the smaller molecules. This result is consistent with a regulation in aperture of individual channels. A more complex alternative cannot be ruled out by these experiments, namely that a junction to begin with is comprised of different-sized channels of different Ca^{2+}-sensitivity.

Physiologically, a graded reduction in channel size has important implications: The junction then becomes a tunable filter for signal transfer from cell to cell.

REFERENCES

Åkerman, K.E.O. 1978. Effect of pH and Ca^{2+} on the retention of Ca^{2+} by rat liver mitochondria. Arch. Biochem. Biophys. 189: 256

Bartley, W., Amoore, J.E. 1958. The effects of manganese on the solute content of rat-liver mitochondria. Biochem. J. 69:348

Carvalho, A., Sanui, H., Pace, N. 1963. Calcium and magnesium binding properties of cell membrane materials. J. Cell. Comp. Physiol. 62: 311

Dahl, G., Isenberg, G. 1980. Decoupling of heart muscle cells: correlation with increased cytoplasmic calcium activity and with changes of nexus ultrastructure. J. Membrane Biol. 53: 63-75.

DeMello, W.C. 1975. Effect of intracellular injection of calcium and strontium on cell communication in heart. J. Physiol.(London) 250: 231-245.

Flagg-Newton, J., Loewenstein, W.R. 1979. Experimental depression of junctional membrane permeability in mammalian cell culture. A study with tracer molecules in the 300 to 800 dalton range. J. Membrane Biol. 50: 65-100.

Flagg-Newton, J., Simpson, I., Loewenstein, W.R. 1979. Permeability of the cell-cell membrane channels in mammalian cell junction. Science 205: 404-407.

Lea, T.Y., Ashley, C.C. 1978. Increase in free calcium in muscle after exposure to CO_2. Nature 275: 236-238.

Loewenstein, W.R. 1966. Permeability of membrane junctions. Ann. N.Y. Acad. Sci. 137: 441-472.

Loewenstein, W.R. 1967. Cell surface membranes in close contact. Role of calcium and magnesium ions. J. Colloid Interface Sci. 15: 34-46.

Meech, R.C., Thomas, R.C. 1977. The effect of calcium injection on the intracellular sodium and pH of snail neurons. J. Physiol. (London) 265: 867-879.

Petersen, O.H., Iwatsuki, N. 1978. The role of calcium in pancreatic acinar cell stimulus-secretion coupling: an electrophysiological approach. Ann. N.Y.Acad. Sci. 307: 599-617.

Rink, T.Y., Tsien,R.J., Warner, A.E. 1980. Free calcium in Xenopus embryos measured with ion-selective electrodes. Nature 283: 658-660.

Rose, B., Loewenstein, W.R. 1976. Permeability of a cell membrane junction and free ionized cytoplasmic calcium. A study with aequorin. J. Membrane Biol. 28: 87-119.

Rose, B., Rick, R. 1978. Intracellular pH, intracellular free Ca, and junctional cell-cell coupling. J. Membrane Biol. 44: 377-415.

Rose, B., Simpson, I., Loewenstein, W.R. 1977. Calcium ion produces graded changes inpermeability of membrane channels in cell junction. Nature 267: 625-627.

Simpson, I. Rose, B., Loewenstein, W.R. 1977. Size limit of molecules permeating the junctional membrane channels. Science 195: 294-296.

Turin, L., Warner, A.E. 1977. Carbon dioxide reversibly abolishes ionic communication between cells of early amphibian embryo. Nature 270: 56-57.

Adv. Physiol. Sci. Vol. 3. Physiology of Non-excitable Cells
J. Salánki (ed.)

CALMODULIN AS A MEDIATOR OF CALCIUM ACTIONS

Wai Yiu Cheung

Department of Biochemistry, St. Jude Children's Research Hospital and University of Tennessee Center for Health Sciences, Memphis, Tennessee 38101, USA

INTRODUCTION

Calcium ion exerts a profound influence on many biological processes such as cell motility, muscle contraction, axonal flow, cytoplasmic streaming, chromosome movement, neurotransmitter release, endocytosis, and exocytosis. Yet, because of the paucity of information about the Ca^{2+} receptors, the mechanism of Ca^{2+} action in most of these processes has remained obscure. Evidence acquired over the past few years suggests that many of the actions of Ca^{2+} are mediated through a homologous class of Ca^{2+}-binding proteins, of which calmodulin, the most widely distributed and versatile, appears to be a primary receptor of this important divalent cation [1-3].

Calmodulin was originally discovered in the late 1960s in our laboratory as an activator of cyclic nucleotide phosphoiesterase [4,5]. Some investigators are not aware of these early reports on calmodulin, then known as protein activator, probably because their titles deal with the activation of phosphodiesterase by snake venom. A more detail account of the discovery of calmodulin has appeared [1,6]. Briefly, I found that phosphodiesterase lost activity during the course of enzyme purification when calmodulin was dissociated. Addition of calmodulin restored the enzyme to its original activity [7-9]. Subsequently calmodulin was shown to regulate brain adenylate cyclase [10,11] and numerous other enzymes and cellular processes (see Table 2). Moreover, there are various calmodulin-binding proteins whose functions have not been identified, and they may be additional calmodulin-regulated enzymes [12].

This communication summarizes some general properties of calmodulin including its assay and preparation, a brief review of the calmodulin-dependent cellular processes, and its central role in cellular regulation. More information on calmodulin is found in several recent reviews [1-3] and a monograph [13]. The references cited herein are not meant to be exhaustive; to do so would have far exceeded the allotted space. The reader is encouraged to consult the vast original literature.

ASSAY OF CALMODULIN

One method to measure calmodulin is based on the stimulation of a Ca^{2+}-dependent phophodiesterase under specified conditions [9]. Theoretically any of the calmodulin-dependent enzymes enumerated in Table 2 can be used as an assay system. Phosphodiesterase has been widely used because the enzyme was the first responsive system to be studied, and it can be prepared easily in bulk.

Bovine brain contains several calmodulin-binding proteins which are capable of competing with phophodiesterase for calmodulin [12]. In fact, all calmodulin-responsive enzymes are potential competitors in the enzyme assay, and the presence of any of these proteins in a tissue extract could cause an underestimation of calmodulin. Fig. I shows the interference of a heat-labile calmodulin-binding protein ($CaM\text{-}BP_{80}$) on the measurement of calmodulin by the phosphodiesterase system [14].

The interference of calmodulin-binding protein on the assay of calmodulin by the phophodiesterase system can be circumvented by a radioimmunoassay, which is based on the recognition of antigenic determinants rather than on enzymic activity, a feature potentially useful in determining calmodulin that may be biologically inactive. In addition, the radioimmunoassay has the further advantage of detecting the sample over a wide range of concentration. (Fig. 2).

PREPARATION OF CALMODULIN

A variety of procedures have been described for preparing calmodulin from different tissues. In our laboratory, the protein was originally isolated from bovine brain by a technique which involved heat denaturation of the bulk of extraneous protein in the tissue extract, chromatography on diethylaminoethyl cellulose and preparative polyacrylamide gel electrophoresis [15]. As properties of calmodulin are better understood, simpler and more efficient isolation procedures have been devised. Anti-psychotic drugs of the phenothiazine type, such as trifluoperazine and chloropromazine, bind calmodulin in the presence of Ca^{2+} [16], a property that has been cleverly exploited to give a simple and efficient affinity-column procedure to prepare calmodulin in high yields [17,18]. Fig. 3 depicts the elution profile of calmodulin prepared from a bovine brain extract on a fluphenazine-agarose column [19]. Fluphenazine is a close derivative of trifluoperazine, having a ethanoic hydroxyl group suitable for chemical coupling to an activated-agarose matrix. Fig. 3 also compares a SDS electrophoretic gel pattern of a preparation before and after the affinity column.

The use of phenothiazine-affinity column for the preparation of calmodulin appears superior to conventional methods: the procedure does not involve harsh conditions, and is simple and efficient, giving a homogenous product essentially by a single step (see Fig. 3). Moreover, the affinity column can be easily regenerated for repeated use.

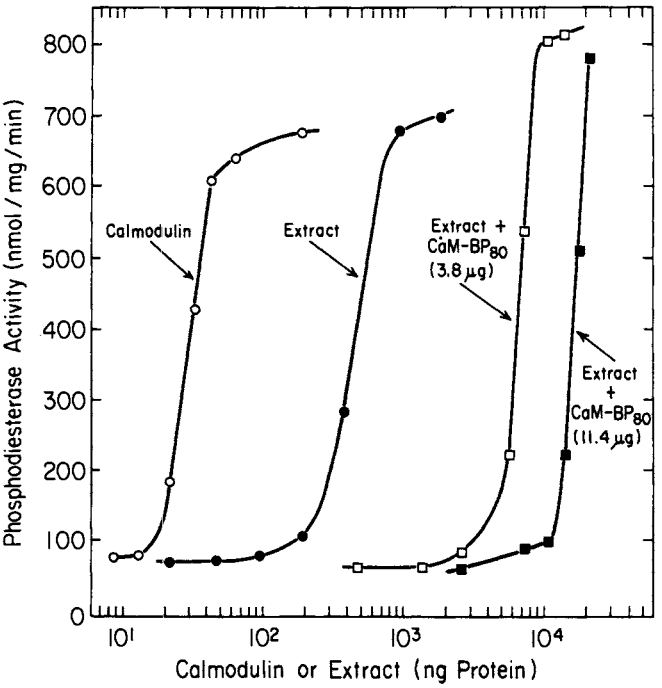

Fig. 1. Assay of calmodulin by Ca^{2+}-dependent phosphodiesterase. Calmodulin-deficient phosphodiesterase was purified from bovine brain cerebral cortex [5]. Pure calmodulin was isolated from bovine brain by a fluphenazine-sepharose affinity column [19] modeled after Charbonneau and Cormier [17]. The heat-treated bovine cerebral extract was prepared according to Wallace and Cheung [14]. Inhibitor - a heat-labile calmodulin-binding protein ($CaM\text{-}BP_{80}$) - was purified to homogeneity from bovine brain. The abscissa refers to the amount of protein contributed by calmodulin or the heat-treated extract. The concentrations of $CaM\text{-}BP_{80}$ (μg protein/0.1 ml of reaction mixture) are indicated by parentheses [From 14].

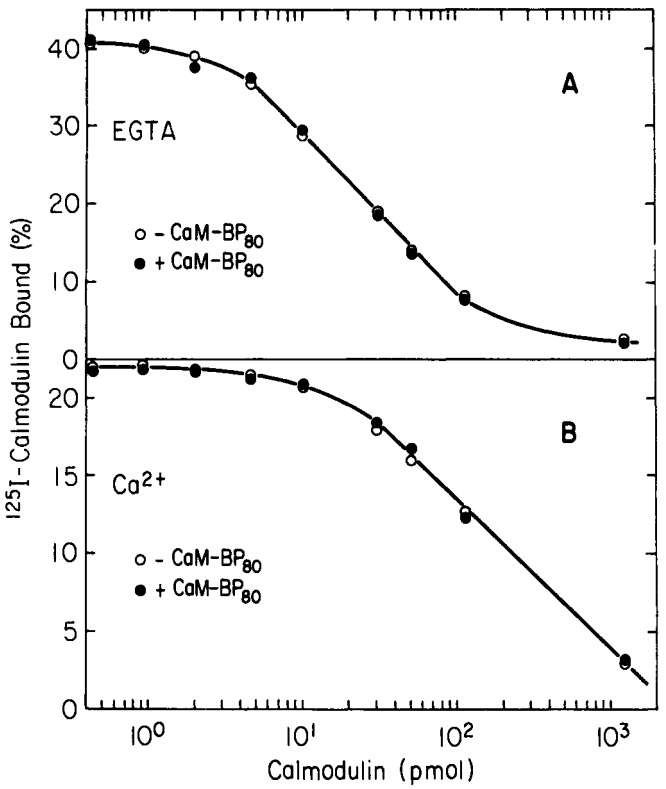

Fig. 2. Radioimmunoassay of calmodulin in the presence or absence of a heat-labeled calmodulin-binding protein ($CaM\text{-}BP_{80}$). Experimental conditions for Panel A and Panel B are comparable except Panel A contained 3 mM EDTA and Panel B contained 0.3 mM Ca^{2+}. When present, the concentration of $CaM\text{-}BP_{80}$ was 3.8 µg or 48 pmol/assay tube [From 14].

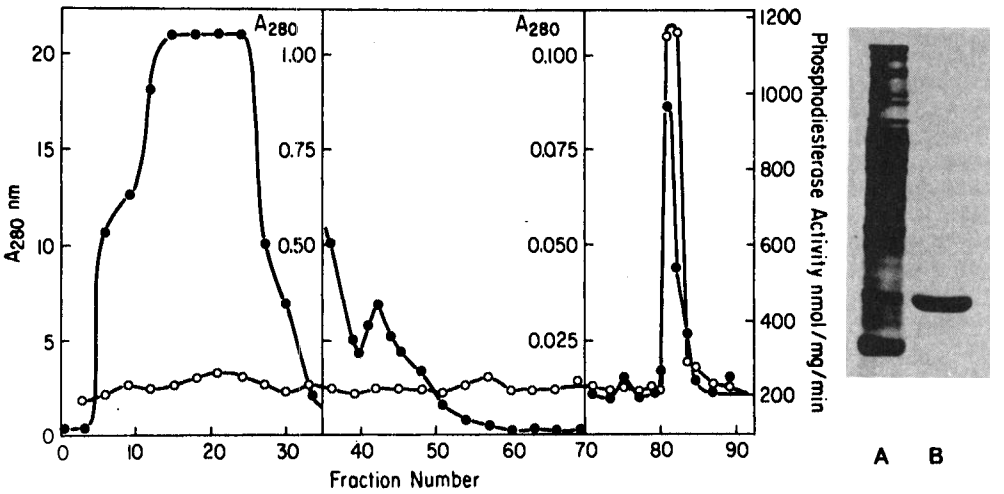

Fig. 3. Preparation of calmodulin by fluphenazine-sepharose affinity column chromatography. One hundred g of bovine brain cerebrum was homogenized with 300 ml of 10 mM PIPES (pH 7.0) containing 0.02% NaN_3. The homogenate was centrifuged at 10,000 x g for 60 min, and the supernatant fluid was applied to a fluphenazine-sepharose (2.6 x 29 cm). The column was washed with 100 ml of PIPES (pH 7.0) containing 1 mM $CaCl_2$, 350 ml of 10 mM PIPES (pH 7.0) containing 1 mM $CaCl_2$ and 0.5 M NaCl, and then eluted with 250 ml of 50 mM Tris-HCl (pH 8.0) containing 0.5 M NaCl and 10 mM EDTA. Ten-ml fractions were collected. The analytical polyacrylamide gel electrophoresis on the right shows the protein pattern of 100 μg of the brain extract before the fluphenazine-sepharose affinity column (Lane A) and that of 15 μg of pure calmodulin collected from portions 81 to 82 in the figure (Lane B) [From 19].

PROPERTIES OF CALMODULIN

A. Physicochemical and Biological Properties

Calmodulin is a heat-stable, globular protein containing 148 amino acids with a molecular weight of 16,723 [20]. Some fifty of the amino acid residues are aspartate and glutamate accounting for an isoelectric point of about 4.3. The molecule contains no cysteine, hydroxyproline, or tryptophan, and only 2 tyrosines. The low content of tyrosine (2 residues) to phenylalanine (8 residues) gives an unusual ultraviolet absorption spectrum with peaks at 253, 259, 265, and 269 nm due to pheylalanine and at 277 nm due to tyrosine. Because of the low content of tyrosine, the extinction coefficient of calmodulin ($E^{1\%}_{1\ cm}$ = 1.8) is small compared to most other proteins [15,21]. Calmodulin does not contain phosphate or carbohydrate, but does have a trimethylated lysine at position 115. Its amino terminus is acetylated. Fig. 4 shows the complete amino acid sequence of bovine brain calmodulin [20].

Calmodulin is very similar to another Ca^{2+}-binding protein, troponin C, and they exhibit approximately 70% conservative sequence homology and 50% direct sequence homology. Troponin C has a slightly higher melecular weight than calmodulin due to an extra eight residues at its amino terminus [20].

Calmodulin contains four Ca^{2+}-binding sites with dissociation constants in the range of 4-18 μM [15]. Binding of Ca^{2+} to calmodulin results in an increase in the α-helical content [21]. Most of the increase in helical content occurs upon binding of the first two molecules of Ca^{2+}. One of the two tyrosine residues, which is situated at the periphery of calmodulin, is further exposed to the solvent upon binding of Ca^{2+} [22]. The Ca^{2+}-induced conformational changes in calmodulin have also been indicated by several independent techniques: an increase in tyrosine fluorescence [22], an increase in refractoriness to cleavage by proteolytic enzymes [21,23], and by nuclear magnetic resonance [24].

One of the most striking characteristics of calmodulin is its stability. The protein may be exposed to 95° or to 8M urea with retention of biological activity. In addition, calmodulin retains its Ca^{2+}-dependent conformation and ability to bind troponin I in an alkaline electrophoresis gel containing 8M urea [25].

Some of the physiochemical properties of calmodulin are summarized in Table 1.

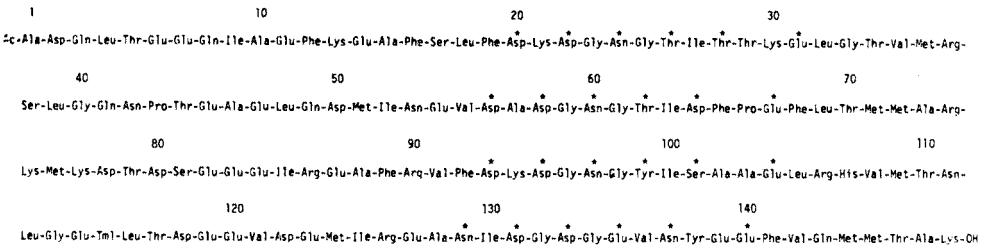

Fig. 4. The amino acid sequence of bovine brain calmodulin as determined by Watterson et al. [20]. The protein contains many acidic amino acids, which furnish carboxylate groups for the reversible binding of Ca^{2+}. The asterisk (*) identifies putative Ca^{2+}-binding residues. The protein, characterized by a trimethylated lysine (Tml) at position 115, lacks tryptophan, cysteine and hydroxyproline, which allows a tertiary structure highly flexible to interact with the various calmodulin-regulated proteins.

Table 1

Physicochemical Properties of Calmodulin

Molecular weight	16,723
$s_{20,w}$ (S)	1.85
D (cm/s)	1.09×10^{-6}
$\bar{v}$ (ml/g)	0.72
Stokes radius (Å)	20.9
Frictional coefficient	1.2
Isoelectric point	4.3
$\varepsilon^{1\%}_{276nm}$	1.8

Calmodulin appears to be ubiquitous throughtout the eukaryotes, lacking both tissue and species specificty. The protein isolated from all sources stimulate brain phosphodiesterase [1]. Moreover, calmodulins from cottonseeds and starfish oocytes cross-react with the antibody directed against bovine brain calmodulin [26], and those from slime mold (Dictyostelium discoideum), algae (Chlamydomonas reinhardii), and the electroplax of electric eel (Electrophorus electricus) cross-react with the antibody directed against rat testicular calmodulin [27]. In addition, the amino acid sequences of calmodulins from bovine brain, uterus, and rat testis are almost identical [20]. The apparent similarity in the amino acid sequence of calmodulin from widely divergent sources suggests that the protein is ancient, with its primary structure highly conserved, an attribute not unexpected of a fundamental regulatory protein.

Comparison of the primary structure of calmodulin with that of other calcium-binding proteins indicates that calmodulin is a member of a homologous series of proteins which include troponin C, myosin light chain, vitamin D-dependent calcium-binding protein and parvalbumins [28]. These proteins may have evolved from a common ancestor through a process of gene duplication and point mutations. Calmodulin appears the most highly conserved member of this family of proteins.

The similarity between calmodulin and troponin C is striking not only in a large common sequence homology, but also because calmodulin substitutes effectively for troponin C in the activation of actomyosin ATPase [25]. Dedman et al. [29] reported that troponin C is one-six-hundredths as active as calmodulin in stimulating brain phosphodiesterase. Wolff and Brostrom [30], however, detected this trace activity only at concentrations of troponin C 2,000-fold higher than calmodulin and attributed the activity to contamination by calmodulin.

In spite of the overwhelming similarities between calmodulin and troponin C, one notable difference exists: calmodulin is widely distributed and governs numerous divergent systems, whereas troponin C appears limited to the skeletal and cardiac muscles. Another difference is that calmodulin contains a trimethylated lysine at position 115. The significance, if any, of the presence of this unusual amino acid is not known.

B. Calmodulin-Regulated Processes

The enzymes which are regulated by calmodulin are fundamental for coordinating cellular activity. As is summarized in Table 2, calmodulin controls the metabolism of cyclic nucleotides, prostaglandins, cellular motility, and other key enzymes and cellular processes.

Table 2

Physicochemical Properties of Calmodulin

Molecular weight	16,723
$s_{20,w}$ (S)	1.85
D (cm/s)	1.09×10^{-6}
$\bar{v}$ (ml/g)	0.72
Stokes radius (Å)	20.9
Frictional coefficient	1.2
Isoelectric point	4.3
$\varepsilon^{1\%}_{276nm}$	1.8

Adenylate cyclase and phosphodiesterase are the only known enzymes involved in the metabolism of cAMP. In the brain and adrenal [49], calmodulin regulates the activities of both enzymes. In many other tissues, at least one form of phosphodiesterase is regulated by calmodulin. The activation of both the synthetic and degradative enzymes by calmodulin in neural tissues by a cellular flux of Ca^{2+} may allow a transient increase of cAMP, first by activating adenylate cyclase (as Ca^{2+} passes through the plasma membrane) and then by phosphodiesterase (as Ca^{2+} diffuses into the cytoplasm) [50]. Alternatively, since brain Ca^{2+}-dependent phosphodiesterase degrades cGMP faster than cAMP at micromolar concentration, the sequential activation of adenylate cyclase and phosphodiesterase may result in an increase of cellular cAMP and a decrease of cellular cGMP (Fig. 5). Another interpretation is based on the observation that calmodulin is released from synaptosomal membranes upon phosphorylation of a membrane protein catalyzed by a cAMP-dependent protein kinase. Activation of adenylate cyclase increases intracellular cAMP, which stimulates a cAMP-dependent phosphorylation of certain

membrane components. This action releases calmodulin from the membrane compartment into the cytoplasm where it activates the Ca^{2+}-dependent phosphodiesterase, returning cAMP to its prestimulated level [51,52]. One uncertainty of this notion is that the concentration of calmodulin in cytosol is invariably higher than that of phosphodiesterase, and the enzyme activity appears more likely to be regulated by the cellular flux of Ca^{2+}.

Muscle contraction is governed by the force generated by the interaction of actin with myosin in response to the cellular level of Ca^{2+}. In skeletal and cardiac muscles the receptor of Ca^{2+} is troponin C, whereas in smooth muscle and non-muscle cells the receptor is calmodulin. Calmodulin is absolutely required for the activity of myosin light chain kinase of smooth muscle or non-muscle cells. The enzyme catalyzes the phosphorylation of a 20,000-dalton light chain of myosin. Phosphorylation of the light chain is obligatory for actomyosin ATPase activity, which catalyzes the hydrolysis of ATP, thereby initiating muscle contraction [53].

Phosphorylase kinase controls the metabolism of glycogen. The enzyme is complex, consisting of four tetramers, $(\alpha\beta\gamma\delta)_4$; α and β are phosphorylatable subunits, and the state of phosphorylation affects the catalytic activity resided in the γ subunit; the δ subunit is calmodulin, tightly bound to the ternary structure. Phosphorylase activity is further increased by an exogenous calmodulin which stimulates the enzyme in response to the cellular flux of Ca^{2+} [32].

A third protein kinase regulated by calmodulin has been found in a membranous fraction of various tissues. In synaptosomes the influx of Ca^{2+} following depolarization leads to the phosphorylation of two membrane proteins with molecular weights of 80,000 and 86,000. These polypeptides also serve as substrates for cAMP-dependent protein kinase [45,46]. Delorenzo *et al.* [47] noted that calmodulin-regulated phosphorylation of certain synaptosomal proteins led to a release of neurotransmitters from synaptic vesicles. In addition, Yamauchi and Fujisawa [54] showed that tryptophan 5-monooxygenase, a key enzyme in the biosynthesis of neurotransmitters, is activated by a calmodulin-induced phosphorylation.

NAD kinase activity in both pea seedling [36] and sea urchin oocyte [37] is governed by calmodulin. The kinase controls the ratio of NAD/NADP which determines the direction of certain metabolic pathways. One of the early events following fertilization of sea urchin egg is an increase of free Ca^{2+}, and a rapid conversion of NAD to NADP [55]. Calmodulin is present at high levels in sea urchin oocyte [56] and is required for the NAD kinase for maximal activity. The rapid increase of Ca^{2+} following fertilization of the egg may be temporally related to the activation of the NAD kinase to generate NADP needed for the many biosynthetic activities.

Phosphoipase A_2 is a key enzyme that governs the availability of arachidonic acid in many tissues. The level of free arachidonic acid is usually low, a rate-limiting step in the synthesis of endoperoxides, thromboxanes, prostaglandins, and prostacyclin. The enzyme depends on

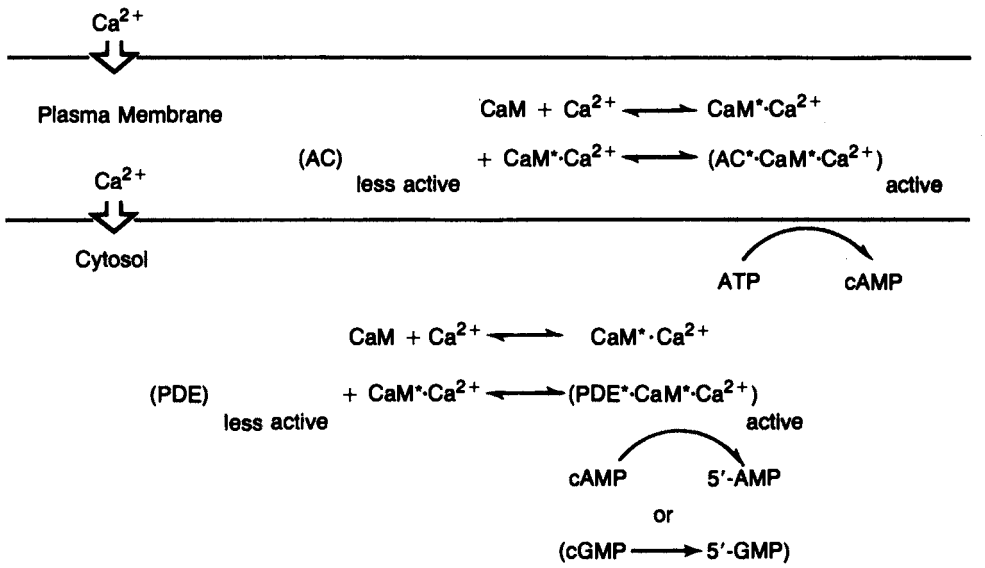

Fig. 5. A speculative scheme for the regulation of brain cAMP metabolism by a cellular flux of Ca^{2+}. Stimulation of the cell leads to an influx of Ca^{2+} or a release of Ca^{2+} from the membrane. The increase of Ca^{2+} first activates adenylate cyclase (as Ca^{2+} passes through the plasma membrane) and then phosphodiesterase (as Ca^{2+} diffuses into the cytoplasm). The sequential activation of the synthetic and then degradative enzyme would allow a transient increase of cAMP. Alternatively, the Ca^{2+}-dependent phosphodiesterase also catalyzes the hydrolysis of cGMP, in fact, at a physiological concentration of substrates, the rate of cGMP hydrolysis is greater than that of cAMP. The influx of Ca^{2+} could result in an increase of cAMP and a concomitant decrease of cGMP. CaM, calmodulin; AC, adenylate cyclase; and PDE, phosphodiesterase (Modified from 50).

activation of the NAD kinase to generate NADP needed for the many biosynthetic activities.

Phosphoipase A_2 is a key enzyme that governs the availability of arachidonic acid in many tissues. The level of free arachidonic acid is usually low, a rate-limiting step in the synthesis of endoperoxides, thromboxanes, prostaglandins, and prostacyclin. The enzyme depends on Ca^{2+} for activity; in human platelets, the effect of Ca^{2+} appears to be mediated through calmodulin [38]. It would be important to determine if the enzyme activity in other tissues is regulated through a similar mechanism.

Another calmodulin-dependent enzyme involved in the metabolism of prostaglandin and prostacyclin is a 15-hydroxyprostaglandin dehydrogenase [39]. Unlike other calmodulin-regulated enzymes, the dehydrogenase is inhibited by calmodulin, and is the first enzyme whose activity is depressed rather than enhanced. The dehydrogenase represents an important enzyme in governing the metabolism of prostacyclin, the most potent anti-platelet aggregating agent so far studied. The potential role of the dehydrogenase in hemostasis has been discussed elsewhere [39].

Calmodulin regulates the activity of Ca^{2+},Mg^{2+}-ATPase of plasma membrane [40-42] and sarcoplasmic reticulum [44]. As intracellular Ca^{2+} increases following stimulation of the cell, calmodulin activates the Ca^{2+},Mg^{2+}-ATPase, which extrudes cytosolic Ca^{2+} into the extracellular space, or takes it up into the sarcoplasmaic reticulum, or both, until the Ca^{2+} concentration returns to a steady-state level. This mechanism constitutes an excellent example of feedback control for the homeostasis of Ca^{2+}. Thus, calmodulin acts not only as a mediator of Ca^{2+} actions in many cellular processes but also as a modulator of its intracellular level [57].

Using indirect immunofluorescence, Welsh *et al.* [58] found that anticalmodulin decorated the mitotic spindle during the division of numerous cultured cells. The fluorescence appeared most intense at the poles of the spindle. Agents such as colcemid and N_2O which disrupt microtubule structure altered the distribution of fluorescence. Following up this observation, the same group showed that calmodulin accelerated the disassembly of microtubules; troponin C exerted similar effect, and was even more active than calmodulin [48].

Wood *et al.* [59] localized calmodulin in mouse basal ganglia. They found that the protein was associated primarily with the postsynaptic densities (PSD) and the dendritic microtubules. This observation is consistent with the work of Grab *et al.* [60] which showed that calmodulin was associated with the PSD isolated by subcellular fractionation. The PSD also contained a Ca^{2+}-dependent protein kinase whose activity is regulated by calmodulin [61].

Harper *et al.* [62] studied the distribution of calmodulin in rat liver, skeletal muscle, and adrenal. In liver calmodulin was associated with the nucleus, plasma membrane, and glycogen granules. Skeletal muscle calmodulin was located at the I band and at the intermyofibrillar region probably in association with glycogen granules and the sarco-

plasmic reticulum. In the adrenal the endocrine state of the animal affected the distribution of calmodulin within the cell. Administration of ACTH to the animal prior to excision of the adrenal greatly appeared to increase calmodulin in the nuclei, implying a role of calmodulin in certain nuclear functions of this organ.

In view of the extensive involvement of Ca^{2+} in cell functions, it would not be surprising that future studies will extend the role of calmodulin to other cellular processes.

MECHANISM OF CALMODULIN ACTION

The mechanism by which calmodulin regulates brain phosphodiesterase, adenylate cyclase, and Ca^{2+}-ATPase has been studied in some detail. As is depicted in the following scheme, the binding of Ca^{2+} to calmodulin brings about a conformation change which allows the Ca^{2+}.calmodulin complex to interact with the apoenzyme to form a ternary complex, which is the active species.

$$CaM + Ca^{2+} \longrightarrow CaM^*.Ca^{2+} \text{ (active)} \qquad (1)$$

$$CaM^*.Ca^{2} + E \text{ (less active)} \longrightarrow CaM^*.Ca^{2+}.E^* \text{ (activated)} \qquad (2)$$

Where CaM stands for calmodulin; E for the apoenzyme, $CaM^*.Ca^{2+}.E^*$ the holoenzyme, and the asterick (*) for a new conformation.

The mechanism depicted by equations (1) and (2) should not be regarded as the only mode by which calmodulin acts. Phosphorylase kinase [32] contains calmodulin as an integral subunit and cannot be removed from the enzyme by EGTA. Lung phosphodiesterase may be another enzyme with a tightly bound calmodulin [63]. Further, calmodulin inhibits adenylate cylase from glioma cells [64] and rat brain under certain conditions [65]. In addition, calmodulin inhibits a 15-hydroxyprostaglandin dehydrogenase [39], and the mechanism of inhibition remains to be elucidated.

CALMODULIN AS AN INTEGRATOR OF CELLULAR REGULATORS

The effects and metabolism of peptide hormones, catecholamines, prostaglandins, cAMP, and Ca^{2+} are often interrelated. Fig. 6 shows the interrelationships of these cellular regulators. Stimulation of a cell leads to the release of hormones, or Ca^{2+}, or both. As discussed in earlier sections, many of the Ca^{2+} effects are mediated through calmodulin, which regulates not only the metabolism of cAMP, cGMP, but also of prostaglandins, prostacyclin and Ca^{2+}. Cyclic AMP, in turn, may control the active uptake of Ca^{2+} by certain organelles. Thus, one cellular regulator may function independently, or may modulate the effect of one of the others. Note that between the Ca^{2+}- and cAMP-regulated pathways in Fig. 6, the response of the Ca^{2+} signal is inherently faster. The hormonal signal is transduced through adenylate cyclase, which catalyzes the synthesis of cAMP. cAMP derepresses protein kinase, and the latter catalyzes the phosphorylation of a receptor protein, probably yet another enzyme. Ca^{2+}, on the other hand, does not need to be synthesized; it interacts with calmodulin which may directly regulate its receptor, as in the case of myosin light chain

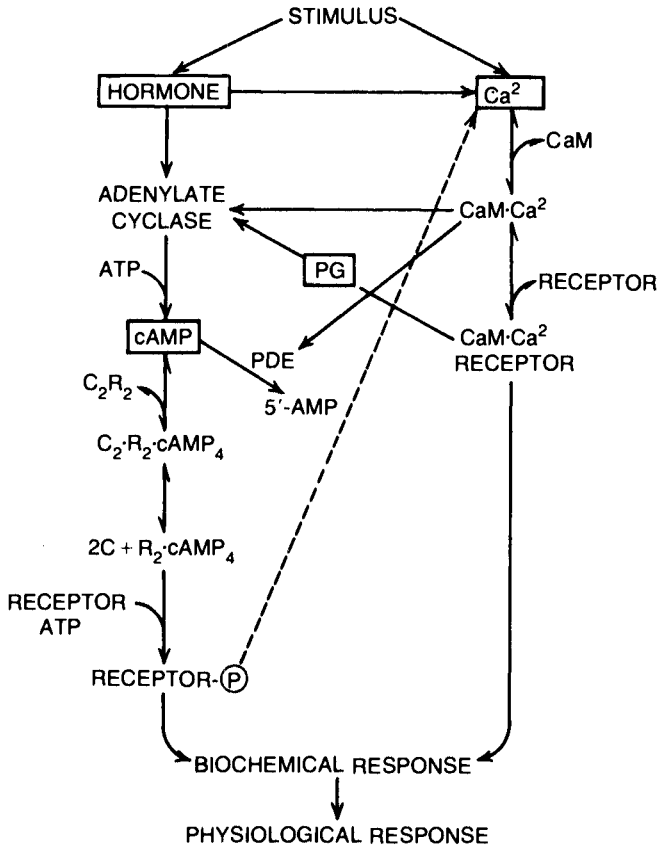

Fig. 6. Integration of cellular regulators by calmodulin. Stimulation of a cell leads to the release of hormones, or Ca^{2+}, or both. Catecholamines, certain peptide hormones, and prostaglandins activate adenylate cyclase and cause the increase of intracellular cAMP. Upon binding cAMP, the regulatory subunit (R) of protein kinase (C_2R_2) is dissociated from the catalytic subunit (C), which becomes active, and catalyzes the phosphorylation of a protein, usually at the serine residue. Phosphorylation of a protein either stimulates or inhibits its biological activity; the phosphorylated protein serves as an effector or a modulator of a cellular process. The influx of Ca^{2+}, or the release of Ca^{2+} from the cell membrane or sarcoplasmic reticulum activates calmodulin, which forms a complex with a receptor protein to initiate a biochemical or physiological response. $E.CaM.Ca^{2+}$ may stand for the active form of adenylate cyclase, phosphodiesterase, or any of the calmodulin-regulated enzymes listed in Table I. An exception is 15-hydroxyprostaglandin dehydrogenase, whose activity is inhibited by calmodulin. Calmodulin regulates the metabolism of cAMP, directly or indirectly, as well as certain prostaglandins (thromboxanes and prostacyclin). cAMP could in turn affects the availability of Ca^{2+}. Thus, the function of metabolism of these cellular regulators are intertwined, and calmodulin integrates them on a molecular basis.

kinase. The less number of intermediate steps in the Ca^{2+}-regulated pathway affords a faster response time.

EPILOGUE

The extensive role of Ca^{2+} in cellular regulation has long been recognized, but there were few clues as to how it exerts its diverse functions. Evidence accumulated during the past several years indicates that many of the Ca^{2+} effects are mediated through calmodulin, a calcium-binding protein ubiquitous in all eukaryotes examined. In view of the extensive interests on Ca^{2+} by numerous investigators dating back to the 1950s, it is surprising that calmodulin was not discovered earlier. Perhaps the abundance and ubiquity of the protein proves to be its own deterrent. An abundance of calmodulin in a tissue would allow the effect of Ca^{2+} to be manifested without the need of an exogenous source. The loss of an enzyme activity during the course of purification, a rather common experience among enzymologists, unexpectedly provided me with an opportunity to discover a missing link in the understanding of Ca^{2+} functions.

ACKNOWLEDGEMENT

This work was supported by USPHS Grant NS08059 and by ALSAC. This article was prepared while I was on sabbatical leave as a Faculty Scholar (1979-1980), Josiah Macy, Jr., Foundation at the Laboratory of Molecular Pharmacology, Howard Hughes Medical Institute, SJ-30, University of Washington, Seattle, Washington. I am grateful to Dr. E. G. Krebs for his generous support and kind hospitality during my tenure in Seattle, and my colleagues R. W. Wallace, T. J. Lynch, E. A. Tallant, Y. M. Liu and Y. P. Liu for their contribution to various phases of this work.

REFERENCES

1. Cheung, W.Y. Calmodulin plays a pivotal role in cellular regulation. Science 207, 19-27, 1980.

2. Klee, C.B., Crouch, T.H. and Richman, P. Calmodulin. Ann. Rev. Biochem. 49, 489-515, 1980.

3. Wang, J.H. and Waisman, D.M. Calmodulin and its role in the second messenger system. Curr. Top. Cell. Regul. 15, 47-107, 1979.

4. Cheung, W.Y. Cyclic 3',5'-nucleotide phosphodiesterase, pronounced stimulation by snake venom. Biochem. Biophys. Res. Commun. 29, 478-482, 1967.

5. Cheung, W.Y. Cyclic 3',5'-nucleotide phosphodiesterase. Preparation of a partially inactive enzyme and its subsequent stimulation by snake venom. Biochim. Biophys. Acta 191, 303-315, 1969.

6. Cheung, W.Y. Calmodulin - An introduction. In Calcium and Cell Function, Vol. 1, Calmodulin, ed. Cheung, W.Y. Academic Press, New York, pp. 1-11, 1980.

7. Cheung, W.Y. Cyclic 3',5'-nucleotide phosphodiesterase. Demonstration of an activator. Biochem. Biophys. Res. Commun. 38, 533-538, 1970.

8. Cheung, W.Y. Cyclic nucleotide phosphodiesterase. Adv. Biochem. Pharmacol. 3, 51-56, 1970.

9. Cheung, W.Y. Cyclic nucleotide phosphodiesterase: evidence for and properties of a protein activator. J. Biol. Chem. 246, 2859-2869, 1971.

10. Brostrom, C.O., Huang, Y.C., Breckenridge, B.M. and Wolff, D.J. Identification of a calcium-binding protein as a calcium-dependent regulator of brain adenylate cyclase. Proc. Natl. Acad. Sci. USA 72, 64-68, 1975.

11. Cheung, W.Y., Bradham, L.S., Lynch, T.J., Lin, Y.M. and Tallant, E.A. Protein activator of cyclic 3':5'-nucleotide phosphodiesterase of bovine or rat brain also activates its adenylate cyclase. Biochem. Biophys. Res. Commun. 66, 1055-1062, 1975.

12. Wang, J.H., Sharma, R.K. and Tam, S.T. Calmodulin-binding proteins. In Calcium and Cell Function, Vol. 1, Calmodulin, ed. Cheung, W.Y. Academic Press, New York, 1980.

13. Cheung, W.Y. (ed.) Calcium and Cell Function, Vol. 1, Calmodulin. Academic Press, New York, 1980.

14. Wallace, R.W. and Cheung, W.Y. Calmodulin. Production of an antibody in rabbit and development of a radioimmunoassay. J. Biol. Chem. 284, 6564-6571, 1979.

15. Lin, Y.M., Liu, Y.P. and Cheung, W.Y. Cyclic 3',5'-nucleotide phosphodiesterase. Purification, characterization, and active form of the protein activator from bovine brain. J. Biol. Chem. 249, 4943-4954.

16. Levin, R.M. and Weiss, B. Mechanism by which psychotropic drugs inhibit adenosine cyclic 3',5'-monophosphate phosphodiesterase of brain. Mol. Pharmacol. 12, 581-589, 1976.

17. Charbonneau, H. and Cormier, M.J. Purification of plant calmodulin by fluphenazine-sepharose affinity chromatography. Biochem. Biophys. Res. Commun. 90, 1039-1047, 1979.

18. Jamieson, G.A. and Vanaman, T.C. Calcium-dependent affinity chromatography of calmodulin on an immobilized phenothiazine. Biochem. Biophys. Res. Commun. 90, 1048-1056, 1979.

19. Wallace, R.W., Tallant, E.A. and Cheung, W.Y. Assay, preparation and properties of calmodulin. In Calcium and Cell Function, Vol. 1, Calmodulin, ed., Cheung, W.Y. Academic Press, New York, 1980.

20. Watterson, D.M., Sharief, F. and Vanaman, T.C. The complete amino acid sequence of the Ca^{2+}-dependent modulator protein (calmodulin) of bovine brain. J. Biol. Chem. 255, 962-975, 1980.

21. Liu, Y.P. and Cheung, W.Y. Cyclic 3',5'-nucleotide phosphodiesterase. Ca^{2+} confers more helical conformation to the protein activator. J. Biol. Chem. 251, 4193-4198, 1976.

22. Klee, C.B. Conformational transition accompanying the binding of Ca^{2+} to the protein activator of 3',5'-cyclic adenosine monophosphate phosphodiesterase. Biochemistry 16, 1017-1024, 1977.

23. Ho, H.C., Desai, R. and Wang, J.H. Effect of Ca^{2+} on the stability of the protein activator of cyclic nucleotide phosphodiesterase. FEBS Lett. 50, 374-377, 1975.

24. Seamon, K.B. Calcium and magnesium-dependent conformation states of calmodulin as determined by nuclear magnetic resource. Biochemistry 19, 207-215, 1980.

25. Amphlett, G.W., Vanaman, T.C. and Perry, S.V. Effect of the troponin C-like protein from bovine brain (brain modulator protein) on the Mg^{2+}-stimulated ATPase of skeletal muscle actomyosin. FEBS Lett. 72, 163-168, 1976.

26. Wallace, R.W. and Cheung, W.Y. Antibody against bovine brain calmodulin cross-reacts with cottonseed calmodulin. Fed. Proc. Fed. Am. Soc. Expt. Biol. 38, 478, 1979.

27. Chafouleas, J.G., Dedman, J.R., Munjaal, R.P. and Means, A.R. Calmodulin. Development and application of a sensitive radioimmunoassay. J. Biol. Chem. 254, 10262-10267, 1979.

28. Kretsinger, R.H. Calcium-binding proteins. Ann. Rev. Biochem. 45, 239-266, 1976.

29. Dedman, J.R., Potter, J.D. and Means, A.R. Biological cross-reactivity of rat testis phosphodiesterase activator protein and rabbit skeletal muscle troponin-C. J. Biol. Chem. 252, 2437-2440, 1977.

30. Wolff, D.J. and Brostrom, C.O. Properties and functions of the Ca^{2+}-dependent regulator protein. Adv. Cyclic Nucleotide Res. 11, 28-88, 1979.

31. Nagao, S., Suzuki, Y. and Watanabe, Y. Activation of a calcium-binding protein of guanylate cyclase in Tetrahymena pyrifomis. Biochem. Biophys. Res. Commun. 90, 261-268, 1979.

32. Cohen, P., Burchell, A., Foulkes, J.G., Cohen, T.W., Vanaman, T.C. and Nairn, A.L. Identification of the Ca^{2+}-dependent modulator protein as the fourth subunit of rabbit skeletal muscle phosphorylase kinase. FEBS Lett. 92, 287-293, 1978.

33. Waisman, D.M., Singh, T.J., Wang, J.H. The modulator-dependent protein kinase. A multi-functional protein kinase activatable by the Ca^{2+}-dependent modulator protein on the cyclic nucleotide system. J. Biol. Chem. 253, 3387-3390, 1978.

34. Dabrowska, R. and Hartshorne, D.J. A Ca^{2+}- and modulator-dependent myosin light chain kinase from non-muscle cells. Biochem. Biophys. Res. Commun. 85, 1352-1359, 1978.

35. Yagi, K., Yazawa, M., Kakiuchi, S., Ohshima, M. and Uenishi, K. Identification of an activator protein for myosin light chain kinase as the Ca^{2+}-dependent modulator protein. J. Biol. Chem. 253, 1388-1340, 1978.

36. Anderson, J.M. and Cormier, M.J. Calcium-dependent regulator of NAD kinase in higher plants. Biochem. Biophys. Res. Commun. 84, 595-602, 1978.

37. Epel, D., Patton, C., Wallace, R.W. and Cheung, W.Y. Calmodulin activates NAD kinase of sea urchin eggs: an early event following fertilization (submitted for publication).

38. Wong, P. Y-K. and Cheung, W.Y. Calmodulin stimulates human platelet phospholipase A_2. Biochem. Biophys. Res. Commun. 90, 473-480, 1979.

39. Wong, P. Y-K., Lee, W.H., Chao, P. H-W. and Cheung, W.Y. The role of calmodulin in prostaglandin metabolism. N. Y. Acad. Sci. (in press).

40. Gopinath, R.M. and Vincenzi, F.F. Phosphodiesterase protein activator mimics red blood cell cytoplasmic activator of (Ca^{2+}-Mg^{2+}) ATPase. Biochem. Biophys. Res. Commun. 77, 1203-1209, 1977.

41. Jarret, H.W. and Penniston, J.T. Partial purification of the Ca^{2+}-Mg^{2+} ATPase activator from human erythrocytes: its similarity to the activator of 3:5'-cyclic nucleotide phosphodiesterase. Biochem. Biophys. Res. Commun. 77, 1210-1216, 1977.

42. Sobue, K., Ichida, S., Yoshida, H., Yamazaki, R. and Kakiuchi, S. Occurrence of a Ca^{2+}- and modulator protein activatable ATPase in the synaptic plasma membrane of brain. FEBS Lett. 99, 199-202, 1979.

43. Hinds, T.R., Larsen, F.L. and Vincenzi, F.F. Plasma membrane Ca^{2+}-transport: stimulation by soluble proteins. Biochem. Biophys. Res. Commun. 81, 455-461, 1978.

44. Katz, S. and Remtulla, M.A. Phosphodiesterase protein activator stimulates calcium transport in cardiac microsomal preparations enriched in sarcoplasmic reticulum. Biochem. Biophys. Res. Commun. 83, 1373-1379, 1978.

45. Schulman, H. and Greengard, P. Stimulation of brain membrane protein phosphorylation by calcium and an endogenous heat-stable protein. Nature 271, 478-479, 1978.

46. Schulman, H. and Greengard, P. Ca^{2+}dependent protein phosphorylation system in membranes from various tissues, and its activation by calcium dependent regulator. Proc. Natl. Acad. Sci. USA 75, 5432-5436, 1978.

47. De Lorenzo, R.J., Freedman, S.D., Yobe, W.B. and Maurer, S.C. Stimulation of Ca^{2+}-dependent neurotransmitter release and presynaptic nerve-terminal protein phosphorylation by calmodulin and a calmodulin-like protein isolated from synaptic vesicles. Proc. Natl. Acad. Sci. USA 76, 1838-1842, 1979.

48. Marcum, J.M., Dedman, J.R., Brinkley, B.R. and Mean, A.R. Control of microtubule assembly-disassembly by calcium-dependent regulator protein. Proc. Natl. Acad. Sci. USA 75, 3771-3775, 1978.

49. Le Donne, N.C. and Coffee, C.J. Properties of the bovine adrenal medulla adenyl cyclase. Fed. Proc. Fed. Am. Soc. Expt. Biol. 38, 469, 1979.

50. Cheung, W.Y., Lynch, T.J. and Wallace, R.W. An endogenous Ca^{2+}-dependent activator protein of brain adenylate cyclase and cyclic nucleotide phosphodiesterase. Adv. Cyclic Nucleotide Res. 9, 233-251, 1978.

51. Gnegy, M.E., Uzunov, P. and Costa, E. Regulation of dopamine stimulation of striatal adenylate cyclase by an endogenous Ca^{2+}-binding protein. Proc. Natl. Acad. Sci. USA 73, 3887-3890, 1976.

52. Gnegy, M.E., Costa, E. and Uzunov, P. Regulation of transsynaptically elicited increase of 3',5'-cyclic AMP by endogenous phosphodiesterase activator. Proc. Natl. Acad. Sci. USA 73, 352-355, 1976.

53. Adelstein, R.S. and Eisenberg, E. Regulation and kinetics of the actin-myosin-ATP interaction. Ann. Rev. Biochem. 49, 921-956, 1980.

54. Yamauchi, T. and Fujisawa, H. Activation of tryptophan 5-monooxyenase by calcium-dependent regulator protein. Biochem. Biophys. Res. Commun. 90, 28-35, 1979.

55. Epel, D. A primary metabolic change of fertilization interconversion of pyridine nucleotide. Biochem. Biophys. Res. Commun. 17, 62-68, 1964.

56. Head, J.F., Mader, S. and Kaminer, B. Calcium-binding modulator protein from the unfertilized egg of the sea urchin egg Arbacia Punctulata. J. Cell Biol. 80, 211-218, 1979.

57. Lynch, T.J. and Cheung, W.Y. Human erythrocyte Ca^{2+}-Mg^{2+}-ATPase: mechanism of stimulation by Ca^{2+}. Arch. Biochem. Biophys. 194, 165-170, 1979.

58. Welsh, M.J., Dedman, J.R., Brinkley, B.R. and Means, A.R. Calcium-dependent regulator protein: localization in mitotic apparatus of eukaryotic cells. Proc. Natl. Acad. Sci. USA 75, 1867-1871, 1978.

59. Wood, J., Wallace, R.W., Whitaker, J.W. and Cheung, W.Y. Immunocytochemical localization of calmodulin and a heat-labile calmodulin-binding protein in basal ganglia of mouse brain. J. Cell Biol. 84, 66-76, 1980.

60. Grab, D.J., Berzins, K., Cohen, P. and Siekevitz, P. Presence of calmodulin in postsynaptic densities isolated from canine cerebral cortex. J. Biol. Chem. 254, 8690-8696, 1979.

61. Grab, D., Carlin, R. and Siekevitz, P. The presence and possible function of calmodulin in isolated cerebral cortex post-synaptic densities. N. Y. Acad. Sci. (in press).

62. Harper, J.F., Cheung, W.Y., Wallace, R.W., Huang, H.L., Levine, S.N. and Steiner, A.L. Localization of calmodulin in rat tissues. Proc. Natl. Acad. Sci. USA 77, 366-370, 1980.

63. Sharma, R.K. and Wirch, E. Ca^{2+}-dependent cyclic nucleotide phosphodiesterase from rabbit lung. Biochem. Biophys. Res. Commun. 91, 338-344, 1979.

64. Brostrom, M.A., Brostrom, C.O., Breckenridge, B.M. and Wolff, D.J. Regulation of adenylate cyclase from glial tumor cells by calcium and a calcium-binding protein. J. Biol. Chem. 251, 4744-4750, 1976.

65. Piascik, M.T., Wisler, P.L., Johnson, C.L. and Potter, J.D. Ca^{2+}-dependent regulation of guinea pig brain adenylate cyclase. J. Biol. Chem. 255, 4176-4181, 1980.

Adv. Physiol. Sci. Vol. 3. Physiology of Non-excitable Cells
J. Salánki (ed.)

TIME IN CELL BIOLOGY. INTRODUCTION

P. Fasella
Instituto Chimica Biologica and Centro di Biologia Molecolare, Città Universitaria, Roma, Italy

Most biological systems are in a steady-state, far from equilibrium. This makes control, performance and evolution possible. Steady-states are determined by the relative rates of the processes involved in them. The ordered flux of matter, energy and information which constitutes life requires that biological systems be ordered in time as well as in space. Knowledge of the characteristic time constants of the various elementary biological systems is indispensable for the understanding of cell physiology since it is the time correlated interplay and succession of the elementary biomolecular events which eventually leads to the ordered performance of cellular functions and to the natural course of the cell life cycle. Moreover, biological selection is often determined by the relative time constants of competing systems be their molecules, cells organisms or populations.

The importance of the time dimension of biological system is explicitly or implicitly recognized and the study of the time structure of cells in the > m sec range is an essential aspect of cellular physiology.

Over the last decades methodological breakthroughs led to the development of "microscopes in the time dimension", which make it possible to measure biologically relevant events down to the pico-second range.

This is providing new insight on the time structure of cells and of their fundamental macromolecular components, with important implications for the understanding of macromolecular self assembly, bio-catalysis, information processing, regulation and selection. Many of the results obtained in this area are quite recent or have been published only in specialized journal and experts-workshop.

This Symposium is an occasion for reviewing the present knowledge of the temporal structure of biological systems in the sub-second time domains. Hans Frauenfelder will introduce

the subject, stress its relevance and outline the problems and approaches to their solutions.
Enrico Gratton will discuss the time dimensions of the fundamental biological macromolecules proteins and nucleic acids and of their mutual complexes.
Thomas Jovin will deal with a more complex system, biomembranes, while Benno Hess will consider events at an even higher level of integration and complexity, namely cellular and metabolic processes.
S. Damjanovich will reconsider all these aspects in a comprehensive way, with special emphasis on energy and information transfer.
The time dimensions of events involved in specialized functions, such as nervous excitation or muscular contraction, will not be dealt with in this Symposium and are the objects of other Sections of this Congress.
However, in an attempt to apply the above views to specific problems in cell physiology, Làbos will briefly discuss the temporal structure in the spikes sequence as a basis for the design of neuronal networks.
A comprehensive discussion will conclude the Symposium.

Adv. Physiol. Sci. Vol. 3. Physiology of Non-excitable Cells
J. Salánki (ed.)

THE TIME DIMENSION OF PROTEIN SYSTEMS

Enrico Gratton
Department of Physics, University of Illinois at Urbana-Champaign, Urbana, IL 61801, USA

Proteins are systems that can exist in a large number of conformations. The complete characterization of these conformations is a very important step in understanding the protein structure and function and generally involves the study of the positions of all the atoms at a given time.

A protein with respect to some specified reference system is described by a set of coordinates $\{x_{j,\ell}(x_i,t)\}$ where j indicates one of the atoms, ℓ a molecule, x is the spatial coordinate and t the time.

The information on the values of $\{\langle x_j(x_i)\rangle_{\ell,t}\}$ is generally obtained using x-ray crystallography. Quite recently, as H. Frauenfelder has shown, information about $\{\langle x_j^2(x_i)\rangle_{\ell,t}\}$ has been obtained (for the whole protein for lysozyme[1] and myoglobin[2]) using the Debye-Waller factors in x-ray, and for the iron atom using Mössbauer spectroscopy.[3]

None of these measurements contains explicitly the time behavior.

It is generally accepted that proteins, specifically enzymes, undergo conformational transitions in every reaction step.

Conformational flexibility is a biologically important property of proteins systems. There is much evidence, essentially from x-ray diffraction studies, that many enzymes change slightly their conformation upon substrate binding. Molecular flexibility is essential in muscle contraction. Recently it has been suggested that protein flexibility is the key for the understanding of enzyme catalysis.[4] Current explanations of allosteric effects involve molecular flexibility. Molecular flexibility is also essential for some structural proteins TBSV (tomato bushy stunt virus)[5] and to explain some membrane properties.[6] Chain flexibility is a key feature in immunoglobulins.

Flexibility means that a protein can exist in many different substates.

Before we enter into a description of the time events in protein systems, it is important to discuss the molecular origin of the protein flexibility.

1) The structure of the polypeptide chain allows rotations about the ϕ and ψ angles. Essentially barriers to rotation are provided by π bonding in the peptide linkage and in the aromatic rings of the side chains of tyrosine, tryptophan, phenylalanine and histidine. Otherwise the primary barrier to rotational motion is van der Waals repulsion resulting from collision with neighboring components of the protein structure.

2) Interaction with external ions and water molecules produce fluctuations in the protein structure in addition to brownian transfer of momentum. Interacting species such as hydrogen ions and water molecules combine or dissociate from particular sites of the protein. The hydrogen ion equilibria can influence the distribution of charge at substantial distances. This association or dissociation can cause conformation transitions. Hydrogen bonding (water) solvents can cause a redistribution of charge and modify the planarity of the peptide linkage.[7)]

How a protein evolves from one state to another is the main goal of the protein dynamics studies. These studies use both theoretical and experimental methods.

In principle, the set of rate of change $\{K^{\ell}_{j\to k}\} = \{d/dt\ x_{j\to k,\ell}(\underset{\sim}{x}_i,t)\}$ plus some coupling plus some initial conditions and the knowledge of the driving forces will completely describe a protein molecule. It is quite obvious that at the present time such a task cannot be completed, and it may be unnecessary.

It is useful to distinguish the $\{K^{\ell}_{j\to k}\}$ in subsets or branches.

Firstly, it is necessary to distinguish between different classes of time events in relation to their time scale. So we distinguish between "fast" and "slow" processes, fast and slow being defined with respect to some reference time. This division is very important because a fast process with respect to a slow one will be seen as an average distribution and the slow one is seen as a slow variable average by a fast one. The two processes cannot be time correlated one with the other because their cross-correlation function averages to zero very rapidly.

Secondly, there are time events dealing with more than one atom of the protein. So it is possible to divide the protein into parts each of which behaves as a rigid body during the time scale of interest. For example, it is useful in the study of the rotation of the entire molecule to consider the protein as a rigid ellipsoid.

Thirdly, it is useful to divide the time events with respect to the molecular process involved.

Fourthly, division can be made in terms of the biologically significant time events.

With these premises in mind, it is possible now to map the different time events in a protein system specifying their time, the part of the protein involved, the molecular process and their biological significance, if any.

At the very beginning of the time scale, see Fig. 1, we have processes found also in the building blocks of the protein. Generally electronic, vibrational and rotational frequencies are not extremely different from that found in the constituent aminoacids. Fortunately some very important differences exist. These frequencies are often used as a probe to characterize some protein conformation.

In the very low frequency region of the Raman spectrum (10-30 cm^{-1}) some conformational dependent features have been observed in proteins and not in the constituent aminoacids. These motions are thought to involve a large portion of the polymer chain.[8] In this time range some theoretical studies have been very useful in clarifying some features of the molecular motions. The dynamics of a folded globular protein (BPTI bovine pancreatic trypsin inhibitor) has been investigated by Karplus and co-workers by Monte Carlo methods solving the equation of motion for the atoms in the neighborhood of their equilibrium conformation.[9] This study involves the internal dynamics of the protein. The average root-mean-square fluctuation of all atoms is found to be 0.9 Å, which is a quite large value. Moreover the largest mean square fluctuation occurs in the side chain at the protein surface and at the two ends of the backbone. The study of the time dependence of the motions reveals a time constant of 1 ps for the decay of atoms fluctuations, the existence of correlated fluctuations, and the occurrence of concerted motions. This study cannot be extended at larger times because of the complexity of the calculations.

NMR techniques have the greatest potentiality for providing detailed information concerning the rotational mobility of individual sites within the protein molecule. p-NMR provide information on environmental characteristics of aromatic aminoacid.[10] C^{13}-NMR and F^{19}-NMR are used to detect aromatic side chains rotations (Tyrosine in alkaline phosphatase[11] $t = 10^{-7}$-10^{-9} sec) and aliphatic side chains rotations (methyl groups 1-5 ps in aortic elastin[12]) in myoglobin[13] (methionine and alanine 10-20 ps).

At longer times we can distinguish between two broad classes of time events: firstly internal processes involving a large part of the protein molecule, secondly surface processes involving the hydration layer and side chains ionization reactions (see ref. 14).

Internal motions have been detected by a large number of methods in the 10^{-10}-10^{-6} sec range. The molecular processes involved are:

a) skeletal motions at the peptide chain (NMR),
b) side chains rotations (NMR, fluorescence),
c) fast isomerizations involving a large part of the protein (spectroscopic relaxation studies),
d) exposure of some internal groups to the solvent (spectroscopy),
e) rotation of the entire molecule (fluorescence-NMR),
f) helix-coil transitions (spectroscopy-ultrasound-NMR, fluorescence)

Surface processes in this time range have been detected both in the hydration layer using dielectric methods and in the side chains ionization reactions using both spectroscopic and ultrasonic methods.

At a longer time scale processes involving the entire protein molecule have been detected. Folding-unfolding transitions require times of the order of 10^{-1}-10^{2} seconds. From dynamic studies of the protein structure

TIME EVENTS IN PROTEIN SYSTEMS (AMBIENT TEMPERATURE)

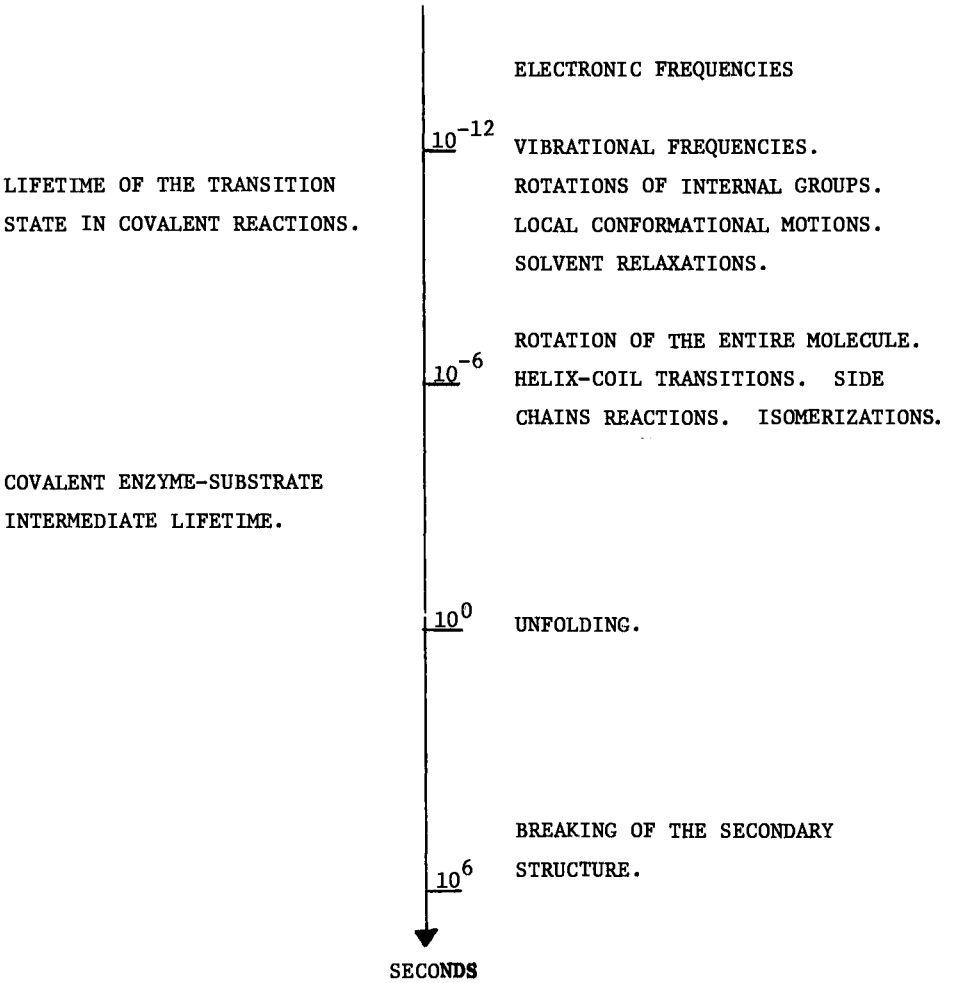

Fig. 1

it appears that a protein exhibits a great flexibility. The frequency and the amplitude of the motions resemble a liquid state. However, many other observations, such as the melting profile, crystallization processes, mechanical properties, packing densities, specificity of the enzymes, point towards a more rigid and solid structure. To solve this basic controversy, a deeper understanding of the intimate protein structure is necessary.

BIBLIOGRAPHY

1) Artymiuk, P. J., Blake, C. C. F., Grace, D. E. P., Oatley, S. J., Phillips, D. C. and Sternberg, M. J. E. Nature (1979) 280, 563-568.

2) Frauenfelder, H., Petsko, G. A., Tsernoglou, D. Nature (1979) 280, 558-563.

3) Dwivedi, A., Pederson, T., Debrunner, P. G. (1978) J. Physique (1979) 40, C2-521.

4) Careri, G., Fasella, P., Gratton, E. Ann. Rev. Biophys. Bioeng. (1979) 8, 69-97.

5) Harrison, S. C., Olson, A. J., Schutt, C. E., Winkler, F. K. and Bricogne, G. Nature (1978) 276, 368-373.

6) Bloom, M. Cand. J. Phys. (1979).

7) Careri, G., Giansanti, A. and Gratton, E. Biopolymers (1979).

8) Brown, K. G., Erfurth, S. C., Small, E. W. and Peticolas, W. L. PNAS USA 69, 1467 (1972).

9) McCammon, J. A., Gellin, B. R. and Karplus, M. Nature (1977) 267, 585-590.

10) Wütrich, K. (1976) Nuclear Magnetic Resonance in Biological Research. Peptides and Proteins. North Holland, Amsterdam.

11) Hull, W. H. and Sykes, B. D. (1975) J. Mol. Biol. 78, 121-153.

12) Urry, D. W. and Mitchell, L. (1976) Biochem. Biophys. Res. Comm. 68, 1153-1160.

13) Jones, W. C., Rothgeb, T. M. and Gurd, F. R. N. (1976) J. Biol. Chem. 251, 7452-7460.

14) Careri, G., Fasella, P. and Gratton, E. (1975) CRC Crit. Rev. Biochem. 3, 141-164.

Adv. Physiol. Sci. Vol. 3. Physiology of Non-excitable Cells
J. Salánki (ed.)

TIME DIMENSION OF CELLULAR METABOLIC PROCESSES

B. Hess and A. Boiteux
Max-Planck-Institut für Ernährungsphysiologie, Dortmund, FRG

I. INTRODUCTION

Time domains of integrated processes in cells or multi-cellular systems result from the individual times of the controlled rates of formation and degradation of the respective metabolites as well as from the times of their transport. Whereas the classical description of cellular processes in terms of enzyme kinetics relies on equilibrium conditions, yielding kinetic properties of "simple and fast" Michaelis-Menten enzymes and "complex and slow" regulatory allosteric enzymes, an understanding of integrated processes relies on the "far from equilibrium" condition, where kinetics might be dependent upon the size and geometry of cells and bodies (1). The function of *in vivo* processes results from the rapid cooperation of free and spatially fixed enzyme sequences, the individual enzyme species in a set serving with some hundred thousands or only a few molecules per cell.

In vivo we observe a large variety of dynamic states in time and space as specific phenomena of living systems: not only classical steady states, but also different types of transitions and oscillations, excitability and dynamic spatial inhomogeneity such as signal transmission over distance, wave propagation and time-dependent spatial patterns which are indeed "dynamic structures". The multiplicity of states being observed in recent years led to a reinvestigation of the time properties of cellular processes and results in the recognition of the creative function of instability, in contrast to the earlier concepts of cellular homeostasis and homogeneity (2).

The true time domains of cellular processes are not immediately displayed by steady state phenomena - rare events in nature or experimental tricks - but rather by careful observation of system instabilities, which may yield turnover and space dimensions from the measured transition times of the respective processes; for example, the periodic and recycling phenomena in metabolism, the mitotic cycle and life cycles of morphogenesis and differentiation of cell populations.

In the following presentation we describe the time domains of some cellular processes of general significance. We treat separately, the domains resulting from a record of enzymic turnover times and the domains resulting from the spatially dependent transport in a given cellular volume, although we know that both are interconnected. It takes time to activate or deactivate enzymes and permeases, to produce and to consume, and it takes time to fill up or deplete a concentration space.

II. TIME DOMAINS OF TURNOVER

1. Steady states

The time domains of metabolic processes are set by the genetic map controlling structure and concentration of metabolic enzymes in a given volume, and thus, determining the kinetic parameters. We realize a perfect kinetic fitting between individual members of the two energy producing pathways of the cell, namely oxidative phosphorylation and glycolysis, though their overall kinetic half-times are quite different. The half-times of kinetics of electron transfer reactions in the cytochrome c segment of the respiratory chain are 1 to 2 msec (3), whereas the glycolytic reactions are about 10 times slower. In general, the concentrations of the catalytic sites of glycolytic enzymes are in the order of 10^{-4} to 10^{-6} molar which is equimolar to many glycolytic intermediates. Most of the glycolytic enzymes are saturated only to about 20% with their respective substrates (4). In fact, this low saturation would yield a rather quick response time, however, most of the time to set the steady state is used for the respective conformational changes of the regulatory enzymes phosphofructokinase and pyruvate kinase. Obviously, velocity here is sacrificed for quality of control. Of course, steady states themselves are silent for the experimentalist and only the rates of input and output indicate the kinetic behaviour of the system.

2. Transient states

The investigation of transition from one steady state to another reveals the "time of operation" of the respective metabolic process. With the help of spectroscopic techniques such transitions can be recorded directly, displaying the time domains we are interested in (5). Well-known transitions are the metabolic responses triggered by the initiation of anaerobiosis or aerobiosis, and the depletion or addition of substrates and enzymatic effectors such as ethanol, glucose or ammonium ions for the carbohydrate metabolism. All of the indicated examples shift well defined metabolic processes from one state to another, and direct recording allows demonstration of the transition times which are necessary to coordinate the various processes until the new state is reached (6).

A typical record of the light absorption of reduced nicotinamide adenine dinucleotide (NADH) in a suspension of yeast cells, given in figure 1, demonstrates first the transition from endogenous respiration to a glycogenetic state triggered

by the addition of ethanol, and later, the transition from glycogenesis to glycolysis triggered by the addition of glucose. We observe transition times in the range of seconds to a minute. The latter case also illustrates the complexity of the transition control which is by no means monotonic, but indicative of classical feedback undershoot and overshoot phenomena (7).

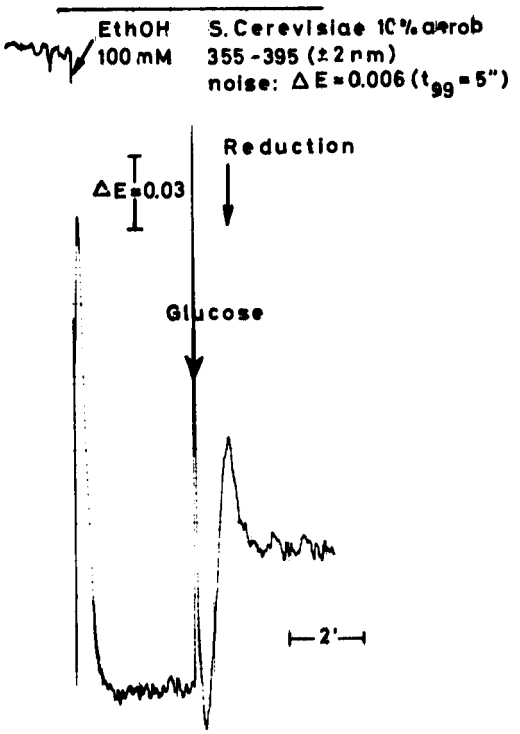

Figure 1
Transition between glycogenesis and glycolysis in yeast cells. A well-stirred aerobic suspension of yeast cells (*S. carlsbergensis*, 10g/100ml) was monitored for changes of intracellular concentration of NADH with a double beam spectrophotometer (λ_1 = 355 nm, λ_2 = 395 nm). Additions of ethanol and glucose shift the redox state of NADH towards reduction and oxidation, respectively, indicative of transitions from endogenous respiration to glycogenesis and from glycogenesis to glycolysis.

3. Oscillatory states
Since the early sixties, oscillatory states have been observed in a large number of cellular processes (1,8,9). In particular, the oscillation of glycolysis allows the study of the large range of its dynamic domain. During oscillation, glycolysis passes through a large range of dynamic states from maximal to

minimal activity of controlling enzymes, with periods between 10 and 100 seconds, A typical example is given in figure 2. The oscillation of (NADH) in a suspension of yeast cells is recorded. The figure demonstrates the time course of the process from the moment when glucose was started to be injected at the rate of 220 m moles per liter per hour to a suspension in anaerobic conditions. Following a short transition time, steady and undamped NAD/NADH oscillations are recorded with a period of 19.6 seconds and a standard deviation of $\pm$ 3.5% (n=15). The record is a section of a series of over 65 cycles (10).

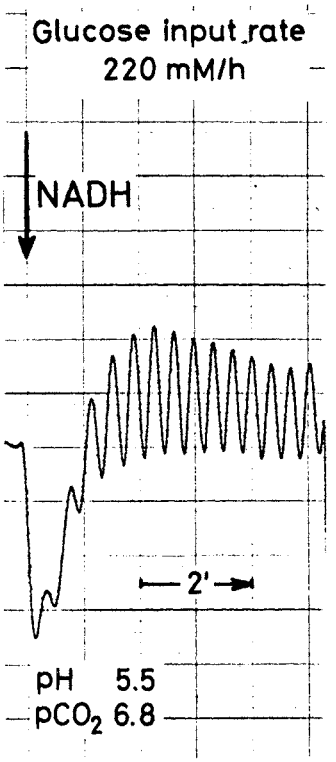

Figure 2
Autonomous oscillation between different glycolytic states in yeast cells. An aerobic suspension of yeast cells (see Figure 1) was injected with a constant flux of glucose (input rate 220 mM per hour). The oscillating trace of the intracellular concentration of NADH indicates periodic changes of glycolytic activity.

Studies of the mechanism of oscillation in glycolysis carried out in yeast extracts have shown that the component responsible for these dynamics is the glycolytic master enzyme phosphofructokinase. This enzyme changes its activity periodically between 1% and 70% of its maximal activity for a given glycolytic flux with periods in the order of minutes. The longer period observed in yeast extracts as compared with intact yeast cells results from dilution of enzymes and intermediates. Model studies in agreement with experimental results show that the period is a complex function of the enzyme concentration and the allosteric kinetic constants: with increasing enzyme concentration, the period shortens for a given overall flux (11,12). Thus, the period of glycolytic oscillations reflects the kinetic design of the master enzyme phosphofructokinase which sets the overall time domain for glycolysis. The oscillation between maximal and minimal glycolytic flux can not reach a higher frequency than the kinetic properties and concentration of phosphofructokinase allow, within a given set of source and sink enzymes.

4. Glycogenesis versus Glycolysis

Time domains of alternation of metabolic processes can also be recorded for the switch from glycogenesis to glycolysis (7,2, 13). Figure 1 demonstrates the relevant transition, which involves inactivation and activation, respectively, of the two enzyme pairs Fructosebisphosphatase/phosphofructokinase and phosphoenol pyruvate carboxykinase/pyruvate kinase. This concerted switching is responsible for the change from glycogenesis to glycolysis. The complex events involved in the onset of the reciprocal inactivation and activation mechanisms of the two pairs of controlling enzymes are the basis for the time range of the transition, which is in the order of seconds to minutes. Though in this context we cannot go into detailed discussion, we want to point out that nature has developed interesting measures to suppress the respective back-reaction effectively in order not to waste energy on futile recycling (see 2).

III. TIME DOMAINS OF TRANSPORT

The intricate coupling of enzymic transformations and transport processes generates a dynamic pattern in time and space of living matter which is essentially inhomogeneous. If transport is fast and transformation limiting slow, intermediates pile up. If transport is limiting slow and transformation fast, steep gradients might occur. The question is how the balance between the two operations is set. The classical volume to surface rule of physiology documents that indeed, metabolic processes depend critically upon spatial dimensions. The flow of substrates and products through the cellular surface seems to be critically matched to the metabolic capacity within the cellular volume. The same balance holds for multicellular systems.

Within the context of this discussion, a consideration of the time domain for transport should relate the capacity for and the velocity of, active transport processes located on the surface of the cell wall, to the capacity and rate of chemical transformation within the cell. In general, we might agree that the kinetic constants of active transport processes are in the range of more or less complex enzymic reactions and only the vectorial feature is added. We expect that the turnover/transfer times for sugar uptake, for example, fit the time of glycolytic turnover.

A simple calculation can give a first approximation to the relation of intracellular transport and turnover. A yeast cell such as *Saccharomyces carlsbergensis* contains soluble glycolytic enzymes in the order of some 10^{-3} molar. This concentration yields an average distance of 400 to 500 Å between enzymic units computed for homogeneous distributions of the enzymes. With this spatial distribution at hand, it is possible to estimate the time of transit of the product of one enzyme from its product releasing site to the substrate binding site of the next enzyme in the glycolytic pathway. For a small molecule like pyruvate, we calculate a transient time between collisions on the active site in the range of some ten microseconds. This is short in comparison to the turnover numbers of the glycolytic enzyme system in the range of some 100 per second per binding site. Although the above calculation neither compensates for the rather different concentrations of various enzymic species, nor takes into account any geometrical or stereochemical considerations, one might conclude that the packing of glycolytic enzymes, at least in yeast cells, is sufficiently dense to prevent diffusion from playing a limiting role.

In order to test the validity of this statement for supercellular dimensions,we recently searched for conditions of spatial inhomogeneities in highly concentrated glycolytic yeast extracts. Using a two-dimensional display of NADH absorbance to detect inhomogeneous distributions of NADH in the glycolyzing system, we observed that spatial analysis readily reveals phenomena of excitability, of signal transmission, propagation, interference of waves, as well as the development and transformation of spatial temporal pattern. Since the glycolytic process is excitable, we found that a local trigger signal can be propagated as a spatiotemporal pulsed signal. The velocity of the propagated pulse is almost two orders of magnitude faster than calculated for propagation by diffusion only. The rate of propagation of an ATP pulse of 0.5 µ mole was 4.8 µm per second. This experiment demonstrates the possible rate for a chemical pulse to propagate over supercellular distances (15,16).

The propagation rate of a supercellular phenomenon can directly be recorded during the life cycle of the slime mould *Dictyostelium discoideum*. After the end of growth,a large population of slime mould cells aggregates in response to chemotactic stimuli

to form the fruiting body. Center cells within such an aggregation territory suddenly start to release periodic pulses of cyclic adenosine monophosphate (cAMP) toward the periphery with a frequency of 0.2 - 0.3 per minute. The cells around the center respond by oriented cell movement and by reproducing the trigger pulse, to which their neighbours respond in just the same way, reproducing the trigger pulse in a relay fashion after a signal input/output delay of approximately 15 seconds. So waves of chemotactic pulses can be propagated over a distance much larger than the chemotactic action radius of a single aggregation center. The speed of wave propagation with a wavelength of 230 µm is about 43 µm per minute. This corresponds to 0.72 µm per second with a pulse height of roughly 15 µM. During the 15 seconds relay time enzymic synthesis leads to an intracellular accumulation of cyclic guanosine monophosphate (cGMP) and cAMP.

The periodic intracellular generation of cGMP and cAMP is coupled with a large number of other intracellular reactions. Using the redox state of cytochrome b or light scattering to monitor intracellular events, we have recorded periodic signals with the frequency of 0.2 per minute. These experiments clearly show that a critical balance between the periodic enzymic synthesis of cAMP as a chemical signal and its transport through the cellular wall right into intercellular space in form of chemical pulses, is a prerequisite for the operation of the biological aggregation process of *Dictyostelium discoideum*.

Interestingly enough, this phenomenon does not rely on a linear gradient established by local enzymic synthesis for transport of metabolites and propagation of signals, but on discrete periodic pulsing. Obviously a pulse mode of operation is more effective for information transfer.

The slime mould *Dictyostelium discoideum* demonstrates macroscopically the perfect coupling of controlled enzymic processes and transport of chemicals. In the future, this system might serve as a biological model to evaluate in more detail, the time dimensions of transport processes and signal propagation over spatial distance.

IV. REFERENCES

1. G. Nicolis and I. Prigogine
   Self-Organization in Nonequilibrium Systems
   John Wiley & Sons, New York, London, Sydney, Toronto
   (1977)

2. A. Boiteux, B. Hess and E.E. Sel'kov
   Creative Functions of Instability and Oscillations
   in Metabolic Systems
   In: Current Topics in Cellular Regulation, 17,
   171-180 (1980)

3. B. Chance
   Biochem. J. 103, 1-18 (1967)

4. B. Hess, A. Boiteux and J. Krüger
   Advances in Enzyme Regulation 7, 149-167 (1969)

5. B. Chance and B. Hess
   Spectroscopic Evidence of Metabolic Control
   Science 129, 700-708 (1959)

6. B. Chance
   Faraday Society Discussions, No. 20, 205-216 (1955)

7. B. Hess
   Organization of Glycolysis: Oscillatory and
   Stationary Control
   In: Rate Control of Biological Processes
   Cambridge: At the University Press XXVII, 105-131
   (1973)

8. B. Hess and A. Boiteux
   Hoppe-Seyler's Z. Physiol. Chem. 349, 1567-1574
   (1968)

9. A. Goldbeter and S.R. Caplan
   Ann. Rev. Biophys. Bioeng. 5, 449 (1946)

10. A. Boiteux, A. Goldbeter and B. Hess
    Proc. Nat. Acad. Sci. USA, 72, 3829-3833 (1975)

11. A. Goldbeter and R. Lefever
    Biophys. Journal 12, 1302-1315 (1972)

12. C.J. Barwell and B. Hess
    FEBS Lett. 19, 1-4 (1971)

13. B. Hess and A. Boiteux
    Heterologous Enzyme-Enzyme Interactions
    In: Protein-Protein Interactions
    Eds. R. Jaenicke, E. Helmreich
    Springer Verlag Berlin, Heidelberg, 271-296 (1972)

14. A. Boiteux and B. Hess
Visualization of Dynamic Spatial Structures in Glycolyzing Cell-Free Extracts of Yeast
In: Frontiers of Biological Energetics
Eds. P.L.Dutton, J. Leigh, A. Scarpa
Acad. Press Inc. New York, San Francisco, London
789-798 (1978)

15. A. Boiteux and B. Hess
Spatial Dissipative Structures in Yeast Extracts
Ber. Bunsenges. Phys. Chem. 84, 346-351 (1980)

16. G. Gerisch
Naturwissenschaften 58, 430-438 (1971)

17. G. Gerisch, D. Hülser, D. Malchow and U. Wick
Phil. Trans. R. Soc. Lond. B. 272, 181-192 (1975)

18. G. Gerisch, Y. Maeda, D. Malchow, W. Roos, U. Wick and B. Wurster
Cyclic AMP Signals and the Control of Cell Aggregation in Dictyostelium discoideum
In: Developments and Differentiation in the Cellular Slime Moulds, Eds. Cappuccinelli and Ashworth
Elsevier/North Holland, Biomedical Press
105-124 (1977)

19. G. Gerisch and B. Hess
Proc. Nat. Acad. Sci. USA, 71, 2118-2122 (1974)

20. G. Gerisch, D. Malchow, W. Roos and U. Wick
J. exp. Biol. 81, 33-47 (1979)

Adv. Physiol. Sci. Vol. 3. Physiology of Non-excitable Cells
J. Salánki (ed.)

STRUCTURE AND DYNAMICS AT MOLECULAR AND CELLULAR LEVELS

S. Damjanovich, L. Trón and B. Somogyi
Department of Biophysics, Debrecen University School of Medicine, Debrecen, Hungary

Molecular as well as cellular events take place in a certain time period and space. The translational and rotational diffusion coefficients are inversely related to the diameter of spheric molecules. The latter has a relationship also to the minus third power of the diameter. Thus it can be stated that the smaller the molecule the faster the motion one can observe at a certain temperature. A similar rule is valid for the vibrational motions of different groups belonging to macromolecules. Since the early experimental approach of Linderstrøm-Lang (1959) many experimental attempts have been made to follow the dynamics of the molecular and cellular events. As Fig.1. demonstrates the available physical methods are also confined to time intervals, therefore in order to study a particular type of motion of our interest we have to select the method having the right correlation time. One of the most intriguing problems in the category of molecular motions is the existence of correlation between protein dynamics and function. This topic has been in the focus of interest since long, however, the decisive evidence is still incomplete. For example to answer the seemingly primitive question if the protein dynamics plays a role in the catalytic ability of enzymes proves to be very difficult. The reason for these adversities comes partly from the manybody problem if we attempt to approach the question on theoretical i.e. quantum chemical grounds. The question is even more complicated than the exact description of the motion of a protein molecule, since the environment and the macromolecular entities have a continuous dynamic energy exchange. Taking into account that the physiological environment of intra- and extracellular macromolecules (e.g. enzymes) is an aqueous solution, furthermore, that the water as a fluid is a very problem-

atic physical entity from dynamic point of view, the theoretical description of energy transfer processes and fluctuations of macromolecules in solutions is rather beyond our present possibilities. McCammon and Karplus (1979) made reputable progress in this field, however, a real breakthrough is still missing.

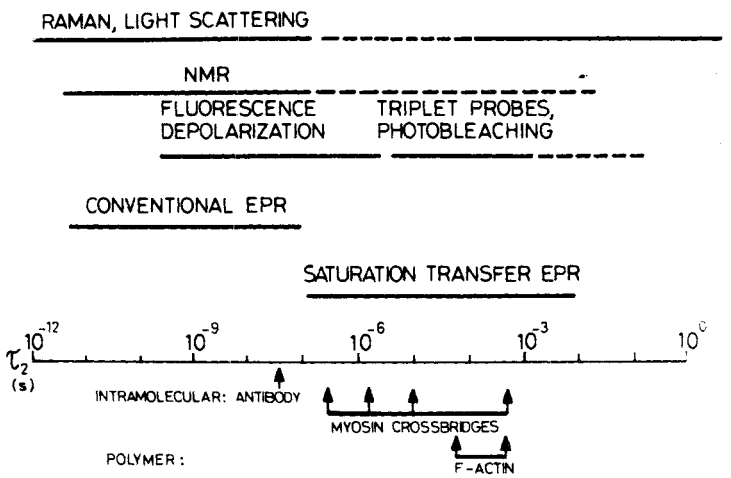

Fig. 1 Overlaps between correlation times and time limits of different methods.

In spite of this pessimistic view considerable efforts have been made in this field. Since the principal aim of the present communication is to introduce our theoretical and experimental work concerning the correlation between macromolecular dynamics and function, we mention here only a few of

the most important works concerning this topic. Green and Ji (1972) elaborated the theory of Electro-Mechano-Chemical energy transduction of the enzymes. A further extension of their work was the piezoelectric theory of Caserta and Cervigni (1974). Gavish (1978), and Gavish and Werber (1979) revived the four decades old (and long forgotten) theory of Kramer's, attributing great importance to environmental viscosity in the enzyme catalysis. Quite a number of other authors dealt with the relationship between ligand binding and fluctuation. The most significant results were gained by Nakanishi and coworkers, and also by Frauenfelder and coworkers (Nakanishi et al., 1972; 1973; Alberding et al., 1978; Austin et al., 1975; Frauenfelder et al., 1979). A well written review of Gurd and Rothgeb (1979) summarizes a part of the relevant experiments.

Our Molecular Enzyme Kinetic Model applied the conception of protein fluctuation and protein-solvent interaction. The significant difference between our theoretical model and most of the contemporary ones was that it took into account the whole protein molecule and besides the specific ligand-protein interaction the dynamic energy exchange of every solvent molecule. The real uniqueness of the MEKM comes from its using manifest physical parameters like environmental microviscosity, mass distribution of the solvent molecules, collisional frequency of the environmental and protein particles (Somogyi and Damjanovich, 1971; 1975; Damjanovich and Somogyi, 1971; 1973; 1978; Somogyi et al., 1978). As a result of the energetic and also stochastic considerations of the model, for example the phenomenological kinetic constants of such simple reaction scheme as

$$E + S \underset{k_{+1}}{\overset{k_{-1}}{\rightleftharpoons}} E\,S \xrightarrow{k_2} E + P \qquad (1)$$

where E, S and P are the enzyme, substrate and product concentrations can be expressed as:

$$k_2 = P_s \cdot \xi \cdot \frac{k\,T}{\mathfrak{N}\,\lambda^2\,\eta\,\bar{\xi}} \cdot \exp\,(-E_p/kT) \qquad (2)$$

or

$$k_{-1} = P_s \frac{k\,T}{\mathfrak{N}\,\lambda^2\,\eta\,\bar{\xi}} \left[(\exp\,(-E_d/kT)\,) - \xi \cdot (\exp\,(E_p/kT)\,)\right] \qquad (3)$$

It can be seen that the rate constants of the decomposition of the ES complex, k_{-1} and k_2 are dependent, besides the well-known Boltzmann factor (kT), upon several parameters having direct physical meaning, characterizing the environment and the enzyme. k_2 and k_{-1} are inversely proportional to the environmental microviscosity (η), the average mass distribution ($\bar{\xi}$), and the lattice distance (λ) characterizing the liquid environment. The P_s and ξ are parameters of the enzyme and the environment as well. E_d and E_p are the energies necessary to dissociate the ES complex into E + S or E + P. Without going into further details (described earlier: Somogyi and Damjanovich, 1975; and Damjanovich and Somogyi, 1978), one can see that the protein fluctuation is included in these equations. The source of such a fluctuation is the mutual energy exchange between environment and macromolecules, described by the energetic factors. The more elaborated expressions (see cit. above) show that the model predicts that both pre-exponential and exponential factors of the equations describing k_2 and k_{-1} rate constants have parameters depending upon the mass composition and microviscosity of the aqueous environment. The former may mean a completely new type of enzyme regulation determined by the environment.

It seems to be relevant to call the attention at this point to the fact that all of the collisional phenomena generating the effects on an enzyme or enzyme-substrate complex have a very different time scale compared to the turnover number of enzyme catalysis. The duration of collisional phenomena for small environmental "particles" is in the range of the frequency of group vibrations i.e. between 10^{-13} and 10^{-12} sec. The small amplitude oscillations of relative distances between various parts of proteins and the large scale fluctuations involving a bigger part of the protein studied by Eftink and Ghiron (1975; 1977), Lakowitz and Weber (1973), and by many other authors (see Gurd and Rothgeb, 1979) belong to the time interval of 10^{-10} - 10^{-8} sec. The average turnover time i.e. the ensemble time average of an ES $\longrightarrow$ E + P transition is generally in the millisecond range. The apparent contradictions can easily be solved if we take into account the P_s probabilistic factor, describing a structure specific collisional pattern, necessary to excite the ES complex and to initiate the transition.

The most conveniently detectable prediction of the MEKM is the effect of viscosity upon catalysis. Changes in enzyme catalysis and regulation were extensively studied while increasing the environmental viscosity and

assuming that the latter must impair the protein fluctuation (e.g. Damjanovich et al., 1972; Laurent and Obrink, 1972; Trón et al., 1976; Jancsik et al., 1976; Varga et al., 1978; Gavish and Werber, 1979). It was a significant observation that upon increasing the environmental microviscosity we may also influence the colloidal properties of the proteins themselves (Jancsik et al., 1976).

The significance of the large amplitude fluctuations, however, was finally established only in the case of the ligand binding of lyzozyme and myoglobin (Nakanishi et al., 1972; 1973; Frauenfelder et al., 1979).

This paragraph of the present communication intends to pursue an experimental line in order to find a possible correlation between the fluctuation and enzyme activity in the same protein simultaneously. As to our knowledge no such experimental attempts have been made. The results of Matkó et al. (1980) can shortly be summarized as follows:

The key enzyme of the glycogen metabolism, the phosphorylase b was selected as test enzyme. It has the advantage of allosteric regulation by an obligatory activator the AMP, and the binding ability of several specific substrates like glucose-1-phosphate (G-1-P), glycogen and inorganic phosphate. We assumed that these facts facilitated the possibility to find a correlation between the fluctuation of the dimeric form of the enzyme (Mw: 185,000 dalton) and the activity. The crucial point of the planning was to find such a method to pursue the fluctuation of the protein matrix where the experimental conditions were compatible with those of the physiological function and regulation of the enzyme. Luckily enough, Eftink and Ghiron (1975) introduced the acrylamide, a small molecular weight (70 dalton), rather inert compound to study the fluorescence quenching of tryptophan residues in proteins. The dynamic quenching of the tryptophans served as a measure of the diffusibility of acrylamide inside the protein matrix. The diffusion of the acrylamide was highly influenced by the nanosecond time scale fluctuation of the protein matrix. Thus the collisional quenching of the tryptophans could serve as a measure of the fluctuation. On the other hand, Eftink and Ghiron have already observed that the acrylamide caused an almost negligible but well defined decrease in the enzyme activities they studied (Eftink and Ghiron, 1977).

In our experiments two lines were followed parallel. On one hand the tryptophan quenching of the twelve tryptophan residues of phosphorylase b served as a measure of the fluctuation of the protein. On the other hand

the decrease in the activity of the enzyme caused by the quencher acrylamide provided a tool for looking towards a possible correlation between fluctuation and catalysis.

The quenching experiments were made with acrylamide concentrations, tested as nondenaturing quantities concerning the enzyme activity. The tryptophan fluorescence of the phosphorylase b was quenched with 0-0.8 M concentration of the acrylamide. The emission spectra of tryptophyl residues of the phosphorylase b are structured. A small shoulder on the right side of the emission peak could easily be identified and probably was due to tryptophyl side chains situated on or near the surface of the protein. Increasing acrylamide concentrations causing greater and greater quenching of the fluorescence at every wavelength, did not cause shifts or changes of a gross, possible quencher induced conformational change of the protein. The Stern-Volmer plot of acrylamide quenching was found to be linear until 0.5 M concentration of acrylamide (Fig.2).

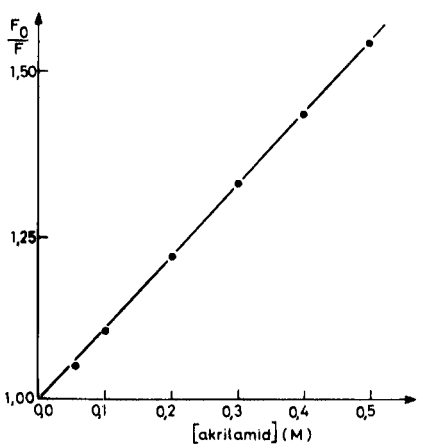

Fig.2 Stern-Volmer plot of acrylamide quenching of tryptophan fluorescence in phosphorylase b enzyme.

Similar quenching experiments carried out with water soluble KI revealed the existence of different classes of tryptophan fluorophors in the enzyme. According to these results only three tryptophans out of the total twelve per monomer enzyme were exposed to the solvent. Thus two further questions had to be answered before interpreting the acrylamide quenching as a measure of the fluctuation of the protein matrix. The first one was the collisional fashion of the quenching itself. It was supported by fluorescence lifetime measurements where in the presence of acrylamide the singlet lifetime of the tryptophans was decreased in the same extent as was the decrease in steady state fluorescence. The second question, namely the number of fluorophors accessible to the quencher in different conditions was calculated using the modified form of the Stern-Volmer plot (Fig.3).

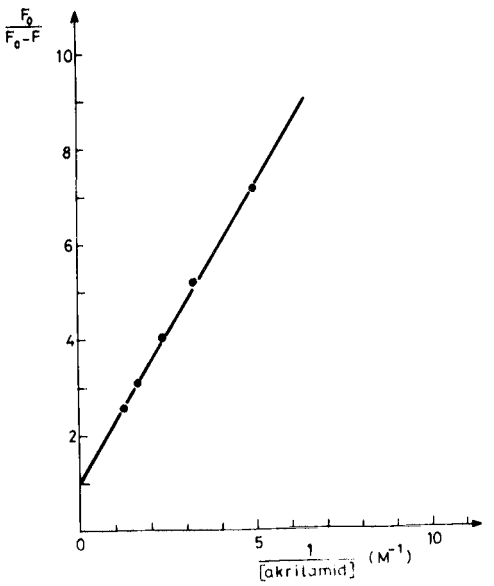

Fig.3 Modified Stern-Volmer plot shows that acrylamide penetrates the interior of phosphorylase b enzyme. The native tryptophan fluorescence is completely quenched at infinite acrylamide concentration.

The results provide straightforward evidence for the permeation of acrylamide molecules to the interior of phosphorylase b since at infinite acrylamide concentration all of the tryptophans were quenched. The straight line also shows that acrylamide penetrates the protein equally at low concentrations. Thus one could conclude that the acrylamide caused quenching served as a measure of the protein fluctuation itself. Thermodynamic analysis of the relevant Arrhenius plots also supported this view.

While increasing the concentration of the acrylamide from 0 to 1 M a monotonous decline in the enzyme activity was observed. As it is shown in Fig.4 the acrylamide did not have any influence on the binding parameters of specific ligands responsible for the catalytic activity and the allosteric regulation of the enzyme.

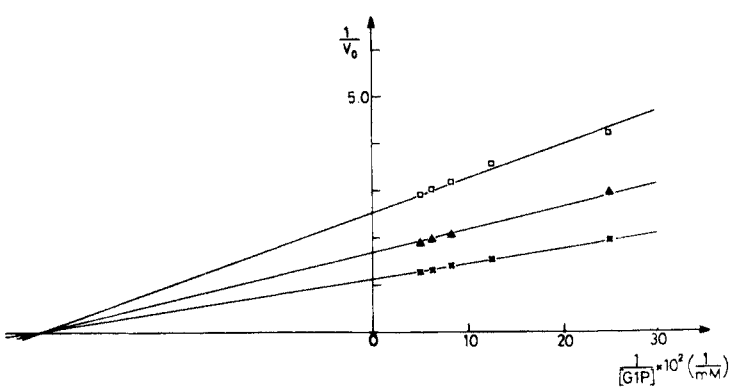

Fig.4 Lineweaver-Burk plot of the activity of phosphorylase b. The G-1-P K_m was not changed at 0.4 (▲-▲) and 0.8 M (□-□) acrylamide concentrations compared to the control (x - x).

The Lineweaver-Burk plot demonstrates only the effect of acrylamide on the G-1-P binding, however similar results i.e. unchanged K_m values were found also with glycogen and AMP. It is noteworthy to observe the significant decrease in the maximal rate of the enzyme action. The intersection of the curves with the $1/V_o$ axis were higher at higher acrylamide concentrations.

The Fig.5 shows the surprisingly linear and very good correlation between the decrease in V_{max} and the quenching of tryptophan fluorescence at different acrylamide concentrations.

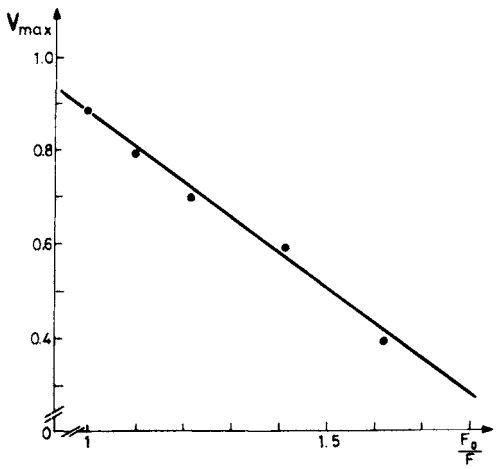

Fig.5 The decrease in the V_{max} of phosphorylase b shows a linear correlation with the decrease of the fluorescence of tryptophan residues upon adding increasing amounts of acrylamide.

The experimental findings in full accord with the theoretical predictions supported the following interpretation:

The quencher molecule, the acrylamide penetrates the protein matrix and colliding with the masked as well as non-masked tryptophans causes a

dynamic quenching. The number of acrylamide molecules per enzyme, assuming an even distribution between solvent and proteins seems to be enough to "fill up" the interior of the protein molecules so as to put a restraint on the internal motion freedom of the different parts. Accepting the necessity of a certain fluctuational freedom of the protein matrix in order to exert the catalytic function of the enzyme, the decreased activity in the presence of acrylamide can easily be explained even without the impairment of ligand binding. Of course the acrylamide molecules inside the protein can also prevent the development of the correct fluctuation pattern resulting in the activation of the enzyme-substrate complex. By such a quasi-mechanical way the acrylamide would produce such a non-competitive inhibition of the enzyme that only the pre-exponential factor of the maximum velocity changes and the activation enthalpy remains constant as it is supported by the thermodynamic analysis of our data.

Besides the ever growing in vitro experimental evidence supporting our theoretical predictions formulated almost one decade ago, the same ideas may suggest experiments to be exploited for in vivo systems. The microscopic viscosity changes may also influence enzyme action and regulation in vivo.

Szöllösi et al. (1980) investigated the rate of fluorescein diacetic acid (FDA) hydrolysis in normal and leukaemic lymphocytes. FDA, a non-fluorescent compound itself is split by nonspecific esterases of the cytoplasm into fluorescein and acetic acid residues. The released fluorescein either accumulates in the cells or effluxes. The esterase activity of the cells can easily be followed by monitoring the fluorescence of the liberated fluorescein. The MEKM was tested in a way by changing the osmolality of the aqueous environment of the cells. Such a change in osmolality is supposed to change the properties of the cytoplasmic matrix, e.g. the microscopic viscosity of the different intracellular compartments, the structural organization and the cell membranes, etc.

The Fig.6 shows a typical kinetics of the esterase activity of normal cells at four different osmolality values (A, B, C, D). The time kinetics was not affected in a great extent in this case. However, a similar experiment, using leukaemic cells of certain strain of mice (AKR:LatixC3H/Ho-mg: Lati/F_1 hybrids) did show a significant sensitivity towards the environmental osmolality (Fig.7).

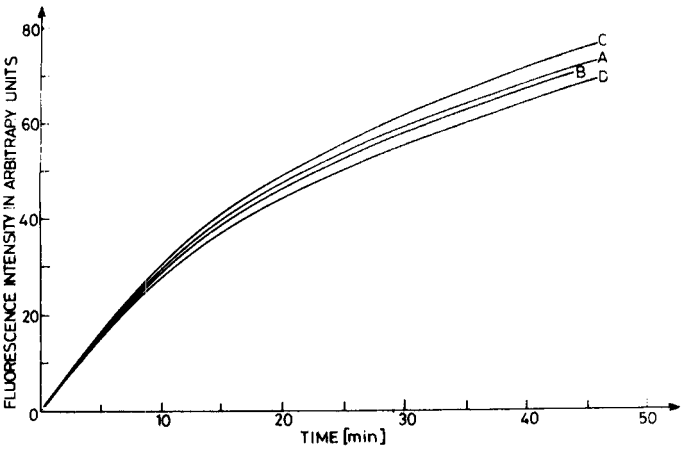

Fig.6 Time kinetics of fluorescein diacetic acid hydrolysis of normal mouse lymphocytes at different osmolality levels.

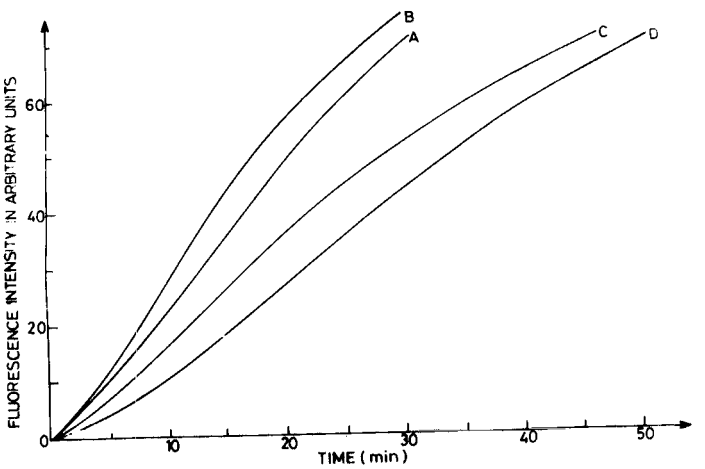

Fig.7 Time kinetics of fluorescein diacetic acid hydrolysis of leukaemic mouse lymphocytes at four different osmolality levels increasing from A to D.

The experiments were carefully repeated with the homogenates of both cell types. In this case there was no difference between normal and leukaemic cells since neither type showed a sensitivity of esterase activity towards the changing osmolality. Another kind of plot of the data shows the viscosity dependence of intact leukaemic and resistance of normal cells (Fig.8).

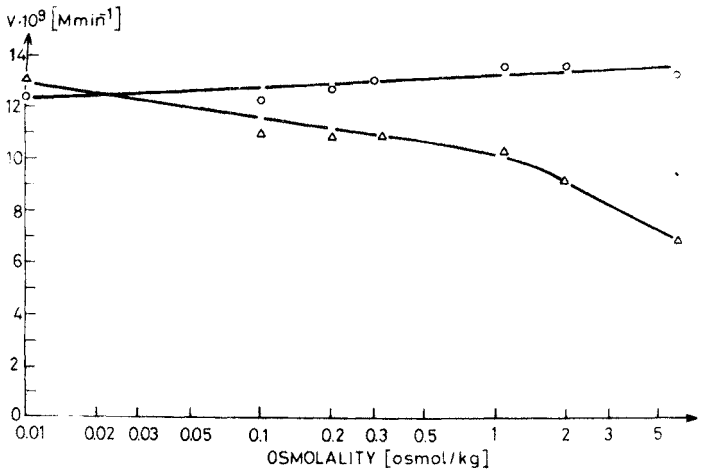

Fig.8 Environmental osmolality dependence of fluorescein diacetic acid hydrolysis of normal (o - o) and leukaemic (-) mouse lymphocytes.

The thorough analysis carried out by Szöllösi et al. (1980) with cell suspensions and also with fluorescence activated cell analysis at single cell level revealed that fluorescein, the product of the hydrolysis accumulates in leukaemic lymphocytes, whereas it easily effluxes from normal ones. The analysis made by flow microfluorimetric methods provided evidence that the fluorescein content of large leukaemic lymphocytes was three times higher than that of normal ones. The observed differences, specific for lymphoid leukaemic cells can be interpreted as differences in the structural organization of the two cell types. This is supported by the negative findings with cell homogenates. Although a cell is far more complicated than a molecular system we believe that the overall mechanism of the action of the

altered environmental osmolality is similar to that predicted by the MEKM. The unquestionable differences between these effects upon normal and leukaemic cells can easily be explained by differences in the structural organization of the esterases. Of course at present the cellular system are not so well understood in these aspects as to carry out a more elaborated analysis. However, in vitro, better approachable systems may suggest tools to characterize differences between important cell types.

REFERENCES

Alberding,N., Frauenfelder,H. and Hanggi,P. (1978): Stochastoc theory of ligand migration in biomolecules
Proc.Natl.Acad.Sci.USA 75, 26-29.

Austin,R.H., Beeson,K.W., Eisenstein,L., Frauenfelder, H. and Gunsalus, I.C. (1975): Dynamicx of ligand binding to myoglobin
Biochemistry 14, 5355-5373.

Caserta,G. and Cervigni,T. (1974): Piezoelectric theory of enzymic catalysis as inferred from electro-mechanochemical principles of bioenergetics.
Proc.Natl.Acad.Sci.USA 71, 4421-4424.

Damjanovich,S. and Somogyi,B. (1971): Viscosity and Enzyme Kinetics.
Proceedings of the First Biophysical Congress, Vol. 6. WMA Verlag, 133-136.

Damjanovich,S. and Somogyi,B. (1973): A molecular enzyme model based on oriented energy transfer.
J. Theoret.Biol. 41, 567-569.

Damjanovich,S. and Somogyi,B. (1978): A possible role of thermodynamic fluctuation in the overall enzyme action. in: New Trends in the Description of the General Mechanism and Regulation of Enzymes (eds Damjanovich,S., Elodi,P. and Somogyi,B.) Symposia Biologica Hungarica Vol.21. Akademiai Kiado, Budapest, 159-184.

Damjanovich,S., Bot,J., Somogyi,B. and Sumegi,J. (1972): Effect of glycerol on some kinetic parameters of phosphorylase b.
Biochim.Biophys.Acta 284, 345-348.

Eftink,M.R. and Ghiron,C.A. (1973): Dynamics of a protein matrix revealed by fluorescence quenching.
Proc.Natl.Acad.Sci.USA 72, 3290-3294.

Eftink,M.R. and Ghiron,C.A. (1977): Exposure of tryptophanyl residues and protein dynamics.
Biochemistry 16, 5546-5551.

Frauenfelder,H., Petsko,A.G. and Tsernoglu,D. (1979): Temperature dependent X-ray diffraction as a probe of protein structural dynamics.
Nature 280, 558-563.

Gavish,B. (1978): The role of geometry and elastic strains in dynamic states of proteins.
Biophys.Struct.Mech. 4, 37-52.

Gavish,B. and Werber,M.M. (1979): Viscosity-dependent structural fluctuations in enzyme catalysis.
Biochemistry 18, 1269-1275.

Green,D.E. and Ji, S. (1972): Electromechanochemical model of mitochondrial structure and function.
Proc.Natl.Acad.Sci.USA 69, 726-729.

Gurd,F.R.N. and Rothgeb,M. (1979): Motions in proteins.
Advances in Protein Chemistry 33, 74-165.

Jancsik,V., Keleti,T., Biczók,Gy., Nagy,M., Szabó,Z. and Wolfram,E. (1975-76): Kinetic properties of aldolase in polymer solutions.
J.Mol.Catal. 1, 137-144.

Keleti,T. (1980): Kinetics and thermodynamics of enzyme action and regulation. in: Bioenergetics and Thermodynamics: Model Systems (ed. Braibanti,A.) D.Reidel Publishing Co., 207-220.

Lakowicz,J.R. and Weber,G. (1973): Quenching of protein fluorescence by oxygen. Detection of nanosecond time scale.
Biochemistry 12, 4171-4179.

Laurent,T.V. and Obrink,B. (1972): On the restriction of the rotational diffusion of proteins in polymer networks.
Eur.J.Biochem. 28, 94-101.

Linderstrøm-Lang,K.V. and Schellman,J.A. (1959): in: The Enzymes (eds. Boyer,P.D., Lardy,H. and Myrback,K.) Academic Press, New York. Vol.I. 443.

McCammon,J.A., Wolynes,P.G. and Karplus,M. (1979): Picosecond dynamics of tyrosine side chains in proteins.
Biochemistry 18, 927-942.

Matko,J., Tron,L., Balazs,M., Hevessy,J., Somogyi, B. and Damjanovich, S. (1980): Correlation between activity and dynamics of protein matrix of phosphorylase b.
Accepted by Biochemistry

Nakanishi, M., Tsuboi,M. and Ikegami,A. (1972): Fluctuation of the lysozyme structure.
J.Mol.Biol. 70, 351-361.

Nakanishi,M., Tsuboi,M. and Ikegami,A. (1973): Fluctuation of the lysozyme structure. II. Effects of temperature and binding of inhibitors.
J.Mol.Biol. 75, 673-682.

Somogyi,B. and Damjanovich,S. (1971): A Molecular Enzyme Kinetic Model.
Acta Biochim.Biophys.Acad.Sci.Hung. 6, 353-364.

Somogyi,B. and Damjanovich,S. (1975): Relationship between the lifetime of an enzyme-substrate complex and the properties of the molecular environment.
J.Theoret.Biol. 51, 393-401.

Somogyi,B., Karasz,F.E., Tron,L. and Couchman,P. (1978): The effect of viscosity on the apparent decomposition rate of enzyme-ligand complexes.
J.Theoret.Biol. 74, 209-216.

Szollosi,J., Kertai,P., Somogyi,B. and Damjanovich,S. (1980): Characterization of living normal and leukaemic mouse lymphocytes by fluorescein diacetate.
Submitted to J.Histochem.Cytochem.

Tron,L., Somogyi,B., Papp,S. and Novak,M. (1976): Effect of viscous media on enzymic action.
Studia Biophys. 60, 157-162.

Varga,M., Fitori,J. and Damjanovich,S. (1978): Conductometric testing of phosphorylase b reaction in the presence of polyethylene glycols.
Studia Biophys. 70, 45-50.

Adv. Physiol. Sci. Vol. 3. Physiology of Non-excitable Cells
J. Salánki (ed.)

MEMBRANE DYNAMICS

Thomas M. Jovin
Abteilung Molekulare Biologie, Max Planck Institut für Biophysikalische Chemie, Postfach 968
D-3400 Göttingen, FRG

The maintenance of cellular viability requires the constant exchange of matter and energy with the environment. The various membrane compartments of the eucaryotic cell (plasma membrane, endoplasmic reticulum, Golgi apparatus, mitochondria) provide the structural, energetic, and regulatory mechanisms for the expression of specialized function such as during growth and differentiation. The fluid mosaic model of the cellular membrane as presented by Singer and Nicolson in 1972 [1] has had a pervasive influence on working concepts and experimental approaches applied to membrane organization and function. (For historical perspective and critical appraisal see ref. 2. Alternative models still arise, 3). Thus, it is now generally accepted that the plasma membrane, in particular, consists of a dynamic assembly of molecules in a constant state of structural and functional rearrangement. The amphipathic phospholipids provide a cohesive yet fluid bilayer matrix in which proteins are integrated with varying degrees of penetration and asymmetric distribution. The carbohydrate moieties associated with certain proteins and lipids function primarily in receptor and recognition mechanisms. Neutral lipids, especially cholesterol, play a regulatory homeostatic role.

The dynamic properties of membranes result necessarily from numerous physical, chemical and biological processes acting in concert. No general review can or will be attempted here. Excellent general sources are given in references 4-6 and in the various Annual Reviews series. An arbitrary yet useful classification of concepts and areas related to membrane dynamics is the following: a) fluidity or microviscosity; b) structural heterogeneity: domains, asymmetry; c) mobility (lateral, rotational, transverse); d) receptor organization and function, and e) transmembranar fluxes and permeation. The underlying molecular events include binding, aggregation, and fusion reactions, conformational transitions, Brownian and electrochemical diffusion, and catalysis. These are subject to the influence of general environmental factors such as ionic composition, temperature, pressure, pH, and and to specific interactions at the external and internal (cytoplasmatic) faces of the membrane, e.g. with hormones and cytoskeletal elements, respectively. It follows that numerous biochemical, biophysical, and biological

techniques have been developed for studies of membrane dynamics (Table 1). I will now discuss briefly some of the fundamental perceptions emerging from their use.

Table 1. Methods for studying membrane dynamics

molecular motion, order
magnetic resonance
electron spin resonance (ESR)
saturation transfer electron spin resonance (STESR)
nuclear magnetic resonance (NMR)
saturation transfer nuclear magnetic resonance (STNMR)
ultrasonic absorption
infrared absorption
light emission (fluorescence, phosphorescence)
spectra, polarization, quantum yield, energy transfer
steady state, time-resolved
recovery after photobleaching (FRP)
correlation spectroscopy
light absorption
linear dichroism
photochromism
electrophoresis (cells, membrane fragments, receptors)
molecular organization, transition
scattering
X-ray
neutron
light: inelastic (resonance Raman), elastic
microscopy
light: fluorescence, reflectance contrast
electron microscope: freeze-fracture, freeze-etch
differential scanning calorimetry (DSC)
(electro)chemical kinetics
perturbation: stopped-flow, temperature & pressure jump
microelectrode: detection & perturbation of potential & flux
(bio)chemical and biological
chemical modification, reconstitution, fusion
catalysis, growth, differentiation

Lipid dynamics

A basic characteristic of the lipid bilayer is the capacity to undergo a reversible cooperative thermotropic transition from a disordered fluid state at high temperature to a gel crystalline state at low temperature [7,8]. The lamellar conformation is conserved. These transitions are influenced by a large number of factors: a) lipid composition and asymmetric distribution in the leaflets of the bilayer; b) state of hydration; c) macrostructure (planar, vesicular, size); d) protein association; e) segregation into adjoining phases or domains. In the case of eucaryotic cellular membranes, the predominant state under normal conditions of growth and function is fluid, i.e., above the characteristic lipid transition temperatures. There is considerable controversy, however, regarding the possible existence and significance of microcrystalline regions [7,9], non-lamellar structures [10], and of homeoviscous mechanisms, especially in microorganisms [7,11], as might be required for the optimal growth, transport, and catalytic efficiency of processes associated with membranes [12].It is instructive to consider the time domains for the characteristic motions of phospholipid molecules in the fluid state of the bilayer (Figure 1). One of the major features is the rapid lateral thermal motion as opposed to the very slow transmembranar redistribution.

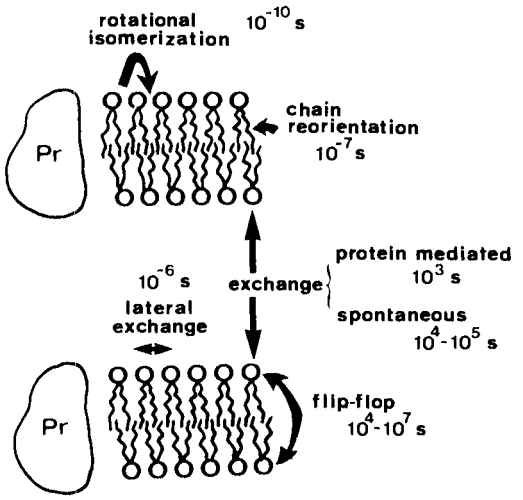

Fig. 1. Phospholipid movements in membranes. Pr, integral proteins. The lateral diffusion coefficient lies in the range 10^{-7}-10^{-9} cm^2 s^{-1}. Random insertion and deletion processes also occur but are not depicted.

Membrane fluidity and microviscosity

The continuous thermal rearrangement of the lipid membrane constituents defines a fluid system yet the extreme degree of structural and thus dynamic anisotropy renders the use of the term "fluidity" ambiguous. This complex subject has been reviewed extensively by Shinitzky and associates [13,14] who identify two distinct regions: a) the hydrocarbon core of the lipid domain. The fluidity in this region is positively correlated with the partial specific volume of the hydrocarbon chains or planar steroid structures; b) the hydrocarbon-water interface and hydrophilic boundary. These are subject to the influence of complex intermolecular forces such that a gradient of fluidity is established from the periphery to the core of the membrane. Magnetic resonance and fluorescence techniques have been applied extensively to these questions [13,14]. In particular, the rotational depolarization of the fluorescence emitted by various external probes and derivatized lipid molecules has been used to define the operational term membrane microviscosity, i.e. a parameter reciprocal to fluidity. Considerable controversy concerns the quantitative interpretation of microviscosity due to the use of steady-state depolarization methods [13,14] as opposed to time-resolved measurements. The latter demonstrate the existence of complex highly anisotropic motions. (For recent discussion and literature see 15-17). Nonetheless, the major factors controlling lipid microviscosity (or microviscosities) in synthetic and biological membranes have been identified [14]: a) the ratio of cholesterol to phospholipid (C/PL); b) the degree of unsaturation and length of the phospholipid acyl chains; c) the ratio of lecithin to sphingomyelin (L/S); and d) the ratio of lipid to protein.

Protein mobility in membranes

In addition to providing the physical boundary of the cell, the plasma membrane is the locus of essential active processes such as a) transduction of sensory, motor, and regulatory signals; b) transport of solutes and metabolites; and c) locomotion and maintenance of morphology. These functions are carried out by proteins together with other constituents of the membrane. The corresponding motions of the proteins (lateral, rotational, transverse) are subject to passive as well as active (metabolically driven) control. The methodology and principal findings in this area have been reviewed extensively [4-6,18-21,Table 1]. Lateral diffusion measurements of proteins in membranes have yielded diffusion coefficients in the range 10^{-9}-$<10^{-12}$ cm^2 s^{-1} and rotational correlation times (calculations of diffusion coefficients are ambiguous) of 20 μs and longer. Many proteins are apparently immobile by the one or the other method. Attempts have been made to reconcile these values with data and concepts [4-6,13,14,15-21] related to: a) membrane fluidity; b) ligand induced redistribution and cytoskeletal interactions [22,23]; c) regulation of the exposure of membrane proteins (passive modulation,24); d) reciprocal influences of proteins and associated (boundary) lipid and ions (especially

Ca^{++}) (see for example ref. 25); e) physical models for diffusion processes in two-dimensional membranes [15-21,26-33]; and f) binding, aggregation, and internalization reactions associated with receptor systems for transduction and regulation (see next section).

I believe it fair to state at this time that the factors determining the motions of proteins in membranes are not yet understood. For example, it is apparent that the constants for lateral diffusion are much smaller than would be predicted from the best (albeit ambiguous as discussed above) estimates of membrane (lipid!) microviscosity.

Membrane receptors

Receptors constitute a class of intrinsic membrane proteins (also lipids?) with high affinity and specificity for ligands controlling distinct cellular functions. Accelerated progress has been made in this area of research due to refined biophysical, biochemical, and cell biological techniques. (For biophysical reviews see refs. 2,34-36). No universal mechanism(s) appear to apply to cell-surface receptor systems. Thus, for example, the catalytic unit of adenylate cyclase responsible for cyclic AMP production, is linked functionally to mobile receptors for different hormones and neurotransmitters through a nucleotide (GTP) binding regulatory component. Stimulation and inhibition of the enzyme depends upon binding and diffusion reactions coupled to different oligomeric complex formation and conformational change(s). All this takes place within the plasma membrane yet functions to transmit signals through it.(The adenylate cyclase system is reviewed in 37,38).

The central role of aggregation states is well established in other systems which, however, provide interesting contrasts: a) the reaction sequence leading to the dramatic degranulation (exocytosis) of mast cells is initiated by the dimerization of the normally monovalent surface receptors for the IgE immunoglobulin [39]. The aggregation is induced by polyvalent antigens or (in the laboratory) by antibodies directed against IgE. b) the receptors for the neurotransmitter acetylcholine are tightly clustered in the post synaptic junctional folds of the motor end plate [34]. The focal release of acetylcholine from the nerve terminal produces a rapid (< 1 ms) depolarization and generation of the characteristic action potential. In addition to the topological requirements for preexisting receptor clustering in this system [34,40], it appears that the contiguity of at least two binding sites for neurotransmitter is essential for channel gating [34,35]. The exact biochemical nature of the ionophore, however, is still a matter of controversy.

c) numerous polypeptide serum factors are required for the maintenance of growth and differentiation (see,for example,41). These hormones (insulin, epidermal growth factor EGF, etc.) bind to specific membrane receptors and initiate a sequence of changes in: a) cell surface distribution of receptors; b) phosphorylation state of integral membrane proteins; c) transport of ions and metabolites, and (more protracted) d) prolife-

ration and differentiation properties of the cell. Recent evidence supports the notion that hormone-induced clustering of the membrane receptors is essential for the initiation of the biological responses [42]. The technical challenge is to demonstrate the existence and key role of microaggregates (as in the case of the mast cell). Larger clusters of hormone-receptor complexes also form and are internalized into the cell by a process of receptor-mediated endocytosis occuring at specialized regions of the cell surface called coated pits [43]. The latter mechanism is also employed for the uptake of nutritionally important proteins and associated small molecules but its significance in the case of hormone internalization is as yet unclear.

New approaches

From the above, it is evident that changes in the lateral and rotational diffusion properties of receptor molecules as a consequence of ligand binding and other interactions may constitute the key initial steps in transmembrane signaling and transduction.

We are currently engaged in studies of membrane receptor dynamics using new biophysical techniques capable of defining the proximity and aggregation states of membrane components:
a) a flow analyzer/sorter equipped with dual-laser source and multiple fluorescence detectors [44] can measure the distance between suitably labeled surface moieties of single cells by resonance energy transfer determinations. In the case of receptors (or more suitably, acceptors, 34) for the lectin concanavalin A, we have obtained evidence for clustering even at low levels of saturation [45,46]. The conclusion is that the cellular surface glycoproteins and glycolipids diffuse and aggregate as a consequence of the multivalent character they share with the lectin.
b) the rotational motion of cell surface proteins in the microsecond-millisecond domain is being measured by timed-resolved phosphorescence anisotropy [47,48], a technique which exploits the long-lived triplet states of suitable extrinsic probes and conjugates [19]. Current experiments on the IgE and hormone receptor systems are providing preliminary evidence for rapid rotational motion in the 10-100 μs region and for aggregation under the influence of environmental conditions (ionic, temperature) and agents (Bartholdi et al; Zidovetzki et al; to be published).The acetylcholine receptor from Torpedo marmorata (Bartholdi et al) as well as the major surface glycoproteins (Band 3, glycophorin) of the human erythrocyte are also under investigation (Bartholdi et al; Matayoshi et al). The attempt is being made to systematically compare the rotational and lateral diffusion properties of proteins in native and reconstituted membranes.

REFERENCES

1. Singer, S.J. and Nicolson, G.L. (1972) Science 175:720-31
2. Sonnenberg, M. and Schneider, A.S., in Receptors and Recognition A4 (eds. P. Cuatrecasas and M.F. Greaves) 1977, Chapman and Hall, London, pp. 1-73
3. Schindler, M., Osborn, M.J. and Koppel, D.E. (1980) Nature 283:346-350
4. Cell Surface Reviews (eds. G. Poste and G.L. Nicolson), North Holland, Amsterdam (especially Vol. 3, 1977)
5. Receptors and Recognition. Series A (eds. P. Cuatrecasas and M.F. Greaves), Chapman and Hall, London
6. Quinn, P.J. and Chapman, D. (1980) CRC Crit. Rev. Biochem. 8:1-117
7. Melchior, D.L, and Steim, J.M. (1976) Ann. Rev. Biophys. Bioeng. 5:205-238
8. Nagle, J.F. (1980) Ann. Rev. Phys. Chem., in press.
9. Klausner, R.D., Kleinfeld, A.M., Hoover, R.L., and Karnovsky (1980) J. Biol. Chem. 255:1286-95
10. de Kruijff, B., Cullis, P.R. and Verkleij, A.J. (1980) TIBS 5:79-81
11. Hauser, H., Hazlewood, G.P. and Dawson, R.M.C. (1979) Nature 279:536-38
12. Shinitzky, M., Borochov, H. and Wilbrandt, W. (1980) in Membrane Transport in Erythrocytes. Albert Benzon Symposium 14, Munksgaard, Copenhagen, in press.
13. Shinitzky, M. and Barenholz, Y. (1978) Biochim. Biophys. Acta 515:367-94
14. Shinitzky, M. and Henkart, P. (1979) Int. Rev. Cytol. 60:121-47
15. Jähnig, F. (1979) Proc. Nat. Acad. Sci. USA 76:6361-65
16. Heyn, M.P. (1979) FEBS Lett. 108:359-64
17. Lakowicz, J.R. and Knutson, J.R. (1980) Biochemistry 19:905-11
18. Edidin, M. (1974) Ann. Rev. Biophys. Bioeng. 3:179-201
19. Cherry, R.J. (1979) Biochim. Biophys. Acta 559:289-327
20. Thomas, D.D. (1978) Biophys. J. 24:439-62
21. Schlessinger, J. and Elson, E.L. (1980) in Biophysical Methods, Methods of Experimental Physics (eds. G. Ehrenstein and H. Lecar), Academic, New York, in press.
22. Edelman, G.M. (1976) Science 192:218-26
23. Klausner, R.D., Bhalla, D.K., Dragsten, P., Hoover, R.L., and Karnovsky, M.J. (1980) Proc. Nat. Acad. Sci. USA 77: 437-41
24. Shinitzky, M. (1979) in Physical Chemical Aspects of Cell Surface Events in Cellular Recognition (eds. C. DeLisi and R. Blumenthal), Elsevier, New York, pp. 173-81
25. Pink, D.A. and Chapman, D. (1979) Proc. Nat. Acad. Sci. USA 76:1542-46
26. Richter, P.H. and Eigen, M. (1974) Biophys. Chem. 2: 255-63
27. Naqvi, K.R. (1974) Chem. Phys. Lett. 28:280-84
28. Saffman, P.G. and Delbrück, M. (1975) Proc. Nat. Acad. Sci. USA 72:3111-13

29. Saffman, P.G. (1976) J. Fluid Mech. 73:593-602
30. Galla, H.-J., Hartmann, W., Theilen, U. and Sackmann, E. (1979) J. Membrane Biol. 48:215-36
31. Hardt, S.L. (1979) Biophys. Chem. 10:239-43
32. Koppel, D.E. and Sheetz, M.P. (1980) Biophys. J. 30: 187-92
33. Andersen, G.R. and Mazo, R.M. (1980) Biopolymers 19: 1597-1602
34. Barrantes, F.J. (1979) Ann. Rev. Biophys. Bioeng. 8: 287-321
35. Stevens, C.F. (1980) Ann. Rev. Physiol. 42:643-52
36. Cell Surface Events in Cellular Recognition (eds. C. DeLisi and R. Blumenthal), Elsevier, New York, pp. 1-393
37. Rodbell, M. (1980) Nature 284:17-22
38. Bell, R.M. and Coleman, R.A. (1980) Ann. Rev. Biochem. 49:459-87
39. Metzger, H. (1978) Immunological Rev. 41:186-199
40. Frank, E. (1979) Nature 278:599-600
41. Carpenter, G. and Cohen, S. (1979) Ann. Rev. Biochem. 48:193-216
42. Schlessinger, J. (1980) TIBS 5:210-14
43. Goldstein, J.L. Anderson, R.G.W. and Brown,M.S. (1979) Nature 279:679-85
44. Arndt-Jovin,D.J.,Grimwade, B.G. and Jovin, T.M. (1980) Cytometry, in press.
45. Chan, S.S., Arndt-Jovin, D.J., and Jovin, T.M. (1979) J. Histochem. Cytochem. 27:56-64
46. Arndt-Jovin, D.J., Grimwade, B.G. and Jovin, T.M. (1980) in preparation.
47. Austin, R.H., Chan, S.S. and Jovin, T.M. (1979) Proc. Nat. Acad. Sci. USA 76:5650-54
48. Moore, C., Boxer, D. and Garland, P. (1979) FEBS Lett. 108:161-66

Adv. Physiol. Sci. Vol. 3. Physiology of Non-excitable Cells
J. Salánki (ed.)

TEMPORAL STRUCTURE OF SPIKE SEQUENCES AS A BASIS FOR DESIGN OF NEURONAL NETWORKS

E. Lábos, E. Nógrádi and D. Ramirez
1st Department of Anatomy, Semmelweis University Medical School, 1450 Budapest, Tűzoltó u. 58 Hungary

INTRODUCTION

The simplest manifestation of temporal structure in unit spike records is the periodical modulation often observable during spontaneous firing. In extreme cases these modulations are resulted in bursting activity or in fairly constant frequency of firing. Concerning to the origin, the increase of firing rate may be endogenous or synaptic activation, while the frequency decrease may be caused by falling of generator potentials, disappearence of synaptic activation or appearence of more or less lasting synaptic inhibition. However, both of them may occur also as a result of refractory cycle or post - tetanic processes.

In theoretical sense, the term "periodic" firing does not correspond to the precise ever-lasting periodicities of certain solutions of given differential equations, i.e. the finitness and noisiness are characteristic to the real records. The term "modulation" is also vague, because an adequate demodulation procedure will not always result in a function which has observable equivalent in the oscillation of membrane potential. This is explicit only if the generator potentials are present and it is hidden if threshold or conductance changes are not accompanied by potential variations.

As it is shown in Fig.1. the internal course of the repeatedly occuring spike sequences includes very minute, but at the same time consequently emerging details. It is also observable that, there are obvious differences between the recurring and preceeding cycles. The two simultaneous records are definitely correlating.

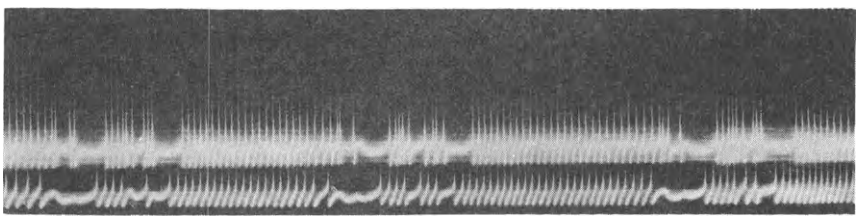

Figure 1. Simultaneous records of two giant neurons of landsnail (Helix pomatia L.)

POINT-PROCESS MODEL OF UNIT RECORDS

In order to extract or translate the information included in intra- or extracellular record the following procedure was followed: (1) The initial R record is the basis of computation of X point-process, which is a set of time points, each of them is corresponding to one and only one spike. (2) The T set of the successive interspike intervals is essentially equivivalent to X, i.e. they may be calculated from each other. (3) Choosing a $d>0$ period of time and dividing the period of observation into equidistant, disjoint and covering dwell times of length d, and finally counting the time points of T in each dwell box an F_d sequence of firing rates is obtained. If d was sufficiently small, than F_d is a sequence consisting only of 0 or 1. These sequences are called (0,1)-words or tapes. Their computation is more or less algorithmic.

During this computational procedure, information is lost, i.e. the computability holds only in the following direction: $R \rightarrow (X \rightleftarrows T) \rightarrow F_d$. The most painful loss of information is that really observed subthreshold oscillations are irreversibly lost. However designing formal neuronal networks on the basis of F_d may result in several solutions, of which the selection is definitely helped by returning to the original R records. Further details is written by Lábos(1980a,1980b,1980c).

EXISTENCE OF TEMPORAL STRUCTURE AND CORRELATION

Both single and double records are often analyzed with linear correlation methods. Auto- and cross-correlation diagrams are suitable to demonstrate the existance of periodicities, delays and also yield measures of the linear correlation. However, it is obvious that correlations are not corresponding to stochastic dependences. There are even invertible deterministic relationships for which the linear correalation coefficients are zeros. For this reason it is reasonable to introduce a method called auto- or cross - communication analysis (Lábos,1978,1980a) which is based upon the computation of Shannonian term called transinformation. It explores exactly the dependence of two e.g. F_d frequency-time diagram. However, in this procedure the actual values of firing rates are ignored. In Fig. 2. for a pair of neuronal records a normalized cross-communication diagram is compared to a cross-correlation one.

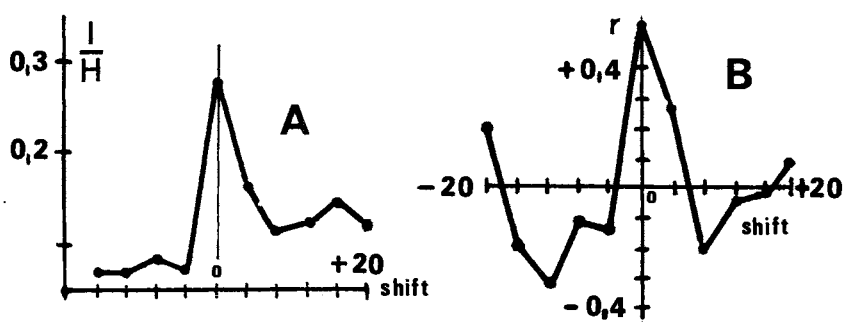

Figure 2. Cross-communication (A) and cross-correlation plots (B)

FORMAL NEURONAL NETWORKS GENERATING GIVEN PATTERNS

The first step of the network synthesis is to find a suitable description of the F_d (0,1) words, where $d \leq \min T$. Any finite words have two important parameters: (1) the length, denoted by L and (2) the order designated with r. The order is the minimal integer number for which

$$G(s_k, s_{k-1}, \ldots, s_{k-r}) = s_{k+1}$$

relation is function. For example W = $(1111010110010000)^{\infty}$ has L=16 length, the consecutive letters are marked with s_k, k=1,...16 and the order is 4. Functions of 3 or less variables are not adequate as e.g. 101 is followed either by 0 or by 1. The following relations hold:

$r < 2^r$, $n < 2^n$, $L \leq 2^n$, $L \leq 2^r$, $r < L$, $n \geq 1$, $r \geq 0$ and $n \lesseqgtr r$.

Here the symbol n means the number of formal neurons or modules in the network of which at least one module generates periodically a previously given W word if the network was starting of its resting state.

A formal neuronal network is here defined as a vector-vector function. Its states are vectors of 0 or 1 components, its connectivity is described by an nxn matrix called N and by the threshold $\underline{T}$, which is a vector. Both N and T have real numbers as entries. The function is as follows: $\underline{s}_{k+1} = \underline{u}(\underline{s}_k . N - \underline{T})$, where the function u is taken by coordinates and its value is 1 if the argumentum was positive and is zero otherwise.

As it is known from the threshold logic (see e.g. Muroga, 1971) to design a neuronal network is equivalent to the solution of a given set of systems of linear inequalities. The aim is to find the values in the matrix N and $\underline{T}$. The starting point is a truth function defined either partially or completely.

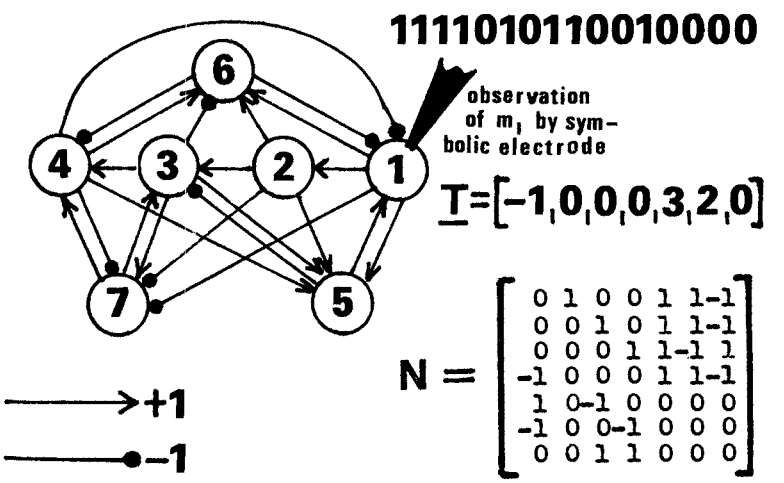

Figure 3. A network of formal neurons of which m_1 module generates cyclically the word (1111010110010000).

The order of ideas resulted in the network in Fig. 3 is as follows. As the G function of 4-order yielded non-solvable system of inequalities, first a simpler network of modules m_1-m_4 were chosen, which is capable to generate the sequence (11110000), i.e. a word which is deficient if compared to the W word to be produced. The modofication of this "core-network" was carried out by recognizing those critical states which lead to errors. This recognition was carried out by additional modules responding by 1 output if and only if the critical state occured. It is often necessary to delay the result of this recognition until the time when the intervention or control becomes important. Thus modules m_5, m_6 and m_7 are critical state-recognizer neurons observing states of the core network (m_1-m_4) and by feeding back their output to the monitored network it is possible to set the core network as it is needed.

This manner of design is called state-recognition method (1980c).

It is similar the way, when the words to be generated are obtained from real neuronal records. E.g. the patterns of the Fig. 1 has the following characteristics: (1) The active phases in the lower record start and end sooner then in the upper one; (2) The rate of firing is fairly constant in the upper record except the shorter interval at the end of activity, while the lower spike sequence shows slow decrease of the rate; (3) Both neurons are stopped by inhibition and in this inhibited phase shorter periodic modulations occur.

The formal network which contains two modules simulating at least partially the phenomena listed above is published in work of Lábos(1980c).

DISCUSSION

The aim of this lecture was to show that interpretatory network can be designed in a more or less canonical way if either real or fictitious sequence are prescribed. The more difficult problems are included in the evaluation and testing of the models. As usually many solutions can be obtained a selection procedure is necessary to exclude irreal cases. Two ways, the experimental test and the searching of optimal solutions are helpful. The other problem is a semantical one. It is not possible to equalize formal and real neurons and it is most probable, that several formal neurons represent parts and processes of real ones whose specification is necessary.

REFERENCES

Lábos, E. (1978) - Distribution of information in neuronal networks of snail (Helix pomatia L.). Annual Meeting of Hungarian Physiological Society, Debrecen.

Lábos, E. (1980a) - Information included in neuronal spike sequences with respect to their generator network. Proc. of the 5th European Meeting on Cybernetics and System Research. Hemisphere Publishing Corporation, Washington (in press).

Lábos, E. (1980b) - Effective extraction of information included in network descriptions and neuronal spike records. Conference on Mathematical and Computer Methodologies in Biology and Medicine. Salerno, 14-18 April, 1980 (in press).

Lábos, E. (1980c) - Optimal design of neuronal networks. Satellite Symposium of 28th IUPS Congress on "Neural Communication and Control" Debrecen, Hungary (in press).

Muroga, S. (1971) - Threshold Logic and its Applications. Wiley-Interscience, New York.

Adv. Physiol. Sci. Vol. 3. Physiology of Non-excitable Cells
J. Salánki (ed.)

SUBSECOND TIME DOMAINS IN BIOLOGICAL SYSTEMS: RELEVANCE, PROBLEMS, APPROACHES

H. Frauenfelder
Department of Physics, University of Illinois at Urbana-Champaign Urbana, IL. 61801, USA

Since biological systems are intricate, a profound understanding can only be reached after exploring the simplest components fully. In physics complex atoms were only understood after the hydrogen atom problem had been solved. Simple proteins such as myoglobin or cytochrome c, are the hydrogen atoms of biology. The present talk will stress the results obtained with such proteins; it is likely that many of the general conclusions and techniques can be applied to more complex biological systems. One of the central problems is characterized by the catch word structure-function relation. This question is intimately related with the spatial and temporal behavior of proteins. The two aspects cannot be separated; in order to discuss the time course of an event intelligently we must know which parts of the macromolecule are involved. Two concepts can be distinguished, conformations and conformational substrates. A conformation is characterized by a particular overall structure and a specific function. A conformation can exist in a very large number of conformational substates that have the same coarse structure but differ in local configurations. All conformational substates perform the same biological function, but possibly with different rates. The problem can now be stated: What are the spatial and temporal properties of conformations and conformational substates? Theory and experiment must go hand in hand to answer this question. In the past few years, theory has progressed

considerably; statistical mechanics, irreversible thermodynamics, and computer calculations provide detailed insight into the temporal and spatial aspects of motion in proteins. Fluctuations around the equilibrium positions and motion of small molecules within proteins are being explored. Experimentally, the spatial and temporal behavior are also being studied. Standard X-ray and neutron diffraction, coupled with improved sources of radiation, detectors, and methods of evaluation, provide the coarse structure of different conformations. Information about the spatial properties of conformational substates has come from a new look at the Debye-Waller factor for all nonhydrogen atoms in proteins. The temporal properties of transitions among conformations and also among substates are investigated by a wide range of techniques, for instance flash photolysis, NMR, ESR, fluorescence experiments, and Mössbauer effect. The result is a picture of a dynamic bimolecule that continuously breathes and moves and where the danamic behavior is the relevant feature for the biological action. The connection between structure and function thus is dynamic and not static.

Adv. Physiol. Sci. Vol. 3. Physiology of Non-excitable Cells
J. Salánki (ed.)

TIME IN CELL BIOLOGY. CONCLUDING REMARKS

P. Fasella
Universita di Roma, II Cattedre di Chimica Biologica, Facultá di Medicina e Chirurgia, Cittá Universitaria, 00185 Roma, Italy

These concluding remarks are personal considerations about the accomplishments, research trends and forecasts emerging from the discussions. They were written on the spur of the moment, as suggested by the Organizers of the Congress. I whish to apologize for the inevitable errors, mis-interpretations, omissions and bias. Specific reference to the work and ideas of the invited participants will often be omitted because obvious. For this also, however, I whish to apologize.

The time structure of the main macromolecular systems constituting the cell begins to be known down to the picosecond range. Thanks to recent theoretical and experimental developments for each class of cell components /proteins, nucleic acids, phospholipid micelles, etc./ events have been identified, described in molecular terms and classified according to the time domain in which they occur. So far only few, but very representative, cases have been studied in depth. The consolidated results and the ideas which generated and were generated by them are so significant that a rapid, rewarding expansion of the field is to be expected.

Of particular interest are the motions typical of macromolecules. Here local events are generally faster than segmental processes, which are in their turn faster than those involving the whole macromolecule. Fluctuations in the macromolecular structure are produced by interaction with external ions and water molecules as well as by brownian transfer of

momentum. Proteins have a flexible structure related to their capacity of existing in different conformational substrates. This flexibility plays a crucial role in biological events such as enzyme catalysis, allosterism, muscular contraction, membrane properties and viral life cycle. Further, systematic work on the relation between the characteristic time constants of the above biological processes and the temporal properties of the macromolecular systems involved in them is highly desirable.

As shown by Frauenfelder, reaction theory as applied to the analysis of the dynamic structure of proteins must be re-examined. Starting from Kramers' model of a chemical reaction /brownian motion of a particle along the reaction coordinate in the presence of a potential energy barrier/ it is possible to overcome the inadequacy of classical transition state theory for the description of reactions in proteins and in complex biological systems. This approach leads to important conclusions, substantiated by measurements of representative systems, such as hemoglobin and the "purple membrane"/cf. Frauenfelder and associates/. First: viscosity exerts a dominant influence on rate coefficients and solvent has a large effect on the local motility inside the protein, variations of solvent viscosity being partially transferred to the reaction site. Second: the static model of a reaction pathway controlled by "barriers" to be overcome should be replaced by a dynamic picture of usually closed "gates", occasionally opened by conformational fluctuations. This is an important notion which should be extended to many mechanisms of biological control.

Gratton, starting from a discussion of the time dimension of proteins, pointed out that a critical comparative study of the characteristic time constants for the different classes of events occurring in the various types of biological macromolecules provides a fundamental clue in the analysis of biologically relevant interactions among the constituents of complex cellular systems: no cross-correlation is possible between processes having greatly different time constants.

Applying this approach to what is in physiological /but certainly not in physical and chemical/ terms an "elementary" process, i.e. an enzyme-catalyzed reaction, the problem arises of defining the relation between the molecular motions occurring in the enzyme protein with time constants of 10^{-7} - 10^{-8} sec and the "chemical" event occurring at the active site with a time constant of 10^{-3} - 10^{-2} sec. The solution of this problem, which has received considerable attention in recent years /e.g. Careri, Gratton and Fasella/, requires further theoretical and experimental work. Useful concepts in this respect are that of protein-mediated cross-correlations of fluctuations at the enzyme active site, and that of the fluctuating enzyme protein as a machine conveying energy from the thermal bath to the reaction site.

The rates for the main elementary reaction steps involving nucleic acids /stacking, base pairing, helix-coil transitions, etc./ determine the rates of information transfer and cleavage of DNA and RNA. The relative rates of contemporaneous or successive events play a crucial role in reduplication, transcription, translation, mutation and repair, as well as in selection. The importance which the dynamic structure of nucleic acids has in determining not just the rates but the specificity of biologically relevant events is demonstrated by recent work carried out by Rigler on tRNA. Here, the existence of a dynamic equilibrium among different conformational states has been defined in its structural and temporal aspects: conformational flexibility is important for the charging of the tRNA with the corresponding amino acid and for the translation of the charged tRNA on the programmed ribosome. Moreover, the role of kinetic effects in "editing" the genetic message by reducing translational errors at the level of the tRNA amino-acid interaction has been demonstrated /cf. also the work of Hopfield and of Fersht/

The role of the dynamics of the DNA Helix, including the opening and closing of base pairs and the formation of branched loops, in the control of enzymological transformations of nucleic

acids has been clearly illustrated by recent kinetic studies, reported by Rigler, of DNA cleavage by restriction endonucleases and of base-specific interactions between DNA and intercalating compounds. The occurrence of specific, "available" conformations of DNA was emphasized during the discussion of the interaction of nucleic acids with regulatory proteins and enzymes.

Recent methodological developments, including time resolved measurements of fluorescence depolarization, dynamic laser light scattering, low-angle X-ray scattering, synchroton radiation sources and NMR, make it possible to extend the above approach to the study of other fundamental processes of gene control and expression. Such work is already carried out in some laboratories and will expand in the near future. The analysis of the time structure of chromatin is one of the most important areas within this field /cf. the intervention of Damjanovich/.

A discussion of the time-resolved structure of biomembranes requires consideration of the characteristic time constants of their components and of the interaction among them during morphogenesis and function. The general properties of biomembranes are illustrated by the selected, representative, cases presented by Jovin /e.g. glycoforin and its interaction with model and natural membranes/. A number of advanced techniques, ranging from NMR to EPR and photochemical bleaching, have been developed and are being applied to the study of biomembranes. The kinetic picture of biomembranes is dominated by the high non-homogeneous viscosity of the medium and by the fluctuating, non-symmetric, mosaic structure. This confers a vectorial character to the chemical reactions occurring in biomembrane. Proteins diffuse in membranes and through membranes. The lateral diffusion constants range between 10^{-8} and 10^{-10} cm^2 sec^{-1}; at least in some cases diffusion occurs by dislocations through existing, fluctuating channels. Transverse diffusion through the membrane is generally slower, except in correspondence of specific "open" gates. The interaction between lipids and proteins are particularly interesting for

the comprehension of these phenomena: in general proteins increase order in the fluid phase and decrease order in the gel phase of the membrane lipid components. Both lateral and transverse diffusion of proteins in membranes are involved in fundamental physiological processes. A good example is transmembrane signalling by receptors aggregation upon effector binding, followed by the formation of coded pits and by internalization. An interesting example of transmembrane signalling is provided by Damjanovich's work about the effect of extracellular osmolality on esterase activity inside lymphocytes and lymphoblasts. Dr. Dancsházy has illustrated the time structure of the electric signals associated with the photocycle of bacteriorhodopsin. This correlates with some of Frauenfelder's observations.

The discussion of the time dimensions of cellular metabolic processes uses all the previous notions concerning the time structure of the cell macromolecular components, introduces new facts and ideas about metabolic pathways and cellular structures and integrates all this complex information in a unitary approach. It is particularly at this level that the physical chemistry of macromolecular complexes meets cell physiology.

Cell anatomy describes the ordered subdivision of cellular space in vesicles, particles, tubules, vacuoles, reticulum and cytoplasmic compartments. Biochemistry identifies the main metabolic networks, formed by interacting series of enzyme-catalyzed reactions, localized in the various subcellular compartments. Interactions between compartments are controlled by transmitters and by protein-mediated transport of metabolites, followed by free-space diffusion. The time dimensions of transport through membranes are the same as those of enzyme reactions. Within each compartment the kinetic properties of all enzyme and transport systems involved and the pool size of the respective metabolites determine the time course of events and hence the fluxes of matter and energy. Thanks to the work of Hess and his associates and of some other laboratories, detailed data are available about the time dimensions

of the most important energy yielding biochemical systems: glycolysis and oxidative phosphorylation. Several representative cell types have been investigated, so that a general picture can be obtained.While over-all turnover numbers are of the same order of magnitude /100 sec^{-1}/ for glycolysis and oxidative phosphorylation, transition times from one metabolic state to another are shorter /0.05-0.1 sec/ for oxidative phosphorylation than for glycolysis /1-20 sec/. In intact cells both processes "oscillate" /i.e. the controlling enzymes go through alternating maxima and minima of activity/ with frequencies ranging between 0.1 and 0.01 sec^{-1}. Such oscillations also provide a means for functional coupling among cells, as shown by the work on the aggregation of slime molds. Moreover, such metabolic oscillation could form the basis for "biological clocks". In free space, metabolic oscillations spread at a rate of 10^{-3} cm sec^{-1}. Coupling of chemical events and spatial transport makes the time dimension of metabolic pathways dependent on the space dimensions of transport and hence on cellular and subcellular anatomy. Metabolic oscillations in space can generate dynamic structures which are time- and metabolic flux dependent. Such pioneering, but fully consolidated, work should and shall be extended to other systems. Of particular interest is the role which the formation of stationary metabolic waves in space could play in morphogenesis by the creation of localized zones of high concentrations of specific compounds.

The symposium was focussed on the time dimensions of cells and their components; however the time structure of multicellular systems is of equal or greater physiological importance and obviously, even more complex. A stimulating, "token" illustration of the type of problems and approaches in this very wide area /which is certainly in rapid expansion as shown by work presented at other sections of this Congress/ has been presented by Lábos and coworkers, who discussed the temporal structure of spike sequences in snail giant neurons as a basis for the design of neuronal networks.

CONCLUSIONS

Because of the eminently dynamic state of living systems, the time dimension is a fundamental aspect of the description of cells. The time structure of cells and of their components in the subsecond range is particularly interesting because fundamental events in biochemical transformations, energy production and utilization, information processing, morphogenesis, development, regulation and selection occur in this time range. Thanks to recent conceptual and methodological developments, the main features of the cell short time structure are being uncovered. Some representative systems, illustrated at this Symposium by pioneers in the respective fields, are now known in considerable detail. The means are there for a rapid and fruitful expansion of their whole research area.

The interest which the physical and molecular approach introduced by many of the speakers has for cell physiologists has been confirmed by the high rate of attendance to this symposium and by the quality and number of interventions in the discussion. I am certain that I correctly interpret the feelings of invited speakers and of the audience, when I express to the Chairman of the Section of Cell Physiology, Professor Salánki, our deep gratitude for this welcome opportunity and for his broad-minded and imaginative support.

INDEX

The page numbers refer to the first page of the article in which the index term appears.

absorbing tubules 71
acetylcholine 23
active oxygen 1
active tranport 57, 187
adhesion 233
adrenaline 209
aggregation 233
amiloride 147, 151, 157
amino acid transport 197
apical membrane 129, 147
astrocyte 23
ATP synthesis 183

Ba^{2+} 135
bactericidal action 1
baseplate 233
brush-border surface 81

Ca^{2+}-ATPase 183
Ca^{2+}-binding proteins 245
calcium 221, 233
  intracellular free 241
calcium ion 1
  function 245
  transport 209
calmodulin 245
cAMP 173
carbonic anhydrase 23
catecholamine 23
cells
  communication of 233
  coupling of 233, 241
  encounter of 233
  interaction of 233
  surface of 233
cell-to-cell channels 241
cellular regulators 245
channel permeability 241
channel size 241
Cl-current 115
Cl-permeability 115
Cl-transport 147
coated vesicles 225
concanavalin A 1
cyclic-3', 5'-adenosine monophosphate 221
cyclic-3', 5'-guanosine monophosphate 221
cyclic nucleotides 245
cytochalasin 1

DTT 147
dynamic metabolic states 275
dynamic structures 275

ependymal cell 23
epithelial transport 157

feed-back inhibition 173
furosemide-sensitive transport 197

GABA 23
glomerulotubular balance 47
glucose metabolism 173
glucose-6-phosphatase 81
glutamate 23
  transport 197
glutamine synthetase 23
Golgi complex 225

$HgCl_2$ 147
hormones 157
H^+ transport 183
hydrogen peroxide 1
5-hydroxytryptamine 23
hypoinsulinemia 173

ionophore 1
instability 71
insulin 173, 209, 221
intracellular communication 241
intracellular macromolecules 233
intracellular pH 241
intracellular substances 233
isoosmotic reabsorption 47
isoosmotic transport 57, 81
isotonic transport 89

K^+-channel 135

latero-basal membrane 129
L-cells 57
leukocyte 1
lipoproteins 225
lymphocytes 197

macromolecule 285, 301
metabolism 187
microglia 23
monolayer cultures 225
mutants 197
myelination 23
myeloperoxidase 1

NADPH oxidase 1
Na^+K^+-ATPase 23, 47, 81, 107, 183
Na^+-K^+-pump 209
Na^+-K^+-transport 209
Na-permeability 151
Na-transport 129, 135, 147, 151, 163
Na-uptake 129
nonequilibrium thermodynamics 187
noradrenaline 209

oligocyte 23
organ formation 233
osmolarity 71
ouabain 107, 147, 157
oxidative metabolism 1
oxytocin 157

paracellular pathway 81
Pasteur effect 173
peritoneal membranes 163
phagocyte 1
phagocytosis 1, 23
phagosome 1
phosphorylase 285
plasma membrane 233
polymorphonuclear leukocyte 1
potassium transport 197
propagation of chemical signals 275
prostaglandins 157
proteins
  dynamics 285, 301
  flexibility 269
proteoglycans 233
proximal nephron 57
proximal rabsorption 47
proximal tubules 47

rate-limiting transport 173
recognition, intercellular 233

Schwann cells 23
sodium transport 157
solute transport 71
standing gradient 71
streptozotocin 173
sugar transport 173, 221
superoxide anions 1
surface macromolecules 233
surface receptors 233

thyroid hormones 209
time domains
  of metabolic processes 275
  of transport processes 275
transcellular channels 81
transcellular transport 107
transepithelial potential 107, 115
transepithelial pressure 57
transepithelial transport 107
transmembrane electrochemical potential 115
transport 71

vibrational motion 285

yeast 173